Synthesis, Biological Evaluation and Surface Applications of Neuritogenic Compounds

Inauguraldissertation

zur

Erlangung der Würde eines Doktors der Philosophie

vorgelegt der

Philosophisch-Naturwissenschaftlichen Fakultät

der Universität Basel

von

Patrick Burch

aus Sarnen, Obwalden

Basel, 2013

Genehmigt von der Philosophisch-Naturwissenschaftlichen Fakultät
auf Antrag von

Prof. Dr. Karl Gademann
Prof. Dr. Thomas R. Ward

Basel, den 12.11.2013

Prof. Dr. Jörg Schibler
Dekan

Für Linda und
meine Familie

„I did it my way“

Frank Sinatra (1915-1998)

Acknowledgements

I would like to express my deepest gratitude to my "Doktorvater" *Prof. Dr. Karl Albert Bernhard Andreas Gademann* for allowing me to join his group, for the guidance and the freedom he has provided me with. I always enjoyed our discussions, especially when we did not agree on something.

Prof. Dr. Thomas Ward is acknowledged not only for accepting the co-examination of my PhD thesis but also for hosting me during my Master thesis and therefore setting the starting point of my on-going tightrope walk between materials chemistry and biology and for telling Karl and Phil to give that guy a chance. I also would like to thank *Prof. Dr. Dennis Gillingham* for chairing my defence.

The joint efforts form *Dr. Henning J. Jessen*, *Dr. Erika Crane* and *Dr. Hideki Miyatake Ondozabal* for critically proofreading this manuscript and therewith improving its quality a lot are deeply appreciated.

It certainly is no secret that without the help of my enthusiastic Master students *Manuel Scherer* and *David Bossert* this thesis probably would not be able to stand upright on a bookshelf just by its-self. Keep up the good work guys! At this place I also like to thank *Massimo Binaghi* for providing most of the fundament on which the gelsemiol project was built on.

Dr. Emma Dunphy and *Dr. York Schramm* are acknowledged for their constant support during the last years as well as for their ability to produce an unbelievable amount of interesting stories, which entertained me a lot.

So many things and people to thank for:

Samuel "Grumpy" Bader, for always being there for me at literarily any time and assuring that I'm not the oldest guy on the dance-floor, this really helped a lot. *Dr. Johannes "Joe" Hoecker* (who was *"raus"* before me) for providing a better understanding of the people from the dark side. *José "Mexican" Gomez* efforts in making me an even better safety inspector cannot be appreciated enough. *Dr. Adrian "Hans-Lee" Laurence* for being my partner in crime before the *Great Escape* out of Lausanne. *Dr. Henning J. Jessen* and *Dr. Chandan K. Jana* for taking me under their wings at the beginning of my doctorate. I might be a bit crazy, but *Christophe Deappen* and *Fabian Schmid* showed me that if it should get worse, one still can be a

great co-worker and friend. *Isabel Keschgerns* (I hope you will get your pony one day), *Elias "Elsbeth" Kaufmann* (nice shirt), *Robin "Röbi" Wehlauch* (nice black shirt), *Dr. Suman "Eagle Eye" De Sakar* (Why is my shirt on the tree), *Dr. Jean-Yves Wach* (scan & dust), *Dr. Claudia Avello Simoes Pires*, *Dr. Elangovan "Ruedi" "E Longerone" "El Angewante" Elamparuthi* (HE BUUCH!!!), *Raphael Liffert* ("Ich nimms jetzt mal chli easy am Afang"), *Dr. Hideki Miyatake Ondozabal* (It's Okey), *Simone "Sisibear" Sieber* ("Thank your for the music, for giving it to me"), *Dr. Erika Crane* (brats and hoppy spritzers for everyone). *Dr. Tom Woods* (The only group member besides me who liked the "Curds"), *Christophe Thommen* (I enjoyed watching our transformation form a very shy guy how broke a lot of glassware to a real man how still breaks a lot of glassware), *Vreni "Verena" Grundler* (you birthed up the group a lot) *Dr. Malika Makhlouf* (ramadamadingdongsong), *Dr. Christof "Oberassistent" Sparr,* (I'm too *** for this shit), *Dr. Cyril Portmann* (the power of positive drinking), You guys really enriched my PhD studies more than any name reaction ever could. *"Paprika", "Trish"* and *"Patricia"* will miss you guys a lot.

A special thanks goes to all people working in this department and keeping it so much alive such as the ground floor *Sonogashirea-Sisters*, the *Be***** Ball Players*, the *Pfaltz Guys*, our former subgroup the *Gillis* and the *Wood-people* who took over the 3th floor after us for good. *The Kellerkinder*, *NMR-guys* and the people form the inorganic department who dared to interact with us organics. The staff how keeps this place running and successfully preventing it form falling apart: *Beatrice Erismann, Marina M. Johnson, Roy Lips, Maurus Maier, Markus Hauri, Andres Kohler* and many more. Sometimes you made me feel working in one big flat-share. That certainly is something that makes this place unique and should be retained by all measures.

I also like to thank everyone how has ever organized an apéro for whatever reason and allowing me to join it, especially, when he or she did not know me at all.

Von ganzem Herzen danke ich auch meiner Familie Lisbeth, Sepp & Jörg für ihre durchgehende Unterstützung in den letzten noch nicht ganz dreissig Jahren. Ein spezieller Dank gebührt meiner Freundin Linda für ihre Liebe und die schönen gemeinsamen Jahre.

Table of Contents

Table of Contents i
Publications iv
Abstract v
Kurzbeschreibung vii

1 Introduction 1
1.1 General Justification 1
1.2 Efficiency of Natural Products Synthesis 2

2 Total Synthesis and Biological Evaluation of Gelsemiol 9
2.1 Introduction 9
2.1.1 Isolation and Neuritotrophic Activity 9
2.1.2 Iridoids 9
2.1.3 Gelsemiol as an Advanced Intermediate 12
2.1.4 Previous Synthetic Contributions 13
2.2 Results and Discussion 19
2.2.1 Retrosynthetic Analysis 19
2.2.2 Total Synthesis 20
2.2.3 Synthesis of Natural Congeners of Gelsemiol 27
2.2.4 Biological Evaluations 28
2.3 Conclusion 31

3 SAR Study on functionally optimized neuritogenic Farinosone C Analogs 35
3.1 Introduction 35
3.1.1 General Outline 35
3.1.2 Parasite Host Control 36
3.1.3 Total Synthesis of Farinosone C by *Jessen et. al*. 38
3.1.4 FOS Approaches form *Gademann* and Co-Workers 40
3.1.5 The *Rat Pheochromocytoma* PC12 Assay as a Brain Model 42

3.2 Results and Discussion 44
3.2.1 Synthesis of Farinosone C Analogs 44
3.2.2 Structure-Activity Relationship Study Results 49
3.3 Conclusion **51**

4 Investigations on the Mode of Action and Molecular Targets of Neuronal Differentiation **55**
4.1 Introduction **55**
4.1.1 General Overview and Known Pathways 55
4.1.2 Neuritogenic Natural Products Bearing long Alkyl Chains 56
4.1.3 Similarity Ensemble Approach 58
4.1.4 The Endocannabinoid System 59
4.1.5 The HIP HOP Assay 62
4.1.6 ATDD and Potentially Psychostimulant Structural Analogs 65
4.1.7 The MTT Assay 70
4.2 Results and Discussion **72**
4.2.1 Computational Results using the SEA Search Tool 72
4.2.2 Synthesis of Tyrosinol Fatty Acid Analogs 4.22a-h 78
4.2.3 Biological Evaluation 80
4.2.4 Examination of the Endocannabinoid System 82
4.2.5 HIP HOP Profiling 84
4.2.6 Amphetamine-Type Bioactivity of Farinosone C Analogs 85
4.2.7 Fluorescent Labelling 88
4.2.8 Neuroprotective Properties 90
4.3 Conclusion **90**

5 Development of Neuritogenic Surfaces using Natural Product Analogs **91**
5.1 Introduction **91**
5.1.1 General Overview 91
5.1.2 Spinal Cord Injuries 91
5.1.3 Surface-Mediated Neuronal Growth and Guidance 92
5.1.4 Gentiside B Analog as Candidate for Coating Applications 93

5.2 Results and Discussion 94
5.2.1 Optimization Studies 94
5.2.2 Scope Exploration 98
5.3 Conclusion **101**

6 Experimental Part **105**
6.1 List of Abbreviations, Acronyms and Symbols **105**
6.2 General Materials and Methods **107**
6.2.1 Synthesis 107
6.2.2 PC12 Assay 108
6.3 Experimental Procedure **109**
6.3.1 Total Synthesis of Gelsemiol 109
6.3.2 Farinosone C Analog Collection 117
6.3.3 Tyrosinol Fatty Acid Analogs Collection 133
6.4 Endocannabinoid System Screen **143**
6.5 Re-Uptake Inhibition Screening **145**
6.6 Surface Coating **146**
6.6.1 Coating Procedure 146
6.6.2 Coating Solutions (CS) 146
6.6.3 Biological Evaluation - General Procedure 147
6.6.4 Restricted Area Coating 147
6.6.5 Recycling Procedure 148
6.6.6 Close Proximity MIE 148
6.6.7 SEM Pictures 148

7 Annexes **153**
7.1 X-Ray Parameters **153**
7.2 NMR Spectra **158**

Parts of this cumulative PhD-Thesis have been or are expected to be published identically or similarly in the following publications and manuscripts:

1) Fabian Schmid, Henning J. Jessen, **Patrick Burch** and Karl Gademann.
"Truncated Militarinone Fragments Identified by Total Chemical Synthesis Induce Neurite Outgrowth"
Med. Chem. Commun. **2013**, *4*, 135-139.

2) **Patrick Burch**, Massimo Binaghi, Manuel Scherer, Corinna Wentzel, David Bossert, Luc Eberhardt, Markus Neuburger, Peter Scheiffele and Karl Gademann.
"Total Synthesis of Gelsemiol"
Chem. Eur. J. **2013**, *19*, 2589-2591. (Chapter 2)

3) Johannes Hoecker, Raphael Liffert, **Patrick Burch**, Robin Wehlauch and Karl Gademann.
"Caged Retinoids as Photoinducible Activators of Neurite Outgrowth"
Org. Biomol. Chem. **2013**, *11,* 3314-3321.

4) Raphael Liffert, Johannes Hoecker, Chandan K. Jana, Tom M. Woods, **Patrick Burch**, Henning J. Jessen, Markus Neuburger and Karl Gademann.
"Withanolide A: Synthesis and Structural Requirements for Neurite Outgrowth"
Chem. Sci. **2013**, *4,* 2851-2857.

5) **Patrick Burch**, Andrea Chicca, Jürg Gertsch and Karl Gademann.
"Discovery of Simplified Neuritogenic Farinosone C Analogs and Investigations on their Mode of Action"
Submitted (Chapter 3 & 4)

6) Elangovan Elamparuthi, Christophe Daeppen, **Patrick Burch**, Simon Glauser, Cedric Hugelshofer and Karl Gademann.
"Structure Activity Relationship and Synthetic Studies on the Cyathin Diterpenoid Cyrneine A"
Manuscript in preparation

7) **Patrick Burch,** Fabian Schmidt and Karl Gademann.
"Neuritogenic Surfaces using Natural Products Analogs"
Submitted (Chapter 5)

Abstract

This thesis is divided into five main chapters which all lay their focus on controlling neuronal cell differentiation using the tools of chemical biology. The individual projects have benefited strongly from cross-pollination of ideas and are all linked in several ways. We hope that our findings could assist the development of therapies for people suffering from neurodegenerative diseases or spinal cord injuries.

Chapter 1 starts with a brief description on the growing impact the diseases we address have on society and introduces different concepts that aim to increase the efficiency of total synthesis and drug discovery.

In **Chapter 2**, the first total synthesis of the neuritotrophic natural product gelsemiol and its biological evaluation is described and discussed.

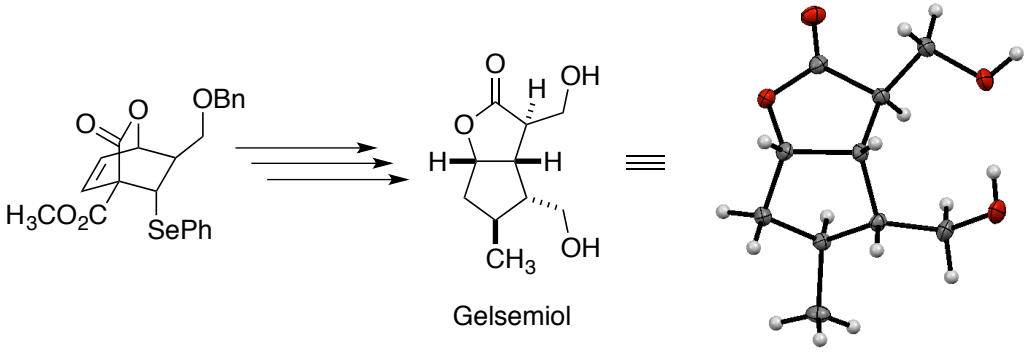

Gelsemiol

After the successful total synthesis of the natural product farinosone C by our group, we aimed to reduce its structural complexity while retaining its unique biological activity. In the present study, farinosone C served as a lead structure and inspired the preparation of small molecules with reduced complexity of which several could induce neurite outgrowth. This in turn allowed the elaboration of a detailed structure-activity relationship and also distinguished the essential from non-essential structural motives, which is discussed in **Chapter 3**.

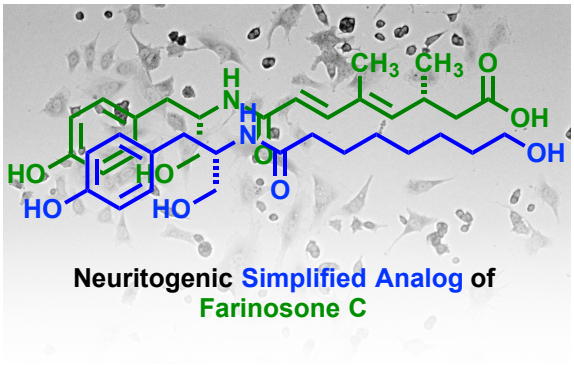

To date, many natural products and their structural analogs with neuritogenic or neuritotrophic properties have been reported. Nevertheless, the underlying biological pathways involved in neuronal cell differentiation, which are influenced by such compounds, are only partially understood. In **Chapter 4**, we attempted to address this issue and present our findings on the mode of action studies.

Chapter 5 describes a facile and modular natural product (NP) analog-based approach to assemble neuritogenic surfaces. The coating procedure involved incubation of glass slides in a solution containing a neurotrophin-like small molecule and an extracellular matrix followed by intense washing and sterilization only. This system has been proven to be very robust and may offer new directions in spinal cord injury treatments.

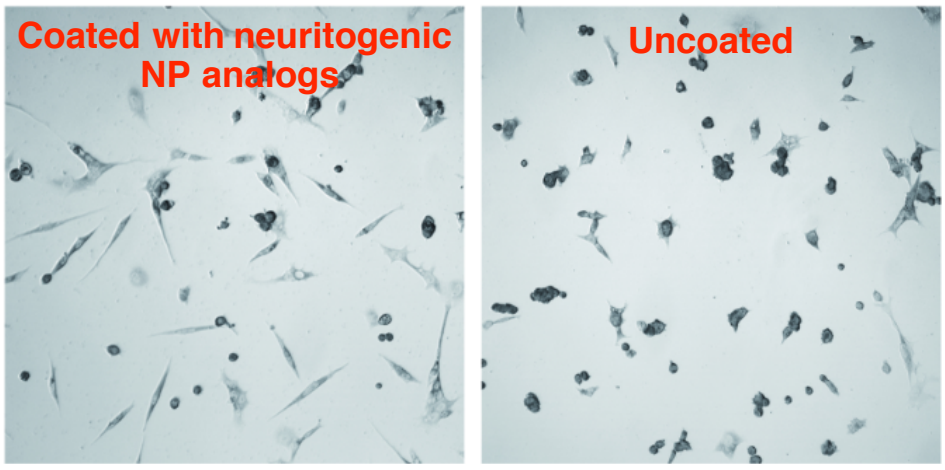

Keywords: • Natural Products • Total Synthesis • Gelsemiol • Neurite Outgrowth • Mode of Action • Spinal Cord Injuries • Neuritogenic Surfaces • Structure Activity Relationship

Kurzbeschreibung

Diese Doktorarbeit gliedert sich in fünf Hauptkapitel, die sich alle damit befassen, wie man die Differenzierung von Nervenzellen kontrollieren kann. Die verschiedenen Projekte haben sich gegenseitig beeinflusst und stark voneinander profitiert. Wir hoffen, mit unseren Ergebnissen die Entwicklung von Therapien für Menschen mit neurodegenerativen Erkrankungen oder Verletzungen des Rückenmarks unterstützen zu können.

Kapitel 1 weist auf die zunehmende Bedeutung von neuronalen Erkrankungen wie Alzheimer in einer immer älter werdenden Gesellschaft hin. Auch werden hier Richtlinien vorgestellt, deren Beachtung die Effizienz einer Synthese oder Wirkstoffentwicklung erhöhen.

In **Kapitel 2** wird die erstmalige enantioselektive Totalsynthese des Naturstoffs Gelsemiol diskutiert. Wir haben eine kurze und effiziente Synthese entwickelt und die Bioaktivität des erhaltenen Naturstoffs evaluiert.

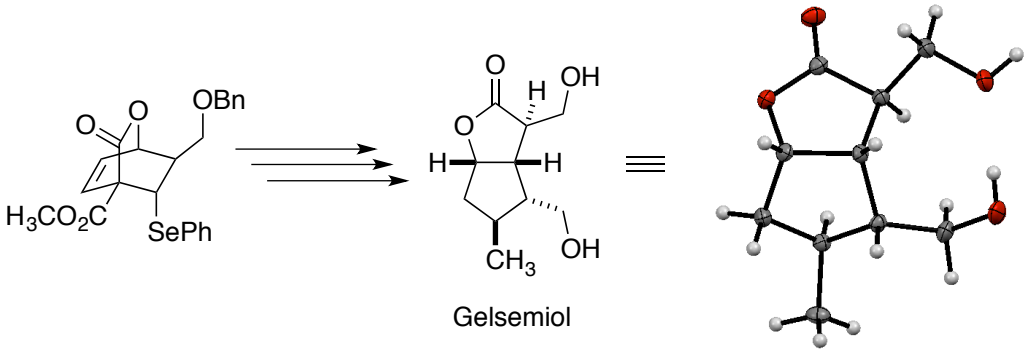

Nachdem der Naturstoff Farinosone C von unserer Gruppe erstmalig in einem Labor hergestellt wurde, haben wir versucht, dessen strukturelle Komplexität, bei gleichbleibender biologischer Aktivität, zu reduzieren. In der im **Kapitel 3** präsentierten Studie diente Farinosone C als Leitstruktur und inspirierte die Herstellung von Molekülen mit reduzierter Komplexität von denen mehrere Neuritenwachstum induzierten. Die Resultate dieser Struktur-Aktivitäts-Beziehung erlaubten uns die wesentlichen, strukturellen Motive von Farinosone C zu identifizieren.

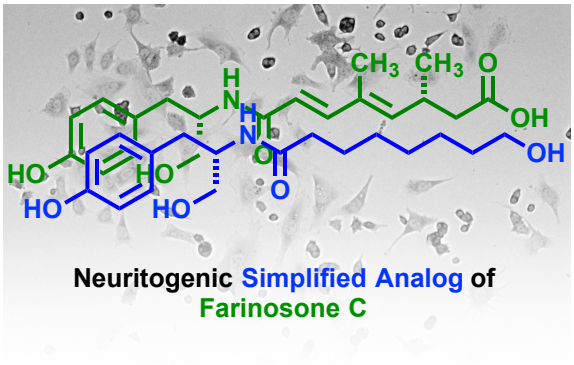

Es sind viele Naturstoffe und deren Derivate bekannt, welche das Neuritenwachstum von verschiedenen Zellen modulieren können. Dennoch sind die zugrunde liegenden biologischen Mechanismen, welche durch solche Verbindungen beeinflusst werden, nur unzureichend begriffen. **Kapitel 4** befasst sich genau mit dieser Frage und präsentiert die Ergebnisse, welche die Untersuchung der Wirkungsweise ergab.

Kapitel 5 beschreibt die Herstellung von neuritogenen Oberflächen unter Verwendung von Naturstoff-Derivaten. Bei diesem Beschichtungverfahren werden Glasplättchen mit Neurotrophin-artigen kleinen Molekülen und einer extrazellulären Matrix inkubiert, gefolgt von intensivem Waschen und Sterilisieren. Diese Methode könnte unserer Meinung nach helfen, neue Wege zur Behandlung von Rückenmarksverletzungen zu beschreiten.

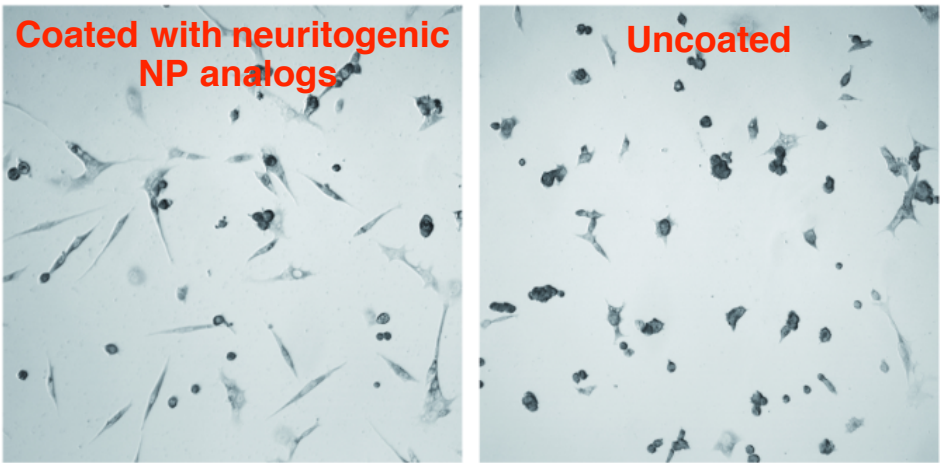

Schlüsselwörter: • Naturprodukte • Totalsynthese • Gelsemiol • Neuritenwachstum • Wirkungsweise • Rückenmarksverletzungen • Neuritogene Oberflächen • Struktur-Aktivitäts-Beziehungen.

CHAPTER 1 -

INTRODUCTION

1

1.1 General Justification

The methods with which physicians treat ill persons have improved tremendously over time and allowed us to live a longer life. The deep-rooted philosophical concept that states that *"There cannot be good without bad"* [1] also comes into play for this matter since in an ageing society, diseases such as neurodegenerative dementias (ND) become increasingly prevalent. Among these sufferings, Alzheimer's disease (AD) is the most prominent one accounting for approximately 60 to 80 % of the diagnosed cases. Other types of ND include Parkinson's or Creutzfeldt-Jakob disease, which gained much public attention in the mid 90's after it was linked to the consumption of beef infected with bovine spongiform encephalopathy (BSE) also known as "mad cow disease". One out of three seniors dies suffering from ND in its different types and stages. AD is currently the 6th leading cause of death and still rising. The very diverse set of symptoms besides memory loss are *e.g.* reduced ability to speak, confusion with time and space, social withdrawal or severe changes in mood and personality. Those in the terminal stages often become bed-bound and cannot precede living without around-the-clock assistance. These symptoms result in tremendous sufferings for patients and their associates. Approved medication only stops, slows down or is reducing the symptoms. To date, there is no therapy available that restores brain function. It is therefore of eminent importance to dedicate recourses and to find ways to overcome this 21st century plague.[2]

While we aim to understand and regulate the formation and restoration of neuronal networks to treat ND we may also find ways to rebuild nerve tracts damaged by spinal cord injuries. Despite of recently made substantial progress in therapy, such as approaches based on electrochemical stimulations[3] or stem cells transplantation,[4] we still are far away from successfully treating chronic paralysis.

---

[1] St. Augustine, T. S. Hibbs, *Enchiridion on Faith, Hope and Love*, Regnery Pub., Washington, D.C, **1996**.
[2] J. Gaugler, B. James, T. Johnson, K. Scholz, W. J, *Alzheimer's & Dementia* **2013**, *9*, 208–245.
[3] R. van den Brand, J. Heutschi, Q. Barraud, J. DiGiovanna, K. Bartholdi, M. Huerlimann, L. Friedli, I. Vollenweider, E. M. Moraud, S. Duis, *et al*., *Science* **2012**, *336*, 1182–1185.

1.2 Efficiency of Natural Products Synthesis

In traditional medicine, plant extracts were applied to cure the most diverse illnesses.[5] The bioactivity of these extracts is typically owed to the present natural products (NP).[6] Since nature was given the appropriate time to optimize these NP in an evolutionary fashion, they can exhibit enormous potencies and still represent a major source of inspiration for modern drug discovery. In fact, approximately half of the available drugs currently on the market contain NP motifs.[7] A fair amount of characterized NP, which can induce desirable biological responses, possess a challenging molecular architecture. Figure 1.1 shows four well-known and very complex NP, which have been synthesized.[8]

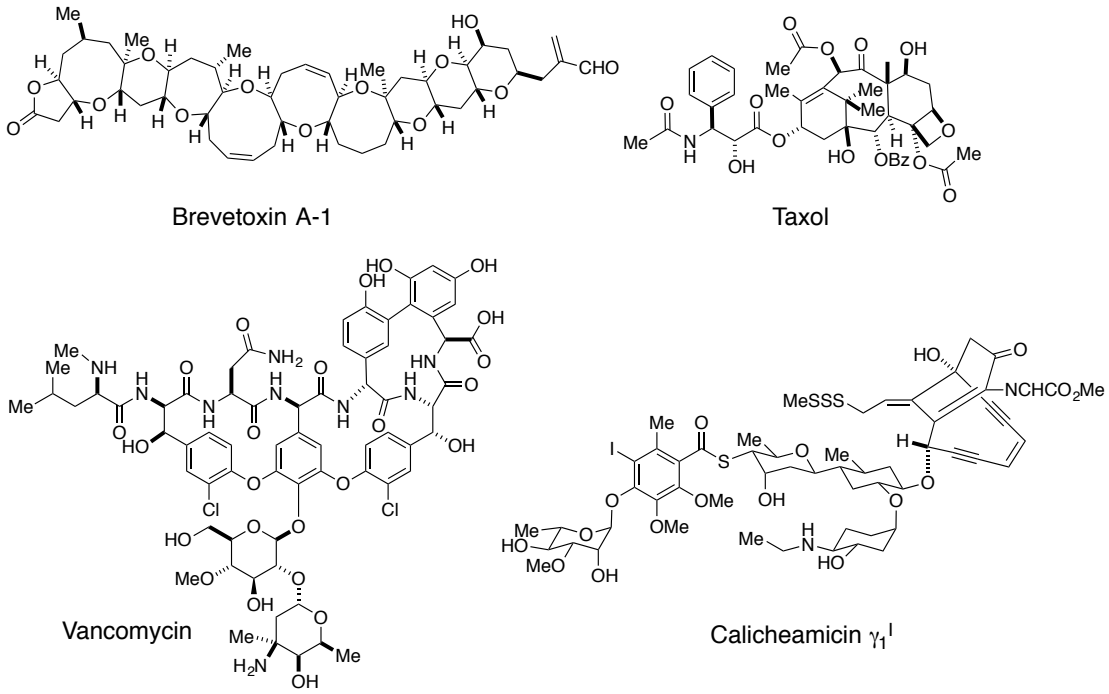

Fig. 1.1. Natural products obtained in synthetic form.

[5] D. S. Fabricant, D. S. Farnsworth, *Environmental Health Perspectives* **2001**, *109*, 69–75.
[6] J. W. Blunt, B. R. Copp, M. Munro, P. T. Northcote, *Nat. Prod. Rep.* **2011**, 196–268.
[7] a) I. Paterson, *Science* **2005**, *310*, 451–453. b) S. Danishefsky, *Nat. Prod. Rep.* **2010**, *27*, 1114-1116. c) D. J. Newman, G. M. Cragg, K. M. Snader, *J. Nat. Prod.* **2003**, *66*, 1022–1037.
[8] K. C. Nicolaou, C. R. H. Hale, C. Nilewski, *Chem. Record.* **2012**, *12*, 407–441.

As one can image, obtaining these NP was neither trivial, quick nor could large amounts of the final natural product be produced.[9] Nevertheless, these remarkable accomplishments illustrate how far organic chemistry has evolved over the last couple of decades. When such total synthesis programs are staged, it is crucial to design a synthetic route that is as efficient as possible. *Hendrickson* defined the ideal or most efficient synthesis as "*The ideal synthesis creates a complex skeleton [...] in a sequence only of successive construction reactions involving no intermediary refunctionalizations, and leading directly to the structure of the target, not only its skeleton but also its correctly placed functionality."*[10] In order to make this general concept more applicable and more specific, guidelines needed to be defined. *Trost* introduced the concept of atom economy, which states that reactions used in a synthesis have to be selective and economical in atom count, meaning that the number of atoms of reactants appearing in the product has to be maximised.[11] The two Nobel Prize laureates *Otto Diels* and *Kurt Alder* introduced the model type reaction that meets these requirements. Diels-Alder reactions are selective and all atoms from the starting material are also present in the product.[12] For the large-scale chemical production atom economy is similar to the E factor (waste per kg product) and of extreme importance to fulfil environmental criteria and be profitable. It also seems obvious that a good synthetic route always should involve as less synthetic transformations as possible. This so-called step economy can be increased by the development of new synthetic strategies and methodology that allows for shorter routes to a target structure.[13]

Baran and *Hoffmann* introduced in 2009 their concept of redox economy. The idea of this concept is to minimise non-strategic redox manipulations in order to achieve an isohypsic synthesis, which consequently leads to a step economic synthesis (Fig. 1.2).[14]

---

[9] K. C. Nicolaou, C. R. H. Hale, C. Nilewski, *Chem. Record*. **2012**, *12*, 407–441.
[10] J. B. Hendrickson, *J. Am. Chem. Soc*. **1975**, *97*, 5784–5800.
[11] a) B. M. Trost, *Angew. Chem. Int. Ed*. **1995**, *34*, 259–281. b) B. M. Trost, *Science* **1991**, *254*, 1471–1477.
[12] O. Diels, K. Alder, *Justus Liebigs Ann. Chem*. **1928**, *460*, 98-122.
[13] a) T. Newhouse, P. S. Baran, R. W. Hoffmann, *Chem. Soc. Rev*. **2009**, *38*, 3010–3021 b) P. A. Wender, V. A. Verma, T. J. Paxton, T. H. Pillow, *Acc. Chem. Res*. **2008**, *41*, 40–49.
[14] N. Z. Burns, P. S. Baran, R. W. Hoffmann, *Angew. Chem. Int. Ed*. **2009**, *48*, 2854–2867.

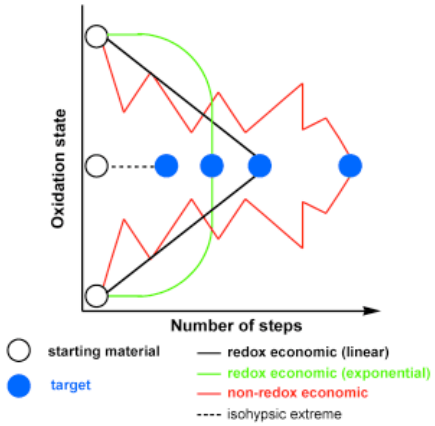

Figure 1.2. Schematic Redox Economy. Reprinted with permission from Ref.: 14, Copyright (2009) Wiley.

These atom-, step- and redox efficiency concepts or guidelines can help chemists to better judge the quality of their synthetic scheme. However, in cases where there is not a precisely defined molecule as the target, but rather a desired biological function, an additional concept can come into play developed by *Wender*: function orientated synthesis (FOS). The concept is based on the reduction of molecular complexity by retained function (bioactivity) resulting in increased step economy (Fig **1.3**).[15]

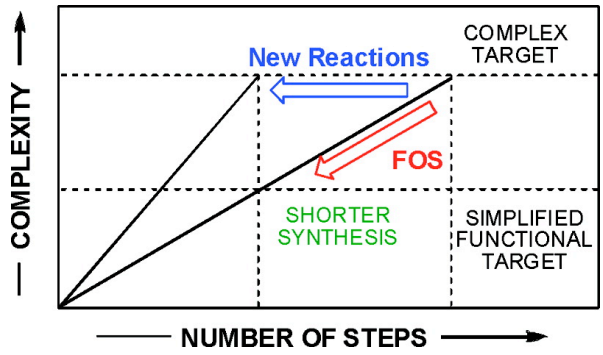

Figure 1.3. Function Orientated Synthesis. Reprinted with permission from Ref.: 15 Copyright (2008) ACS.

FOS concept has been applied to several therapeutically important natural product leads and is gaining importance.[16] Often simplified structures can mimic or even exceed the function of those from which they are inspired but can be supplied

[15] a) P. A. Wender, V. A. Verma, T. J. Paxton, T. H. Pillow, *Acc. Chem. Res.* **2008**, *41*, 40–49.
[16] S. L. Schreiber, *Science* **2000**, *287*, 1964–1969.

easier.[17] For instance, the sesquiterpen artemisin (**1.1**) a widely used antimalarial, FOS allowed medicinal chemists to generate its NP analog **1.2** with improved activity and step economy as shown in scheme **1.1**.[18] Dynemicin (**1.3**) can act as an antitumor agent by generating a diradical species through a Bergman cyclization[19] that can cleave DNA. The simplified derivative **1.4** is an effective functional mimic of the NP **1.3** and kills tumour cells through the identical mode of action.[20] Another anti-tumour agent that gained strong interest is bryostatin 1 (**1.5**). This NP **1.5** represents an enormous synthetic challenge and requires over 70 synthetic steps to obtain. *Wender* and co-workers were able to dramatically reduce the step count by FOS approach. Not only did they reduce the number of steps by more than half, the resulting bryostatin 1 analog **1.6** was also more potent than the parental NP **1.5**.[21]

[17] P. A. Wender, V. A. Verma, T. J. Paxton, T. H. Pillow, *Acc. Chem. Res.* **2008**, *41*, 40–49.
[18] a) C. Zhu, S. P. Cook, *J. Am. Chem. Soc.* **2012**, *134*, 13577-13579. b) G. H. Posner, P. M. O'Neill, *Acc. Chem. Res.* **2004**, *6*, 397-404. c) G. H. Posner, J. N. Cumming, S.-H. Woo, P. Ploypradith, S. Xie, T. A. Shapiro, *J. Med. Chem.* **1998**, *41*, 940–951.
[19] R. R. Jones, R. G. Bergman, *J. Am. Chem. Soc.* **1972**, *6*, 660-661.
[20] a) M. D. Shair, T. Y. Yoon, K. K. Mosny, T. C. Chou, S. J. Danishefsky, *J. Am. Chem. Soc.* **1996**, *118*, 9509–9525. b) P. A. Wender, C. K. Zercher, *J. Am. Chem. Soc.* **1991**, *131*, 2311-2313.
[21] a) P. A. Wender, V. A. Verma, T. J. Paxton, T. H. Pillow, *Acc. Chem. Res.* **2008**, *41*, 40–49. b) I. Paterson, *Science* **2005**, *310*, 451–453.

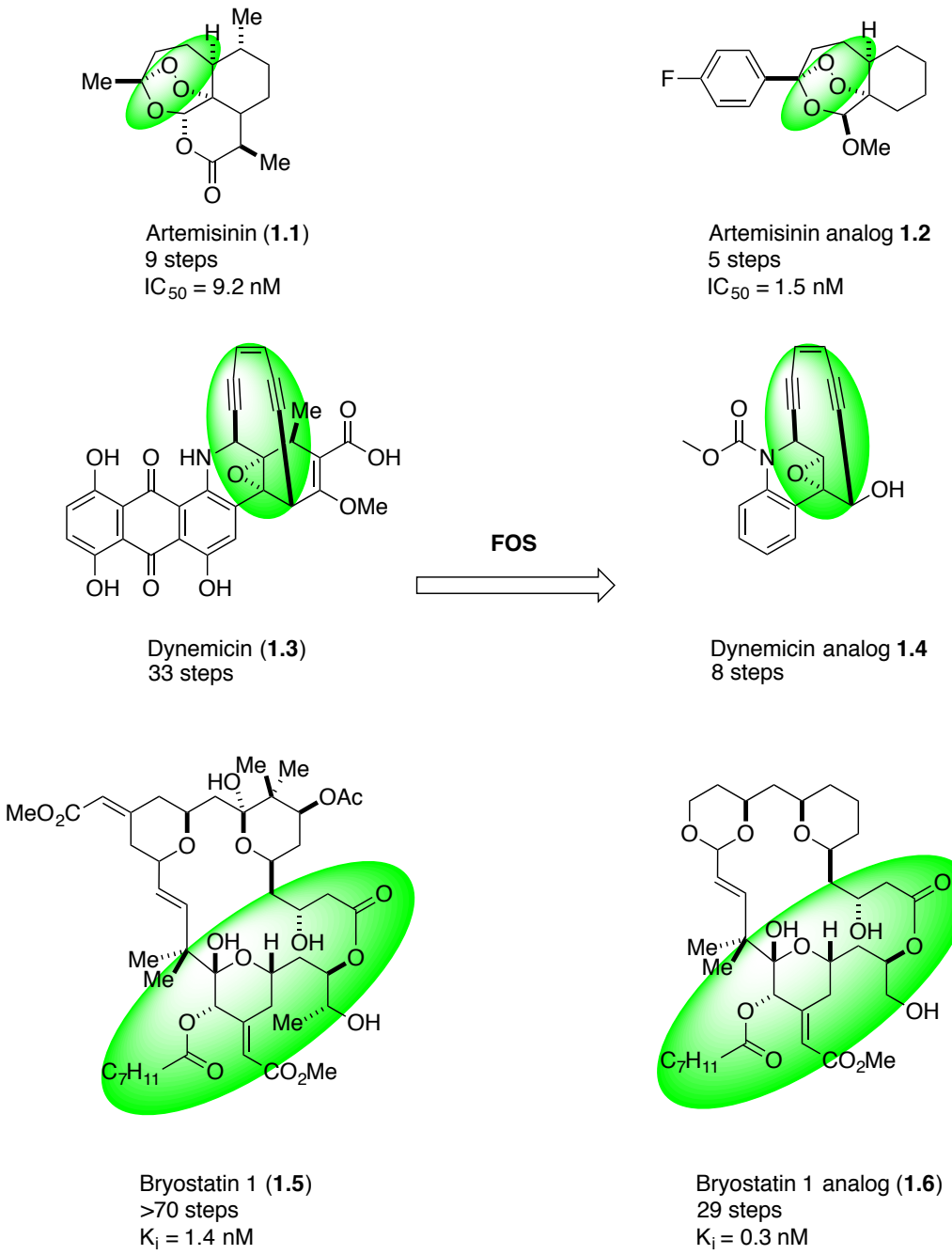

Scheme 1.1. Natural products simplified applying FOS

Another approach is to truncate certain parts of the target molecule.[22] A prominent example of this approach is the removal of the polycyclic side chain of halichondrin B (**1.7**) by *Kishi* and co-workers, where the shortened analog E 7389

[22] a) F. Schmid, H. J. Jessen, P. Burch, K. Gademann, *MedChemComm* **2013**, *4*, 135–139. b) J.-Y. Wach, K. Gademann, *Synlett* **2011**, *2012*, 163–170.

(**1.8**) has successfully reached the market to treat metastatic breast cancer (Scheme 1.2).[23]

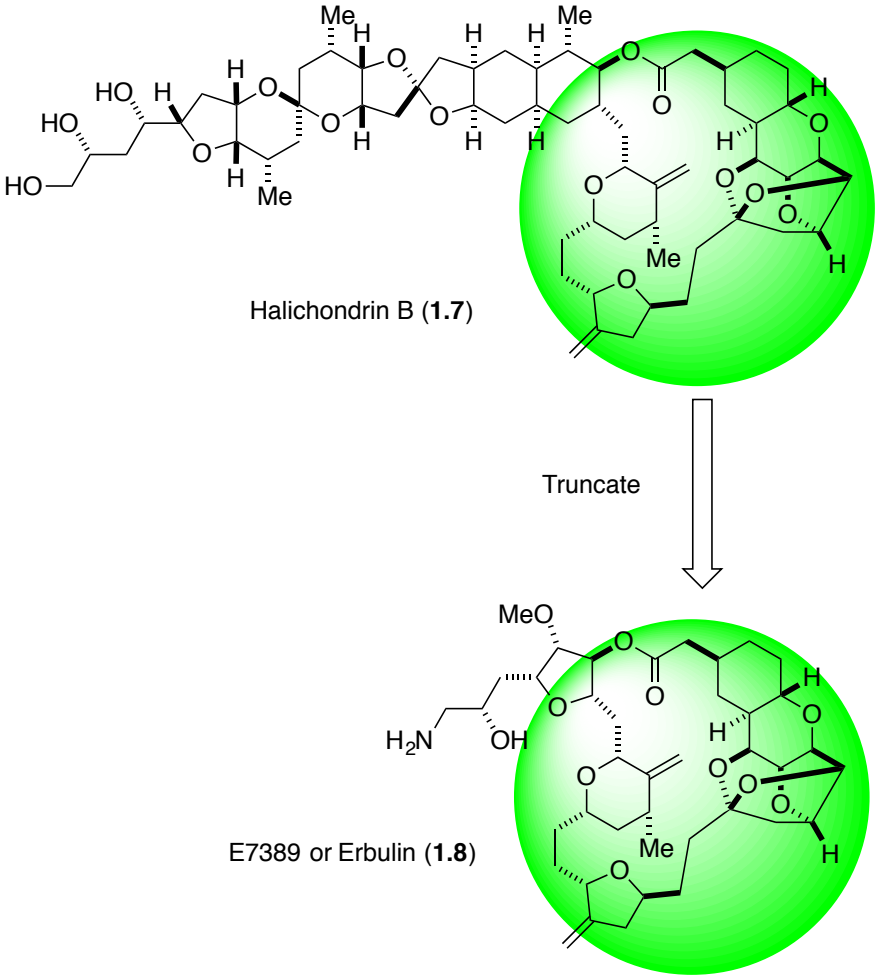

Scheme 1.2. Truncation of halichondrin B (**1.7**).

[23] a) D. P. Stamos, S. S. Chen, Y. Kishi, *J. Org. Chem.* **1997**, 7552–7553. b) M. J. Towle, K. A. Salvato, J. Budrow, B. F. Wels, G. Kuznetsov, K. K. Aalfs, S. Welsh, W. Zheng, B. M. Seletsky, M. H. Palme, *et al.*, *Cancer Res.* **2001**, *61*, 1013–102. c) T. D. Aicher, K. R. Buszek, F. G. Fang, C. J. Forsyth, S. H. Jung, Y. Kishi, M. C. Matelich, P. M. Scola, D. M. Spero, S. K. Yoon, *J. Am. Chem. Soc.* **1992**, *114*, 3162–3164.

2

CHAPTER 2 - TOTAL SYNTHESIS AND BIOLOGICAL EVALUATION OF GELSEMIOL

Parts of this chapter are published similarly or identically.[24]

2.1 Introduction

2.1.1 Isolation and Neuritotrophic Activity

Gelsemiol (**2.1**) was first isolated from *Gelsemium semprevirens* (Gentianales) and characterized in 1987 by *Jensen* and co-workers.[25] Seven years later **2.1** was also found in the leaves of *Gelsemium elegans* (Gentianales).[26] A subsequent publication by *Ohizumi* and co-workers reported the isolation of **2.1** from *Verbena littoralis* (Lamiales) and demonstrated its neuritotrophic properties in the PC12D cell-line in the presence of nerve growth factor (NGF).[27] Moreover, these plants which produce **2.1** can be found on different continents and their use in traditional medicine to treat *e.g.* diarrhea, typhoid fever or migraine is reported.[28] These findings made gelsemiol (**2.1**) an ideal candidate for our program on the synthesis and biological evaluation of neuritogenic natural products, which is described in this chapter.

2.1.2 Iridoids

A large number of plant families and some insects rely on iridoids as secondary metabolites, of which to date over 1000 have been isolated and characterized.[29] The first isolation dates back to 1835 and is credited to *Geiger*.[30] The name however originates from *Cavill* and co-workers who characterized the 1,3-dialdehyde iridodial (**2.2**, Scheme 2.1) and named it after the Australian ants

---

[24] a) P. Burch, M. Binaghi, M. Scherer, C. Wentzel, D. Bossert, L. Eberhardt, M. Neuburger, P. Scheiffele, K. Gademann, *Chem. Eur. J.* **2013**, *19*, 2589–2591. b) M. Scherer, Master Thesis, **2012**. c) D. Bossert, Master Thesis, **2012**.
[25] S. R. Jensen, O. Kirk, B. J. Nielsen, R. Norrestam, *Phytochem.* **1987**, *6*, 1725–1731.
[26] H. Takayama, Y. Morohoshi, M. Kitajima, N. Aimi, S. Wongseripipatana, D. Ponglux, S.-I. Sakai, *Nat. Prod. Lett.* **1994**, *5*, 15–20.
[27] a) Y. S. Li, K. Matsunaga, R. Kato, Y. Ohizumi, *J. Pharmacy. Pharmacol.* **2001**, *53*, 915–919. b) Y. S. Li, M. Ishibashi, M. Satake, Y. Oshima, Y. Ohizumi, *Chem. Pharm. Bull.* **2003**, *51*, 1103–1105 b) Y. Li, Y. Ohizumi, *Yakugaku Zasshi* **2004**, *124*, 417–424.
[28] a) Y.-S. Li, K. Matsunaga, M. Ishibashi, Y. Ohizumi, *J. Org. Chem.* **2001**, *66*, 2165–2167 b) F. Sun, Q. Y. Xing, X. T. Liang, *J. Nat. Prod.* **1989**, *52*, 1180–1182.
[29] A. Oudin, M. Courtois, M. Rideau, M. Clastre, *Phytochem. Rev.* **2007**, *6*, 259–276.
[30] P. L. Geiger, *Ann.* **1835**, *14*, 206.

(*Iridomyrmex detectus*) from which it was isolated.[31] The hemiacetal form of iridodial (**2.2**) characterized by a methylcyclopentan[c]pyran backbone which is formed out of ten carbon atoms represents the common structural motif for the vast majority of iridoids.[32] These compound possess a wide range of interesting pharmacological properties such as anti-inflammatory, anti-fungal, anti-bacterial or immunomodulatory activities.[33]

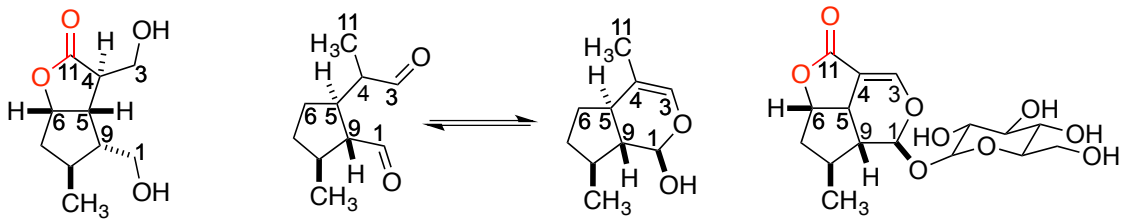

Scheme 2.1. Gelsemiol (**2.1**), iridodial (**2.2**) and (–)-brasoside (**2.3**).

Gelsemiol (**2.1**) also belongs to the iridoid family, as one might see on the second glance. If iridodial (**2.2**, Scheme **2.1**) is oxidized at the C(6) and C(11) position followed by lactonization and both aldehydes are reduced, gelsemiol (**2.1**) could be obtained.[34] In all plant extracts where **2.1** has been isolated to date, the iridolactone (–)-brasoside (**2.3**) was also found.[35] We therefore speculated that these compounds originate from an overlapping biosynthetic pathway. The iridoid biosynthesis is well investigated.[36] Starting from pyruvate and glyceraldehyde-3-phosphate, 7-deoxyloganic acid (**2.4**) is formed in over a dozen enzymatic steps.

---

[31] G. Cavill, D. L. Ford, H. D. Locksley, *Aust. J. Chem.* **1956**, *9*, 288–293.
[32] PhD Thesis of I. K. Mangion, *Development of Organocatalytic Direct Aldol Transformations, Total Syntheses of Brasoside and Littoralisone, and Progress Toward the Total Synthesis of Diazonamide A*, Cal. Tech., **2006**.
[33] B. Dinda, S. Debnath, R. Banik, *Chem. Pharm. Bull.* **2011**, *59*, 803–833.
[34] a) H. Takayama, Y. Morohoshi, M. Kitajima, N. Aimi, S. Wongseripipatana, D. Ponglux, S.-I. Sakai, *Nat. Prod. Lett.* **1994**, *5*, 15–20 b) P. Burch, M. Binaghi, M. Scherer, C. Wentzel, D. Bossert, L. Eberhardt, M. Neuburger, P. Scheiffele, K. Gademann, *Chem. Eur. J.* **2013**, *19*, 2589–2591.
[35] a) S. R. Jensen, O. Kirk, B. J. Nielsen, R. Norrestam, *Phytochem.* **1987**, *6*, 1725–1731. b) H. Takahashi, Y. Haga, T. Shibata, K. Nonoshita, T. Sakamoto, M. Moriya, T. Ohe, M. Chiba, Y. Mitobe, H. Kitazawa, *et al. Bioorg. Med. Chem. Lett.* **2009**, *19*, 5436–5439 c)Y. S. Li, M. Ishibashi, M. Satake, Y. Oshima, Y. Ohizumi, *Chem. Pharm. Bull.* **2003**, *51*, 1103–1105.
[36] a) R. van der Heijden, A. Lefeber, R. Verpoorte, *FEBS Lett.* **1998**, *343*, 313-316. b) A. Oudin, M. Courtois, M. Rideau, M. Clastre, *Phytochem. Rev.* **2007**, *6*, 259–276.

Intermediate **2.4** could then undergo selective oxidation at the C(6) position yielding the alcohol **2.5**, which is also present in *Gelsemium sempervirens*.[37] Such oxidations are known for similar substrates.[38] Intermolecular lactonization would then lead to the tricyclic (–)-brasoside **2.3**. Following the previously mentioned keto-hemiactetal tautomerism, the dialdehyde **2.7** could be formed after deglycosylation of **2.3**. The final step would involve the reduction of both aldehydes to obtain gelsemiol (**2.1**).

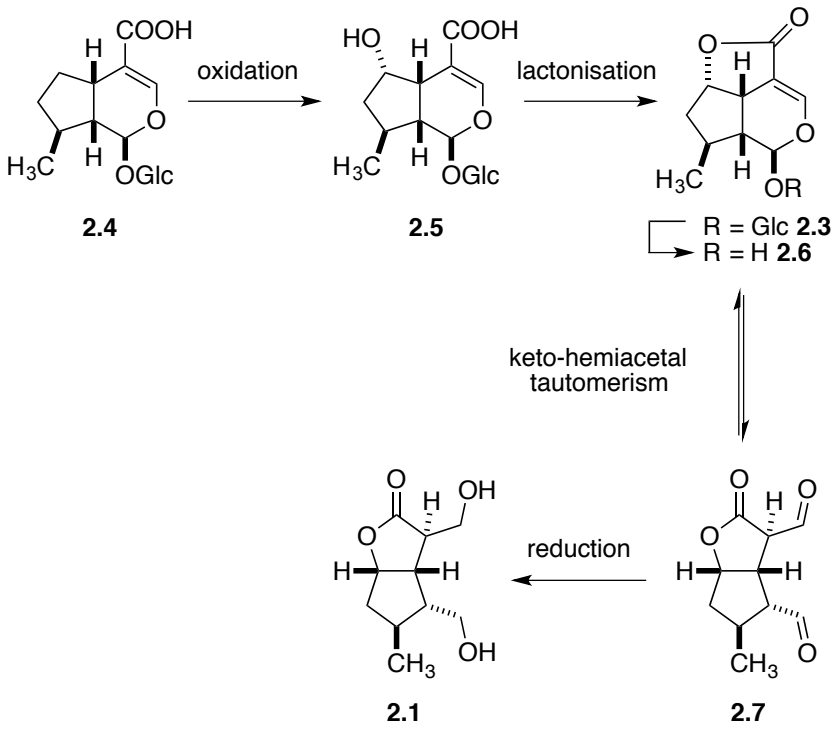

Scheme 2.2. Proposed biosynthetic pathway of gelsemiol (**2.1**)

[37] a) Y.-S. Li, K. Matsunaga, M. Ishibashi, Y. Ohizumi, *J. Org. Chem.* **2001**, *66*, 2165–2167. b) F. Sun, Q. Y. Xing, X. T. Liang, *J. Nat. Prod.* **1989**, *52*, 1180–1182.
[38] a) A. Oudin, M. Courtois, M. Rideau, M. Clastre, *Phytochem. Rev.* **2007**, *6*, 259–276. b) N. Rønsted, E. Göbel, H. Franzyk, S. R. Jensen, C. E. Olsen, *Phytochem.* **2000**, *55*, 337–348.

2.1.3 Gelsemiol as an Advanced Intermediate

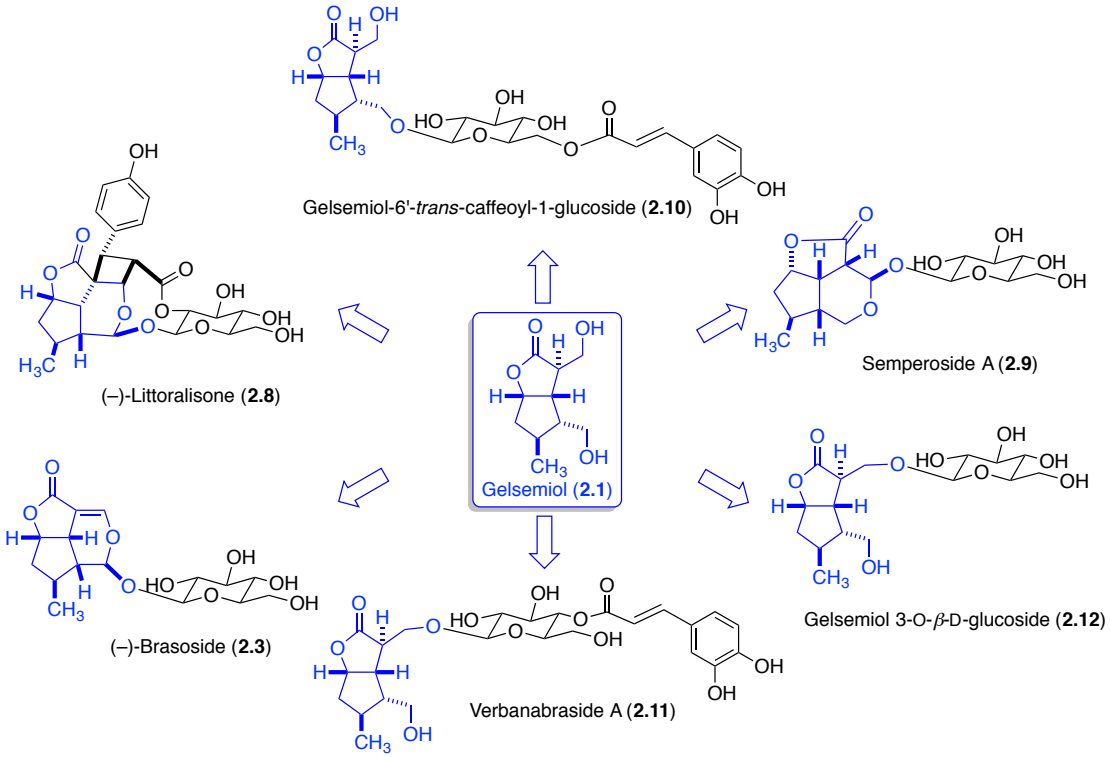

Scheme 2.3. Natural products that could be derived from gelsemiol **2.1**

Out of these six natural products (NP) shown in scheme **2.3**, three of them have been synthesized to date. An elegant biomimetic route to access (–)-littoralisone (**2.8**) and (–)-brasoside (**2.3**) has been established by *MacMillan* and *Mangion*.[39] *Zanoni et al*., synthesized semperoside A (**2.9**), which has also been isolated from *Gelsemium sempervirens*.[40] The glycosylated congeners of gelsemiol **2.10**, **2.11** and **2.12** have not yet been synthetically produced and none of these six NP has been investigated regarding their neuritogenic properties. We envisioned that gelsemiol (**2.1**) could be an excellent advanced intermediate to access such interesting compounds. For **2.10**, **2.11** and **2.12** an elaborate protecting group strategy should allow their production. If one could oxidize **2.1** to the dialdehyde **2.7**, hemiacetal formation could lead to tricycle **2.13a**. The acetylated derivative **2.13b** was used by *MacMillan* to synthesize (–)-littoralisone (**2.8**) and (–)-brasoside (**2.3**) in two

[39] a) P. L. Geiger, *Ann*. **1835**, *14*, 206. b) I. K. Mangion, D. MacMillan, *J. Am. Chem. Soc*. **2005**, *127*, 3696–3697.
[40] a) G. Cavill, D. L. Ford, H. D. Locksley, *Aust. J. Chem*. **1956**, *9*, 288–293. b) P. Piccinini, G. Vidari, G. Zanoni, *J. Am. Chem. Soc*. **2004**, *126*, 5088–5089 c) S. R. Jensen, O. Kirk, B. J. Nielsen, R. Norrestam, *Phytochem*. **1987**, *6*, 1725–1731.

additional steps each (Scheme 2.4).[44] With the dialdehyde **2.7** in hand, a selective reduction at the C(1) position would allow the formation of the hemiacetal starting form the opposite side than in the case of **2.13**. After glycosylation, semperoside A (**2.9**) should be available for biological evaluation.

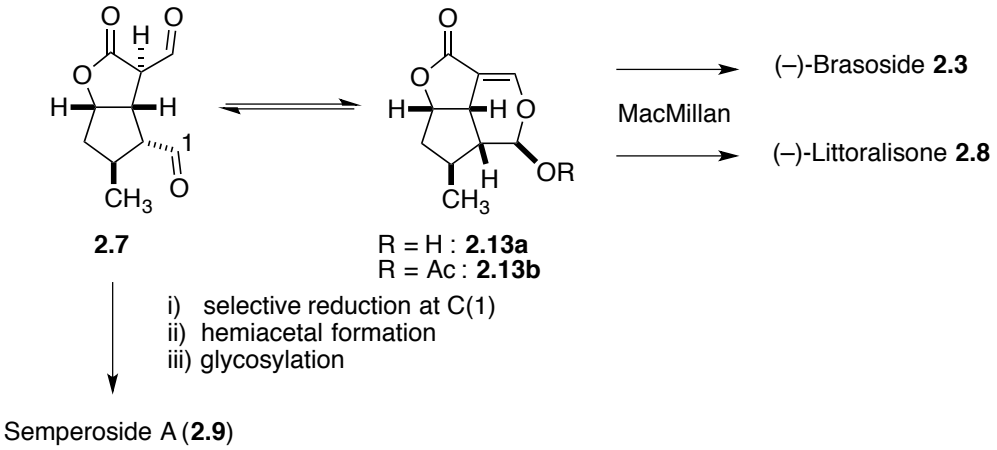

Scheme 2.4 Synthetic strategy towards semperoside A (**2.9**), (–)-brasoside (**2.3**) and (–)-littoralisone (**2.8**) starting form dialdehyde **2.7**.

2.1.4 Previous Synthetic Contributions

In 1981 *Grieco* reported the total synthesis of (+)-iridomyrmecin (**1.14**) starting from the bicyclo[2.2.1]heptane derivative **2.15**, which can be accessed in seven steps. The key step involved a Baeyer-Villiger oxidation using H_2O_2 and subsequent treatment of the resulting carbonyl acid with BF_3 to yield bicyclic compound **2.16**. The lactone **2.16** was then methylated twice. First, *via* enolate formation using LDA followed by a cuprate mediated anti-S_N2' alkylation. Deprotection with Raney-Nickel then initiated the lactonization and furnished (+)-iridomyrmecin (**2.14**, Scheme 2.5).[41] Later in 1997, *Gibbs* also reported the total synthesis of (+)-iridomyrmecin (**2.14**) using a partly different approach. The key intermediate **2.17** was synthesized in five steps. Iodolactonization followed by HI

[41] a) PhD Thesis of I. K. Mangion, *Development of Organocatalytic Direct Aldol Transformations, Total Syntheses of Brasoside and Littoralisone, and Progress Toward the Total Synthesis of Diazonamide A*, Cal. Tech., **2006**. b) P. A. Grieco, C. V. Srinivasan, *J. Org. Chem.* **1981**, *46*, 2591–2593.

elimination using DBU yielded compound **2.16** in 86% over two steps. Three additional steps similar to *Grieco's* approach then led to (+)-iridomyrmecin (**2.14**).[42]

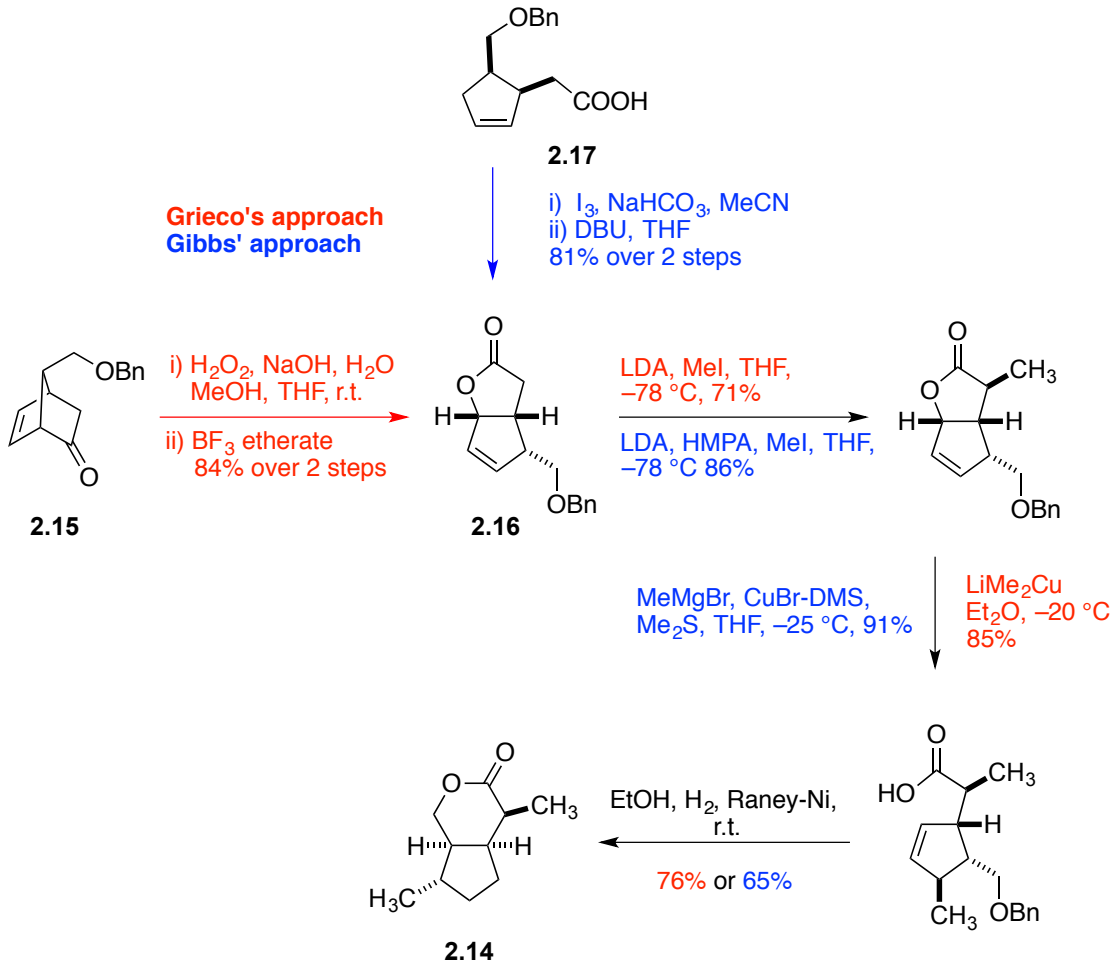

Scheme 2.5. Total synthesis of (+)-iridomyrmecin (**2.14**) by *Grieco* and *Gibbs*.

As previously mentioned, *Zanoni* reported the total synthesis of semperoside A (**2.9**) in 2004. In his strategy he employed synthetic knowledge, which he and his group had acquired earlier.[43] A Baeyer-Villiger oxidation turned the Weiss diketone **2.18** into the lactone **2.19,** which upon a reduction-elimination sequence yielded the regioisomers **2.20a/b** as an equimolar mixture. The *Zanoni* group found two different ways to convert this mixture into lactone **2.21**. Both approaches started with the saponification of the **2.20a/b** mixture, which was then either followed by lipase

[42] a) D. M. Hodgson, A. R. Gibbs, *Synlett* **1997**, *6*, 657–658. b) D. M. Hodgson, A. R. Gibbs, M. G. B. Drew, *J. Chem. Soc., Perkin Trans. 1* **1999**, 3579–3590.
[43] a) P. Piccinini, G. Vidari, G. Zanoni, *J. Am. Chem. Soc.* **2004**, *126*, 5088–5089. b) G. Zanoni, A. Porta, A. Meriggi, M. Franzini, G. Vidari, *J. Org. Chem.* **2002**, *67*, 6064–6069.

catalysed kinetic resolution in vinyl acetate/Et_3N (5:1) as solvent system[44] or by a sequence that is more suitable for scale up. For this approach a catalytic combination of Pd(II)- and $Cu(II)(OAc)_2$ was applied. With this new type of Pd(II)-mediated lactonization **2.21** was obtained on gram scale. After acetylation, the Curran reaction was used for diastereoselective methylation and yielded the six-membered lactone **2.22**. Saponification followed by KI_3 promoted iodolactonization gave the lactone **2.23** in excellent yield. Raney-Nickel mediated hydrodeiodination followed by protection of the hydroxyl group and formylation yielded the SEM ether **2.24**. Seven additional steps, including a mercury mediated 6-*endo*-trig cyclisation then led to semperoside A (**2.9**, Scheme 2.6).[45]

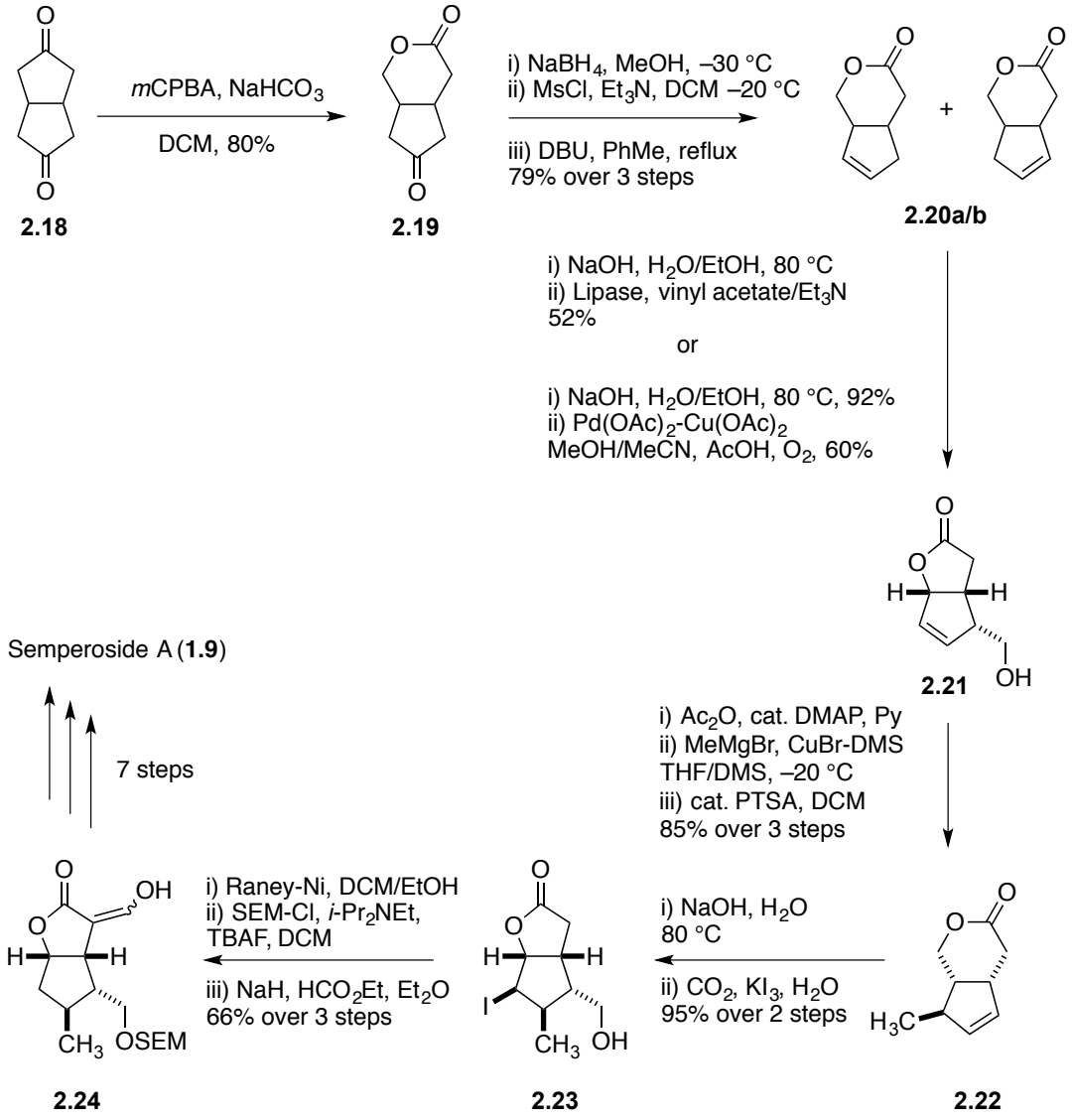

Scheme 2.6 Total synthesis of semperoside A (**1.9**) by *Zanoni*.

[44] G. Zanoni, F. Agnelli, A. Meriggi, G. Vidari, *Tetrahedron Asym*. **2001**, 1779-1784.
[45] P. Piccinini, G. Vidari, G. Zanoni, *J. Am. Chem. Soc*. **2004**, *126*, 5088–5089.

In 2004, *Robertson* described their attempt towards the total synthesis of (–)-brasioside (**2.3**).[46] Even though their approach to cyclised compound **2.25** was unsuccessful, they discovered an efficient route for the synthesis of the bicyclic carbon backbone of gelsemiol-like iridoids in only three steps. First, cyclopent-2-enone (**2.26**) was subjected to Luche reduction followed by esterification to furnish compound **2.27**. Now the stage was set for a one pot radical reaction/olefination sequence initiated by dilauroyl peroxide (DLP, CH_3-$(CH_2)_{10}$-$COO)_2$) to give rise to **2.28**. After ozonolysis and ketal-protection, the α-position of the carbonyl group could then be modified.[46]

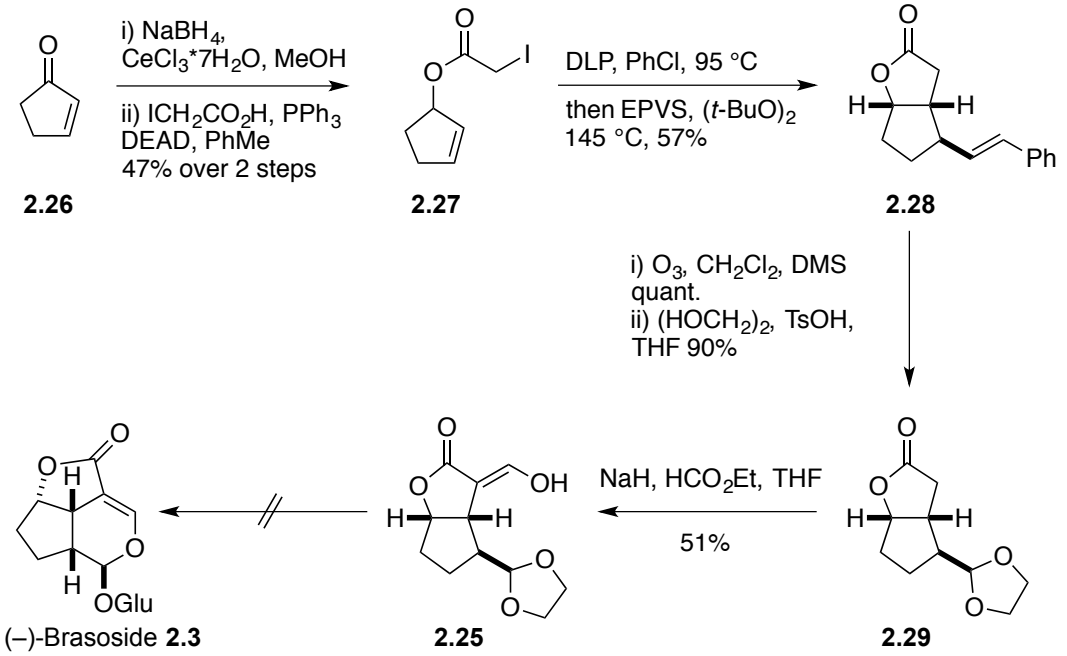

Scheme 2.7. Efforts towards the synthesis of (–)-brasioside (**2.3**) by *Robertson*.

Our attention was also caught by the work of *Markó* and co-workers. An enantioselective copper-mediated inverse electron demanding Diels-Alder reaction (IEDDA) sets the stage for a radical cascade/skeletal rearrangement leading to the oxabicyclo[3.3.0]octanone skeleton (Scheme 2.8). Depending on the ligand and metal of choice, both isomers could be obtained in high yields, practical selectivity and only two steps.[47]

[46] J. Robertson, M. Menard, R. Ford, *Synlett* **2004**, *15*, 2788–2790.
[47] a) I. E. Markó, S. L. Warriner, B. Augustyns, *Org. Lett.* **2000**, *2*, 3123–3125. b) B. Augustyns, N. Maulide, I. E. Markó, *Tetrahedron Lett.* **2005**, *46*, 3895–3899.

Efforts towards the structurally similar Corey *endo*-lactone (Scheme 2.8) used in the synthesis of prostaglandins are not discussed as the stereochemistry at C(9) position is inverted.[48]

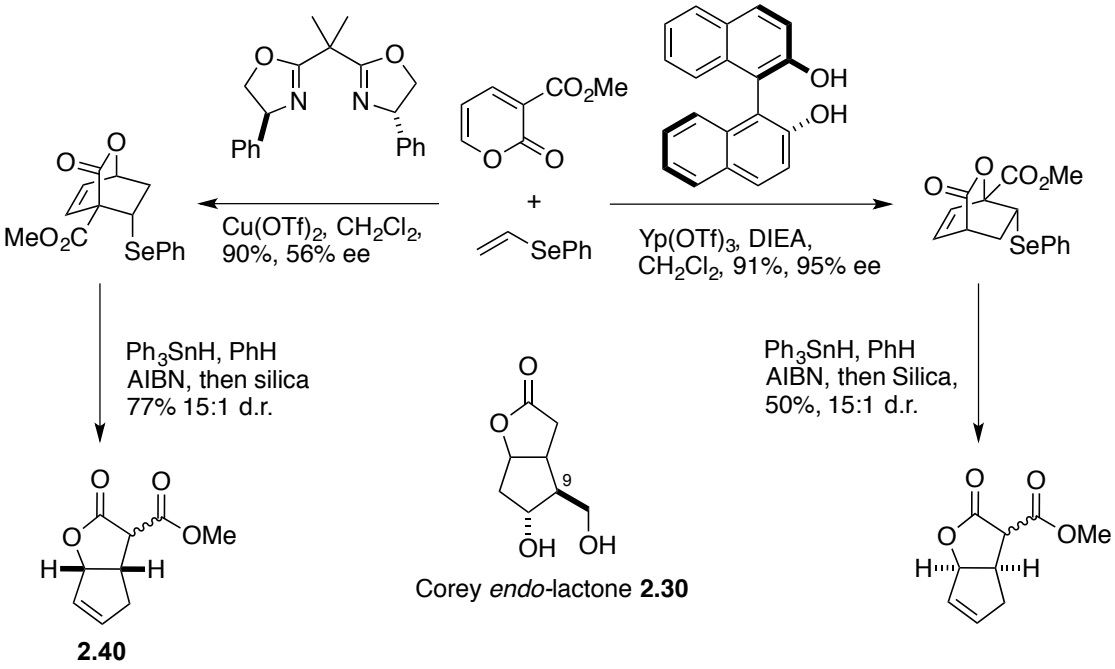

Scheme 2.8. Selective IEDDA and the Corey *endo*-lactone (**2.30**).

Recently, *Waldmann* reported an interesting conceptional approach that led to the discovery of two novel NP-inspired neuritogenic compound classes. Different sesquiterpenoids and iridoids, including gelsemiol (**2.1**) and (–)-littoralisone (**2.2**) were analysed and the pentaleone **2.31** and iridoid-inspired scaffold **2.32** were defined as lead structures. **2.31** can be derived form a [3+2]-cycloaddition employing a chiral phosphine catalyst. These pentalenones **2.31** could then be further converted into the cyclopental[*c*]pyranone scaffold **2.32** by regioselective Baeyer-Villiger oxidation. With this methodology, they were able to build up a library with over 35 compounds and found several neurite outgrowth-promoting small molecules (**2.33-2.37**). These results proved their rational design approach to be valid and therefore presenting an antetype example how NP synthesis and function oriented drug discovery are able to

c) J.-H. Liao, N. Maulide, B. Augustyns, I. E. Markó, *Org. Biomol. Chem.* **2006**, *4*, 1464–1467 d) I. E. Markó, I. Chellé-Regnaut, B. Leroy, S. L. Warriner, *Tetrahedron Lett.* **1997**, *97*, 4269-4271.

[48] a) G. Zanoni, A. Porta, A. Meriggi, M. Franzini, G. Vidari, *J. Org. Chem.* **2002**, *67*, 6064–6069. b) E. J. Corey, N. M. Weinshenker, T. K. Schaaf, W. Huber, *J. Am. Chem. Soc.* **1969**, *91*, 5675–5677.

interlock frictionless.[49]

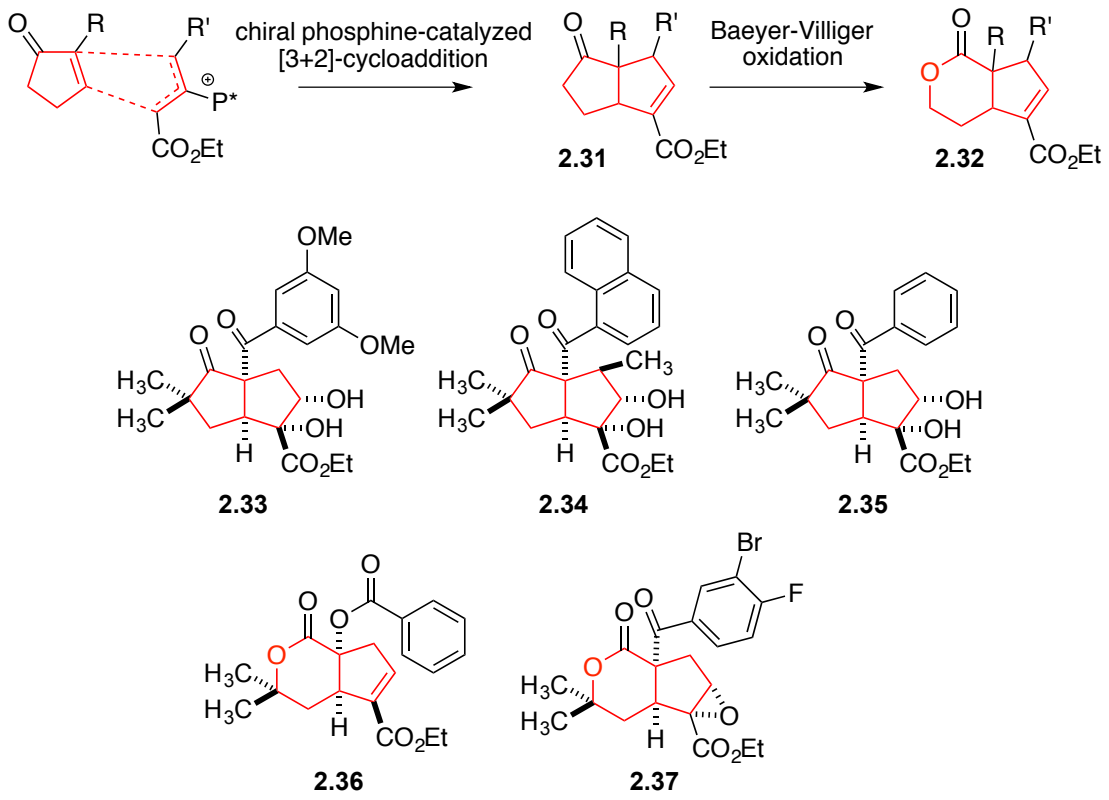

Scheme 2.9. NP inspired neuritogenic compounds reported by *Waldmann* and co-workers.

From the different approaches discussed in this section, several parts are interesting for our synthetic endeavour. By applying *Zanoni's* strategy, the formation of gelsemiol (**2.1**) might be possible if the lactone **2.21** or **2.23** can be reduced selectively at the C(4)-position in around 14 steps (Scheme **2.6**). Walking on the synthetic pathways of either *Grieco* or *Gibbs* towards the lactone **2.16** in seven to nine steps might also be a promising route (Scheme **2.5**). Lactone **2.16** then would be selectively formylated at the C(4) and alkylated at the C(8) position. If the radical reaction developed by *Robertson* and co-workers would also proceed smoothly with a methyl group present at the C(8) position, one might use his approach to obtain gelsemiol (**2.1**). However, since *Markó* provided the chemistry community with the shortest route to the oxabicyclo[3.3.0]octanone skeleton, we based our retrosynthetic analysis upon his approach.

[49] P.-Y. Dakas, J. A. Parga, S. Höing, H. R. Schöler, J. Sterneckert, K. Kumar, H. Waldmann, *Angew. Chem. Int. Ed.* **2013**, *52*, 9576–9581.

2.2 Results and Discussion

2.2.1 Retrosynthetic Analysis

Gelsemiol (**2.1**) bears five stereocenters in a ten carbon atom skeleton, therefore its total synthesis in a selective, scalable and economic fashion remains challenging. From a retrosynthetic point of view, we envisioned that the best way to start might be with the cleavage of the C(6)-O bond, followed by the C(3) alcohol oxidation to obtain the desymmetrized diacid **2.38**. Next, the removal of the methyl group was considered in a retro anti-S_N2' fashion. Intermediate **2.39** shows strong structural similarities with **2.40** (Scheme 2.8) arising form the previously introduced and by definition atom economic IEDDA reaction followed by the radical reaction/skeleton rearrangement.[50]

If this reaction sequence tolerates a C(9) functionalization, **2.39** should be accessible from the selenium containing dienophil **2.41** and the diene **2.42**. We also envisioned that the protection of the alcohol **2.41** might be beneficial to improve the selectivity of the IEDDA and the methylation process. A benzyl protection group seemed the most appropriate since it can be removed simultaneously during the deiodination step at the end of the synthesis using reductive hydrogenation conditions.

[50] a) I. E. Markó, S. L. Warriner, B. Augustyns, *Org. Lett.* **2000**, *2*, 3123–3125. b) B. I. Augustyns, N. Maulide, I. E. Markó, *Tetrahedron Lett.* **2005**, *46*, 3895–3899 c) J.-H. Liao, N. Maulide, B. Augustyns, I. E. Markó, *Org. Biomol. Chem.* **2006**, *4*, 1464–1467 d) I. E. Markó, I. Chellé-Regnaut, B. Leroy, S. L. Warriner, *Tetrahedron Lett.* **1997**, *97*, 4269-4271.

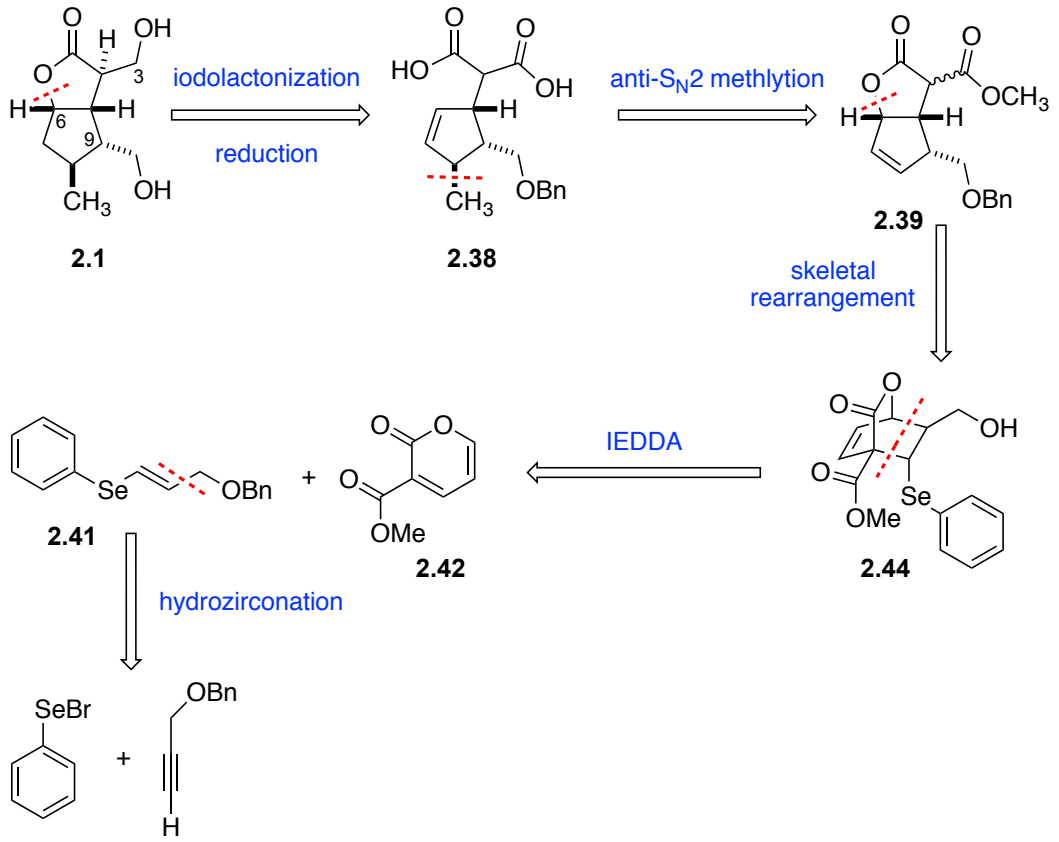

Scheme 2.10. Retrosynthetic analysis of gelsemiol (**2.1**).

2.2.2 Total Synthesis

The synthesis began with the benzyl protection of propargyl alcohol (**2.43**) following a known literature procedure[53] pursued by its *trans*-selective hydrozirconation using Schwartz's reagent with PhSeBr to afford the stable vinylselenide **2.44** in 72% yield.[52] Separate preparation of the Schwartz's reagent resulted in higher yields and absolute stereocontrol compared to *in situ* procedures. Synthesis of intermediate **2.44** proved to be more challenging than anticipated. We initially attempted the IEDDA reaction at ambient pressure and in the presence of a catalytic amount of the *in situ* formed Cu(II)-complex chelated by the *tert*-BuBox ligand, which was prepared following a procedure from *Evans*,[53] but mostly the [2+2] product was obtained. Interestingly, conducting the IEEDA reaction under reduced

[51] B. L. Ashfeld, S. F. Martin, *Tetrahedron* **2006**, *62*, 10497–10506.
[52] a) Z. Z. Huang, X. Huang, L. S. Zhu, *Tetrahedron* **1996**, *29*, 9819–9822. b) S. L. Buchwald, S. J. LaMaire, R. B. Nielsen, B. T. Watson, S. M. King, *Org. Synth* **1998**, *9*, 162. b) J. Schwartz, J. A. Labinger, *Angew. Chem. Int. Ed.* **1976**, *15*, 333–340. c) D. W. Hart, J. Schwartz, *J. Am. Chem. Soc.* **1974**, *26*, 8115–8116.
[53] D. A. Evans, G. S. Peterson, J. S. Johnson, D. M. Barnes, K. R. Campos, K. A. Woerpel, *J. Org. Chem.* **1998**, 63, 4541–4544.

pressure in neat conditions led to the bicyclic compound **2.44** in high yields and with a reasonable enantiomeric excess of 83% (Scheme 2.11).

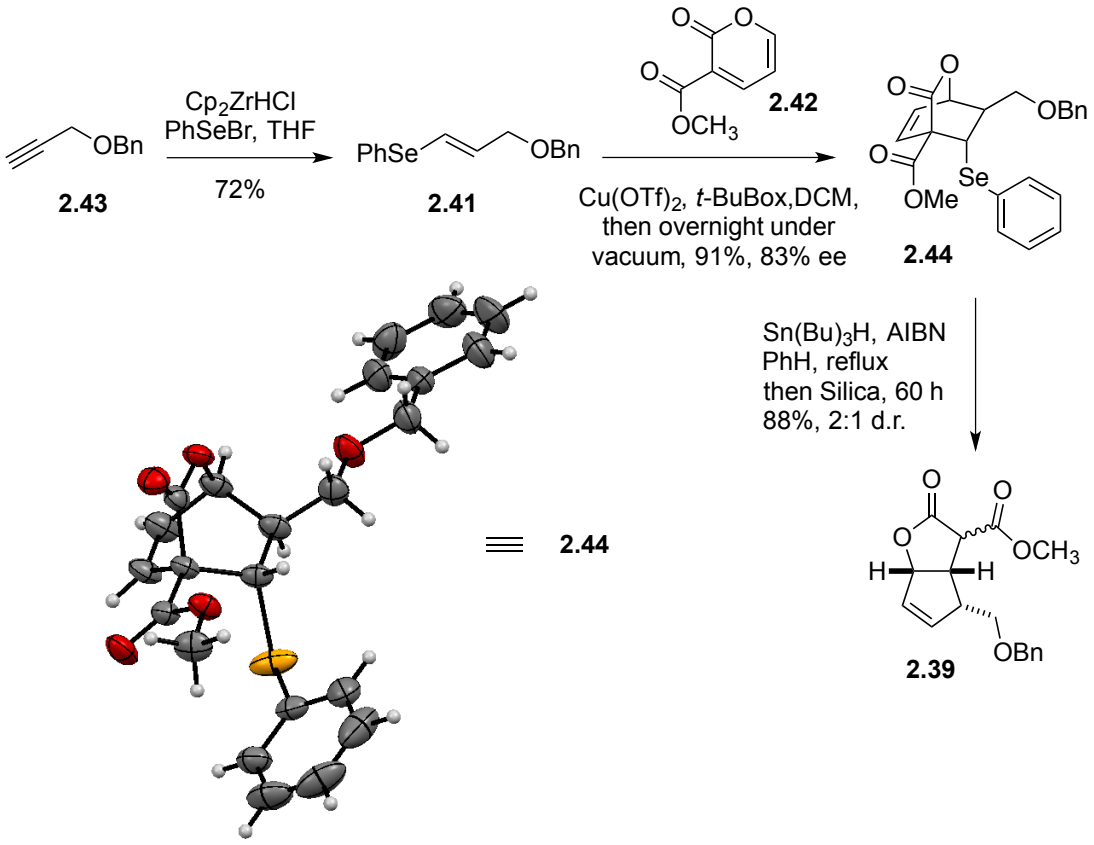

Scheme 2.11. Synthesis of bicycle **2.39**.

In principle, four different transition states are possible for the IEDDA reaction. However, only one seems sterically favoured. By protecting the propargyl alcohol, we assume that this effect contributes to the enhanced selectivity in comparison to the reported 56% ee by *Markó* as speculated earlier (Fig. 2.1).[54]

[54] I. E. Markó, S. L. Warriner, B. Augustyns, *Org. Lett.* **2000**, *2*, 3123–3125.

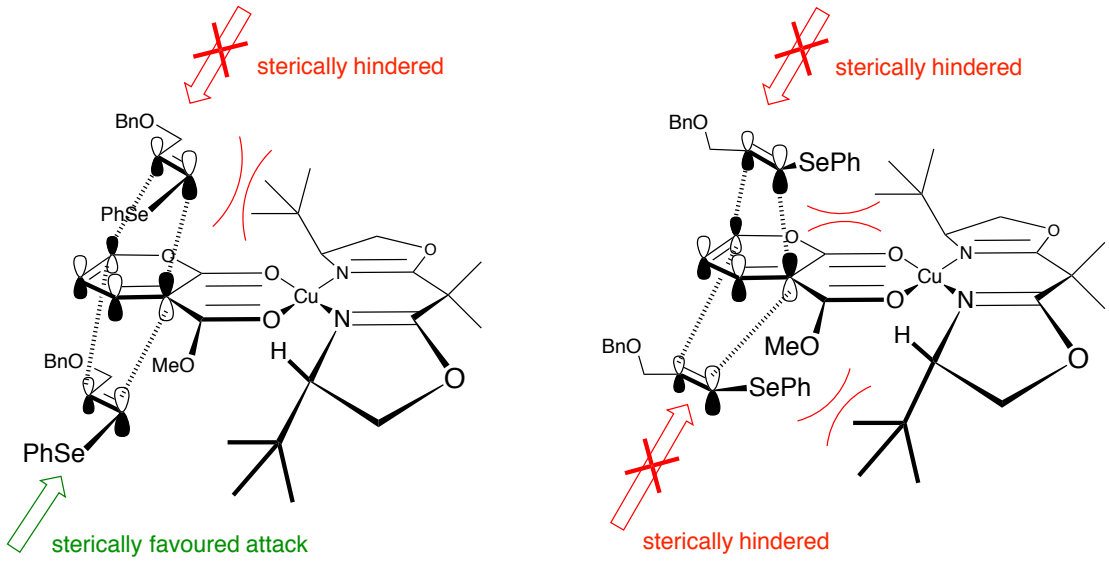

Figure 2.1. Visualization of the possible transition states during the IEDDA reaction.

With **2.44** in hand, we were then able to obtain the rearranged bicyclic lactone **2.39** in high yield *via* the radical reaction/skeleton rearrangement developed by *Markó*. The mechanism for this cascade reaction was proposed by the authors and is shown in scheme **2.12**.[55] With the help of AIBN, the radical **2.45** is generated, which then attacks the proximal sp^2-carbon leading to cyclopropylmethyl intermediate **2.46**. This 3-membered ring is then opened in the opposite direction to its closure, forming the stable tertiary radical **2.47**. This intermediate **2.47** is then intercepted by the $Sn(Ph)_3H$ to yield the primary adduct **2.48**. A [1,3]-shift of the carboxyl function results in the formation of lactone **2.39**. *Markó* reported a diastereomeric ratio of 15:1, but we only obtained 2:1 in favour of the *R*-configured diastereoisomer of **2.39**. Nevertheless, in our strategy, this stereocenter is irrelevant. In this step, the exclusion of oxygen was important, also requiring degasing of the silica gel.[56]

[55] a) B. I. Augustyns, N. Maulide, I. E. Markó, *Tetrahedron Lett*. **2005**, *46*, 3895–3899. b) J.-H. Liao, N. Maulide, B. Augustyns, I. E. Markó, *Org*. *Biomol*. *Chem*. **2006**, *4*, 1464–1467 b) I. E. Markó, S. L. Warriner, B. Augustyns, *Org*. *Lett*. **2000**, *2*, 3123–3125.

[56] a) I. E. Markó, S. L. Warriner, B. Augustyns, *Org*. *Lett*. **2000**, *2*, 3123–3125. b) J.-H. Liao, N. Maulide, B. Augustyns, I. E. Markó, *Org*. *Biomol*. *Chem*. **2006**, *4*, 1464–1467 c) I. E. Markó, I. Chellé-Regnaut, B. Leroy, S. L. Warriner, *Tetrahedron Lett*. **1997**. 97, 4269-4271.

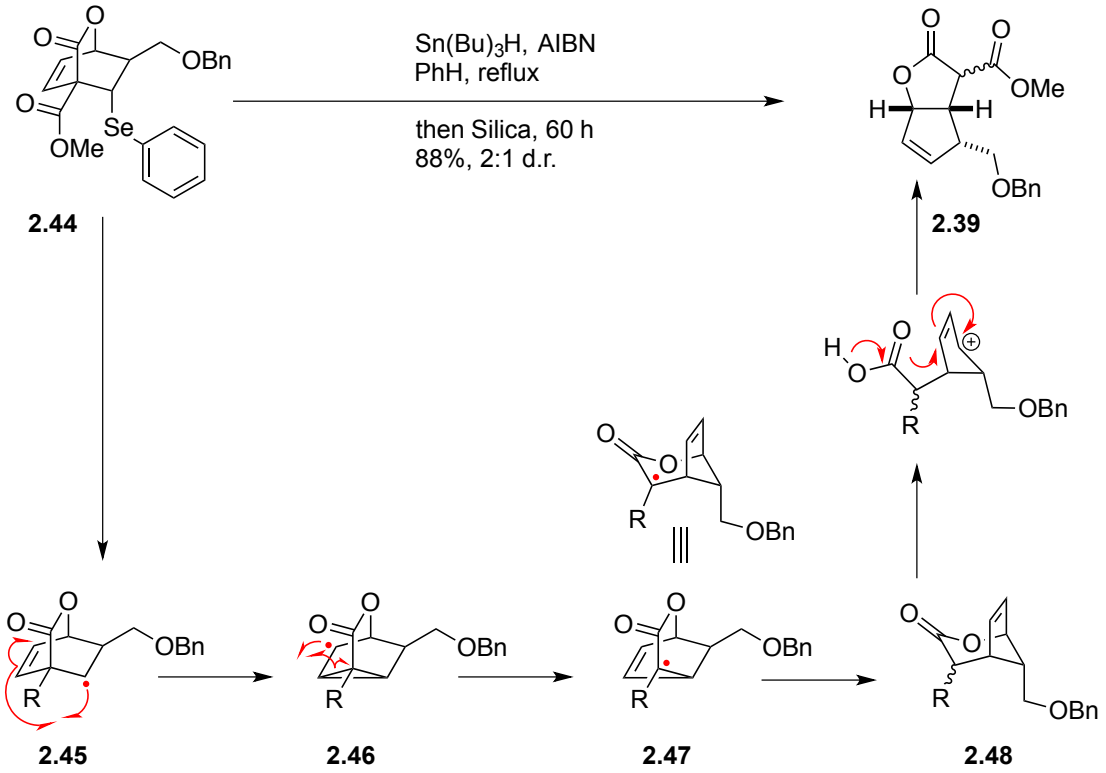

Scheme 2.12. Radical rearrangement and [1,3]-shift of the carboxyl function.

Preparation of compound **2.49** was realized from olefin **2.39** without purification or isolation of the different intermediates. The bicyclic lactone **2.39** was treated with methyl cuprate, prepared *in situ*, in the presence of trimethylchlorosilane to undergo alkylation followed by opening of the lactone **2.39** in a anti-S_N2' type reaction.[57] Saponification of the *mono*-ester malonate moiety in water, mild pH-acidification of the mixture with solid CO_2 to prevent decarboxylation, followed by iodolactonisation[58] gave the carboxylic acid **2.49** in 45% yield over three steps. X-ray crystallographic analysis of **2.49** unambiguously confirmed the absolute configuration of all six stereogenic centres (Scheme **2.13**).

[57] a) D. P. Curran, M.-H. Chen, *Tetrahedron Lett*. **1985**, *26*, 4991–4994. b) D. P. Curran, M. H. Chen, D. Leszczweski, *J. Org. Chem*. **1986**, *51*, 1612–1614. c) H. Weinmann, E. Winterfeldt, *Synthesis* **1995**, *9*, 1097–1101.
[58] P. Piccinini, G. Vidari, G. Zanoni, *J. Am. Chem. Soc*. **2004**, *126*, 5088–5089.

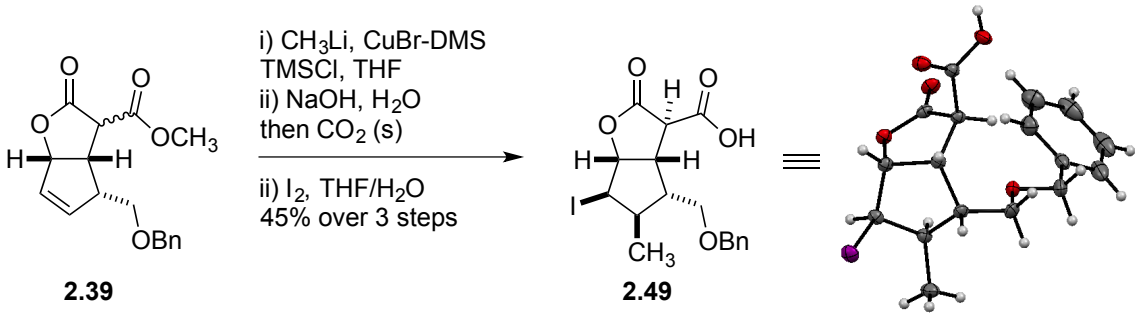

Scheme 2.13. The synthesis of bicyclic lactone **2.49** *via* selective methylation and iodolactonization.

Finding an acceptable way to reduce the acid **2.49** became the most challenging part of the synthesis. After screening multiple conditions including: $NaBH_4$ in combination with the Vilsmeier salt or ethyl chloroformate in combination with $NaBH_4$, BH_3-DMS and DIBAL-H, or $NaBH(OAc)_3$ without activator using different solvents and temperatures. The best yields were obtained by making a detour *via* the lactol **2.50**. Initially, the acid **2.49** was successfully reduced with an excess of BH_3-DMS. After a solvent exchange from THF to EtOH, Raney-Nickel was added and a hydrogen atmosphere applied to trigger the benzyl group deprotection[59] and the deiodination,[60] which led to the desired NP **2.1** and the lactol **2.50** in a 2:3 mixture. To our delight, Raney-Nickel was able to oxidize lactol **2.50** to gelsemiol (**2.1**) at a slow rate but quantitatively. Since compound **2.1** and **2.50** could be separated, we were able to show that only lactol **2.50** could undergo oxidation to yield gelsemiol (**2.1**) using Raney-Nickel in EtOH without hydrogen at room temperature (Scheme 2.14).

[59] K. Horita, T. Yoshioka, T. Tanaka, Y. Oikawa, O. Yonemitsu, *Tetrahedron* **1986**, *42*, 3021–3028.
[60] a) P. Piccinini, G. Vidari, G. Zanoni, *J. Am. Chem. Soc.* **2004**, *126*, 5088–5089. b) R. Di Florio, M. A. Rizzacasa, *J. Org. Chem.* **2002**, 4392–4398.

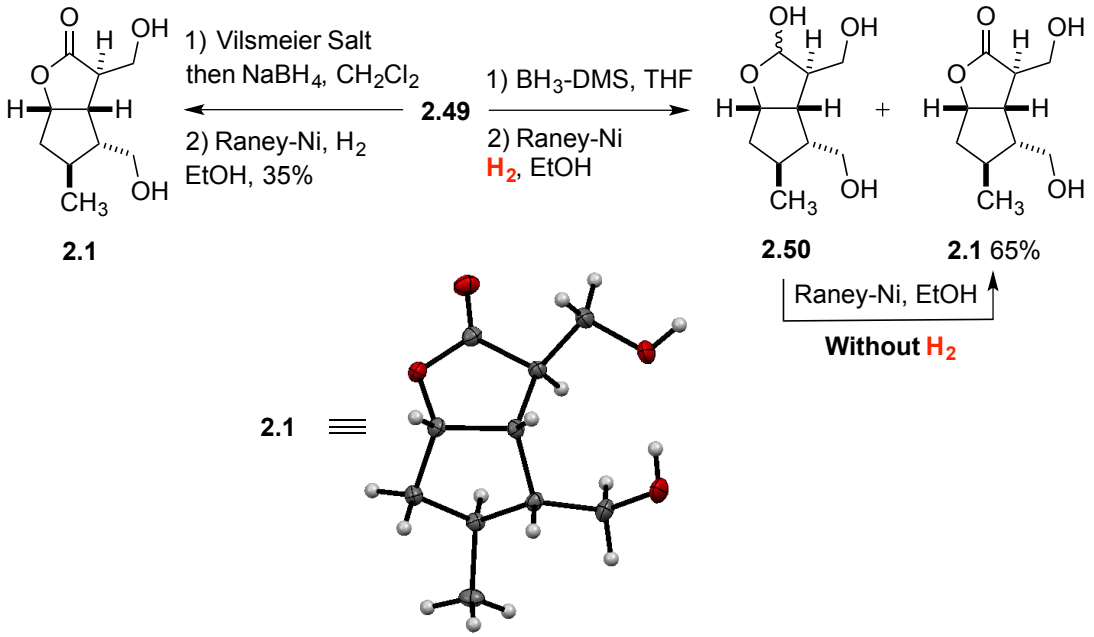

Scheme 2.14. Endgame of the total synthesis of gelsemiol (**2.1**).

Even though oxidations of secondary alcohols to ketones using refluxing Raney-Nickel conditions are known[61] this example represents the first Raney-Nickel-mediated lactol oxidation at room temperature to our knowledge. We wondered about the generality of this reaction and performed a very limited screen of similar commercially available compounds. However, no successful oxidations were observed (Scheme 2.15).

Another finding made during this project was that $NaBH(OAc)_3$ was able to fully decarboxylate the acid **2.49** in quantitative yields, even at catalytic amounts. In literature, many examples for decarboxylations are known, including the use of simple alkali metals salts as NaCl or LiCl,[62] but to the best of our knowledge, examples with catalytic amounts of $NaBH(OAc)_3$ have never been reported.

[61] a) M. E. Krafft, W. J. Crooks, B. Zorc, S. E. Milczanowski, *J. Org. Chem.* **1988**, *53*, 3158–3163. b) M. E. Krafft, B. Zorc, *J. Org. Chem.* **1986**, *51*, 5482–5484.
[62] A. P. Krapcho, J. F. Weimaster, J. M. Eldridge, *J. Org. Chem.* **1978**. *1*, 138-147.

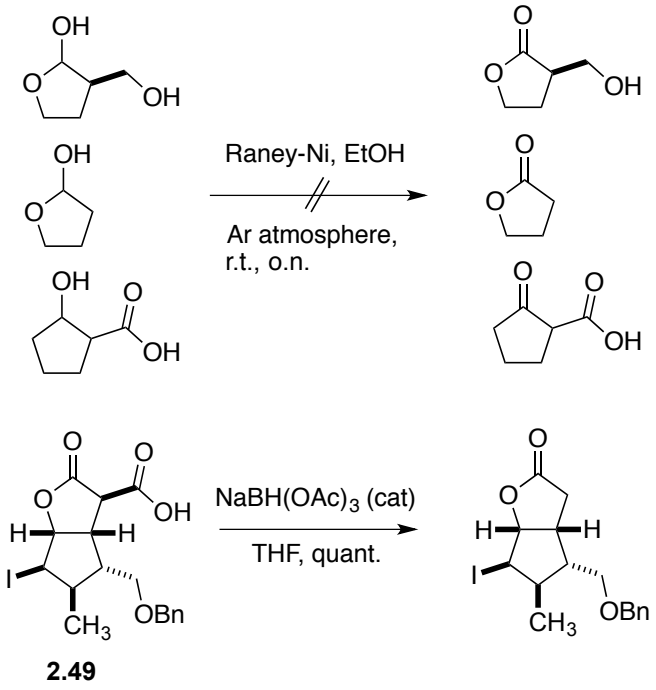

Scheme 2.15. Limited scope explorations of lactol oxidations using Raney-Nickel and decarboxylation using $NaBH(OAc)_3$.

Iridoid **2.1** was also synthesized without the formation of the lactol **2.50** *via* the activation of the acid **2.49** using the Vilsmeier salt, followed by $NaBH_4$ reduction[63] giving rise to alcohol **2.51**. This alcohol is then treated under similar conditions for the last step (Scheme 2.14). This route however, resulted in a much lower yield (35% over two steps).

The ^{1}H and ^{13}C NMR spectra were then compared with the literature data.[64] They were in excellent agreement besides a small misassignment in the original isolation paper we could manage to clarify. In the isolation paper it is claimed that the C(4) carbon signal is displayed at 51.1 ppm and the C(9) at 44.7 ppm, but according to 2D-NMR experiments, the assignment is interchanged.

For analytical proposes, *Jensen* and co-workers acetylated gelsemiol (**2.1**) on both alcohols and compared the analytical data with the data from natural glycosylated gelsemiol congeners. We decided to acetylate **2.1** as well and synthesize the diacetylated gelsemiol analog **2.52**, which had the same chemical shifts as the reported ones.[66] To dispel eventual last doubts, single crystals of **2.1** were grown in

[63] T. Fujisawa, T. Mori, T. Sato, *Chem. Lett.* **1983**, *6*, 835–838.
[64] S. R. Jensen, O. Kirk, B. J. Nielsen, R. Norrestam, *Phytochem.* **1987**, *6*, 1725–1731.

pentane/CH_2Cl_2 mixture and were then subjected to X-ray diffraction analysis (Scheme 2.14).

2.2.3 Synthesis of Natural Congeners of Gelsemiol

After having established a versatile route to gelsemiol (**2.1**), we intended to synthesize some of the previous mentioned natural congeners of gelsemiol (Scheme 2.3). First, we focused on the oxidation of **2.1** to the dialdehyde **2.7** as briefly discussed in scheme 2.1 to find a pathway towards the (–)-brasoside (**2.3**), (–)-littoralisole (**2.8**) or semperoside A (**2.9**) core structure. Unfortunately, all attempts to oxidize both lactones were unsuccessful as shown in table 2.1 below. Since *MacMillan* and *Zanoni* already have reported elegant ways to obtain these three cyclic iridolactones **2.3**, **2.8**, **2.9** we decided not to spend further recourses on these targets.

Entry	Oxidation Method	Activation Agent	Solvent	Temp.	Observation
1	TPAP	NMO	MeCN	r.t.	Mono-oxidation
2	MnO_2	-	DCM	r.t.	No reaction
3	PCC	-	DCM	r.t.	Mono-oxidation
4	PCC	$MeCO_2Na$	DCM	r.t.	Mono-oxidation
5	DMP	-	DCM	0 °C	Mono-oxidation
6	Swern	-	THF	–78 °C	No reaction
7	Swern	-	DCM	–78 °C	Decomposition
8	Moffatt	DCC	DMSO	r.t.	Decomposition
9	Moffatt	EDC	DMSO	r.t.	Decomposition

Table 2.1. Conditions attempted towards the synthesis of dialdehyde **2.7** (Scheme 2.2 and 2.4)

2.2.4 Biological Evaluation

Gelsemiol **2.1** is known to induce neurite outgrowth in combination with nerve growth factor (NGF) in the PC12 cell line (*rat adrenal pheochromocytoma*) as mentioned previously.[65] First, we successfully reproduced these reported results as shown (Fig. 2.2), then we attempted to find a similar morphological response using primary cells.

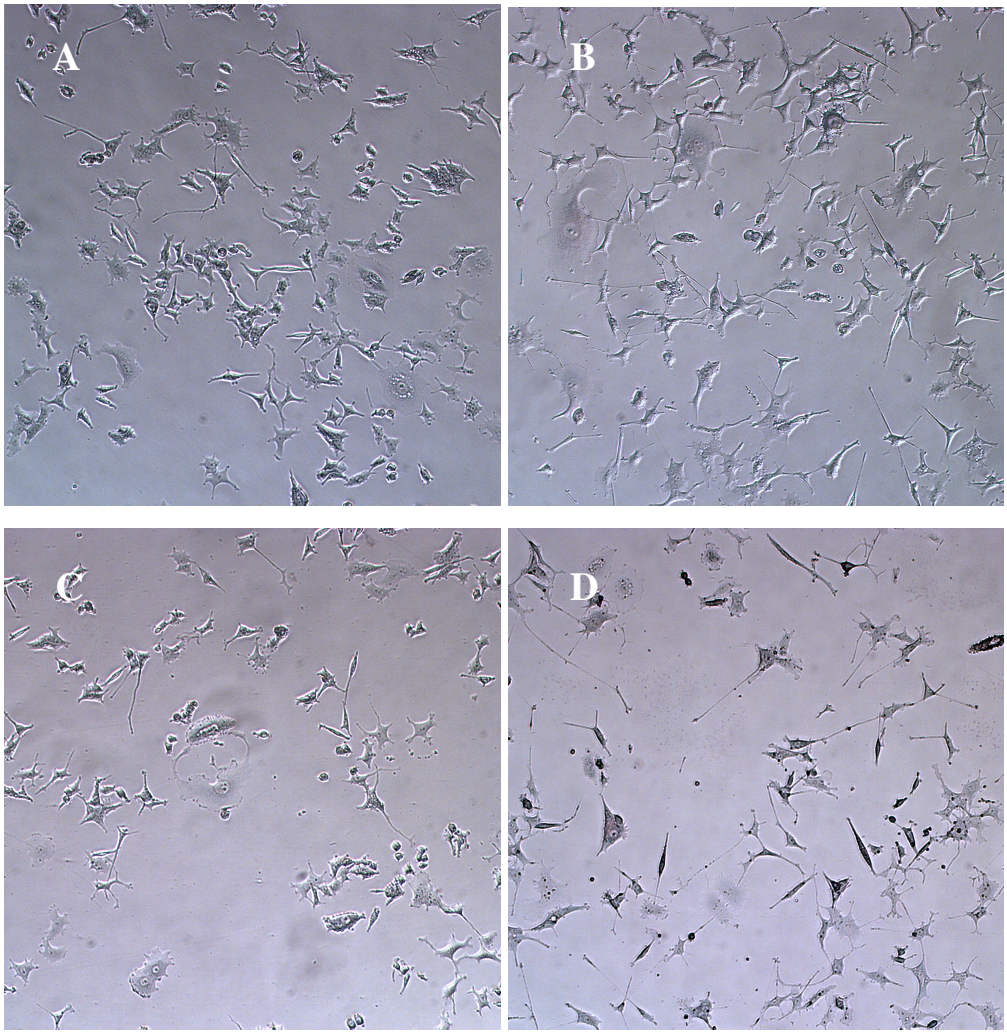

[65] a) Y. S. Li, K. Matsunaga, R. Kato, Y. Ohizumi, *J. Pharmacy. Pharmacol*. **2001**, *53*, 915–919. b) Y. Li, Y. Ohizumi, *Yakugaku Zasshi* **2004**, *124*, 417–424.

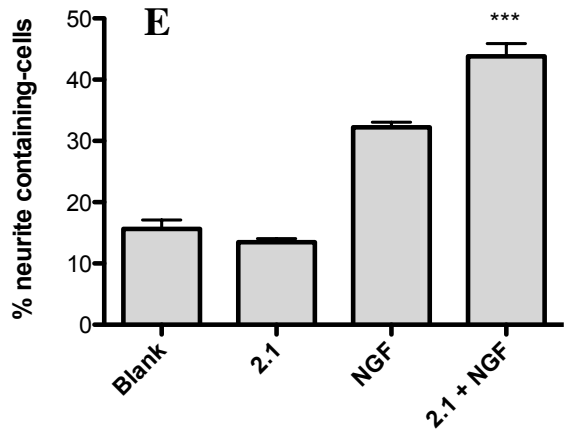

Figure 2.2. A: Blank (DMSO 0.1 %), B: Blank (NGF 7S 10 ng mL^{-1} + DMSO 0.1 %), C: gelsemiol (**2.1**) (50 µM) D: gelsemiol (**2.1**) (50 µM + NGF 7S ng mL^{-1}), E: plotted activity, Incubation period: 2 days. Values are reported as mean ± SEM. (unpaired tow-tailed t-test significance: *** = $P < 0.0001$)

We therefore sacrificed mice pups to extract their primary cerebellar granule cells following a known procedure[66] in collaboration with the group of *Prof. Dr. Peter Scheiffele* (Biozentum, Basel). For this type of primary neurons we had to establish a different way to analyse the neurite outgrowth than in the PC12 cell model. The difference is that all of these cells bear long axons and dendrites and are forming an unmanageable network. Therefore, we focused on the amount of branching-points, meaning how much processes (axon and dendrites) of a single neuron cross the eight concentric cycles being focused on the soma, to see if gelsemiol (**2.1**) initiates any morphological changes. To be able to do so, the cells were transfected with green fluorescent protein (GFP). In only a small percentage of the primary cells the transfection was successful and the few fluorescent neurons were distinguishable from the rest. Since we knew that **2.1** was only active in combination with NGF, we speculated that brain-derived neurite growth factor (BDGF) might be an appropriate substitution for this model. However, we could only find a significant difference in branching-points when samples with and without BDGF where compared. The addition of gelsemiol (**2.1**) made no difference.

[66] C. Dean, F. G. Scholl, J. Choih, S. DeMaria, J. Berger, E. Isacoff, P. Scheiffele, *Nat. Neurosci*. **2003**, *6*, 708–716.

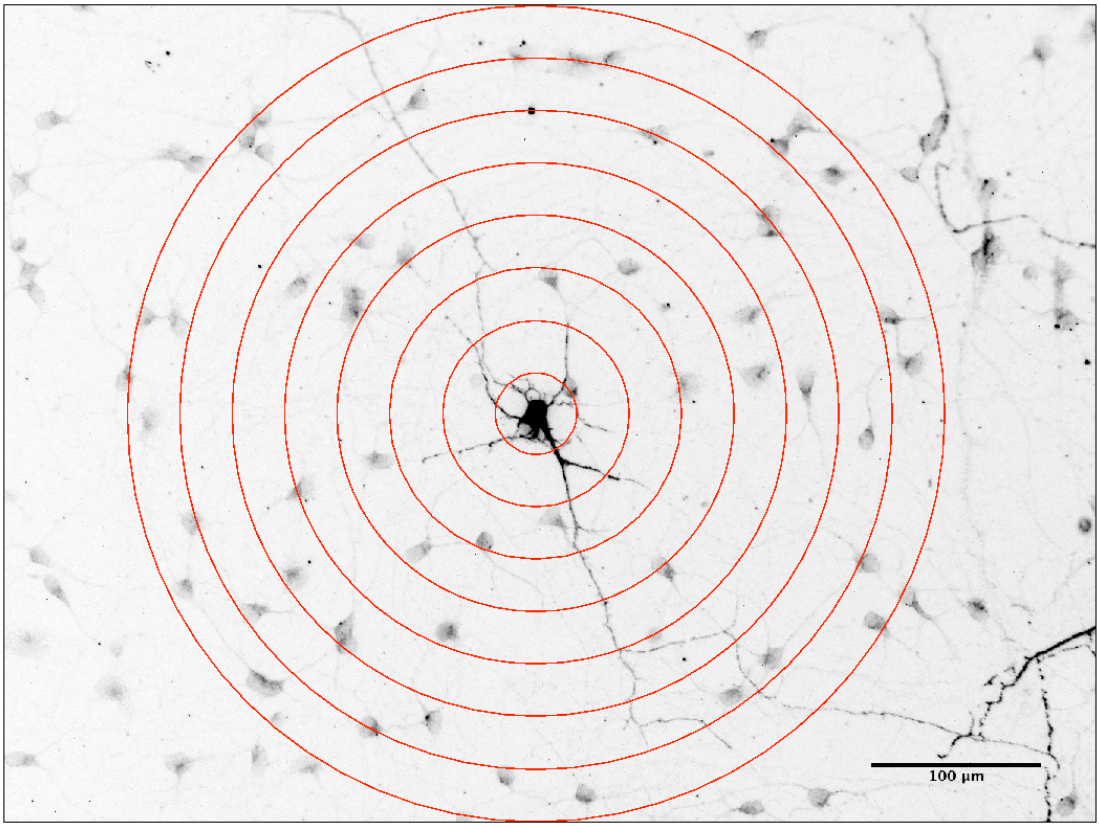

Figure 2.3. Representative inverted image of a GFP expressing primary granule cell and the eight concentric cycles.

In order to restore brain function, it is not only sufficient to induce neurite outgrowth, but is also mandatory to form new synapses. A synapse consists of a pre- and postsynapse (also see Fig. 4.10). Only if these are overlapping, a port for neuronal signal transaction can be formed. The formation of synapses is called synaptogenesis and can be investigated using an elaborate antibody staining methodology. Therefore the primary cerebellar granule cells were again seeded in a 24-well plate, transfected with GFP as before and incubated for 2 days with 50 µM of gelsemiol (**2.1**). Then the cells were fixed and stained using pre- and postsynaptic specific and their respective fluorescent secondary antibodies. When these blue (postsynapes) and red (presynapse) dots overlap, they represent a functionable synapse. If this overlap is located on the green neuron of interest, a yellow dot can be observed as shown (Fig. 2.4). The amount of these spots is then analysed using a confocal microscope and compared to the control experiments. Our findings suggest that synaptogenesis cannot be attributed to gelsemiol (**2.1**).

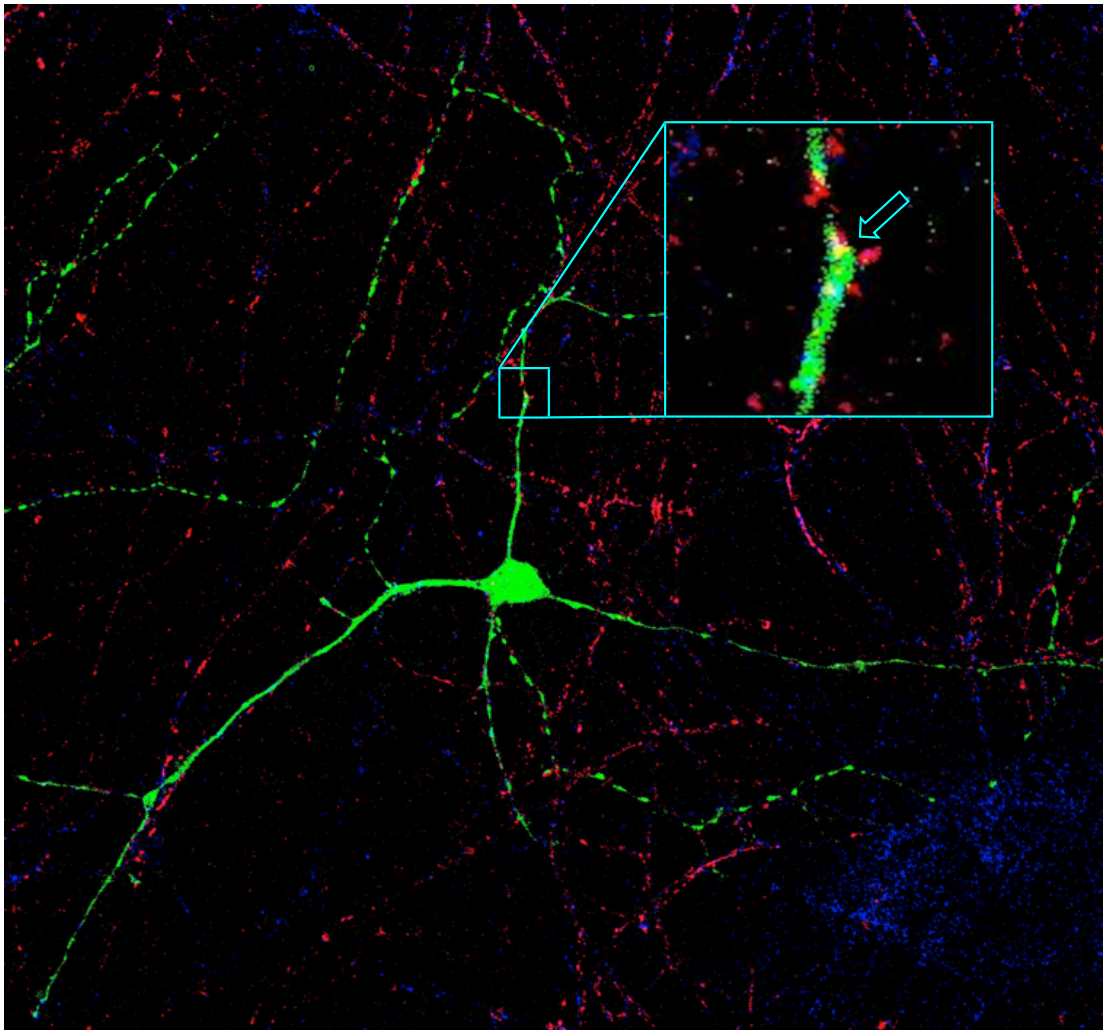

Figure 2.4. Representative image of a GFP expressing primary granule cell stained with post- and presynaptic antibody markers.

2.3 Conclusion

The first enantioselective total synthesis of gelsemiol (**2.1**) was accomplished in nine steps and an overall yield of 14 %. The key features of the synthesis involved a stereoselective IEDDA as well as the following radical rearrangement, and the highly efficient and stereoselective iodolactonisation. Selective reduction of carboxylic acid **2.39** kept the lactone moiety intact and retained the absolute configuration of the six stereogenic centers. Additionally, the final three transformation can be performed in one pot. This versatile synthetic approach, which also follows some of the in chapter 1.2 introduced criteria for an efficient total synthesis, is expected to be widely utilized for the syntheses of iridoids and

iridoalkaloids. The biological evaluation reproduced the neuritogenic activity in the PC12 cell line but could not be transferred onto primary cell models.[67]

[67] P. Burch, M. Binaghi, M. Scherer, C. Wentzel, D. Bossert, L. Eberhardt, M. Neuburger, P. Scheiffele, K. Gademann, *Chem. Eur. J.* **2013**, *19*, 2589–2591.

3

CHAPTER 3 - SAR STUDY ON FUNCTIONALLY OPTIMIZED NEURITOGENIC FARINOSONE C ANALOGS

3.1 Introduction

3.1.1 General Outline

Our group accomplished the total synthesis of several neuritogenic alkaloids originating from entomopathogenic fungi such as pretenellin (**3.1**), farinosone A (**3.2**), militarinone D (**3.3**) or farinosone C (**3.4**) and assigned their absolute configurations (Fig. 3.1).[68] The biosynthesis of these compounds is likely to be related, as recent contributions suggested.[69] From a very limited structure-activity relationship (SAR) study of farinosone C (**3.4**), we found that the simplified L-tyrosinol-propionamide analog **3.5** was able to induce neuronal differentiation, albeit at higher concentration than the parent NP **3.4**. We therefore aimed to synthesize structurally optimized derivatives of farinosone C (**3.4**), which retain or even display more potent neurite outgrowth-inducing capability. At the same time, this endeavour would also result in a more defined description of the pharmacophore. In this chapter, we report the results of this SAR study on farinosone C analogs.

[68] a) H. J. Jessen, A. Schumacher, T. Shaw, A. Pfaltz, K. Gademann, *Angew. Chem. Int. Ed.* **2011**, 4222–4226 b) Y. Li, Y. Ohizumi, *Yakugaku Zasshi* **2004**, *124*, 417–424 c) H. J. Jessen, D. Barbaras, M. Hamburger, K. Gademann, *Org. Lett.* **2009**, *11*, 3446–3449 d) Y. Cheng, B. Schneider, U. Riese, B. Schubert, Z. Li, M. Hamburger, *J. Nat. Prod.* **2004**, *67*, 1854–1858.

[69] a) J. Xu, L. Trzoss, W. K. Chang, E. A. Theodorakis, *Angew. Chem.* **2011**, *123*, 3756–3760 b) S. Bergmann, J. Schümann, K. Scherlach, C. Lange, A. A. Brakhage, C. Hertweck, *Nat. Chem. Biol.* **2007**, *3*, 213–217 c) L. Trzoss, J. Xu, M. H. Lacoske, W. C. Mobley, E. A. Theodorakis, *Chem. Eur. J.* **2013**, *19*, 6398–6408 d) L. M. Halo, J. W. Marshall, A. A. Yakasai, Z. Song, C. P. Butts, M. P. Crump, M. Heneghan, A. M. Bailey, T. J. Simpson, C. M. Lazarus, *et al.*, *Chembiochem* **2008**, *9*, 585–594.

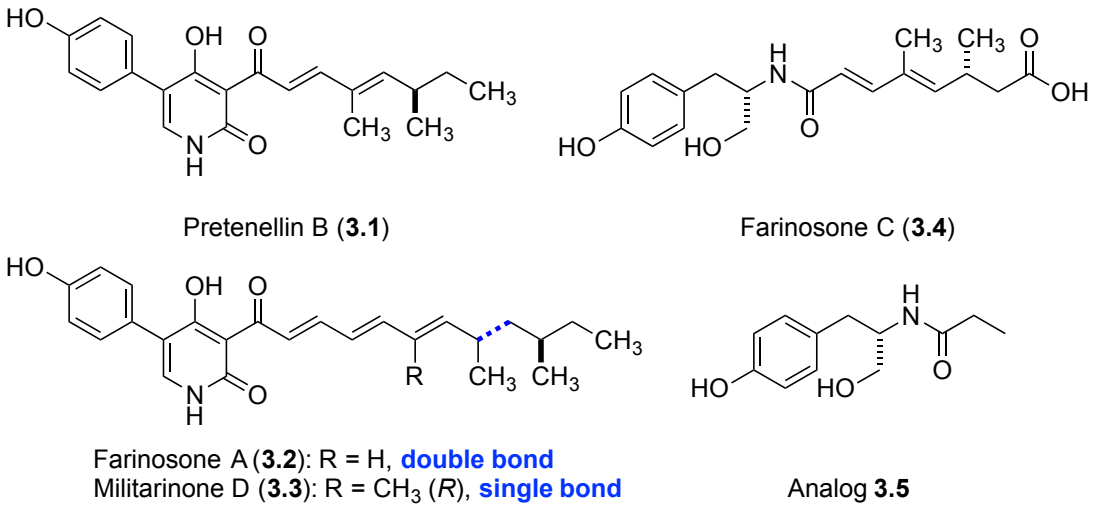

Figure 3.1. Neuritogenic natural products and lead analog **3.5**.

3.1.2 Parasite Host Control

Understanding the ways in which parasites are able to manipulate the behaviour of their hosts has become a popular research field.[70] An interesting example is the effects *Toxoplasma gondii* has on rats and mice. These rodents are in a classic predator/prey system with cats and it was essential for their survival to develop efficient defence strategies. The native fear of the odour of cat urine is one of these strategies rodents have developed to avoid contact with their predators. But when mice are infected by *Toxoplasma gondii*, this fear turns into a fatal attraction. This parasite must find its way to a cat's intestines for sexual reproduction. After successful copulation, the formed oocytes are excreted in the cat's feces and rodents are then employed to serve as transport vesicles to the next cat host. The way *Toxoplasma gondii* is affecting the rodents behaviour is not fully, but quite well understood: This parasite is one of the few pathogens that is able to cross the blood-brain-barrier of the host. Once in the brain, it increases the dopamine (**4.12**) levels up to 15%. When in contrary the dopamine receptors of infected mice are blocked, the natural fear of cat's urine could be restored. This strongly suggests a link between the behavioural changes of the host and the neurotransmitter that is known to be key for reward and decision-making. The effects *Toxoplasma gondii* has on humans have been investigated intensively, but not considered a major health risk. Hence 20-40%

[70] a) R. Poulin, *Adv. Stud. Behav.* **2010**, *41*, 151–186. b) F. Libersat, A. Delago, R. Gal, *Annu. Rev. Entomol.* **2009**, *54*, 189–207.

of the world's population is infected by *Toxoplasma gondii*, this is important.[71]

In addition, entomopathogenic fungi that infect and kill insects can physically control their hosts using a variety of complex interactions, of which some are believed to be mediated by small molecules.[72] These organisms receive growing interest from the scientific community, not only because their host-parasite interactions could potentially led to new insecticides, but also because these fungi have been widely used in traditional Chinese medicine over centuries and understanding their effects on humans in detail is important.[73]

In 2004, *Hamburger* and co-workers (Pharmazentrum Basel) reported on the isolation and partial characterization of farinosone A (**3.2**), B, and C (**3.4**) originating from the entomopathogenic fungi *Paecilomyces farinosus*,[74] also known as *Isaria farinose.*[75] If these compounds are involved in the observed behavioural changes is unclear. Nevertheless, these compounds are known to significantly induce neurite outgrowth in PC12 cells and, therefore lie exactly in the overlap of two of our main research focuses: natural product synthesis and restoration of brain function.[76]

---

[71] a) P. K. House, A. Vyas, R. Sapolsky, *PLOS ONE* **2011**, *6*, e23277. b) A. Vyas, S.-K. Kim, N. Giacomini, J. C. Boothroyd, R. M. Sapolsky, *Proc. Natl. Acad. Sci.* **2007**, *15*, 6442-6447. c) G. Schatz, *Jenseits Der Gene*, Wiley-VCH Verlag GmbH & Co. KGaA, Weinheim, **2012**.

[72] a) A. E. Hajek, R. S. Leger, *Annu. Rev. Entomol.* **1994**, *39*, 293–322. b) H. E. Roy, D. C. Steinkraus, J. Eilenberg, A. E. Hajek, J. K. Pell, *Annu. Rev. Entomol.* **2006**, *51*, 331–357. c) M. Rohlfs, A. C. L. Churchill, *Fungal Genetics and Biology* **2011**, *48*, 23–34. d) H. J. Jessen, A. Schumacher, F. Schmid, A. Pfaltz, *Org. Lett.* **2011**. *16*, 4368-4370.

[73] R. Paterson, *Phytochem.* **2008**, *69*, 1469–1495.

[74] Y. Cheng, B. Schneider, U. Riese, B. Schubert, Z. Li, M. Hamburger, *J. Nat. Prod.* **2004**, *67*, 1854–1858.

[75] G. Zimmermann, *Biocontrol. Sci. Tech.* **2008**, *18*, 865–901.

[76] Y. Cheng, B. Schneider, U. Riese, B. Schubert, Z. Li, M. Hamburger, *J. Nat. Prod.* **2004**, *67*, 1854–1858.

Figure 3.2. Entomopathogenic fungus *Paecilomyces farinosus* growing out of an insect corpse.[77]

3.1.3 Total Synthesis of Farinosone C by *Jessen et al.*

With the absolute stereochemistry of the natural products not clearly assigned, all four possible farinosone C isomers had to be synthesized to elaborate the absolute stereochemistry by comparing the analytical data of the synthesized compounds with the isolated natural product. The synthesis began by TIPS protection of iodoethanol that was then coupled with either (+)- or (–)-pseudoephedrine-propionamide, following an optimized procedure from *Myers*.[78] Direct reductive cleavage of the obtained amide **3.6** employing LAH resulted in the formation of the respective aldehydes **3.7** in high to excellent enantiomeric excess. The *trans*-selective double bond was introduced by a Wittig reaction using the ylid **3.8**. The resulting ester was reduced with DIBAL-H before it was re-oxidized with activated manganese dioxide to obtain the aldehyde **3.9** (Scheme 3.1a). The second double-bond was introduced via a Horner-Wadsworth-Emmons reaction giving rise to the (*E,E*) configured ester **3.10** in both enantiomers in quantitative yields. These compounds proved to be unstable and partial racemization was observed. Separation of the isomers could be performed

[77] Photograph reprinted with permission of Renée Lebeuf, **2011**
[78] A. G. Myers, B. H. Yang, H. Chen, L. McKinstry, D. J. Kopecky, J. L. Gleason, *J. Am. Chem. Soc*. **1997**, *119*, 6496–6511.

satisfyingly at a later stage of the synthesis, and this issue could be resolved. After TIPS removal, a mild two step oxidation sequence of a Swern oxidation, followed by sodium chlorite oxidation yielded compound **3.11** in high yields. *Tert*-butylation of acid **3.12** and selective LiOH saponification, then set the stage for the peptide coupling with either L- or D-tyrosinol. The total synthesis was completed by deprotection of the acid terminus with TFA. The analytical data of the 1'*S*,3*R* configurated isomer was in full agreement with the reported values for farinosone C (**3.4**). This first, enantioselective total synthesis of **3.4** required 14 steps and achieved an overall yield of 23% (Scheme 3.1b).[79]

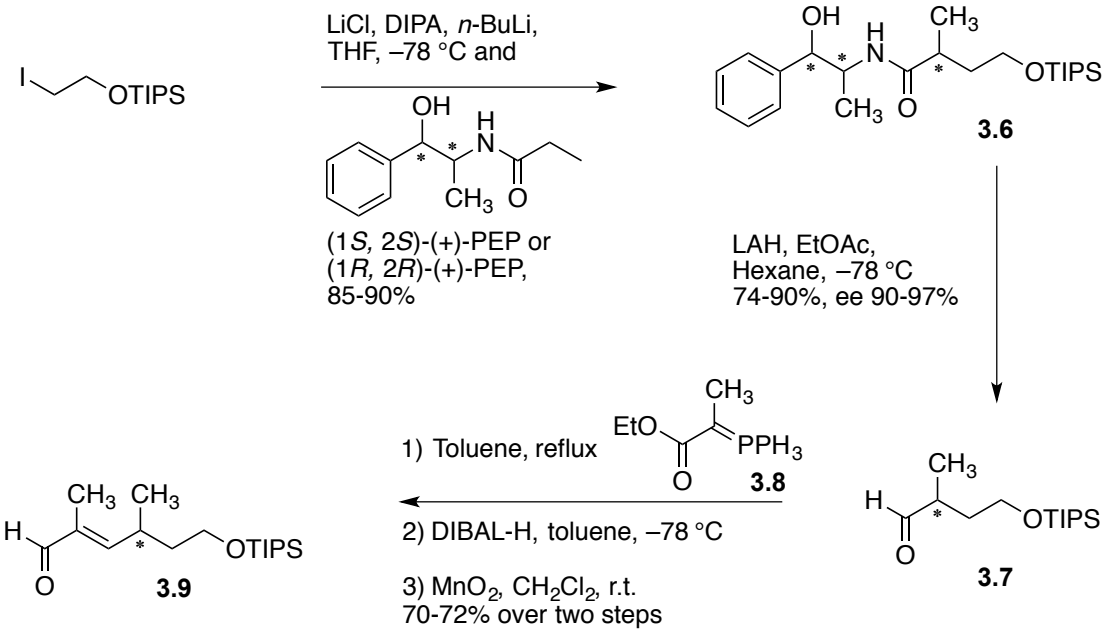

Scheme 3.1a. Total Synthesis of farinosone C (**3.4**) by *Jessen et al.* part A.

[79] H. J. Jessen, D. Barbaras, M. Hamburger, K. Gademann, *Org. Lett.* **2009**, *11*, 3446–3449.

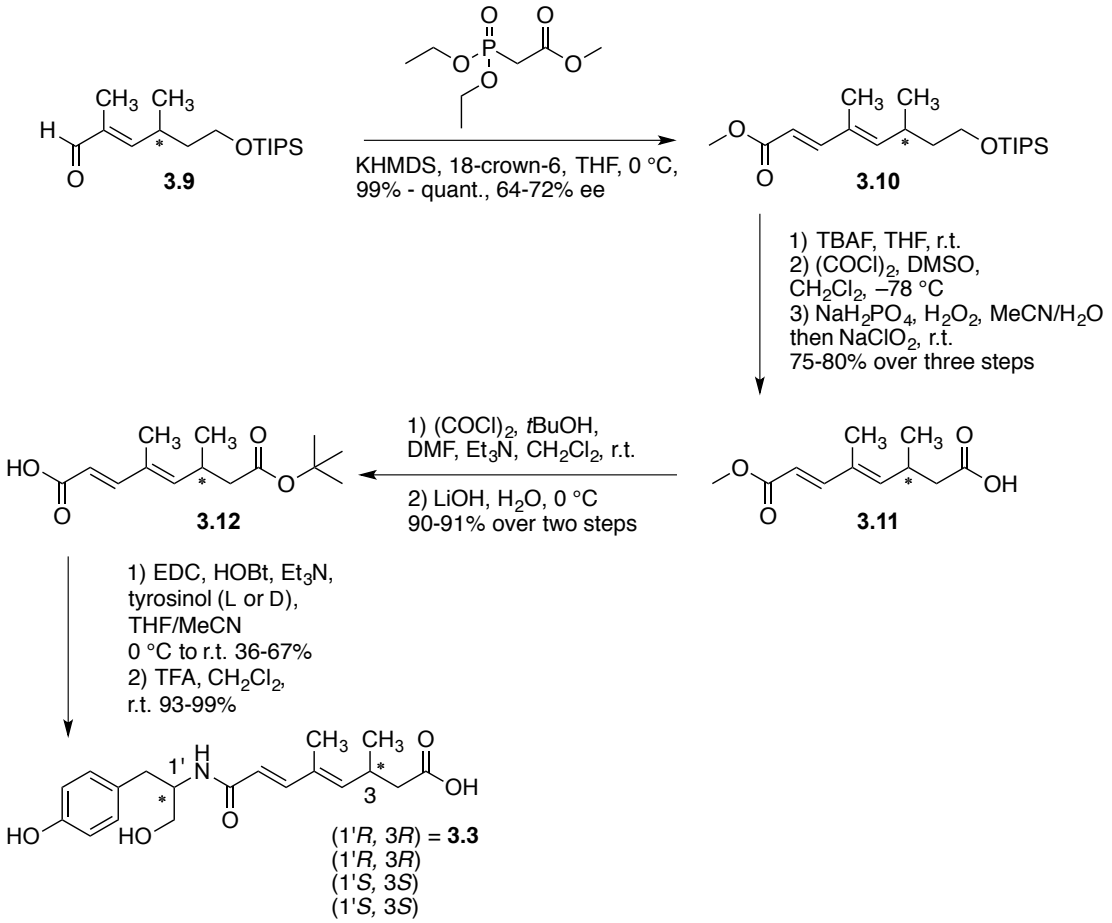

Scheme 3.1b. Total Synthesis of farinosone C (**3.4**) by *Jessen et al.* part B.

3.1.4 Function Oriented Synthetic Approaches from *Gademann* and Co-Workers

The *Gademann* laboratory has a long-standing tradition in exploring the biological and synthetic scope of natural products and their analogs after successful completion of their total synthesis. As outlined in section 1.2, simplification of a NP while retaining the bioactivity will facilitate its supply. *Bonazzi et al.* for example showed that the potent CRM1 nuclear export inhibitors anguinomycin C (**3.13**) and D (**3.14**) can be strongly simplified by truncation of the polyketide chain, hence the resulting analog **3.15** retained most of the biological activity (Fig. 3.2).[80] Another satisfying endeavour was the truncation of polypeptide chain from farinosone A (**3.2**) and militarinone D (**3.16**). In this investigation, not only was the side chain subtracted, but also the pharmacophore was optimized during the SAR study. The most potent analog SF33 (**3.17**) origination from this project conducted by *Schmid et*

[80] S. Bonazzi, O. Eidam, S. Guettinger, J.-Y. Wach, I. Zemp, U. Kutay, K. Gademann, *J. Am. Chem. Soc.* **2010**, *132*, 1432–1442.

al. was able to induce neuronal differentiation in the PC12 assay at a 20-fold lower concentration than the parent NP **3.2** and **3.16**.[81] Other SAR investigations focused on the A ring of the neuritogenic NP withanolide A (**3.18**) conducted by *Liffert* and *Hoecker et al.*[82] or the antibacterial alkaloid nostocarboline (**3.18**) and its dimeric analogs synthesized by *Barbaras* and *Bonazzi et al.*[83] These two latter approaches did not lead to significantly simplified analogs, but did provide valuable insight in to the structural requirements for bioactivity. Moreover, in the case of nostocarboline (**3.19**), several derivatives showed strongly improved selectivity and bioactivity.

[81] F. Schmid, H. J. Jessen, P. Burch, K. Gademann, *MedChemComm* **2013**, *4*, 135–139.
[82] a) R. Liffert, J. Hoecker, C. K. Jana, T. M. Woods, P. Burch, H. J. Jessen, M. Neuburger, K. Gademann, *Chem. Sci.* **2013**, *4*, 2851–2857. b) C. K. Jana, J. Hoecker, T. M. Woods, H. J. Jessen, M. Neuburger, K. Gademann, *Angew. Chem.* **2011**, *123*, 8557–8561. c) C. K. Jana, J. Hoecker, T. M. Woods, H. J. Jessen, M. Neuburger, K. Gademann, *Angew. Chem. Int. Ed.* **2011**, *50*, 8407–8411.
[83] a) J. F. Blom, T. Brütsch, D. Barbaras, Y. Bethuel, H. H. Locher, C. Hubschwerlen, K. Gademann, *Org. Lett.* **2006**, *8*, 737–740. b) D. Barbaras, M. Kaiser, R. Brun, K. Gademann, *Bioorg. Med. Chem. Lett.* **2008**, *18*, 4413–4415. c) H. H. Locher, D. Ritz, P. Pfaff, M. Gaertner, A. Knezevic, D. Sabato, S. Schroeder, D. Barbaras, K. Gademann, *Chemotherapy* **2010**, *56*, 318–324. d) S. Bonazzi, D. Barbaras, L. Patiny, R. Scopelliti, P. Schneider, S. T. Cole, M. Kaiser, R. Brun, K. Gademann, *Bioorg. Med. Chem.* **2010**, *18*, 1464–1476.

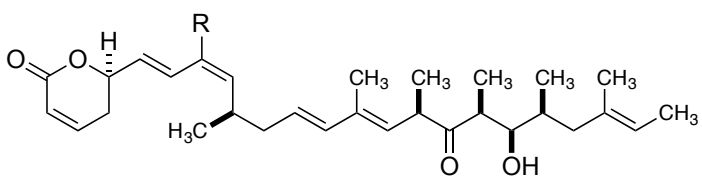

Anguinomycin C (**3.13**): R = CH_3
Anguinomycin D (**3.14**): R = C_2H_5

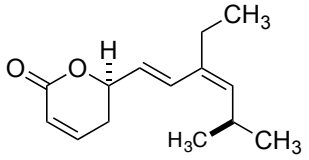

Analog **3.15**

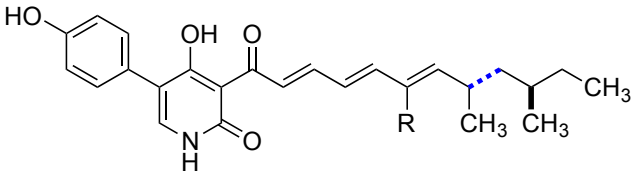

Farinosone A (**3.2**): R = H, **double bond**
Militarinone D (**3.3**): R = CH_3 (*R*), **single bond**

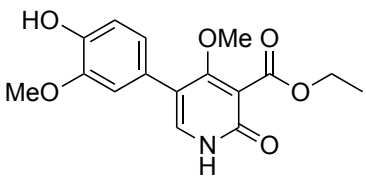

Analog **3.17**

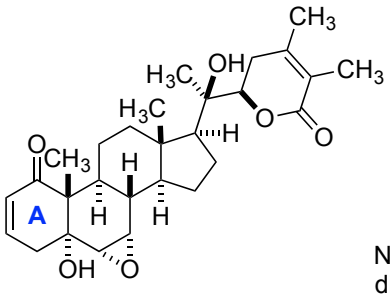

Withanolid A (**3.18**)

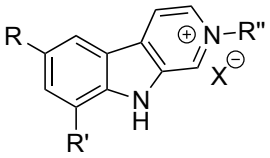

Nostocarboline (**3.19**): R = Cl, R' = H, R=CH_3, X = I
dimers where connected with different linkers
at the R" position

Figure 3.2. FOS approaches by *Gademann* and co-workers.

3.1.5 The *Rat Pheochromocytoma* PC12 Cell Assay as a Brain Model

In 1976, *Greene* and *Tischler* set the foundation for the *rat pheochromocytoma* PC12 assay. This immortal cell line was harvested from a solid tumour located in the adrenal glands from a New England Deaconess Hospital strain white rat; washed, cultivated and made accessible for the scientific community. In their publication they stated that: "*The PC12 line appears to be a useful model system for the study of numerous problems in neurobiology and neurochemistry*"[84] which is evident by hundreds of scientific contributions, including at least four originating form our laboratory.[85]

[84] L. A. Greene, A. S. Tischler, *Proc. Natl. Acad. Sci.* **1980**, *77*, 1701–1705.
[85] a) P. Burch, M. Binaghi, M. Scherer, C. Wentzel, D. Bossert, L. Eberhardt, M. Neuburger, P. Scheiffele, K. Gademann, *Chem. Eur. J.* **2013**, *19*, 2589–2591.
b) F. Schmid, H. J. Jessen, P. Burch, K. Gademann, *MedChemComm* **2013**, *4*, 135–

These cells also respond to the nerve growth factor (NGF). This neurotrophin initiates the formation and elongation of dendrites and axons.[86] Certain NP such as gelsemiol (**2.1**) promote the effects of NGF and lead to a more pronounced differentiation, but show no effect when NGF is not present.[87] Other compounds such as the ones discussed in this chapter induce neurite outgrowth without the need to supply NGF. Nevertheless, the screening is facilitated by overnight priming of the PC12 cells using 20-120 ng/mL concentration of NGF, increasing the cell sensitivity towards potential neuritogenic compounds.[88] NGF also represents our standard positive control and, thus allows for quality judgment of each single run. Even though research on neuritogenic compounds is shifting more and more towards primary cell models,[89] this relatively stable and robust *in vitro* assay does allow a chemical laboratory to efficiently screen their promising molecules in house.

The large protein NGF lacks metabolic stability and is incapable to cross the Blood-Brain-Barrier. Therefore, a NGF-based treatment of neuronal diseases would rely on direct injection of NGF in the patient's brain. Despite the fact that this approach showed acceptable results in animal studies, adaption of this procedure to humans is unpractical.[90] More promising in this regard are gene therapy-based strategies. In these approaches the NGF-expressing gene is delivered into neuronal cells using a virus vector. After successful implementation of the gene, the neurons are able to increase the NGF concentrations permanently.[91] However, one could

---

139. c) H. J. Jessen, A. Schumacher, T. Shaw, A. Pfaltz, K. Gademann, *Angew. Chem. Int. Ed.* **2011**, 4222–4226. d) H. J. Jessen, D. Barbaras, M. Hamburger, K. Gademann, *Org. Lett.* **2009**, *11*, 3446–3449.

[86] a) L. A. Greene, A. S. Tischler, *Proc. Natl. Acad. Sci.* **1976**. *7*, 2424-2428. b) I. Dikic, J. Schlessinger, I. Lax, *Curr. Biol.* **1994**, *4*, 702–708.

[87] a) Y. S. Li, K. Matsunaga, R. Kato, Y. Ohizumi, *J. Pharmacy Pharmacol.* **2001**, *53*, 915–919. b) P. Burch, M. Binaghi, M. Scherer, C. Wentzel, D. Bossert, L. Eberhardt, M. Neuburger, P. Scheiffele, K. Gademann, *Chem. Eur. J.* **2013**, *19*, 2589–2591. c) Y. S. Li, M. Ishibashi, M. Satake, Y. Oshima, Y. Ohizumi, *Chem. Pharm. Bull.* **2003**, *51*, 1103–1105.

[88] L. Trzoss, J. Xu, M. H. Lacoske, W. C. Mobley, E. A. Theodorakis, *Org. Lett.* **2011**, *13*, 4554–4557.

[89] P.-Y. Dakas, J. A. Parga, S. Höing, H. R. Schöler, J. Sterneckert, K. Kumar, H. Waldmann, *Angew. Chem. Int. Ed.* **2013**, *52*, 9576–9581.

[90] U. Bickel, T. Yoshikawa, W. M. Pardridge, *Adv. Drug Deliv. Rev.* **2001**, *46*, 247–279.

[91] a) R. J. Mandel, *Curr. Opin. Mol. Ther.* **2010**, *12*, 240–247. b) M. H. Tuszynski, L. Thal, M. Pay, D. P. Salmon, H. S. U, R. Bakay, P. Patel, A. Blesch, H. L. Vahlsing,

consider a small molecule-driven approach that would ultimately lead to an oral treatment more efficient.[92]

3.2 Results and Discussion

3.2.1 Synthesis of Farinosone C Analogs

Initially, compound **3.5** was intended to be obtained by combining L-tyrosinol hydrochloride with propionic acid using EDC and HOBt as coupling reagents, but the yields were unsatisfying. Replacing HOBt/EDC with PyBoB also gave in impractical results and the combination the DMF/THF as solvent mixture in both cases was inconvenient regarding its removal. We then tried the Schotten-Baumann method, which employs a biphasic solvent mixture of H_2O and THF (or MeCN in some cases) in combination with the respective acid chloride and potassium carbonate.[93] With this method, the amide **3.5** could be obtained in high yields. This method was then used to perform most of the corresponding amide formations. We noted that if the acid chloride is added approximately 0.5 h later, the reactions proceeded with higher yields and less reaction times. This might be due to the fact that if the amine is deprotonated beforehand, it will react faster with the acid chloride, thereby reducing the ability of the acid chloride to decompose. Using this method, all target compounds expect **3.20s,p,l** could be successfully prepared in yields ranging form 9 to 99% (Fig. 3.2 and Table 3.1).

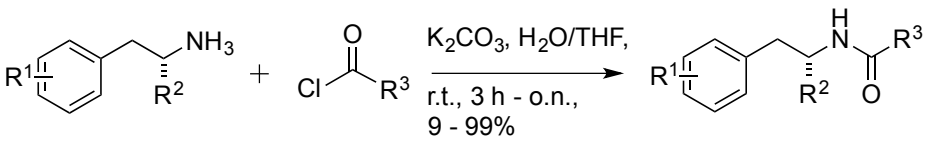

Scheme 3.2. General procedure for the tyrosinol amide synthesis.

G. Ho, *et al*., *Nat Med* **2005**, *11*, 551–555. a) E. D. Roberson, L. Mucke, *Science* **2006**, *314*, 781–784.

[92] F. M. Longo, S. M. Massa, *Nat. Rev. Drug Discovery* **2013**, *12*, 507–525.

[93] L. Kürti, B. Czako, *Strategic Applications of Named Reactions in Organic Synthesis: Background and Detailed Mechanisms*, Elsevier, Amsterdam, **2005**.

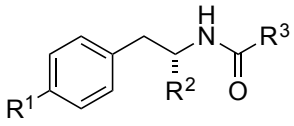

Cpd	R^1	R^2	R^3
3.5	OH	CH_2OH	CH_2CH_3
3.20a	H	CH_2OH	CH_2CH_3
3.20b	OCH_3	CH_2OH	CH_2CH_3
3.20c	$OCOCH_2CH_3$	CH_2OH	CH_2CH_3
3.20d	OH	CH_2OCH_3	CH_2CH_3
3.20f	OCH_3	CH_2OCH_3	CH_2CH_3
3.20g	OH	COOH	CH_2CH_3
3.20h	OH	$COOCH_3$	CH_2CH_3
3.20j	OH	H	CH_2CH_3
3.20m	OH	CH_2OH	Ph
3.20n	OH	CH_2OH	$CH(CH_3)_2$
3.20o	OH	CH_2OH	$C(CH_3)_3$
3.20r	OH	CH_2OH	$(CH_2)_7CH_3$
3.20s	OH	CH_2OH	$(CH_2)_7COOH$
3.20t	OH	CH_2OH	$(CH_2)_7OH$

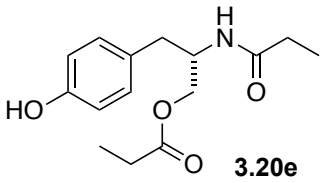

3.20e

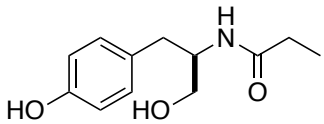

3.20i

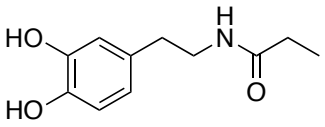

3.20k

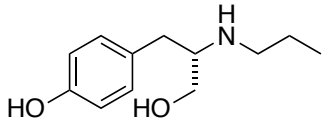

3.20l

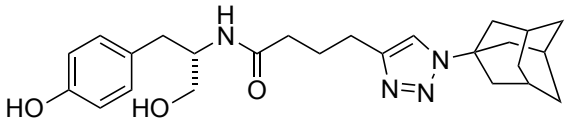

3.20p

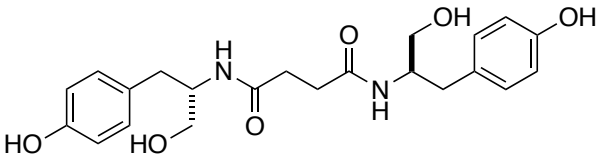

3.20q

Table 3.1. Complete farinosone C analog (**3.5**, **3.20a-t**) collection.

During the production of compound **3.5** the two isomeric diester side products **3.20c** and **3.20r** were also formed and therefore added to the analog collection. ^{1}H NMR analysis of the OH signals of each isomer allowed differentiation of their structures. The phenolic proton signal of **3.20e** is more downfield shifted than the primary alcohol of **3.20c** as shown in the spectra below (Fig. 3.3).

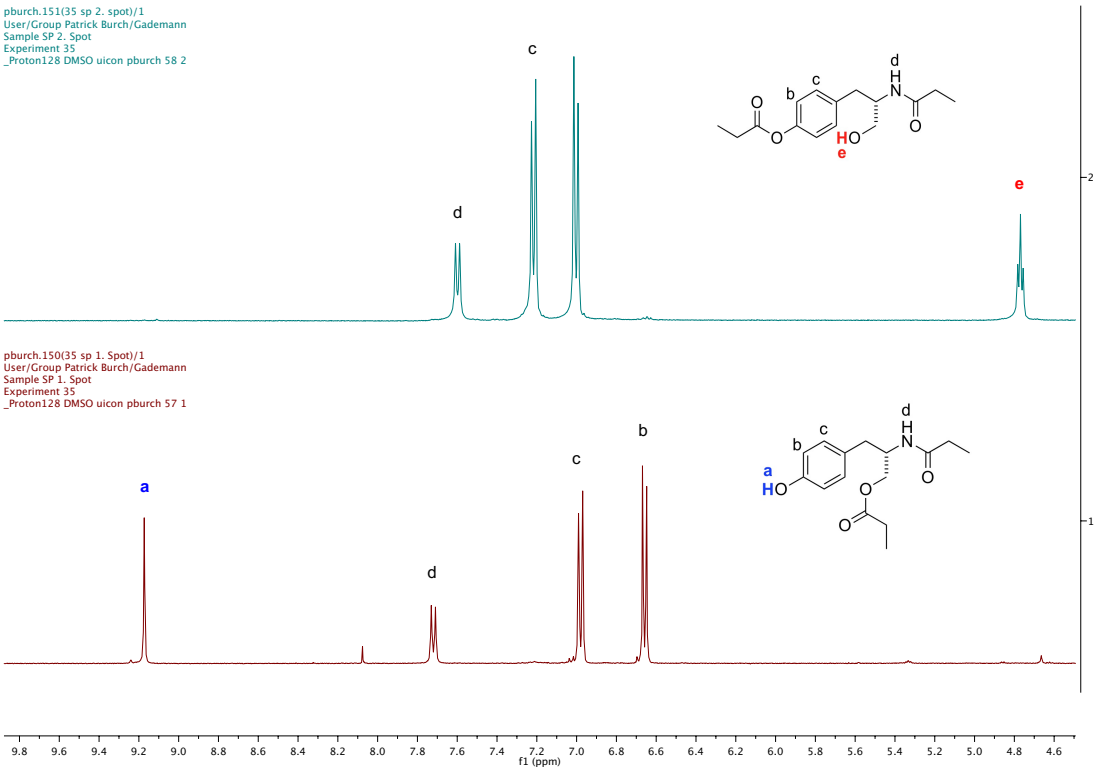

Figure 3.3. ^{1}H NMR in deuterated DMSO of the diesters **3.20c** (upper) and **3.20e** (lower).

Selective methylation of the hydroxyl groups was accomplished using caesium carbonate as base in combination with methyl iodide.[94] Mostly methylation of the phenolic hydroxyl group **3.20b** and a minor amount the dimethylated product **3.20e** were observed (Scheme 3.3).

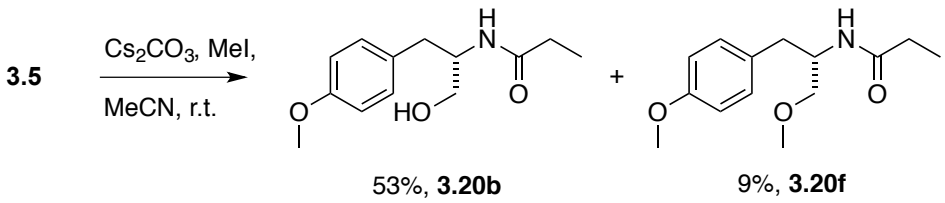

Scheme 3.3. Selective phenolic hydroxyl group methylation.

[94] G. Balboni, V. Onnis, C. Congiu, M. Zotti, Y. Sasaki, A. Ambo, S. D. Bryant, Y. Jinsmaa, L. H. Lazarus, I. Lazzari, *Bioorg. Med. Chem.* **2007**, *15*, 3143–3151.

The selective methylation of the less basic, primary alcohol was not as straightforward. Therefore, the previously prepared methyl ester **3.20h** was protected with TBSCl using a catalytic amount of DMAP. Then, the protected methyl ester **3.21** was reduced employing $LiAlH_4$ to furnish the primary alcohol **3.22**. This alcohol was then methylated utilizing methyl iodide and sodium hydride, followed by a TBAF deprotection yielding ether **3.20d** (Scheme 3.4).

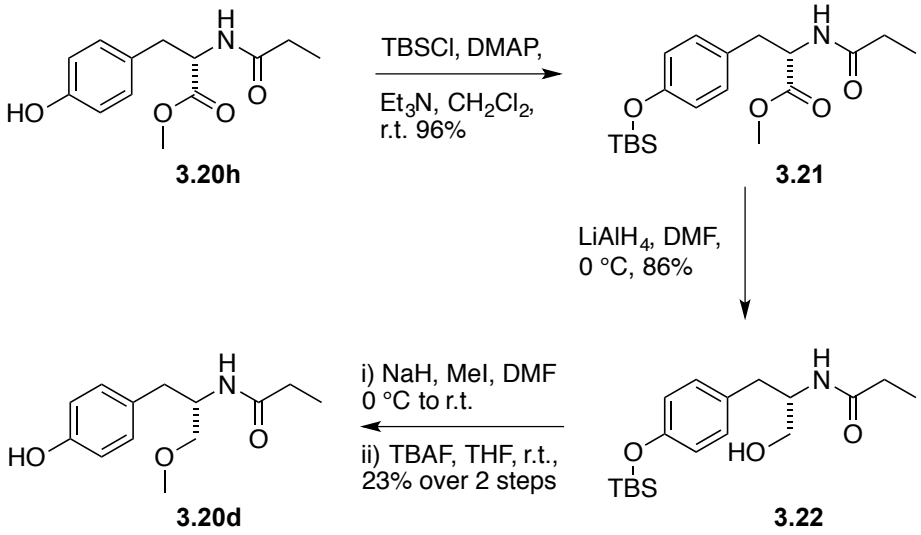

Scheme 3.4. Methylation of the primary alcohol **3.20d**.

Reduction of the carbonyl functionality was more challenging than anticipated. First attempts with $LiAlH_4$, even under refluxing conditions, demonstrated no reactivity. Activation of the amide function with TMSCl in combination with HMDS, followed by reduction with BH_3-DMS complex solution was unsuccessful as well, even though this approach was applied for the synthesis of similar compounds, as it will be discussed in chapter 4. The same was observed for the reductive amination with L-tyrosinol (**3.23**) and propionaldehyde. At this point, we turned our synthetic efforts towards a direction we wanted to avoid in the first place: 1-bromopropane (1 equiv.) was added to a solution of L-tyrosinol (1 equiv.) and potassium carbonate in a mixture of THF/H_2O. At room temperature no reactivity was observed, but at 70 °C, the expected overalkylation occurred. ^{1}H NMR and UPLC analysis (data not shown) indicated that all three possible dialkylation products and one monoalkylated product were formed. Neither temperature reduction to 45 °C nor change of the base to Et_3N or DBU in DMF improved selectivity. We then reduced the amount of 1-bromopropane to 0.5 equiv. and tried the aforementioned Schotten-Baumann conditions. UPLC analysis revealed mainly the monoalkylated

product and semi-preparative HPLC separation yielded the pure amine **3.20l** in 39% yield.

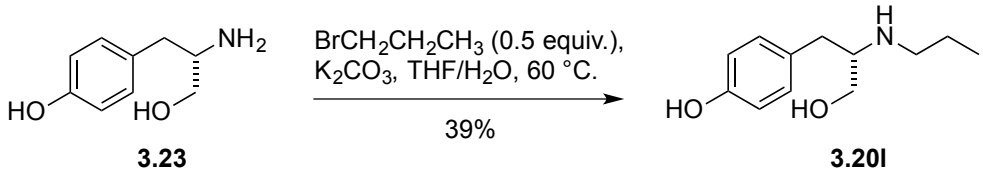

Scheme 3.5. Synthesis of amine **3.20q**.

The adamantyl derivative **3.20p** was synthesized employing the copper-catalyzed Huisgen 1,3-dipolar cycloaddition, commonly known as the "click reaction". To improve the process, TBTA **3.24** was added as catalyst (Scheme 3.5). *Sharpless* and *Fokin* noticed in early mechanistic investigations that the reaction rates of some polyvalent substrates were remarkably high and that these "click reactions" were autocatalytic. They then prepared and screened a collection of polyvalent triazoles and discovered that TBTA **3.24** (Scheme 3.6) was able to accelerate the model reaction the most; the [1,2,3]-triazole groups and the tertiary amine were postulated to work therefore in concert. The amine nitrogen is expected to provide additional electron density to the copper, which results in a higher reactivity. The [1,2,3]-triazole rings on the other hand shield the metal centre from potential destabilizing interactions but nevertheless are labile enough to allow the copper(I)-acetylide/ligand complex formation. This complex is then carried through the catalytic cycle.[95]

[95] T. R. Chan, R. Hilgraf, K. B. Sharpless, V. V. Fokin, *Org. Lett.* **2004**, *6*, 2853–2855.

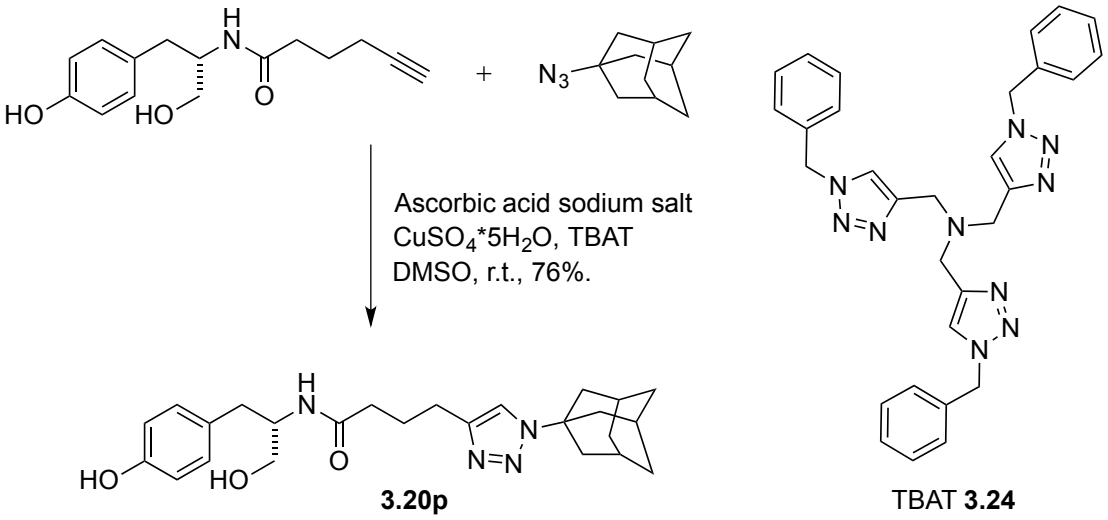

Scheme 3.6. Synthesis of the [1,2,3]-triazole analog **3.20p**.

The formation oft the acid **3.20s** was accomplished by monoactivation of suberic acid (**3.25**) with pentafluorophenol (PFP) using EDC after direct amide coupling approaches with ByPoP failed. The activated PFP-ester was reacted with L-tyrosinol (**3.23**) under basic conditions (Scheme 3.6).[96] Regular flash chromatography proved to be insufficient for purification, but preparative HPLC gave rise to the pure acid (**3.20s**). This amphipilic product crystalized and was investigated by X-ray diffraction analysis (chapter 7).

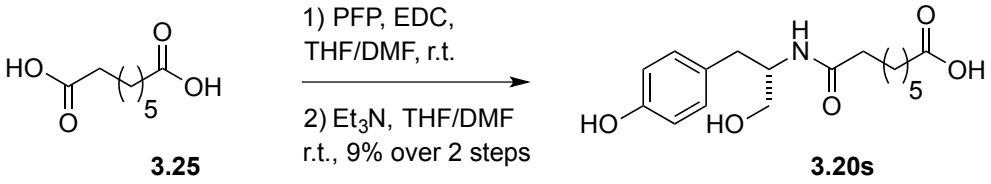

Scheme 3.6. Synthesis of the acid analog **3.20s**.

3.2.2 Structure-Activity Relationship Study Results

First, the role of the phenolic OH group was evaluated. Since phenols are known to be easily oxidized in an enzymatic environment,[97] we envisioned that the removal (→ **3.20a**), methylation (→**3.20b**) or esterification (→**3.20c**) of the hydroxyl group might be beneficial for metabolic stability. However, all these modifications led

[96] K. J. Hamblett, B. B. Kegley, D. K. Hamlin, M.-K. Chyan, D. E. Hyre, O. W. Press, D. S. Wilbur, P. S. Stayton, *Bioconjugate. Chem.* **2002**, *13*, 588–598.
[97] A. M. Mayer, *Phytochem.* **2006**, *67*, 2318–2331.

to a complete loss of bioactivity, which suggested that this functional group is essential for activity. The role of the primary hydroxyl group was investigated next. Again, methylation and esterification were not tolerated, as the corresponding compounds **3.20d** and **3.20e** were found to be inactive, as was the doubly methylated compound **3.20f**. Interestingly, however, oxidation to the carboxylic acid **3.20g** and derivatization to its methyl ester analog **3.20h** led to biologically active compounds. We then investigated the influence of the stereogenic center: Formation of the D-tyrosinol-propionamide **3.20i** or complete removal of the CH_2OH side chain in **3.20j** resulted in inactivity, showing that the presence of the hydroxymethylene moiety in the (*S*)-configuration is mandatory for neuritogenic activity. The close catechol analog of **3.20j**, the dopaminyl propanoate (**3.20k**) caused cytotoxicity at our standard concentration of 50 µM and was inactive at 5 µM. The amide moiety was also shown to be essential, as the secondary amine **3.20l** was inactive. Modifications of the amide only tolerated a planar aromatic substituent (→**3.20m**), as the more 3D space demanding isobutyramide **3.20n** and pivalamide analogs **3.20o** displayed no significant activity.

With these results in hand, we turned our attention towards the alkyl chain, the part of farinosone C (**3.4**) that had synthetically been the most demanding. The very bulky triazole-adamantyl derivative **3.20p** was not active, however the dimer **3.20q** of the L-tyrosinol-propionamide (**3.5**) showed significant bioactivity. Finally, we were interested in the role of the acidic terminus of farinosone C (**3.5**). It appears that a polar terminus is required for the long chain aliphatic compounds, as the apolar amide **3.20r** showed no activity. Terminal acid **3.20s** and the terminal alcohol **3.20t** showed good activity; the latter compound was even able to induce cell differentiation at 10 µM concentration, thus rendering the triol **3.20t** an even more potent compound than the parent NP (**3.4**). This interesting result demonstrated that the synthetically challenging side chain of farinosone C (**3.4**) can be replaced by an unbranched and fully saturated one.

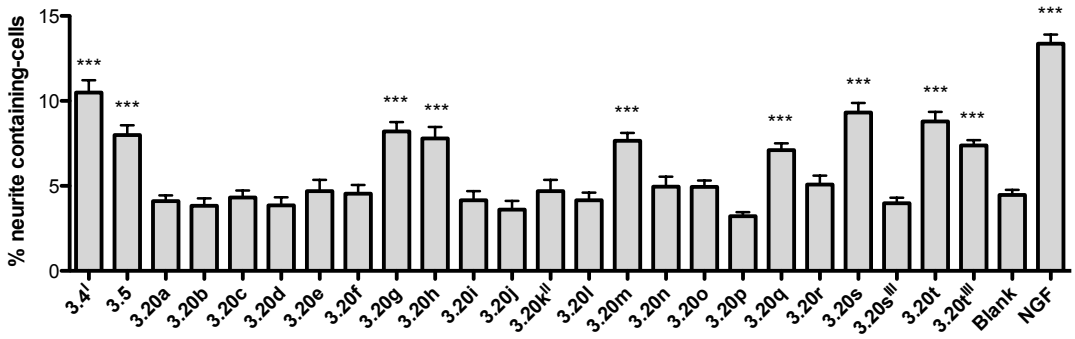

Figure 3.3. Neuritogenic activity of the simplified farinosone C analogs in the PC12 assay. All values were determined at 50 µM, except; I: 20 µM, II: 5 µM, III: 10 µM. Positive control: Nerve growth factor (NGF): 20 ng mL^{-1}. Solvent

3.3 Conclusion

With our synthesized collection of farinosone C analogs we were able to differentiate the essential from the non-essential structural moieties from farinosone C (**3.4**) as summarized in figure 3.4.

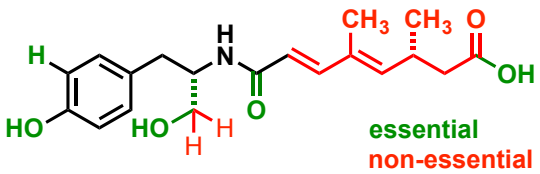

Farinosone C (**3.4**)

Figure 3.4. Visual summary of the SAR study results.

It was demonstrated that the branched and unsatured side chain can be simplified or truncated. The phenolic hydroxyl group allowed no alteration, but the primary one did to a certain extend. This SAR study unearthed six novel active molecules **3.20f,g,m,q,s,t**, of which the triol **3.20t** possessed superior neurotrophin-like functionality than the parental NP **3.4** itself, but with much reduced molecular complexity. Both can be obtained from cheap commercial starting materials in one step, hereby fulfilling the economical requirements outlined in chapter 1.

CHAPTER 4 - INVESTIGATIONS ON THE MODE OF ACTION AND MOLECULAR TARGETS OF NEURONAL DIFFERENTIATION

4

4.1 Introduction

4.1.1 General Overview and Known Pathways

Reported NP and their analogs with neuritogenic properties are numerous. Only in the first half of 2013, at least seven new compounds from four different molecule classes have been reported.[98] But, the underlying biological pathways involved in neuronal cell differentiation are only partially understood. It is *e.g.* known that $MEK_{1/2}$, also called MAP kinases, which function in a mitogen-activated protein kinase cascade, can control cell differentiation and growth. In PC12 cells, this pathway can be activated *via* NGF. It has been shown that if $MEK_{1/2}$ are inhibited using the selective antagonist PD 098059 (**4.1**, Fig. 4.1), NGF cannot induce cell differentiation further.[99] We then showed that the neuritogenic activity of the pyridone SF33 (**3.16**), the truncated NP analog introduced in section 3.1.4, can also be suppressed by $MEK_{1/2}$ inhibition using antagonist **4.1**. This led to the assumption that the mode of action for **3.1** is involving the MAP kinase pathway.[100] Nonetheless, from this data we cannot define the molecular binding site, hereafter referred to as target, which **4.1** preferentially modulates, initiating the signal cascade that results in morphological changes. In general, it can be stated that not much is known about the targets to which neuritogenic small molecules bind to thereby triggering cell differentiation. Therefore we started a program to shed some more light on the mode of action and the targets involved in neuronal cell differentiation.

---

[98] a) P.-Y. Dakas, J. A. Parga, S. Höing, H. R. Schöler, J. Sterneckert, K. Kumar, H. Waldmann, *Angew. Chem. Int. Ed.* **2013**, *52*, 9576–9581. b) M. B. Hadimani, M. K. Purohit, C. Vanampally, R. Van der Ploeg, V. Arballo, D. Morrow, K. E. Frizzi, N. A. Calcutt, P. Fernyhough, L. P. Kotra, *J. Med. Chem.* **2013**, *56*, 5071–5078. c) M. Kubo, R. Ishii, Y. Ishino, K. Harada, N. Matsui, M. Akagi, E. Kato, S. Hosoda, Y. Fukuyama, *J. Nat. Prod.* **2013**, *76*, 769–773.

[99] a) D. R. Alessi, A. Cuenda, P. Cohen, D. T. Dudley, A. R. Saltiel, *J. Biol. Chem.* **1995**, *270*, 27489–27494. b) L. Pang, T. Sawada, S. J. Decker, A. R. Saltiel, *J. Biol. Chem.* **1995**, *270*, 13585–13588. c) C. M. Crews, A. Alessandrini, R. L. Erikson, *Science* **1992**, *258*, 478–480.

[100] F. Schmid, H. J. Jessen, P. Burch, K. Gademann, *MedChemComm*, **2013**, 4, 135–139.

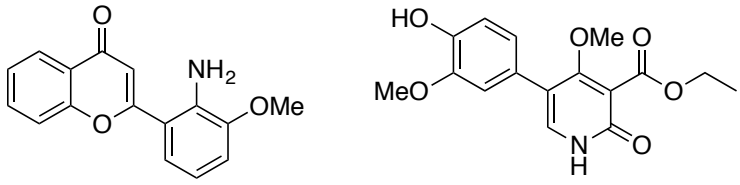

PD 098059 (**4.1**) SF33 (**3.16**)

Fig. 4.1. The selective $MEK_{1/2}$ antagonist (**4.1**) and SF33 (**3.16**).

4.1.2 Neuritogenic Natural Products Bearing Long Alkyl Chains

Several neurotrophin-like NP and close analogs are reported which bear long aliphatic chains such as lembehyne A (**4.2**),[101] docosahexaenoic acid (**4.3**)[102] and gentiside B (**4.4**, Fig.4.2).[103] An analog of the latter compound will be further discussed in in chapter 5.

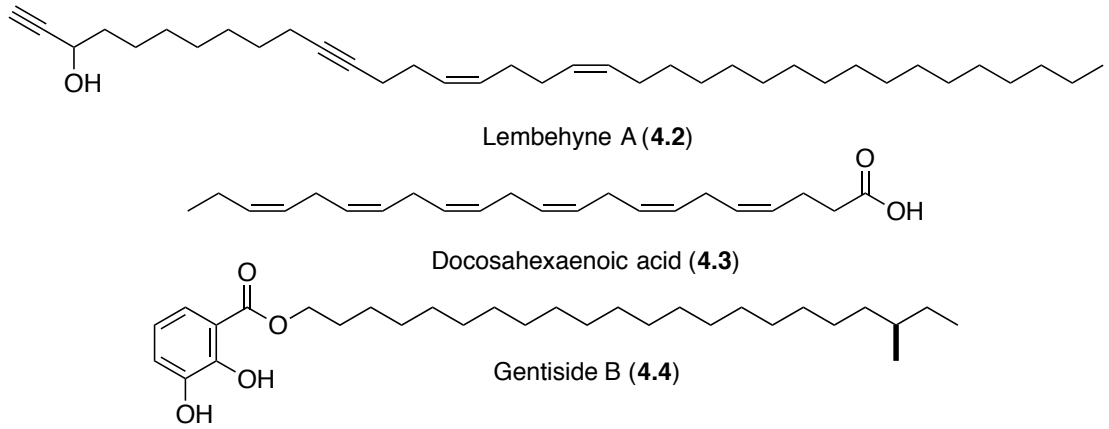

Fig. 4.2. Neurotrophin-like natural products bearing long alkyl chains.

However, our compounds of interest are the tryptamine-derived alkaloids isolated from the seeds of *Annona atemoya* and initially reported with no associated bioactivity.[104] Due to the structural similarity with melatonin (**4.5**, Table 4.1), which is known to initiate neuronal differentiation, *Figadère* and co-workers investigated

[101] a) S. Aoki, K. Matsui, T. Takata, W. Hong, *Biochem. Biophys. Res. Commun.* **2001**, 558–563. b) F. Schmidt, P. Champy, B. Seon-Meniel, X. Franck, R. Raisman-Vozari, B. Figadere, *Plos One* **2009**, *4*, e6215.
[102] F. Calderon, H.-Y. Kim, *J. Neurochem.* **2004**, *90*, 979–988.
[103] a) Y. Luo, K. Sun, L. Li, L. Gao, G. Wang, Y. Qu, L. Xiang, L. Chen, Y. Hu, J. Qi, *ChemMedChem* **2011**, *6*, 1986–1989. b) L. Gao, L. Xiang, Y. Luo, G. Wang, J. Li, J. Qi, *Bioorg. Med. Chem.* **2010**, *18*, 6995–7000. c) J. Qi, Y. Luo, L. Gao, *Mini-Rev. Med. Chem.* **2011**, 658–677.
[104] M. Leboeuf, A. Caré, M. E. Tohami, J. Pusset, *J. Nat. Prod.* **1982**, 617–623.

this compound class in more detail. They performed an SAR study using primary dopaminergic neurons, which indeed confirmed their hypothesis and identified several potent novel neurotrophin-like melatonin derivatives. Table 4.1 shows the 18 NP and close analogs, which were synthesized and evaluated. At a 10 nM concentration, all compounds showed some bioactivity, but four (**4.6c,l,q,r,** highlighted in red) showed superior neuritogenic properties. They found that the length of the aliphatic chains is crucial, with the strongest hits all bearing a 16-atom chain. Another general trend observed was that secondary amines were more active than the amides. Unsaturated aliphatic chains are also well tolerated, even when the chain length is increased by two carbon atoms.[105]

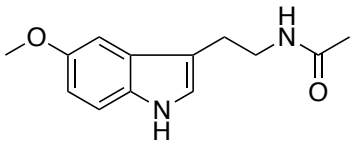

Melatonin (**4.5**)

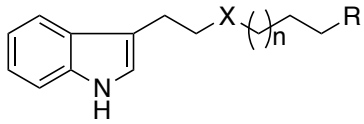

Gerneral structure

Cpd	X	n	R	Cpd	X	n	R
4.6a	NH_2–C=O	9	CH_3	**4.6j**	NH_2–CH_2	9	CH_3
4.6b	NH_2–C=O	11	CH_3	**4.6k**	NH_2–CH_2	11	CH_3
4.6c	NH_2–C=O	12	CH_3	**4.6l**	NH_2–CH_2	12	CH_3
4.6d	NH_2–C=O	13	CH_3	**4.6m**	NH_2–CH_2	13	CH_3
4.6e	NH_2–C=O	14	CH_3	**4.6n**	NH_2–CH_2	14	CH_3
4.6f	NH_2–C=O	16	CH_3	**4.6o**	NH_2–CH_2	16	CH_3
4.6g	NH_2–C=O	19	CH_3	**4.6p**	NH_2–CH_2	19	CH_3
4.6h	NH_2–C=O	5	∇	**4.6q**	NH_2–CH_2	5	∇
4.6i	NH_2–C=O	11	OH	**4.6r**	NH_2–CH_2	11	OH

Table 4.1. NP and close analogs used in the SAR study of *Figadère*.
∇ = [CH=CH–CH_2–CH=CH–$(CH_2)_4$–CH_3].[107]

[105] F. Schmidt, G. Le Douaron, P. Champy, M. Amar, B. Seon-Meniel, R. Raisman-Vozari, B. Figadere, *Bioorg. Med. Chem.* **2010**, *18*, 5103–5113.

4.1.3 Similarity Ensemble Approach

Information technology has fundamentally changed our daily life but also had a big impact on chemistry and drug discovery in particular, as exemplified by the 2013 Nobel Prize in chemistry. In this field, the techniques can be separated into two major principles: the ligand-based or receptor-based approach. Pharmaceutical research is applying these two strategies in combination with fragment-based lead discovery. Together these two approaches are considered to be complementary to high-throughput screening that has become the primary source of innovation for several pharmaceutical enterprises, which will be discussed later. As the name already suggests, an accurate 3D receptor model is required for a receptor-based approach. Virtual screening then allows analysis of enormous compound collections to find appropriate chemical keys for the particular lock. In ligand-based or chemocentric approaches, the structural features of a given ligand can virtually be screened against thousands of ligands of which the molecular target is known. Several methods are known for ligand- and receptor based-approaches and a combination of both is possible if required.[106] Besides making the discovery of lead structures more efficient, computational approaches also aim to estimate the safety of potential drugs. Often, promising drug candidates fail in late-stage clinical trials due to adverse side effects and toxicity issues, which represents a tremendous financial loss. Consequently, possible adverse effects of a drug candidate should be predicted and confirmed as early as possible in the development process (also see section 4.1.5). With *in silico* assessments, researchers also aim to reduce animal testing, where financial recourses are not the only concern that has to be considered.[107]

One ligand-based technique is called Similarity Ensemble Approach (SEA) developed by *Shoichet* and colleagues.[108] This program relates receptors to each other quantitatively based on the structural similarity of their binding ligands. In this seminal study, they applied 246 drug relevant receptor subsets. For each subset, the binding affinities of multiple ligands are known, resulting in a total number of over

[106] a) Y. Tanrikulu, G. Schneider, *Nat. Rev. Drug Discovery* **2008**, *7*, 667–677. b) J. Hert, P. Willett, D. J. Wilton, P. Acklin, *J. Chem. Inf. Modl.* **2006**. *46*, 462-470.
[107] a) A. Vedani, M. Dobler, M. Smieško, *Toxicol. Appl. Pharm.* **2012**, *261*, 142-153. b) S. Eid, A. Zalewski, M. Smieško, B. Ernst, A. Vedani, *IJMS* **2013**, *14*, 684–700.
[108] a) M. J. Keiser, B. L. Roth, B. N. Armbruster, P. Ernsberger, J. J. Irwin, B. K. Shoichet, *Nat. Biotech.* **2007**, *25*, 197–206. b) www.sea.bkslab.org/search

65'000 ligands. Then, every ligand of each subset was compared to each ligand in every other set. If two ligand ensembles (or sets) score high regarding structural similarity, the two receptors subsets can quantitatively be related and visually mapped in close proximity. With this information, medicinal chemists have an indication which other receptor types are likely to interfere if a particular compound is developed as a drug candidate. This approach was proven valid since its results are in accordance with known polypharmacological interactions. This method also allows investigations of molecules not related to a certain protein target by comparing its chemical topology to the previously investigated 65'000 ligands.[109]

4.1.4 The Endocannabinoid System

The hemp plant *Cannabis sativa L.* has been used by humans for either ritualistic or therapeutic purposes, dating back 5'000 years ago, starting in China. Over the centuries, traditional medicine used extracts of *Cannabis sativa L.* to treat various medical conditions such as pain or loss of appetite.[110] Despite the constant medical use of cannabis, it was not before 1964 until *Gaoni* and *Mechoulam* isolated and characterized the main psychoactive constituent from this plant: Δ^9-tetrahydrocannabinol (THC, **4.7**, Fig. 4.3) and reported its first total synthesis one year after.[111] In 1990 *Matsuda*[112] and, three years later, *Abu-Shaar*[113] identified and cloned cannabinoid (CB) receptors 1 and 2, which are the cellular targets of THC **4.7** and other natural cannabinoids.[114] The two receptors display a divergent distribution pattern throughout the organisms; CB_1 is mainly found in the central nervous system and CB_2 in the peripheral and immune cells.[115]

---

[109] M. J. Keiser, B. L. Roth, B. N. Armbruster, P. Ernsberger, J. J. Irwin, B. K. Shoichet, *Nat. Biotech.* **2007**, *25*, 197–206.
[110] D. M. Lambert, C. J. Fowler, *J. Med. Chem.* **2005**, *48*, 5059–5087.
[111] a) Y. Gaoni, R. Mechoulam, *J. Am. Chem. Soc.* **1964**, *86*, 1646–1647. b) R. Mechoulam, Y. Gaoni, *J. Am. Chem. Soc.* **1965**, *87*, 3273–3275.
[112] L. A. Matsuda, S. J. Lolait, M. J. Brownstein, A. C. Young, T. I. Bonner, *Nature* **1990**, *346*, 561–564.
[113] S. Munro, K. L. Thomas, M. Abu-Shaar, *Nature* **1993**, *365*, 61–65.
[114] Cannabinoids: compounds, which bind to the $CB_{1/2}$ receptors
[115] D. M. Lambert, C. J. Fowler, *J. Med. Chem.* **2005**, *48*, 5059–5087.

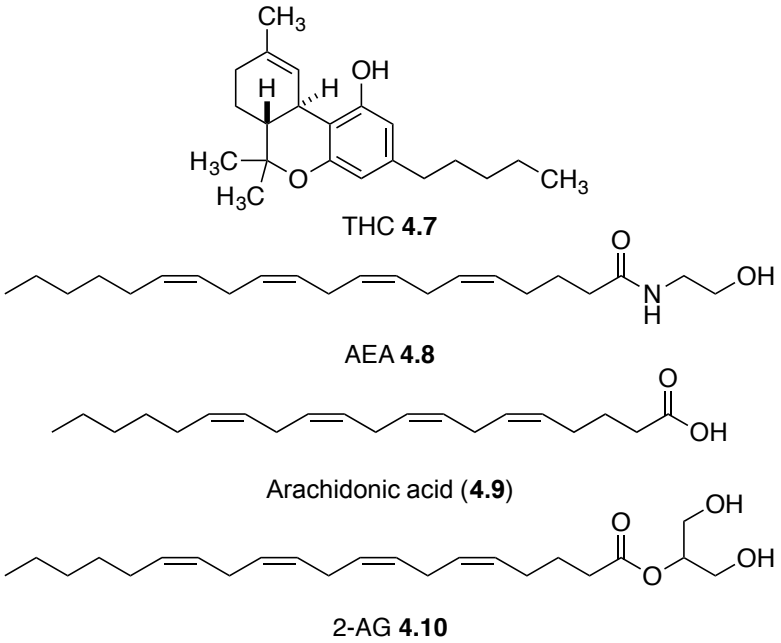

Fig 4.3. THC **4.7**, arachidonic acid (**4.9**) and the two main endocannabinoids AEA **4.8** and 2-AG **4.10**.

Once the cannabinoid receptors were discovered, research focused on the identification of the endogenous ligands that would modulate these receptors. Because THC **4.7** is rather lipophilic, extraction approaches focused on apolar substances. Anandamide (AEA, **4.8**) was the first endogenous cannabinoid (endocannabinoid) discovered.[116] Other endocannabinoids where then reported in high frequency, most derived from arachidonic acid (**4.9**), of which 2-arachidonylglycerol (2-AG, **4.10**) is the most prominent.[117] Other important pillars of the endocannabinoid system (ECS) signalling processes include the fatty acid amide hydrolase (FAAH), the monoacylglycerol lipase (MAGL) and the α,β-hydrolase-6 and -12 (ABHD-6 and -12) which end the bioactivity of AEA **4.8** or 2-AG **4.10**, respectively after cellular re-uptake.[120] Additionally, the putative bidirectional endocannabinoid membrane transporter (EMT) has also become a dynamic research topic establishing an

[116] W. Devane, L. Hanus, A. Breuer, R. Pertwee, L. Stevenson, G. Griffin, D. Gibson, A. Mandelbaum, A. Etinger, R. Mechoulam, *Science* **1992**, *258*, 1946–1949.
[117] R. Mechoulam, S. Ben-Shabat, L. Hanus, M. Ligumsky, N. E. Kaminski, A. R. Schatz, A. Gopher, S. Almog, B. R. Martin, D. R. Compton, *et al., Biochem. Pharmacol*. **1995**, *50*, 83–90.
[118] a) M. K. McKinney, B. F. Cravatt, *Annu. Rev. Biochem*. **2005**, *1*, 411–432. b) A. Chicca, J. Marazzi, S. Nicolussi, J. Gertsch, *J. Biological Chem*. **2012**, *287*, 34660–34682. c) T. P. Dinh, T. F. Freund, D. Piomelli, *Chem. Phys. Lipids* **2002**, 149–158.

alternative rational to passive membrane diffusion of endocannabinoids in recent years.[119]

An increasing number of pathophysiological conditions related to the ECS, such as fertility, cancer and cardiovascular diseases in addition to the previously mentioned (pain, appetite) explains the interest of the pharmaceutical industry and the multiple drug candidates which are in clinical trials now. The main entry point to modulate the ECS is *via* FAAH inhibitors.[120] Moreover, there is increasing evidence that the ECS is involved in the progression and potential healing of neurodegenerative disorders. The brain region that controls movement, *basal ganglia* is strongly disturbed by patient suffering from Parkinsons' and Huntingtons' disease. Hence these sufferings can also be classified as movement disorders, this is consistent. It has been shown that 1) CB_1 receptors are highly overexpressed in this brain area, 2) endocannabinoids are abundant in these area as well, 3) natural or synthetic cannabinoids have potent effects on motor activity and 4) people suffering from movement disorders express altered CB_1 receptors and endocannabinoid levels in that region. As a consequence, there is broad agreement that the ECS is heavily involved in the evolution of these suffering based on these and other findings.[121] The most abundant neurodegenerative disorder, Alzheimers' disease, characterised by the formation of β-amyloid (βA) plaques (also see section 4.1.7) seems to be influenced by the ECS as well. *Milton* showed that AEA (**4.8**) can prevent βA-induced toxicity.[122] Additionally, the memory deficit induced by βA admission could be improved by CB_1 receptor inhibition in animal models.[123] Others report that the

[119] a) A. Chicca, J. Marazzi, S. Nicolussi, J. Gertsch, *J. Biological Chem*. **2012**, *287*, 34660–34682. b) N. Battista, M. Di Tommaso, M. Bari, M. Maccarrone, *Front. Behav. Neurosci*. **2012**, *9*, 1-7.

[120] a) K. Ahn, S. E. Smith, M. B. Liimatta, D. Beidler, N. Sadagopan, D. T. Dudley, T. Young, P. Wren, Y. Zhang, S. Swaney, *et al*., *J. Pharm. Exp. Ther*. **2011**, *338*, 114–124. b) S. Kathuria, S. Gaetani, D. Fegley, F. Valiño, A. Duranti, A. Tontini, M. Mor, G. Tarzia, G. L. Rana, A. Calignano, *et al*., *Nat. Med*. **2002**, *9*, 76–81. c) V. Di Marzo, *Nat. Rev. Drug Discovery* **2008**, *7*, 438–455. d) E. L. Scotter, M. E. Abood, M. Glass, *Br. J. Pharmacol*. **2010**, *160*, 480–498.

[121] a) T. Nagayama, A. D. Sinor, R. P. Simon, J. Chen, S. H. Graham, K. Jin, D. A. Greenberg, *J. Org. Chem*. **1999.** b) P. Pacher, S. Bátkai, G. Kunos, *Pharmacol. Rev*. **2006**. *58*, 389-462.

[122] N. Milton, *Neurosci. Lett*. **2002**, *332*, 127–130.

[123] C. Mazzola, V. Micale, F. Drago, *Euro. J. Pharmaco*. **2003**, *477*, 219-225.

overexpression of FAAH and CB_2 receptors in brains of patients suffering from Alzheimers' disease.[124]

4.1.5 The HIP HOP Assay

Despite enormous financial costs and novel technologies, surprisingly low numbers of new drugs receive approval each year. In 2006 a study conducted by *Overington, Al-Lazikani,* and *Hopkins* counted 21'000 licenced drug products. However, when duplicates, salt forms, vitamins, supplements, along with others are removed, only 1'357 unique drugs remain. Out of these drugs, 1'204 are small molecule drugs and 166 are "biological" drugs such as therapeutic antibodies.[125] And all these drugs act on only 324 molecular targets, of which 266 are located in humans and the remaining 58 in pathogens. In 2010, only 21 new drugs had been approved by the FDA. This represents the lowest number in at least 15 years (Fig. 4.4). On the contrary, the R&D expenditures are constantly increasing and since 2002, have almost doubled, reaching over 120 billion USD in 2010. This means that the development of one new drug costs, on average, approximately five billion USD and will take around 13 years. This costs however also include unsuccessful endeavours.[126]

[124] C. Benito, E. Núñez, R. M. Tolón, E. J. Carrier, A. Rábano, C. J. Hillard, J. Romero, *J. Neurosci*. **2003**, *23*, 11136–11141.
[125] a) O. H. Brekke, I. Sandlie, *Nat. Rev. Drug Discovery* **2003**, *2*, 52–62. b) J. P. Overington, B. Al-Lazikani, A. L. Hopkins, *Nat. Rev. Drug Discovery* **2006**, *5*, 993–996.
[126] E, Pisani, *The Pharmaceutical Industry and Global Health: Facts and Figures,* IFPMA, Geneva, **2011**.

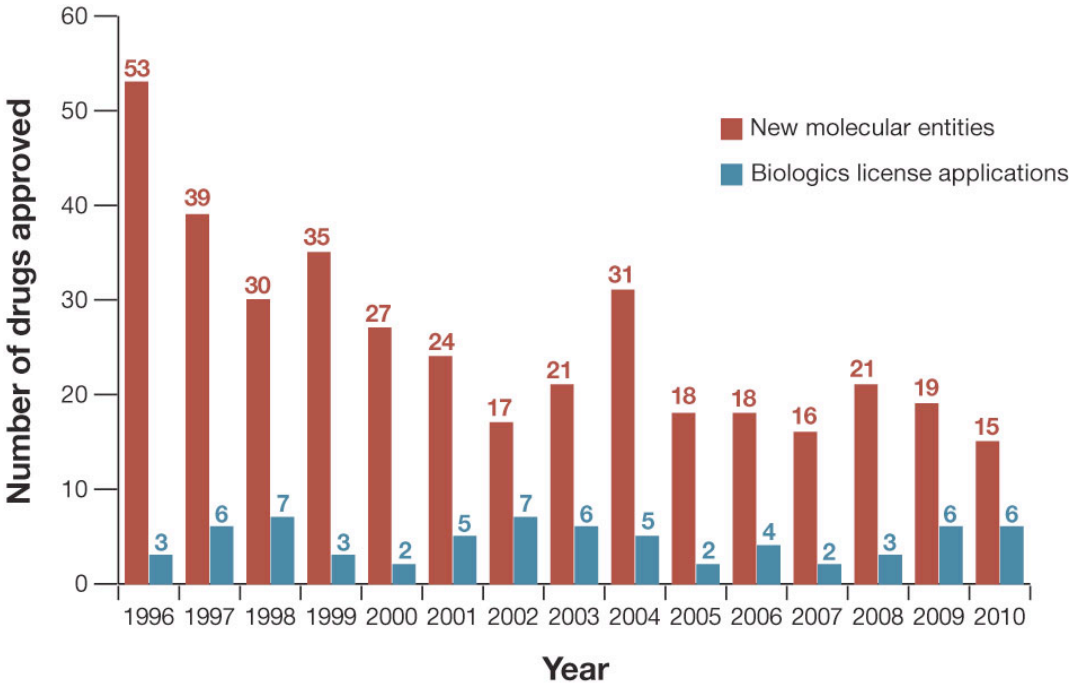

Fig. 4.4. Number of FDA approved drugs per year. (Reprinted from Ref.: 127 with permission from NPG)

While looking at these numbers, the pharmaceutical industry cannot be too confident regarding its performance and a higher efficiency should be aimed for where possible. One way in achieving this goal, are innovative, high-throughput screening platforms.[129] To build up, steadily improve and adequately operate these platforms has become a very important part of today's drug discovery. Consequently, a multitude of quite diverse methodologies have evolved, and companies consider a strong screening facility a market advantage.[128] *Novartis*, a major drug producer, operates several high-throughput screening platforms, and is the only company running a phenotypic screen using yeast *Sacharomyces cerevisiae* (the first eukaryotic genome decoded in 1995)[129] called HIP HOP assay, on this scale.

The term HIP HOP originates in this regard from **h**aplo**i**nsufficiency **p**rofiling and **ho**mozygous **p**rofiling. This screening platform can help to identify potential drug targets. While target recognition is not essential for drug development, it does

[127] M. Allison, *Nat. Biotech.* **2012**, *30*, 41–49.
[128] R. Macarron, M. N. Banks, D. Bojanic, D. J. Burns, D. A. Cirovic, T. Garyantes, D. V. S. Green, R. P. Hertzberg, W. P. Janzen, J. W. Paslay, *et al., Nat. Rev. Drug Discovery* **2011**, *10*, 188–195.
[129] S. Hoon, R. S. Onge, G. Giaever, C. Nislow, *Trends Pharmacol. Sci.* **2008**, *10*, 499-504.

facilitate the optimization of a compound's inhibitory activity. For the haploinsufficiency profiling (HIP), one functional copy of a specific gene was deleted. If one copy cannot overcome growth inhibition, this indicates supersensitive pathways that are affected directly and allows direct identification of the molecular target. In the homozygous profiling (HOP), both gene copies are deleted and the synthetic lethality is examined. Synthetic lethality occurs when a compound is able to block pathways which compensate for the deleted one.[130] This assay takes advantage on the evolutionary certainly beneficial tendency of organisms to preserve buffering schemes that grant phenotypic stability, despite genetic variation or environmental changes (scheme 4.6).[131] While homozygous profiling (HOP) is less approvingly for target identification, it can help to confirm haploinsufficiency profiling (HIP) results and more importantly, identify off-target effects of drug candidates at an early stage (also see section 4.1.4).[132]

Since each strain is labelled using a unique barcode derived from around 20 base-pairs incorporated in the DNA, microarray analysis allows to pool many different strains in the same well.[133] Then, these microorganisms are grown in the presence and absence of the compounds of interest for several generations on an automated system. Strains that are sensitive to the added chemicals are then identified by their lower relative abundance, as compared to the reference strains.[134] In the HIP case genome-wide specific gene deletion is tolerated where in the HOP case only deletion of non-essential genes are possible. Limitation of this assay include that only genes influencing the growth rate of the yeast can be detected and the fact that the investigated compounds need to be able to enter the yeast cells prior to potential gene interactions.[135]

---

[130] D. L. Richie, K. V. Thompson, C. Studer, V. C. Prindle, T. Aust, R. Riedl, D. Estoppey, J. Tao, J. A. Sexton, T. Zabawa, *et al*., *Antimicrob. Agents Chemother.* **2013**, *57*, 2272–2280.

[131] a) J. L. Hartman, B. Garvik, L. Hartwell, *Science* **2001**, *291*, 1001–1004. b) S. Hoon, R. S. Onge, G. Giaever, C. Nislow, *Trends Pharmacol. Sci.* **2008**. *10*, 499-504.

[132] S. Hoon, R. S. Onge, G. Giaever, C. Nislow, *Trends Pharmacol. Sci.* **2008**, *10,* 499-504

[133] S. E. Pierce, E. L. Fung, D. F. Jaramillo, A. M. Chu, R. W. Davis, C. Nislow, G. Giaever, *Nat. Meth.* **2006**, *3*, 601–603.

[134] D. L. Richie, K. V. Thompson, C. Studer, V. C. Prindle, T. Aust, R. Riedl, D. Estoppey, J. Tao, J. A. Sexton, T. Zabawa, *et al*., *Antimicrob. Agents Chemother.* **2013**, *57*, 2272–2280.

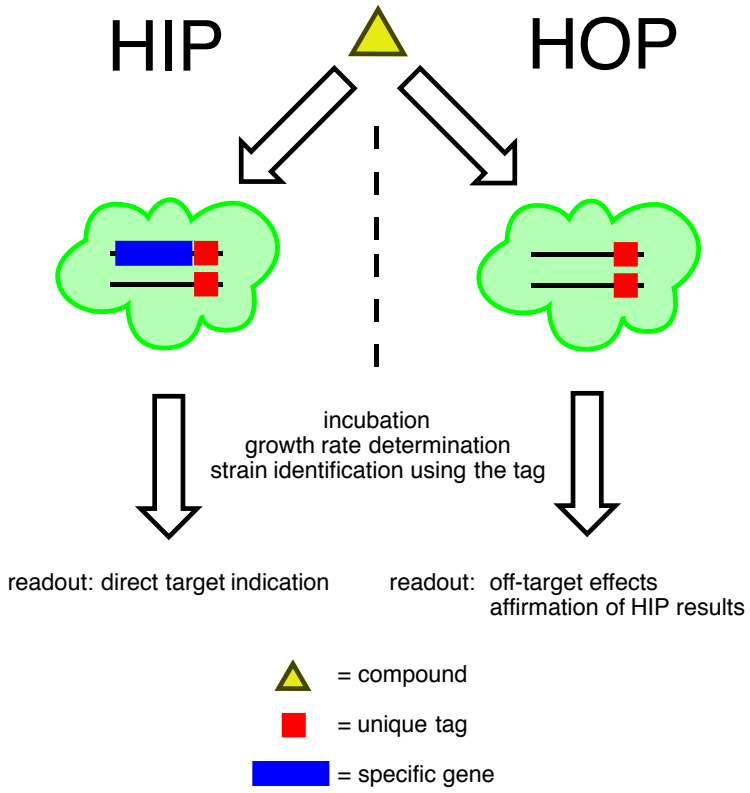

Scheme 4.6. Difference of HIP vs. HOP profiling.

4.1.6 Amphetamine-Type Designer Drugs and Potentially Psychostimulant Structural Analogs

Given that substances **3.20a-t** originating from our SAR study on farinosone C structurally resemble the psychostimulant amphetamine-type designer drugs (ATDD), in part of their molecular structure, we investigated the activity of our library at amphetamine targets in the brain. The background and dangers of ATDD effects are specified in this section. The emergence of new psychoactive designer drugs and the willingness of drug abusers to look for new alternatives to traditional ATDD make it necessary to consider the psychoactive potential of our library, ideally to demonstrate absence of any potential psychoactive effects. Thereby we prevent drug users to experiment with substances designed in accordance to our lead structure.

ATDD have long been abused for their psychostimulant properties. Well-known and popular psychostimulants are amphetamine ("speed", **4.10a**), methamphetamine ("crystal-meth", **4.10b**) and 3,4-methylenedioxymethamphetamine (MDMA, "ecstasy", **4.11a**). While amphetamine (**4.10a**) and methamphetamine

(**4.10b**) are psychostimulants, MDMA's psychoactive properties are less distinct.[135] MDMA **4.11a** triggers the feelings happiness and subjective closeness to other people.[136] The widespread popularity of these ATDD drugs revealed their dangers in the last decades. Amphetamine **4.10a** and particularly methamphetamine **4.10b** have a considerable potential for inducing addiction.[137] While MDMA **4.11a** is considered as less addictive compared to the other two **4.10a** and **4.10a**,[138] its neurotoxic potential is a matter of on-going research to finally predict the long-term impact on regular user's mental health.[139] Furthermore, ATDD are potentially life-threatening on acute dosing. Methamphetamine (**4.10b)** and MDMA **4.11a** both typically are cardiostimulants and might lead to hyperthermia. Organ failure due to untreated hyperthermia has caused many deaths in young drug users.[140] MDMA **4.11a** might also lead to brain oedema.[141] The health risks and consequences of these drugs are well understood. However, a new problem in terms of stimulant drug use emerged in the last decade. The evolution of the internet made it possible for dealers to distribute legal substances world-wide, thereby offering drug abusers a wide set of alternatives to their "traditional" ATDD.[142] By modulation of functional groups of amphetamine **4.10a**, new molecular entities with potentially psychoactive properties come into existence. Some of these ATDD **4.10a-f** (Fig. 4.7) and **4.11a-g** (Fig. 4.8) are shown. The motivation to sell or consume some of these drugs besides their psychoactivity, is the fact that they are legal, at least as long as authorities banned the single substances. This, however, drives the production of different derivatives, causing an unknown accumulation of new psychoactive drugs for availability to consumers. The European

---

[135] a) H. Kalant, *CMAJ* **2001**, *165*, 917–928. b) J. C. Cole, H. R. Sumnall, *Pharmacol. Therapeutics* **2003**, *98*, 35–58. c) C. C. Cruickshank, K. R. Dyer, *Addiction* **2009**, *104*, 1085–1099.

[136] M. Liechti, *Neuropsychopharmacology* **2000**, *22*, 513–521.

[137] A. M. Barr, W. J. Panenka, W. G. MacEwan, A. E. Thornton, D. J. Lang, W. G. Honer, T. Lecomte, *J. Psychiatry. Neurosci.* **2006**, *31*, 301–314.

[138] Z. Wang, W. L. Woolverton, *Psychopharmacology* **2006**, *189*, 483–488.

[139] a) M. H. Baumann, J. S. Partilla, K. R. Lehner, *Euro. J. Pharmaco.* **2012**, 1–5. b) J. P. Capela, H. Carmo, F. Remião, M. L. Bastos, A. Meisel, F. Carvalho, *Mol Neurobiol* **2009**, *39*, 210–271. c) J. H. Halpern, A. R. Sherwood, J. I. Hudson, S. Gruber, D. Kozin, H. G. Pope Jr, *Addiction* **2011**, *106*, 777–786.

[140] a) H. Kalant, *CMAJ* **2001**, *165*, 917–928. b) J. C. Cole, H. R. Sumnall, *Pharmacol. Therapeutics* **2003**, *98*, 35–58. c) C. C. Cruickshank, K. R. Dyer, *Addiction* **2009**, *104*, 1085–1099.

[141] H. Kalant, *CMAJ* **2001**, *165*, 917–928.

[142] S. L. Hill, S. H. L. Thomas, *Clin. Toxicol.* **2011**, *49*, 705–719.

Monitoring Centre for Drug and Drug Addiction (ECDDA) highlights in their annual report 2013 that the threat arising by these novel psychoactive substances.[143] Even though the parent molecules of these drugs are well investigated, the effects induced in humans by similar drugs can dramatically change between analogs. As an example, the pharmacology of 3,4-methylenedioxypyrovalerone (MDPV, "bath salt", **4.11g**), is unlike the pharmacology of both MDMA **4.11a** and methamphetamine (**4.10b**). MDPV **4.11g** is an extraordinarily highly potent drug that has caused enormous damages to abusers.[144] Therewith MDPV **4.11g** demonstrates that the concern about the unknown risks of new psychoactive substances is a justified one.

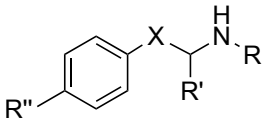

R = H, R' = CH_3, R" = H, X = CH_2 : Amphetamine (**4.10a**)
R = CH_3, R' = CH_3, R" = H, X = CH_2 : Methamphetamine (**4.10b**)
R = H, R' = CH_3, R" = H, X = CO : Cathinone (**4.10c**)
R = CH_3, R' = CH_3, R" = H, X = CO : Methcathinone (**4.10d**)
R = CH_3, R' = CH_3, R" = CH_3, X = CO : Methedrone (**4.10e**)
R = CH_3, R' = CH_3, R" = F, X = CO : Flephedrone (**4.10f**)

Figure 4.7. ATDD derived from amphetamine (**4.10a**)

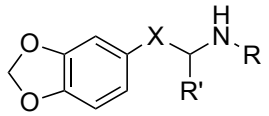

R = CH_3, R' = CH_3, X = CH_2 : MDMA (**4.11a**)
R = CH_3, R' = CH_2CH_3, X = CH_2 : MBDB (**4.11b**)
R = CH_2CH_3, R' = CH_3, X = CH_2 : MDEA (**4.11c**)
R = CH_3, R' = CH_2CH_3, X = CO : Methylone (**4.11d**)
R = CH_2CH_3, R' = CH_3, X = CO : Butylone (**4.11e**)
R = CH_3, R' = CH_2CH_3, X = CO : Ethylone (**4.11f**)

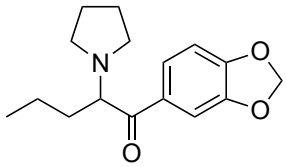

MDPV **4.11g**

Figure 4.8. ATDD derived from MDMA (**4.11a**)

[143] EMCDDA, **2013**, 1–80.
[144] a) L. D. Simmler, T. A. Buser, M. Donzelli, Y. Schramm, L.-H. Dieu, J. Huwyler, S. Chaboz, M. C. Hoener, M. E. Liechti, *Br. J. Pharmacol*. **2012**, *168*, 458–470. b) M. H. Baumann, X. Wang, R. B. Rothman, *Psychopharmacology* **2006**, *189*, 407–424.

The main site of action for these drugs is at the synapse of monoaminergic neurons present in the brain. The effects of ATDD are mainly due to re-uptake inhibition of dopamine (DA, **4.12**), norepinephrine (NE, **4.13**) and serotonin (5-hydroxytryptamine, 5-HT, **4.14**) shown in figure 4.9.

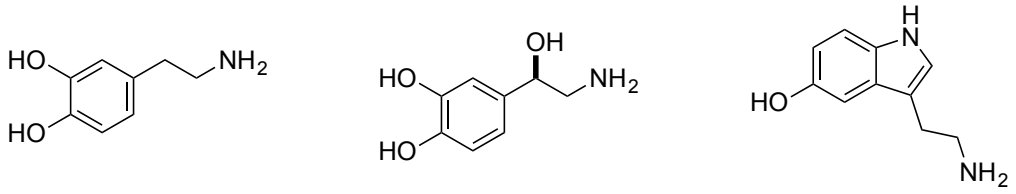

Dopamine (DA, **4.12**) Norepinephrine (NE, **4.13**) Serotonine (5-HT, **4.14**)

Figure 4.9. The neurotransmitters, which concentrations are mostly affected by ATDD.

The mode of action ATDD act is descripted as follows: The neurotransmitters are released by the presynapse, transmiting neuronal signals by binding and, therefore activating or deactivating the postsynaptic receptors. To end this signalling cascade, monoamine re-uptake transporters remove the neurotransmitters from the synaptic cleft back to the presynapse. If these transporters are inhibited by ATDD, a higher neurotransmitter concentrations results, subsequently causing profound changes in signal transmission (Fig. 4.10).[145]

[145] a) A. S. Kristensen, J. Andersen, T. N. Jorgensen, L. Sorensen, J. Eriksen, C. J. Loland, K. Stromgaard, U. Gether, *Pharmacol. Rev.* **2011**, *63*, 585–640. b) G. E. Torres, R. R. Gainetdinov, M. G. Caron, *Nat. Rev. Neurosci.* **2003**, *4*, 13–25.

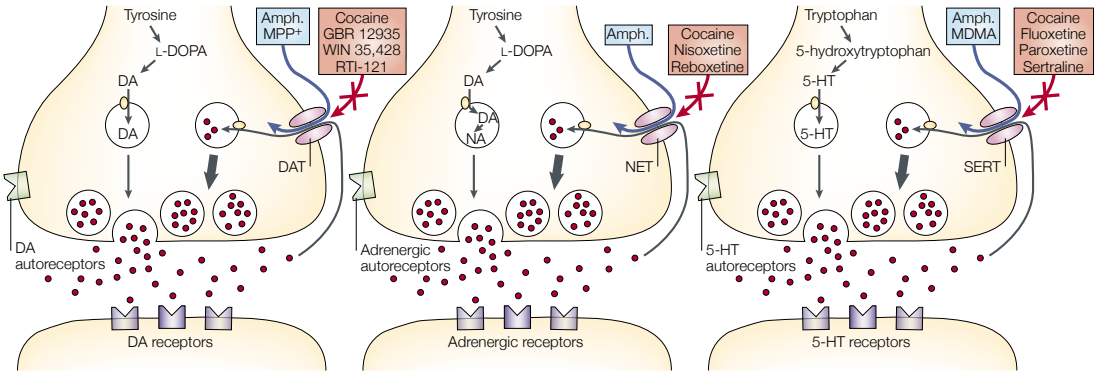

Figure 4.10. Schematic drawing of monoaminergic synapse, indicating the target transporters of ATDD, like **4.10a** and **4.11b**. These ATDD inhibit the DA (**4.12**), NE (**4.13**), and 5-HT (**4.14**) re-uptake inhibitors and prevent the transporters from neurotransmitter recycling, leading to increased neurotransmitter levels in the synaptic cleft and an increase in signal transmission. (Reprinted from Ref.: 147b with permission from NPG)

The diverse psychological and physical responses of ATDD are based on the different potencies by which they inhibit the respective monoamine transporters. The effects of MDMA **4.11a** on abusers are "entactogenic", meaning that the drug induces delightful psychotropic effects such as increased empathy and confidence or intensified sensory perception. These effects derive from an expanded serotonin (**4.14**) concentration upon MDMA's preferential action on the serotonin transporter. Methamphetamine on the other hand acts more potently on the dopamine and norepinephrine transporters. This preference results in reduced appetite, improved attention or decreased need of sleep.[146] Since these are qualities useful to soldiers, methamphetamine was widely used by military personnel during the 2nd World War on both sides.[147] Dopamine (**4.12**) is the crucial neurotransmitter involved in the development of an addiction, which explains that "crystal-meth" **4.12** causes stronger addictions than "ecstasy" **4.14**. Since a wide range of medical complications caused

[146] C. C. Cruickshank, K. R. Dyer, *Addiction* **2009**, *104*, 1085–1099.
[147] M. D. Anglin, C. Burke, B. Perrochet, E. Stamper, S. Dawud-Noursi, *J. Psy. Drugs*. **2000**, *32*, 137–141.

by ATDD are known, illegalization of these substances is reasonable to improve public health.[148]

When new psychoactive drugs appear to become popular among drug users, pharmacological studies are conducted to gain information about their possible effects and dangers for abusers. One way to address this is by *in vitro* monoamine re-uptake inhibition studies. Therefore, human embryonic kidney (HEK) 293 cells that stably express human DA, NE or 5-HT transporters, respectively, are grown in well plates.[149] Then, the compounds of interest are added before the respected tritium (^{3}H) labelled neurotransmitter. After a short incubation time, the cells are washed. After cell lysis it is then possible to determine the amount of neurotransmitter present in the cells by β–count measurements. A small radioactive signal then corresponds to a strong re-uptake inhibition.[150]

4.1.7 The MTT Assay

Our brain accounts for only a few percent of the human body weight, but demands around 20% of the oxygen consumed. This results in high levels of reactive oxygen species (ROS) and, therefore, leads to oxidative stress. Our brain evolved mechanisms to manage a certain amount of oxidative stress well. The βA peptide however is known to facilitate the formation of ROS. One of the significant characteristics of Alzheimer's disease is the βA peptide overproduction and its miss-folding, leading to the formation and deposition of βA plaques, as well as increased oxidative stress by free radicals for the brain. To address the oxidative stress problem, the consumption of external antioxidants such as phenolic phytochemicals or vitamins

[148] a) J. C. Cole, H. R. Sumnall, *Pharmacol. Therapeutics* **2003**, *98*, 35–58 b) L. D. Simmler, T. A. Buser, M. Donzelli, Y. Schramm, L.-H. Dieu, J. Huwyler, S. Chaboz, M. C. Hoener, M. E. Liechti, *Br. J. Pharmacol.* **2012**, *168*, 458–470.
[149] M. Tatsumi, K. Groshan, R. D. Blakely, E. Richelson, *Euro. J. Pharmaco.* **1997**, *340*, 249–258.
[150] a) L. D. Simmler, T. A. Buser, M. Donzelli, Y. Schramm, L.-H. Dieu, J. Huwyler, S. Chaboz, M. C. Hoener, M. E. Liechti, *Br. J. Pharmacol.* **2012**, *168*, 458–470. b) C. M. Hysek, L. D. Simmler, V. G. Nicola, N. Vischer, M. Donzelli, S. Krähenbühl, E. Grouzmann, J. Huwyler, M. C. Hoener, M. E. Liechti, *PLOS ONE,* **2012**, *7*, e36476.

seems a valid general defence strategy.[151] Since farinosone C (**3.4**) and most of its analogs contain a phenolic moiety, we aimed to examine their antioxidant properties by investigating their neuroprotective properties.[152] *Kim* developed a procedure to address this question using a modification of the widely used MTT assay.[153] MTT stands for 3-(4,5-dimethylthiazol-2-yl)-2,5-diphenyl tetrazolium bromide (**4.15**). This yellow, water soluble MTT (**4.15**) is reduced by NADH to the purple and insoluble formazan (**4.16**) inside living cells. After a given time, the growth medium is replaced by DMSO, which solubilizes the dye (**4.16**). Since only living cells can reduce MTT, absorption measurements allow for quantitative determination of viability. The more purple a solution is, the more cells survived a given conditions.[154]

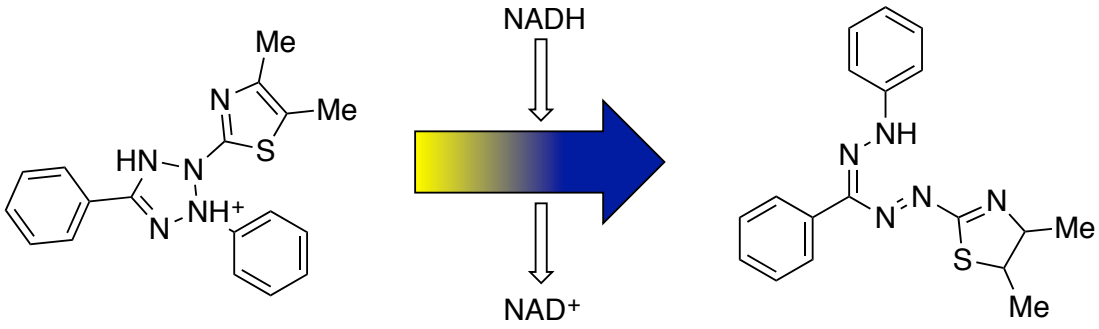

MTT (**4.15**) Formazan (**4.16**)

Figure 4.11. Schematic view of the MTT assay.

[151] a) S. G. Lee, H. Lee, T. G. Nam, S. H. Eom, H. J. Heo, C. Y. Lee, D.-O. Kim, *J. Food Sci*. **2011**, *76*, C250–C256. b) J. Gaugler, B. James, T. Johnson, K. Scholz, W. J, *Alzheimer's & Dementia* **2013**, *9*, 208–245.
[152] H. J. Jessen, D. Barbaras, M. Hamburger, K. Gademann, *Org. Lett*. **2009**, *11*, 3446–3449.
[153] a) M. B. Hadimani, M. K. Purohit, C. Vanampally, R. Van der Ploeg, V. Arballo, D. Morrow, K. E. Frizzi, N. A. Calcutt, P. Fernyhough, L. P. Kotra, *J. Med. Chem*. **2013**, *56*, 5071–5078. b) S. G. Lee, H. Lee, T. G. Nam, S. H. Eom, H. J. Heo, C. Y. Lee, D.-O. Kim, *J. Food Sci*. **2011**, *76*, C250–C256.
[154] a) R. D. Brinton, R. S. Yamazaki, *Pharmaceu. Res*. **1998**, *15*, 386–398 b) T. Mosmann, *J. Immuno. Met*. **1983**, *65*, 55-63. c) J. Qi, Y. Luo, L. Gao, *Mini-Rev. Med. Chem*. **2011**, 658–677.

We set out to combine application of our compounds with βA peptide in PC12 cells to allow us to find small molecules that are able to protect neurons from oxidative stress using MTT as visual readout.[155]

4.2. Result and Discussion

4.2.1 Computational Results using the SEA Search Tool

As mentioned in chapter 3, our SAR study revealed triol **3.20t** as the most potent farinosone C analog. Its structure was therefore submitted to the online SEA search tool (SEArch), developed by the *Shoichet* group.[156] The molecular descriptor used to encode the submitted compounds, was Scitegic ECFP4 and the database to search against was the ChEMBL Medical Chemistry Database Version 10. For triol **3.20e**, the SEArch tool suggested 45 different protein targets. The targets are ranked according to their maximum Tanimoto coefficient (mTC). The value describes the amount of similarity to the nearest neighbour of the submitted structure to the annotated ligands in the respective receptor subset and the e-value allows judgement of the quality of this result (Table 4.2).[157]

#	Code	Lds	Receptor Subset	e-Value	mTC
1	GRIA1_HUMAN_10000	125	Glutamate receptor ionotropic, AMPA 1	8.66e-42	0.44
2	OPRM_RAT_10000	2143	Mu opioid receptor	8.26e-25	0.43
3	ACHD_HUMAN_10000	12	Acetylcholine receptor protein delta chain	2.26e-27	0.43
4	SOAT1_RAT_10000	480	Acyl coenzyme A: cholesterol acyltransferase 1	3.29e-5	0.42
5	NEP_HUMAN_10000	490	Neprilysin	1.52e-21	0.41
6	HYES_HUMAN_10000	763	Epoxide hydratase	1.62	0.41
7	HDAC9_HUMAN_10000	354	Histone deacetylase 9	1.51e-21	0.4

[155] a) S. G. Lee, H. Lee, T. G. Nam, S. H. Eom, H. J. Heo, C. Y. Lee, D.-O. Kim, *J. Food Sci*. **2011**, *76*, C250–C256. b) J. Gaugler, B. James, T. Johnson, K. Scholz, W. J, *Alzheimer's & Dementia* **2013**, *9*, 208–245.
[156] www.sea.bkslab.org/search
[157] M. J. Keiser, B. L. Roth, B. N. Armbruster, P. Ernsberger, J. J. Irwin, B. K. Shoichet, *Nat. Biotechnol*. **2007**, *25*, 197–206.

8	HDAC5_HUMAN_10000	364	Histone deacetylase 5	4.38e-21	0.4
9	HDAC1_HUMAN_10000	1521	Histone deacetylase 1	4.22e-29	0.4
10	HDAC2_HUMAN_10000	614	Histone deacetylase 2	3.62e-29	0.4
11	HDAC3_HUMAN_10000	489	Histone deacetylase 3	8.64e-27	0.4
12	**CNR2_HUMAN_10000**	**1759**	**Cannabinoid CB2 receptor**	**1.88e-01**	**0.39**
13	**CNR1_HUMAN_10000**	**2267**	**Cannabinoid CB1 receptor**	**1.56**	**0.39**
14	CEGT_HUMAN_10000	6	Ceramide glucosyltransferase	1.43e-8	0.39
15	OPRD_RAT_10000	1622	Delta opioid receptor	2.87e-10	0.38
16	ACE_HUMAN_10000	654	Angiotensin-converting enzyme	3.51e-1	0.38
17	GRIA1_RAT_10000	113	Glutamate receptor ionotropic, AMPA 1	2.33e	0.37
18	**CNR1_RAT_10000**	**1279**	**Cannabinoid CB1 receptor**	**2.13e-6**	**0.37**
19	ACE_RABIT_10000	95	Angiotensin-converting enzyme	1.68e-11	0.37
20	**CNR2_MOUSE_10000**	**237**	**Cannabinoid CB2 receptor**	**7.92e-9**	**0.37**
21	OPRM_HUMAN_10000	2816	Mu opioid receptor	3.32e-6	0.37
22	MMP8_HUMAN_10000	628	Matrix metalloproteinase 8	1.18e	0.36
23	OPRD_MOUSE_10000	413	Delta opioid receptor	1.11e-8	0.36
24	ACE_RAT_10000	253	Angiotensin-converting enzyme	1.43e-9	0.35
25	PIN1_HUMAN_10000	26	Peptidyl-prolyl cis-trans isomerase NIMA-interacting 1	2.30e-4	0.35
26	OPRD_HUMAN_10000	2216	Delta opioid receptor	1.02e-3	0.35
27	GLCM_MOUSE_10000	12	Beta-glucocerebrosidase	5.99e-31	0.34
28	ATS5_HUMAN_10000	88	ADAMTS5	2.02	0.33
29	OPRM_MOUSE_10000	256	Mu opioid receptor	5.87e-4	0.33
30	PAPA1_CARPA_10000	52	Papain	9.5	0.33
31	AMPN_HUMAN_10000	92	Aminopeptidase N	1.23e-1	0.33
32	PA21B_PIG_10000	11	Phospholipase A2 group 1B	2.96e-15	0.32
33	MIF_HUMAN_10000	40	Macrophage migration inhibitory factor	3.91e	0.32
34	OPRK_MOUSE_10000	137	Kappa opioid receptor	1.81e-2	0.31
35	A2AMS1_MOUSE_10000	172	Sigma opioid receptor	7.92e-1	0.31
36	OPRK_RAT_10000	552	Kappa opioid receptor	5.88e-1	0.31
37	NMT2_HUMAN_10000	82	Peptide N-	2.38e-3	0.31

			myristoyltransferase 2		
38	NMT1_HUMAN_10000	89	Peptide N-myristoyltransferase 1	5.01e-3	0.31
39	**CNR2_RAT_10000**	**81**	**Cannabinoid CB2 receptor**	**2.41e-6**	**0.31**
40	CASP1_HUMAN_10000	460	Caspase-1	1.20e-3	0.3
41	LYAM3_HUMAN_10000	9	P-selectin	3.82e-4	0.3
42	NK3R_HUMAN_10000	342	Neurokinin 3 receptor	4.09e-3	0.3
43	KPCB_HUMAN_10000	537	Protein kinase C beta	3.07	0.29
44	CATB_RAT_10000	15	Cathepsin B	4.27e-2	0.29
45	HIS7_CRYNE_10000	22	Imidazoleglycerol-phosphate dehydratase	2.29e-4	0.29

Table 4.2. Results of the similarly search against triol **3.20e** using the SEArch tool developed by *Shoichet* (Lds = amount of ligands in this subset).[158]

The ligand set of the ionotropic glutamate receptor AMPA 1 showed the highest proximity.[159] These receptors are present in many parts of the brain and are the most frequently found receptors in the nervous system.[160] It is, therefore, no surprise that these ion channels are modulated by glutamate (**4.17**) as this compound is the most abundant excitatory neurotransmitter in the mammalian cortex. The biogenic amine of glutamate, γ-aminobutyric acid (GABA, **4.18**) is the chief inhibitory neurotransmitter that primarily acts on the GABA receptor ion channel complexes. These two neurotransmitters can be enzymatically transformed into each other and their interplay mediates the fast excitatory synaptic transmission and underlying several forms of synaptic plasticity, among other things (Fig. 4.12).[161]

[158] a) M. J. Keiser, B. L. Roth, B. N. Armbruster, P. Ernsberger, J. J. Irwin, B. K. Shoichet, *Nat. Biotechnol.* **2007**, *25*, 197–206. b) www.sea.bkslab.org/search
[159] O. A. Petroff, *The Neuroscientist* **2002**, *8*, 562–573.
[160] S. R. Platt, *Vet. J.* **2007**, *173*, 278–286.
[161] a) A. Nilsen, P. M. England, *J. Am. Chem. Soc.* **2007**, *129*, 4902–4903. b) O. A. Petroff, *The Neuroscientist* **2002**, *8*, 562–573.

Glutamate (**4.17**) GABA (**4.18**)

Figure 4.12. The two most abundant neurotransmitters glutamate (**4.17**) and GABA (**4.18**).

A closer look on the top three ranked ionotropic glutamate receptor AMPA 1 subset ligands, the philanthotoxin derivatives **4.19a-f** reveals the structural similarities with the triol **3.20t**. These compounds **4.19a-f** are able to block AMPA receptors in the low μM range (Fig. 4.13).[162] However, due to the enormous breadth of this receptor family, other active receptor subsets might provide more insight.

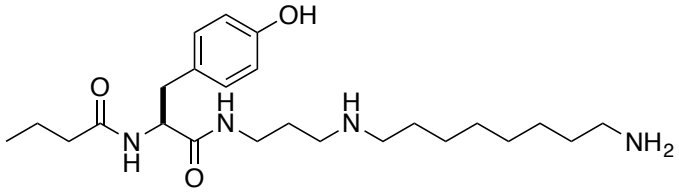

4.19a Rank 1, TC: 0.4386

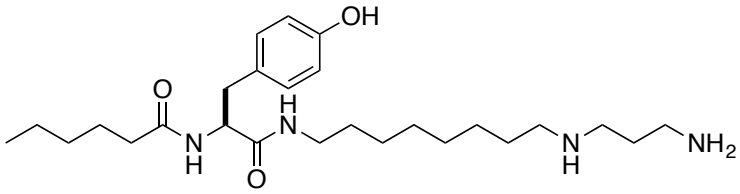

4.19b Rank 2, TC: 0.4310

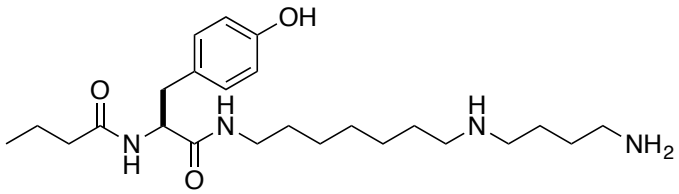

4.19c Rank 3, TC: 0.4035

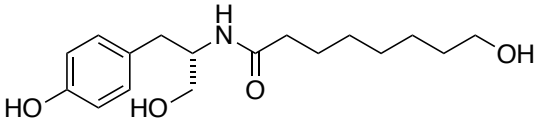

Triol **3.20t**

Figure 4.13. Top three ionotropic glutamate receptor AMPA 1 inhibitors **4.19a-c** according to their Tanimoto coefficient, and triol **3.20t**.

[162] a) H. Kromann, S. Krikstolaityte, A. J. Andersen, *J. Med. Chem.* **2002**, *45*, 5745-5754. b) A. Nilsen, P. M. England, *J. Am. Chem. Soc.* **2007**, *129*, 4902–4903.

Other receptor subsets of interest involve the histone deacetylase, opioid and cannabinoid receptors. We then visually screened hundreds of ligands associated to these receptors. The ideal ligand would be a close structural mimics of **3.20t** that bears a tyrosinol moiety, due to this being the common structural motive every member of our farinosone C derivative collections has in common.

Our initial attempts where unsuccessful identifying the L-tyrosinol-derived ligands. However, in the CB_1 receptor subset (CNR1_RAT_10000) the 44 ligands, which scored the highest out of 1279, are all AEA **4.8** and 2-AG **4.10** analogs, which comes as no surprise (Fig 4.14). Of special interest is compound **4.20** (Fig 4.14) that ranked 13th. It does not contain a tyrosinol-derived ligand, but the *para*-phenolic moiety was encouraging enough for us to perform a literature search where we replaced the 4-hydroxybenzyl part of this amphiphile **4.20** by L-tyrosinol.

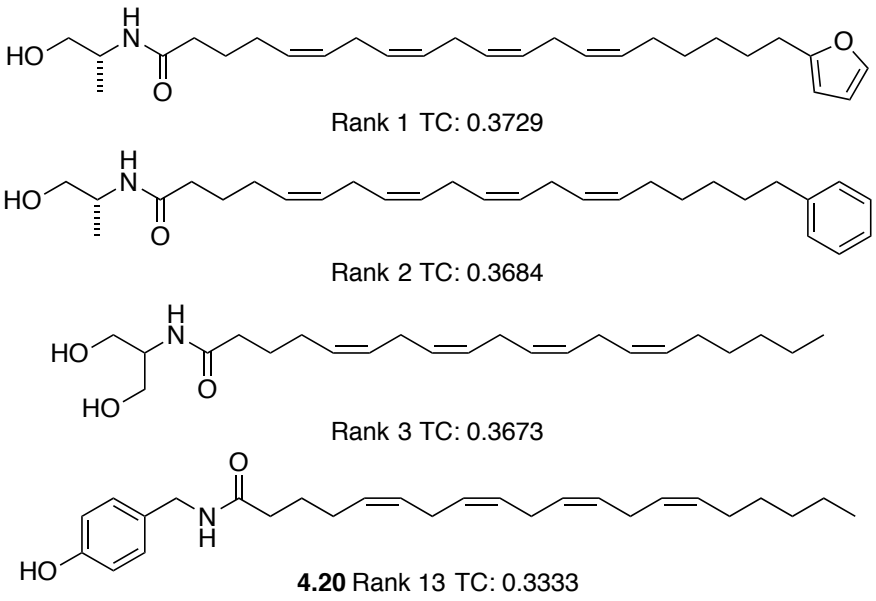

Figure 4.14. Top three CB_1 inhibitors according to their Tanimoto coefficient and the dopamine derived analog **4.20**.

To our delight, we found this exact compound and close analogs, which where descripted as potent CB1 receptor agonists.[163] These tyrosinol-derived fatty acid analogs are not registered in the ChEMBL Medical Chemistry Database and could, therefore, not attract our attention on the first glance.

[163] F. Schmidt, G. Le Douaron, P. Champy, M. Amar, B. Seon-Meniel, R. Raisman-Vozari, B. Figadere, *Bioorg. Med. Chem.* **2010**, *18*, 5103–5113.

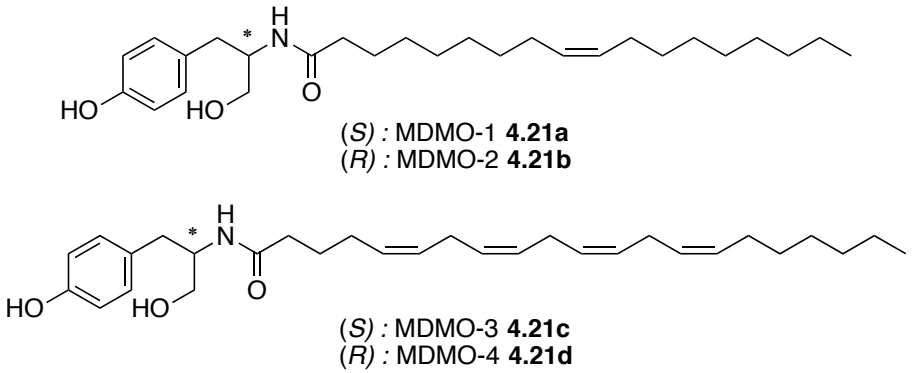

Fig. 4.15. Selective tyrosinol derived CB_1 inhibitors developed by *Di Marzo*.[164]

This literature search revealed inconclusive results regarding the relationship between tyrosinol-derived CB_1 inhibitors and neuronal differentiation. As discussed in section 4.1.2 *Figadère* reported on tryptamine derived fatty acid derivatives with neuritogenic properties.[165] We speculated that if we replace the tryptamine with a tyrosinol unit, eventually compounds would be furnished which 1) interact with the CB_1 receptor system, and 2) are able to induce neuronal differentiation which may allow a connection to be made between these to phenomenas.

As highlighted in table 4.1, a 16-atom alkyl chain yielded the best results. Consequently, we also intended to use the same length for the fully saturated alkyl chains. Table 4.3 shows the molecular probes we synthesized. We were especially interested in the bioactivity of compound **4.22b/f** since both also bear a hydroxyl group terminus as the neuritogenic triol **3.20t** does.

[164] G. Ortar, A. Ligresti, L. De Petrocellis, E. Morera, V. Di Marzo, *Biochem. Pharmacol*. **2003**, *65*, 1473–1481.
[165] F. Schmidt, G. Le Douaron, P. Champy, M. Amar, B. Seon-Meniel, R. Raisman-Vozari, B. Figadere, *Bioorg. Med. Chem*. **2010**, *18*, 5103–5113.

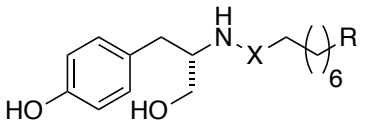

Cpd	X	R
4.22a	$–CH_2$	$–(CH_2)_7–CH_3$
4.22b	$–CH_2$	$–(CH_2)_7–OH$
4.22c	$–CH_2$	$–CH=CH–CH_2–CH=CH–(CH_2)_4–CH_3$
4.22d	$–CH_2$	$–(CH=CH–CH_2)_3–CH_3$
4.22e	–C=O	$–(CH_2)_7–CH_3$
4.22f	–C=O	$–(CH_2)_7–OH$
4.22g[166]	–C=O	$–CH=CH–CH_2–CH=CH–(CH_2)_4–CH_3$
4.22h	–C=O	$–(CH=CH–CH_2)_3–CH_3$

Table 4.3. Tyrosinol fatty acid analogs **4.22a-h**.

4.2.2 Synthesis of Tyrosinol Fatty Acid Analogs 4.22a-h

We first synthesized the tryptamine-derived compounds **4.6c** and its amine analog **4.6l** following the reported procedure, obtaining similar yields.[167] These two compounds will then later serve as reference compounds. As previously mentioned (section 4.1.2), *Figadère* and co-workers evaluated the neuritogenic properties using primary dopaminergic neurons,[169] therefore we also had to examine if these results could be repeated in our PC12 cell model.

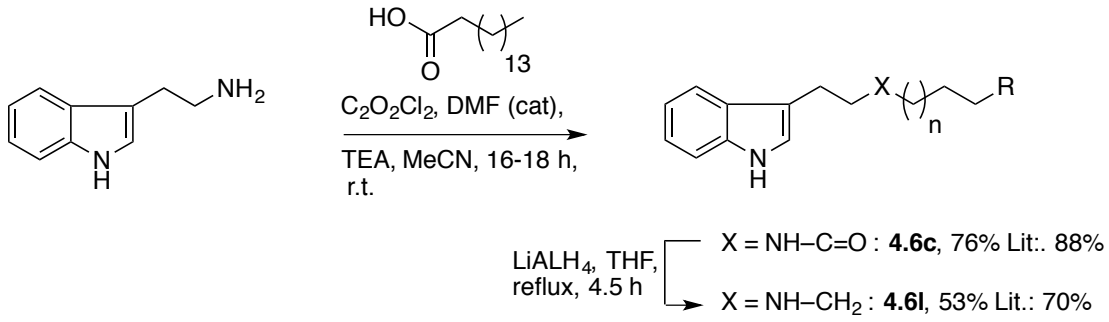

Scheme 4.1. Synthesis of reference compounds **4.6c/l** as described by *Figadère*.[169]

[166] also referred as **BSL34**

[167] F. Schmidt, G. Le Douaron, P. Champy, M. Amar, B. Seon-Meniel, R. Raisman-Vozari, B. Figadere, *Bioorg. Med. Chem.* **2010**, *18*, 5103–5113.

We initially planed to adopt the peptide coupling/reduction sequence using $LiAlH_4$ for our L-tyrosinol derived analogs. However, we were not able to synthesize compound **4**.**22e**, **4.22f**, or the double unsaturated amide **4.22g** using oxalyl chloride and catalytic amounts of DMF. The same was true for these three compounds when PyBOB **4.23** was used as coupling agent. We instead found that HOBt in combination with EDC afforded compound **4**.**22e** and **4.22f** in reasonable yields (scheme 4.2). Nevertheless, using $LiAlH_4$ to reduce the amide bond was insufficient and no conversion of the starting material was observed. Also, neither acetic acid with $NaBH_4$ salt nor BH_3-THF complex solution under reflux transformed amide **4.22e** into the amine **4**.**22a**.[168] Since these direct reduction approaches were not successful, we employed HDMS in combination with a catalytic amount of TMSCl, first mixed with amides **4.22e** or **4.22f** and refluxed for up to 2 h in MeCN to give rise to the respective TMS-formimidate analogs. The MeCN was then replaced by dioxane and BH_3-DMS complex solution was added in excess. Reflux overnight yielded the desired secondary amines **4**.**22a** and **4**.**22b**.[169]

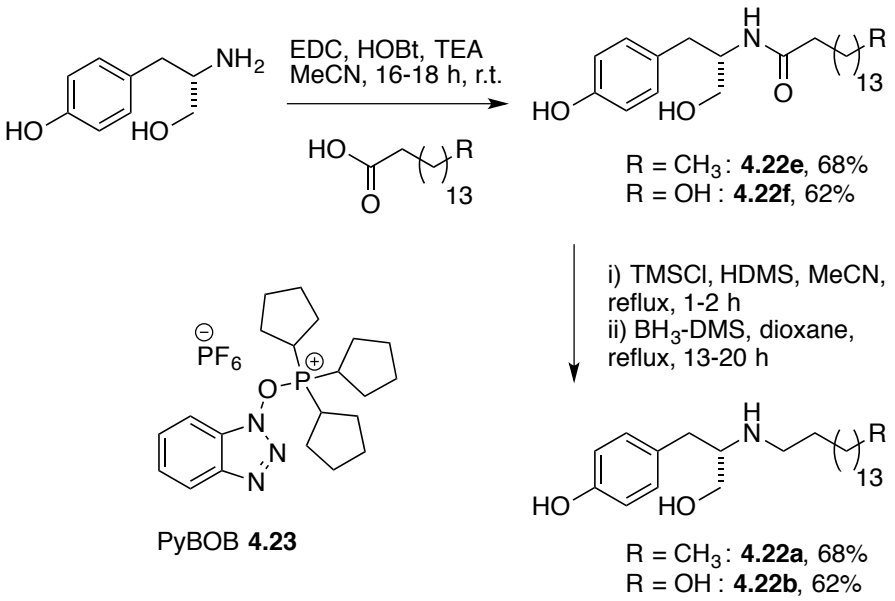

Scheme 4.2. Peptide coupling/reduction sequence for fully saturated tyrosinol analogs.

[168] a) T. M. Fong, S. B. Heymsfield, *Int. J. Obes.* **2009**, *33*, 947–955. b) R. Lan, Q. Liu, P. Fan, S. Lin, S. R. Fernando, D. McCallion, R. Pertwee, A. Makriyannis, *J. Med. Chem.* **1999**, *42*, 769–776.

[169] a) B. Ravinder, S. R. Reddy, A. P. Reddy, *Tetrahedron* **2013,** *54***,** 4908-4913. b) A. Giannis, K. Sandhoff, *Angew. Chem. Int. Ed.* **1989**, *28*, 218–220.

This established sequence could not be applied to the unsaturated fatty acid derivatives. Activation of the fatty omega-3 or omega-6 fatty acid using DCC and PFP yielded the desired amides **4.22g** and **4.22h** (Scheme 4.3). Reduction of amide **4.22g** using $LiAlH_4$ under reflux overnight led to a complex mixture, including starting material. The previously applied approach using HMDS/TMS and BH_3-DMS resulted in complete saturation of all non-aromatic double-bonds. We then decided to try to bypass the amide reduction *via* a reductive animation. Ethyl linoleate **4.24** or ethyl linolenate **4.25** were dissolved in toluene and cooled to –78 °C before 1 equiv. of a pre-cooled DIBAL-H solution was added. A standard work-up after 50 minutes afforded the crude aldehyde, which was then dissolved in MeOH and glacial acetic acid, L-tyrosinol and sodium cyanoborohydride were added at room temperature to provide the remaining members of the desired collection, as shown in table 4.3.

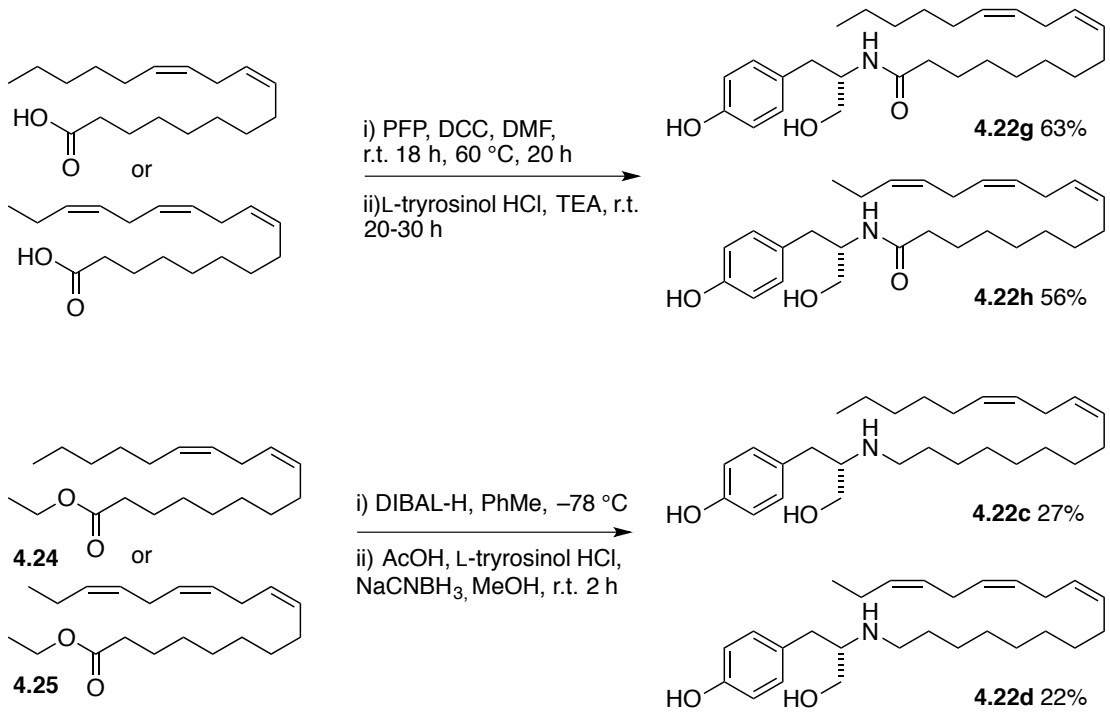

Scheme 4.3. Synthesis of OMDM-2 **4.21b** analogs **4.22c-g**.

4.2.3 Biological Evaluation

Compounds **4.6c** and **4.6l** and the commercially available CB_1 selective antagonist OMDM-2 (**4.21b**) were first screened for neurite outgrowth at 10 μM concentration using the same assay conditions as in chapter 3, but with a higher NGF concentration (40 ng/mL instead of 20 ng/mL) for the overnight priming. All

compounds (**4.22a-d** and **4.6l**) bearing a secondary amine function were not tolerated by the PC12 cells, resulting in partial or complete cell death. After reduction of the concentration by one order of magnitude, neither toxicity nor neuritogenic activity could be observed for these amines. Among the amide bearing amphiphiles **4.22f-h**, only **4.22g** (hereafter referred to as **BSL34)** showed a significant activity at 10 µM concentration (Fig. 4.16), suggesting that the degree of unsaturation of the alkyl chain plays a crucial role. Also, the length of the alkyl chain is of importance as expected; triol **3.20t** was been identified as the most potent compound, whereas triol **4.22f** was inactive, but they only differ in the length of the alkyl chain (C7 versus C14). Trypatmine-derived compounds were either toxic (**4.6l**) or completly inactive (**4.6c**), even at a 100-fold higher concentration. This results is contraty to *Figadère's* findings,[170] demonstrating the difficulty in transforming obeservations from one cell type to another.

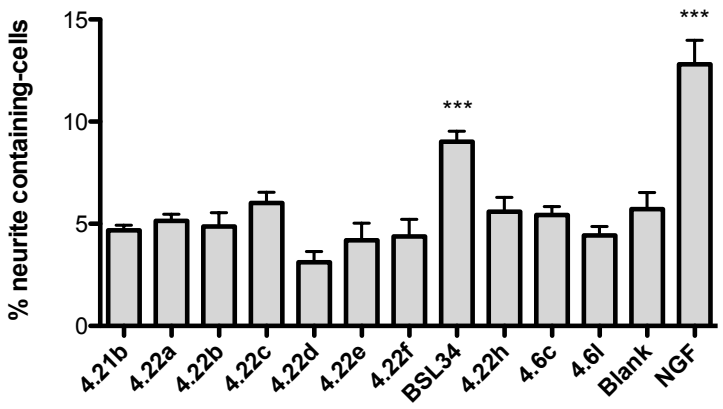

Fig. 4.16. Neuritogenic activity of OMDM-2 (**4.21b**) and fatty acid analogs. Values were determined at 10 µM (**4.21b**, **4.22e-h**, **BSL24**, **4.6c**) or 1 µM (**4.22a-d**, **4.6l**), NGF control: 20 ng mL^{-1}. DMSO control: 0.1%. Incubation period: 2 days. Values are reported as means ± SEM (unpaired tow-tailed t-test significance: *** = $P < 0.0001$).

[170] F. Schmidt, G. Le Douaron, P. Champy, M. Amar, B. Seon-Meniel, R. Raisman-Vozari, B. Figadere, *Bioorg. Med. Chem.* **2010**, *18*, 5103–5113.

4.2.4 Examination of the Cannabinoid System

Next the $CB_{1/2}$ binding affinities for this set of compounds (Fig. 6.1A and 6.1B) were evaluated in collaboration with *Prof. Dr. Jurg Gertsch* and *Dr. Andrea Chicca* (University of Bern). We were very pleased to discover that **4.22b** and, more importantly, the neuritogenic omega-6 fatty acid amide derivative **BSL34** selectively bind to the CB_1 receptor with moderate K_i potencies values of 530 and 810 nM, respectively (Fig. 4.17).[171]

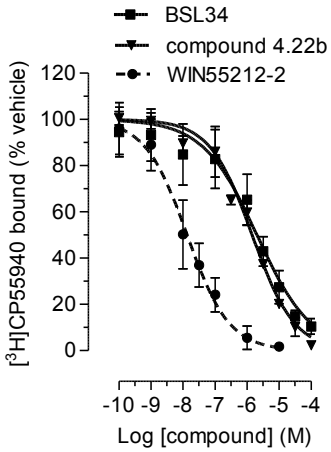

Fig. 4.17. EMT inhibition parameters. EC_{50} values and maximal effect were determined from full concentration-dependent curves performed in U937 cells as previously described.[173]

To further clarify the role of the CB_1 receptor, we performed a co-incubation study in the PC12 system using the CB_1 selective antagonists rimonabant or AM251.[172] Despite multiple attempts under a variety of conditions, neuronal differentiation could not be suppressed using the above-mentioned selective CB_1 antagonists in combination with **BSL34**, nor were phenotypic changes detected when AM251 or rimonabant was administered alone. The same results were observed when the CB_1 selective agonist O-689[173] at a 100 nM concentration was investigated. Extra-

[171] A. Chicca, J. Marazzi, S. Nicolussi, J. Gertsch, *J. Biological Chem*. **2012**, *287*, 34660–34682.
[172] a) T. M. Fong, S. B. Heymsfield, *Int. J. Obes*. **2009**, *33*, 947–955 b) R. Lan, Q. Liu, P. Fan, S. Lin, S. R. Fernando, D. McCallion, R. Pertwee, A. Makriyannis, *J. Med. Chem*. **1999**, *42*, 769–776.
[173] S. Lin, A. D. Khanolkar, P. Fan, A. Goutopoulos, C. Qin, D. Papahadjis, A. Makriyannis, *J. Med. Chem*. **1998**, *41*, 5353–5361.

and intercellular endocannabinoid levels can also be controlled by the putative endocannabinoid membrane transporter (EMT) or the enzymes FAAH, ABHDs, and MAGL as introduced earlier (section 4.1.4). Modulation of these targets' functions is known to affect the endocannabinoid concentrations, indicating indirect $CB_{1/2}$-dependent effects.[174] Consequently, we tested our compounds (both collections) in this regard. All compounds showed no or only a weak inhibition (up to 20-25%) at 1 μM of fatty acid amide hydrolase (FAAH, Fig. 6.2). Similarly, 2-AG hydrolysis by MAGL and ABHDs is not significantly inhibited at the screening concentration of 1 μM (6.3A and 6.3B). Next, we examined the EMT inhibition capacities (Fig. 6.4). We discovered fatty acid analogs displaying excellent EMT inhibitory patterns (Table 4.4). Four of the tested compounds inhibited AEA (**4.8**) cellular re-uptake with sub-micromolar EC_{50} values. The most potent compound was again **BSL34** with a 10-fold higher activity than UCM707, a potent benchmark inhibitor.[175]

Cpd	EC_{50} ± SEM (nM)	Max Inhibition
4.22c	975 ± 201	51 %
4.22d	966 ± 252	60 %
4.22f	757 ± 326	73 %
BSL34	228 ± 139	52 %
UCM707	1800 ± 801	80 %

Table 4.4. EMT inhibition parameters. EC50 values and maximal effect were determined from full concentration-dependent curves performed in U937 cells as previously described.[176]

[174] A. Chicca, J. Marazzi, S. Nicolussi, J. Gertsch, *J. Biological Chem*. **2012**, *287*, 34660–34682.
[175] a) A. Chicca, J. Marazzi, S. Nicolussi, J. Gertsch, *J. Biological Chem*. **2012**, *287*, 34660–34682 b) P. Hasanein, K. Javanmardi, *Fund. Clin. Pharmacol*. **2008**, *22*, 517–522 b) E. de Lago, J. Fernández-Ruiz, S. Ortega-Gutiérrez, A. Viso, M. L. López-Rodríguez, J. A. Ramos, *Euro. J. Pharmaco*. **2002**, *449*, 99–103.

4.2.5 HIP HOP Profiling

The tyrosinol fatty acid analogs **4.22a-h** and all members of the farinosone C collection (**3.5**, **3.20a-t**) were investigated in the HIP HOP assay at *Novartis* by *Dr. Dominic Höpfner* and co-workers. Most of the compounds already failed the initial uptake screening with the yeast cells. Of the few compounds that passed this first hurdle, **4.22b** expressed an interesting profile (Fig. 4.18). It is unclear why only one members of the tyrosinol fatty acid collection **4.22a-h** was taken up by the yeast cells, although their structural similarity is very high. However, at a concentration of 150 µM, **4.22b** induced lipid stress. This observation is supported by the fact that yeast strains in which one gene copy of APL6 and NEO1 has been deleted (HIP) showed reduced viability. Both genes are linked to membrane stress.[176] Moreover, TDA10 is a "frequent hitter" associated with compounds known to induce membrane destabilisation.[177] Due to the lipophilicity of compound **4.22b**, this was expected. Moreover, besides also being associated to lipid stress, ERG24 inhibition indicates that the sterol biosynthesis is affected.[178] This result is supported by the synthetic lethality of the UPC2 strain. This gene decodes the main relator unit of the sterol biosynthesis.[179] As explained in section 4.1.5, when a compound inhibits a compensating pathway (ERG24) and the main pathway (UPC2) is abundant, HOP allows for confirmation of HIP results.

GEF1 is known for membrane destabilisation as well[180] and ILM1 is expected to be an experiment-specific false positive, because it was observed with unrelated compounds during this run but never before. These results however do not allow the conclusion that **4.22f** directly inhibits ERG24 or that the compound's ability to induce membrane stress is the main reason for sterol biosynthesis inhibition. In summary, the

---

[176] a) C. R. Cowles, G. Odorizzi, G. S. Payne, S. D. Emr, *Cell* **1997**, *91*, 109–108. b) S. Wicky, H. Schwarz, B. Singer-Kruger, *Molec. Cell. Biol.* **2004**, *24*, 7402–7418. c) H. R. Panek, *The EMBO J.* **1997**, *16*, 4194–4204.
[177] *Personal communication from Dr. Dominic Höpfner*, **2013**.
[178] N. Jia, B. Arthington-Skaggs, W. Lee, C. A. Pierson, N. D. Lees, J. Eckstein, R. Barbuch, M. Bard, *Antimicrob. Agents Chemother.* **2002**, *46*, 947–957.
[179] L. W. Parks, W. M. Casey, *Annu. Rev. Microbiol.* **1995**, *49*, 95–116.
[180] A. Lopez-Rodriguez, A. Carabez-Trejo, L. Coyne, R. F. Halliwell, R. Miledi, A. Martinez-Torres, *FEMS Yeast Res.* **2007**, *7*, 1218–1229.

HIP HOP assay represents an impressive target identification platform, but did not support us in our attempt to find the lock to our neuritogenic keys.[181]

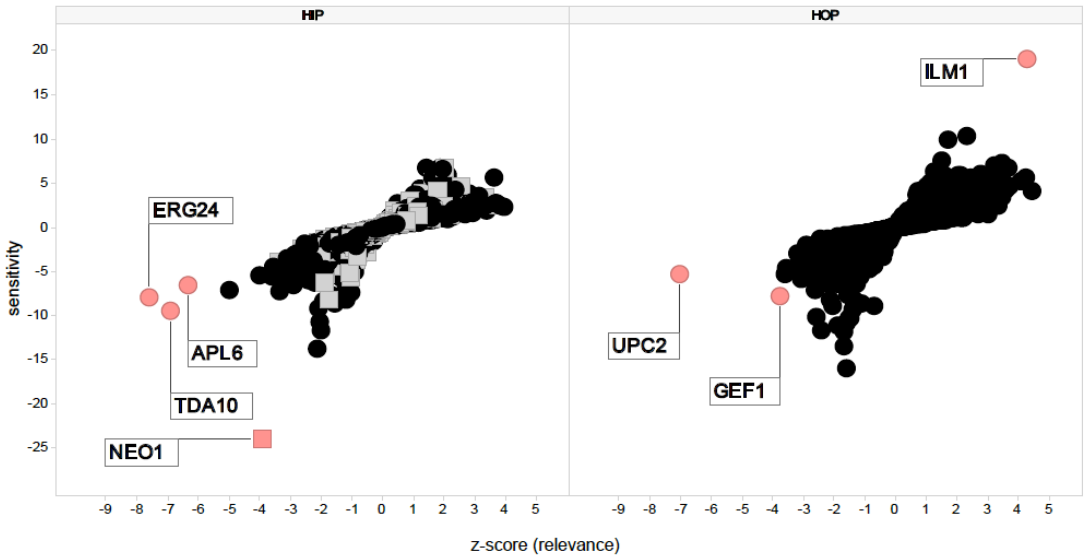

Fig. 4.18. Results obtained form the HIP HOP assay conducted at *Novartis* in Basel by *Dr. Dominic Höpfner* and co-workers. The z-score (= sensitivity score / standard deviation) allows judging the relevance of the obtained results: > ± 5 is considered interesting.

4.2.6 Amphetamine-Type Bioactivity of Farinosone C Analogs

As described in section 4.1.6, multiple ATDD are well established. Examination of the structures shown in figure 4.7 and 4.8 reveals that re-uptake transporters tolerate a wide range of different structural moieties. This fact, in combination with a certain structural analogy from ATDD drugs and members of our farinosone C library, made their potential to act on monoamine re-uptake transporters of interest. Therefore, a dozen compounds where selected (Fig. 4.19) and screened for re-uptake transport inhibition (Fig. 4.20) in collaboration with *Dr. Linda Simmler* and *PD Dr. Matthias Liechti* (University Hospital, Basel). At 20 µM concentration, the compounds **3.20l** and **3.20o** showed weak dopamine (DA, **4.12**) and norepinephrine (Ne, **4.13**) re-uptake inhibition. The amine **3.20l** inhibited DA re-uptake to 53 ± 9% and NE re-uptake to 64 ± 4%, and the molecular probe **3.20o** inhibited DA re-uptake to 52 ± 14% and NE re-uptake to 81 ± 5%. It was expected that amine **3.20l** showed

[181] www.yeastgenome.org

superior properties than analogs bearing an amide group. Consequently, no amide bond is present in the introduced amphetamine-derivatives. However, a drug that exhibits about 50% re-uptake inhibition efficacy at 20 µM would not be considered as pharmacologically relevant DA or NE re-uptake inhibitor, as known transporter inhibitors like MDMA and methamphetamine inhibit DA transport and NE transport have a 50% inhibitory concentration below 1 µM in this assay. MDMA **4.11a** inhibits 50% of NE re-uptake at 0.5 µM and methamphetamine inhibits 50% NE re-uptake at 6 nM and DA re-uptake at 1 µM concentration.[182] The abnormal negative binding observed by the dopamine-derived amide **3.20k** in case of the dopamine transporter is hard to rationalize. *In vitro* hydrolysis of the amide bond revealing dopamine would lead to re-uptake inhibition.[183] Another reason for this type of observation are pH-changes, hence acid **3.20g** did not induce such an effect, the catechol **3.20k** should not either. However, if **3.20k** acts as a substrate for the DA transporter, a general re-uptake acceleration could eventually occur. In Summary, these findings did not justify further investigation such as determination of K*i* values for transporter affinity or transporter-mediated release properties. Possible ethical considerations prior to publication are therefore not necessary, as we did not discover a potent monoamine re-uptake transporter inhibitor that can be obtained in one-step form non-controlled substances.

[182] L. D. Simmler, T. A. Buser, M. Donzelli, Y. Schramm, L.-H. Dieu, J. Huwyler, S. Chaboz, M. C. Hoener, M. E. Liechti, *Br. J. Pharmacol.* **2012**, *168*, 458–470.
[183] R. B. Rothman, M. H. Baumann, C. M. Dersch, D. V. Romero, K. C. Rice, F. I. Carroll, J. S. Partilla, *Synapse* **2001**, *39*, 32–41.

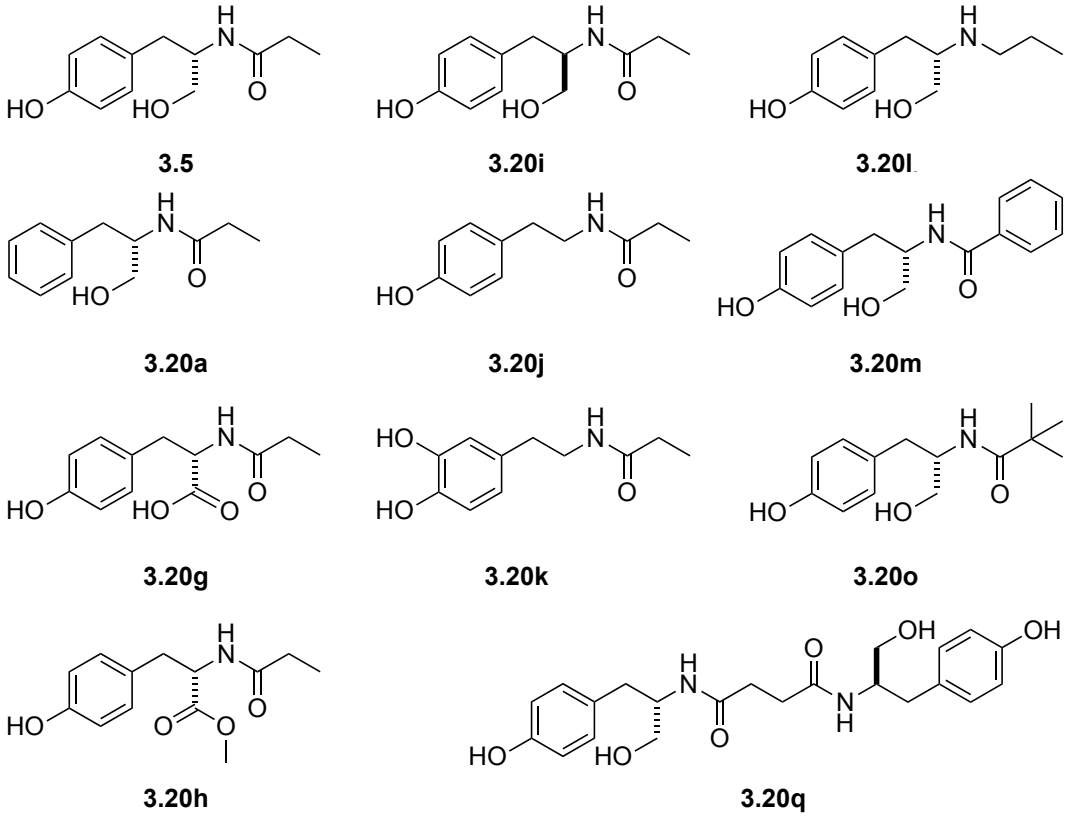

Fig. 4.19. Compounds selected for monoamine re-uptake inhibition studies.

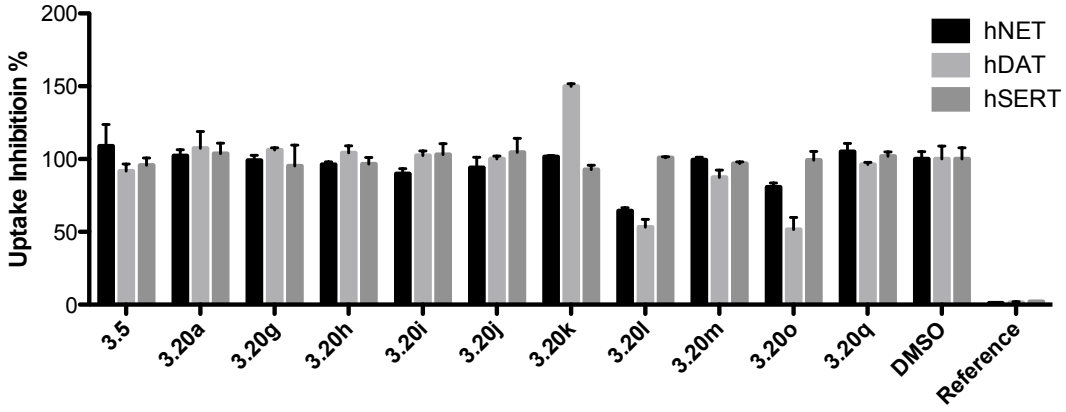

Fig. 4.20. Re-uptake inhibition study results. Reference: fluoxetine (hSERT), mazindole (hDAT) and nisoxetine (hNET) all at 10 μM.

4.2.7 Fluorescent Labelling

A common method to localize a general cell region, such as the membrane, nucleolus or mitochondrion core in which active compounds interacted with their respective receptors is fluorescent labelling.[184] We envisioned that a tyrosinol-type pharmacophore linked to a fluorescent label may retain its neuritogenic activity and, if so, the interaction of our fluorescent ligand with its respected molecular target might be strong enough to allow for a local accumulation. This eventually would narrow down the possible molecular targets. Therefore, dansyl chloride (**4.26**) was coupled with 6-aminocaproic acid (**4.27**) following a literature procedure.[185] The resulting dansyl tag **4.28** was attached to L-tyrosinol using HATU **4.29**, which proceeded well and yielded the fluorescently labelled compound **4.30** (Scheme 4.4).

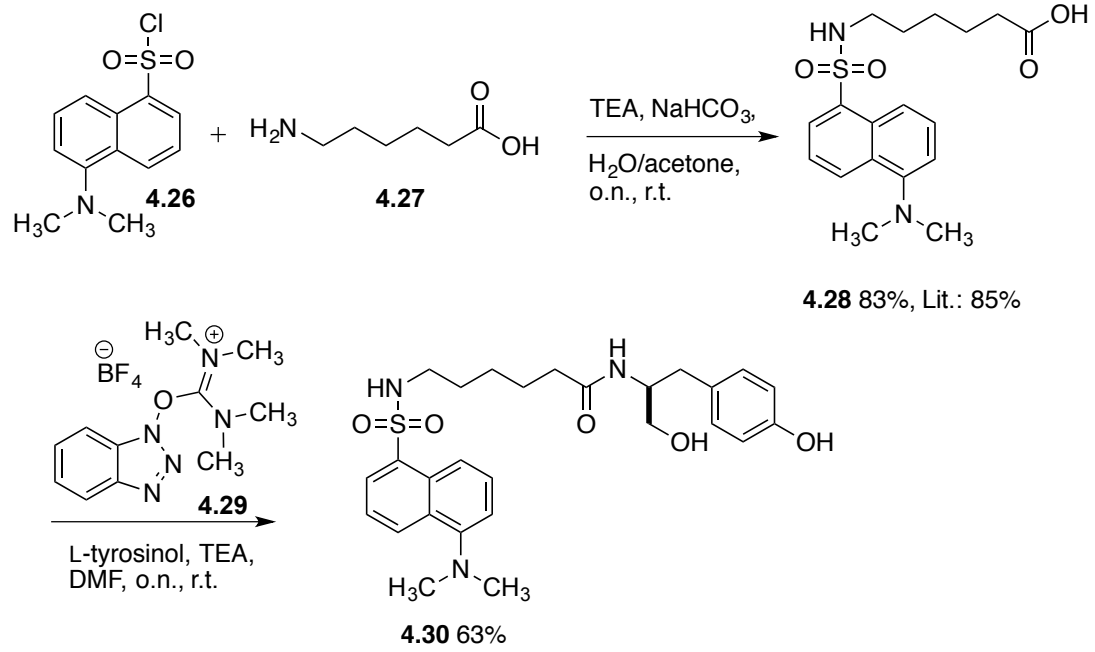

Scheme 4.4. Synthesis of fluorescent L-tyrosinol derived label **4.30**.

With the labelled tyrosinol derivative **4.30** in hand, we investigated its neuritogenic properties. Unfortunately, no bioactivity could be observed under standard PC12 assay conditions. Nevertheless, fluorescent staining investigations

[184] a) G. Zimmermann, B. Papke, S. Ismail, N. Vartak, A. Chandra, M. Hoffmann, S. A. Hahn, G. Triola, A. Wittinghofer, P. I. H. Bastiaens, *et al*., *Nature* **2013**, *497*, 638–642. b) H. Sahoo, *RSC Advances* **2012**, *2*, 7017–7029.

[185] T. H. Walls, S. C. Grindrod, D. Beraud, L. Zhang, A. R. Baheti, S. Dakshanamurthy, M. K. Patel, M. L. Brown, L. H. MacArthur, *Bioorg. Med. Chem.* **2012**, *20*, 5269–5276.

were performed. Compound **4.30** did stain the cells fluorescently, but no specific localisation could be recognized (Fig. 4.20A), even at higher magnification (picture not shown). **4.28** was used as control, to see if the L-tyrosinol terminus does make any difference (Fig. 4.20B). Comparison of these two different picture series however revealed no difference.

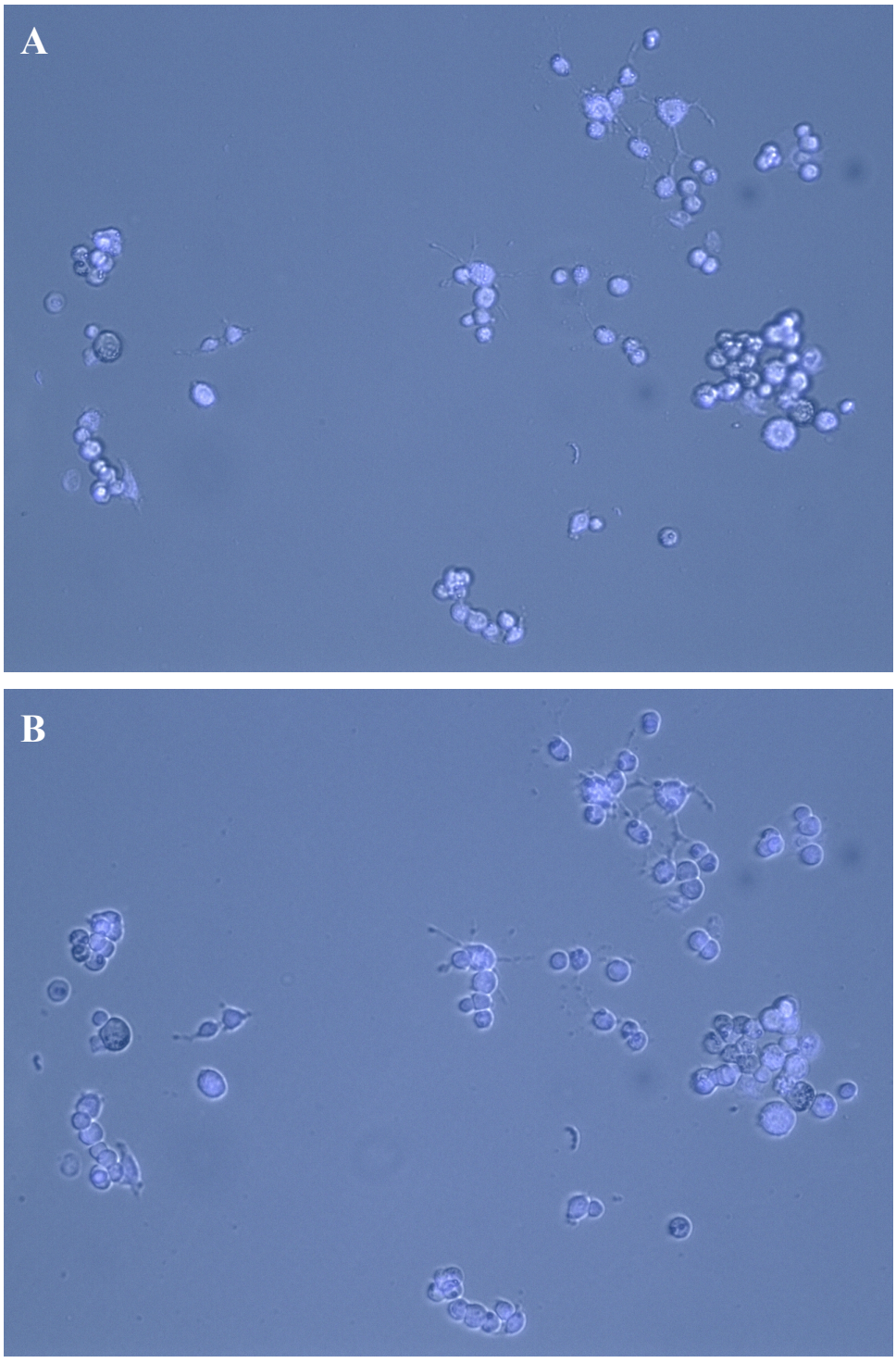

Fig. 4.20. Fluorescently stained PC12 cells. A: **4.30** 50 µM, B: **4.28** 50 µM.

4.2.8 Neuroprotective Properties

The attempts to establish the MTT assay were unsuccessful. The procedure of *Kim*[186] was followed as described using the same (40 μM) or higher (100 μM) concentrations of βA peptide fragment 25-35. The incubation times were also extended from the proposed 2 h to 1-2 days but no βA–induced cytotoxicity could be detected and, therefore, prevented any neuroprotective examination in combination with our compounds. Experiments using higher concentrations of βA were not conducted due to high material costs.

4.3 Conclusion

Our investigations discussed in this chapter did not result in the definition of a precise molecular target responsible for neurite outgrowth. Nevertheless, a broad insight into various tools of chemical biology was acquired and evidence was found that the ECS might be involved in neuronal differentiation mediated by some of our compounds. We consider the discovery of four simple and potent EMT inhibitors an important one. Especially since **BSL34** clearly outruns the potent benchmark inhibitor UCM707. This advancement is expected to by appreciated by numerous researchers working on the endocannabinoid system.

[186] S. G. Lee, H. Lee, T. G. Nam, S. H. Eom, H. J. Heo, C. Y. Lee, D.-O. Kim, *J. Food Sci*. **2011**, *76*, C250–C256.

CHAPTER 5 - DEVELOPMENT OF NEURITOGENIC SURFACES USING NATURAL PRODUCT ANALOGS

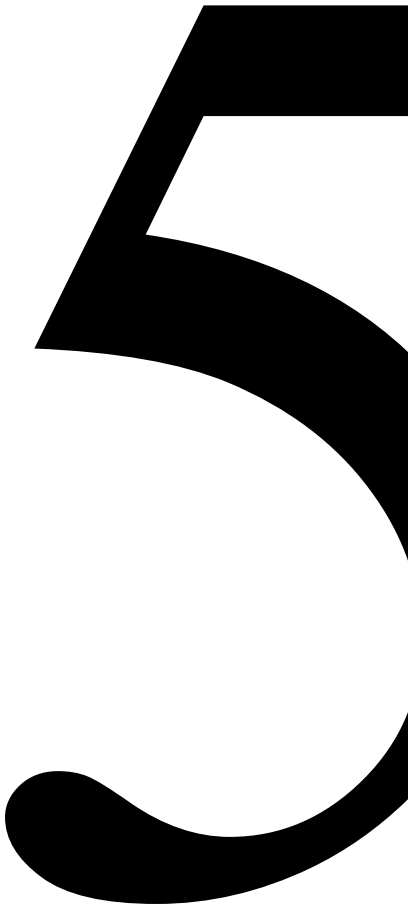

5.1 Introduction

5.1.1 General Outline

The previous three chapters have presented results that could potentially contribute to establishing small molecule-based therapies for patients suffering from neurodegenerative dementia (ND). This chapter however addresses a different unmet medical condition: Spinal cord injuries (SCI). Although, ND and SCI disable patients in different ways, both conditions could be addressed if neuronal cells are forced to re-connect in a controlled fashion. To help paralyzed people to regain their locomotor control, researchers from distinguish fields such as medicine, natural sciences and engineering have to join efforts. An increasing number of new therapeutic approaches emerged from research laboratories and seek transformation into clinical trials.[187] This chapter reports on a facile, robust and carefully explored method to turn glass slides into neuritogenic surfaces.

5.1.2 Spinal Cord Injuries

In the US, every year 10'000 new people are being diagnosed with traumatic SCI. More than one third is caused by motor vehicle accidents followed by falls and violence (primarily gunshot wounds).[188] Depending on which section of the spinal column and the ferocity the traumatic interruption has occurred, the symptoms differ from light chronic pain to total paralysis. It is also crucial to receive adequate medical treatment within the first couple of hours after the incident to prevent secondary lesions. In order to prevent further damage of the spinal cord, the removal of bone fragments or internal stabilization of the injured area showed to be critical for the success of later rehabilitation.[189] Another major problem is caused by inflammation resulting from the uncontrolled release of chemicals from damaged blood vessels, axons and cells. Healthy axons *e.g.* normally deliver small and controlled amounts of

[187] a) B. K. Kwon, E. B. Okon, W. Plunet, D. Baptiste, K. Fouad, J. Hillyer, L. C. Weaver, M. G. Fehlings, W. Tetzlaff, *J. Neurotrauma* **2011**, *28*, 1589–1610. b) W. Tetzlaff, E. B. Okon, S. Karimi-Abdolrezaee, C. E. Hill, J. S. Sparling, J. R. Plemel, W. T. Plunet, E. C. Tsai, D. Baptiste, L. J. Smithson, *et al.*, *J. Neurotrauma* **2011**, *28*, 1611–1682.

[188] *Spinal Cord Injury: Facts and Figures at a Glance*, The National SCI Statistical Center, **2012**, University of Alabama, Brimingham.

[189] J. W. McDonald, C. Sadowsky, *The Lancet* **2002***, 359*, 417-425.

the neurotransmitter glutamate (**4.17**) to stimulate other cells to fire electrical impulses (also see section 4.2.1). Nevertheless, injuries can result in an uncontrolled release of glutamate (**4.18**), which then leads to over-excitation. This can results in the formation of free radicals resulting in the death of healthy cells. This process is called excitotoxicity and one way to prevent this is the local admission of glutamate-receptor blockers shortly after the injury.[190]

Approved long-term treatments include additional surgeries, medication, electrical stimulations and large amount of physical therapies. A good combination of these methods can enable heavily paralysed people to regain back some of their locomotor control, eventually after years of intensive therapy. However, full recovery remains very rare.[191] Experimental therapies include stem cell transplantations,[192] electrochemical neuroprosthesis in combination with a robotic interface[193] or antibody treatments.[194] Another approach is to engineer materials that can promote and guide neuronal growth and at the same time also act as stabilizing and bridging device.[195]

5.1.3 Surface-Mediated Neuronal Growth and Guidance

Multiple approaches, mainly originating form the field of neural interfaces, are reported where surface-based neuronal differentiation and guidance was induced. These results were achieved *e.g. via* topographical changes of surfaces using lithographic modifications and pattering,[196] the alignment of nanofibers, -particles or

[190] a) D. D. Yang, C. Y. Kuan, A. J. Whitmarsh, M. Rincón, T. S. Zheng, R. J. Davis, P. Rakic, R. A. Flavell, *Nature* **1997**, *389*, 865–870. b) C. Matute, M. V. Sánchez-Gómez, L. Martínez-Millán, R. Miledi, *Proc. Natl. Acad. Sci.* **1997**, 8830–8835.
[191] J. W. McDonald, C. Sadowsky, *The Lancet* **2002***, 359*, 417-425.
[192] a) J. W. McDonald, *Sci. Am.* **1999**, 64–73. b) O. Tsuji, K. Miura, Y. Okada, K. Fujiyoshi, M. Mukaino, N. Nagoshi, K. Kitamura, G. Kumagai, M. Nishino, S. Tomisato, *et al.*, *Proc. Natl. Acad. Sci.* **2010**, *107*, 12704–12709. b) J. W. McDonald, X. Z. Liu, Y. Qu, S. Liu, S. K. Mickey, D. Turetsky, D. I. Gottlieb, D. W. Choi, *Nat. Med.* **1999**, *5*, 1410–1412.
[193] R. van den Brand, J. Heutschi, Q. Barraud, J. DiGiovanna, K. Bartholdi, M. Huerlimann, L. Friedli, I. Vollenweider, E. M. Moraud, S. Duis, *et al., Science* **2012**, *336*, 1182–1185.
[194] I. C. Maier, R. M. Ichiyama, G. Courtine, L. Schnell, I. Lavrov, V. R. Edgerton, M. E. Schwab, *Brain* **2009**, *132*, 1426–1440.
[195] J. W. McDonald, C. Sadowsky, *The Lancet* **2002** *, 359*, 417-425.
[196] a) N. A. Kotov, J. O. Winter, I. P. Clements, E. Jan, B. P. Timko, S. Campidelli, S. Pathak, A. Mazzatenta, C. M. Lieber, M. Prato, *Adv. Mater.* **2009**, *21*, 3970–4004.

–tube arrays,[197] or with biomimetic polymers.[198] The fabrication of these materials however, often requires multiple layers and a combination of several specific components. Other approaches include the decoration of surfaces with neurotrophic proteins such as NGF to promote neuronal differentiation.[199] Nevertheless, this method is linked to several drawbacks such as 1) the rapid metabolic degradation, 2) slow tissue penetration, 3) the relatively large size of NGF and 4) potential toxicity at high concentrations of growth factors.[200]

5.1.4 Gentiside B Analog as ideal Candidate for Coating Applications

Recently *Qi et al.* reported the isolation and neuritogenic evaluation of the gentiside family (also see section 4.1.2). These amphiphlic natural products originate from the plant *Gentiana rigescens* used in traditional Chinese medicine. A subsequent SAR study showed that simplified analogs also possess similarly strong neurite outgrowth inducing capabilities in the PC12 cell line. The most potent among them is compound (**5.1**, Fig. 5.1).[201] Since amphiphiles[202] and catechols[203] are known to absorb to surfaces, we hypothesized that this natural product analog (**5.1**) might allow

b) F. Patolsky, B. P. Timko, G. Yu, Y. Fang, A. B. Greytak, G. Zheng, C. M. Lieber, *Science* **2006**, *313*, 1100–1104.

[197] a) A. Solanki, S.-T. D. Chueng, P. T. Yin, R. Kappera, M. Chhowalla, K.-B. Lee, *Adv. Mater.* **2013**, 38, 5477-485. b) T. D. B. Nguyen-Vu, H. Chen, A. M. Cassell, R. Andrews, M. Meyyappan, J. Li, *Small* **2006**, *2*, 89–94. c) A. F. Quigley, J. M. Razal, B. C. Thompson, S. E. Moulton, M. Kita, E. L. Kennedy, G. M. Clark, G. G. Wallace, R. M. I. Kapsa, *Adv. Mater.* **2009**, *21*, 4393–4397. d) M. K. Gheith, V. A. Sinani, J. P. Wicksted, R. L. Matts, N. A. Kotov, *Adv. Mater.* **2005**, *17*, 2663–2670.

[198] C. B. Gumera, Y. Wang, *Adv. Mater.* **2007**, *19*, 4404–4409.

[199] S. Tang, J. Zhu, Y. Xu, A. P. Xiang, M. H. Jiang, D. Quan, *Biomaterials* **2013**, *34*, 7086–7096.

[200] P. Tayalia, D. J. Mooney, *Adv. Mater.* **2009**, *21*, 3269–3285.

[201] a) L. Gao, J. Li, J. Qi, *Bioorg. Med. Chem.* **2010**, *18*, 2131–2134. b) L. Gao, L. Xiang, Y. Luo, G. Wang, J. Li, J. Qi, *Bioorg. Med. Chem.* **2010**, *18*, 6995–7000. c) Y. Luo, K. Sun, L. Li, L. Gao, G. Wang, Y. Qu, L. Xiang, L. Chen, Y. Hu, J. Qi, *ChemMedChem* **2011**, *6*, 1986–1989.

[202] A. B. Jòdar-Reyes, J. L. Ortega-Vinuesa, A. M. Rodrìguez, *J. Colloid. Interface. Sci.* **2005**, *282*, 9–9.

[203] a) J. Gomes, A. Grunau, A. K. Lawrence, L. Eberl, K. Gademann, *Chem. Commun.* **2013**, *49*, 155–157. b) S. Zürcher, D. Wäckerlin, Y. Bethuel, B. Malisova, M. Textor, S. Tosatti, K. Gademann, *J. Am. Chem. Soc.* **2006**, *128*, 1064–1065. c) B. Malisova, S. Tosatti, M. Textor, K. Gademann, S. Zürcher, *Langmuir* **2010**, *26*, 4018–4026. d) P. B. Messersmith, *Science* **2008**, *319*, 1767–1768. e) R. Wehlauch, J. Hoecker, K. Gademann, *ChemPlusChem* **2012**, *77*, 1071–1074.

the assembly of neuritogenic surfaces (NS) by simple absorption on a given solid support.

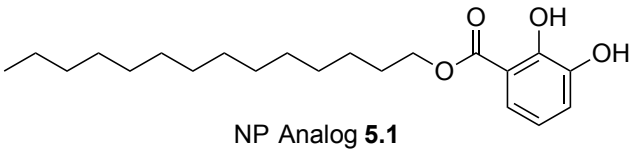

NP Analog **5.1**

Fig. 5.1. The potent neuritogenic genteside B analog **5.1**.

5.2 Results and Discussion

5.2.1 Optimization Studies

In the context of this surface functionalization study, initial experiments showed promising results and therefore justified a broad and systematic exploration of these first findings. To start with, the best concentration of **5.1** had to be determined. Given that the ideal solution concentration of **5.1** is 1 μM[204] we chose to screen a range from 10 mM to 10 nM. Therefore amphiphile **5.1** was dissolved in DMSO and mixed in a 1:10 ratio with a 0.01% collagen aqueous solution. Collagen is widely used to support cell attachment to surfaces.[205] Microscope cover slides were then incubated with this coating solution (CS) for 4 h at 36 °C and afterwards intensively washed with H_2O. These slides were then placed in a new collagen coated 24-well plate, dried and sterilized under UV-light for 2 h. NGF primed PC12 cells were then grown on these slides and incubated for two days, fixed, stained and examined following known procedures (also see Fig. 5.12).[206] As in the earlier discussed projects, NGF (20 ng mL^{-1}) can be used as positive control, similar as in chapters 2-4. In this case, glass slide coated only with collagen, for the cells to grow on, were used as blanks. Another positive control was the normal addition of the NP analog used for coating, to ensure compound specific quality control where needed. These runs are marked with "*". Values are reported as means (unpaired tow-tailed t-test

[204] L. Gao, J. Li, J. Qi, *Bioorg. Med. Chem.* **2010**, *18*, 2131–2134.
[205] a) T. D. B. Nguyen-Vu, H. Chen, A. M. Cassell, R. Andrews, M. Meyyappan, J. Li, *Small* **2006**, *2*, 89–94. b) J. Heino, *Bioessays* **2007**, *29*, 1001–1010.
[206] a) P. Burch, M. Binaghi, M. Scherer, C. Wentzel, D. Bossert, L. Eberhardt, M. Neuburger, P. Scheiffele, K. Gademann, *Chem. Eur. J.* **2013**, *19*, 2589–2591. b) K. Schmidt, W. Gunther, S. Stoyanova, B. Schubert, Z. Li, M. Hamburger, *Org. Lett.* **2002**, *4*, 197–199. c) L. A. Greene, A. S. Tischler, *Proc. Natl. Acad. Sci.* **1980**, *77*, 1701–1705. d) Y. Obara, T. Aoki, M. Kusano, Y. Ohizumi, *J. Pharm. Exp. Ther.* **2002**, *301*, 803–811. d) I. Dikic, J. Schlessinger, I. Lax, *Curr. Biol.* **1994**, *4*, 702–708.

significance: *** = P < 0.0001, **P = < 0.001, *P = < 0.01) and the error bars denote SEM.

Figure 5.2 illustrated that concentrations from 1 mM to 100 nM significantly induce neurite outgrowth. At 10 mM, and to a much lesser extent at 1 mM concentration, the PC12 cells did not attach to the surface anymore, but are still viable. This phenomenon was examined in more detail by placing droplets of 1 mM solution of **5.1** on the bottom of a collagen coated 6-well plate. After evaporation, PC12 cells were incubated for two days, fixed and fluorescently stained using 4,6-diamidin-2-phenylindol (DAPI). As figure 5.3 clearly visualizes, the neurons only attached to the non-modified surface areas, but they are doing this in close proximity to the "restricted area", indicating that a high concentration of the neurotrophin-like compound **5.1** prohibits surface adherence only, but shows no visual toxicity. However, from the results summarized in figure 5.2 a 10 µM to 100 µM concentration was considered best for further evaluations.

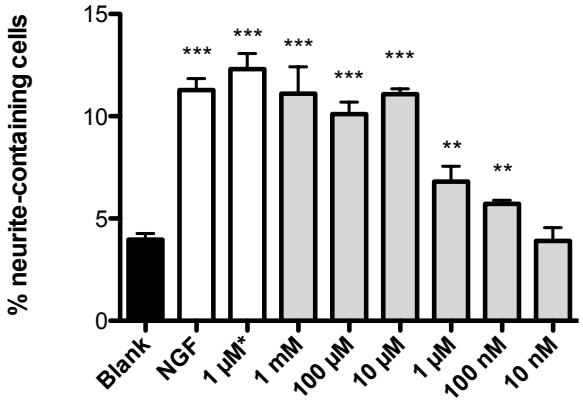

Fig 5.2 Activity of NS using **5.1** at different concentrations in the PC12 assay.

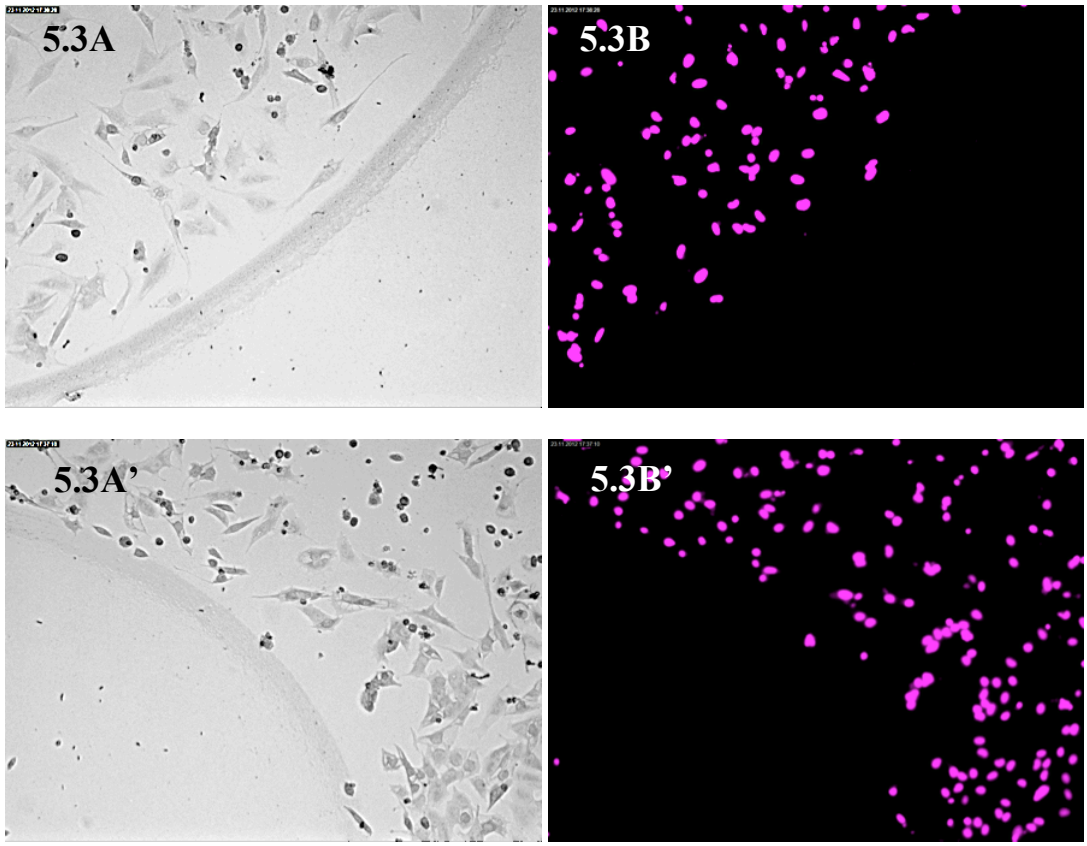

Fig. 5.3 Assambly of "restricted areas". 100 µL droplets of a **5.1** solution (EtOH, 0.01% collagen aqueous solution, 1:10, v:v) were added directly on the plastic 6-well bottom. 5.3A and A' are contrast micrograph and 5.3B and B' their respected fluorescent images.

Next, we performed a solvent screen with water-miscible solvents. DMSO, 1,4-Dioxane, THF, MeOH, EtOH, MeCN, DMF solutions of **5.1** were therefore mixed again with 0.01% collagen aqueous solution (1:10, v:v) to a final concentration of 100 µM. After two days of incubation and examination, all glass slides showed neuritogenic properties and all solvents were acceptable (Fig. 5.4). Since DMSO is non-toxic in low concentrations[207] and widely used in medical applications[208] all additional experiments were performed using this solvent. To further optimize our method we turned our focus towards the incubations conditions.

[207] G. Da Violante, N. Zerrouk, I. Richard, G. Provot, J. C. Chaumeil, P. Arnaud, *Biol. Pharm. Bull.* **2002**, *25*, 1600–1603.
[208] N. C. Santos, J. Figueira-Coelho, J. Martins-Silva, *Biochem. Pharmacol.* **2003**, *65,* 1035–1041.

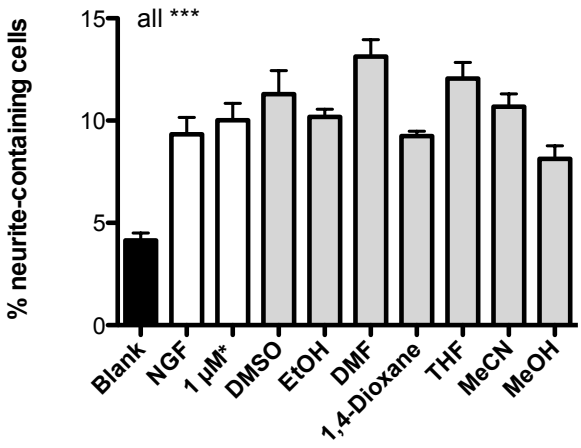

Fig. 5.4. Activity of NS using different water-miscible solvents for coating. For **5.1** 1 µM* and blank DMSO was used as solvent.

Figure 5.5 shows that time and temperature play the expected critical role in the coating procedure. One hour of coating time is not sufficient to detect any bioactivity. Coating of 4 h is only effective at 36 °C. Coating for 16 h at 4 °C resulted in no biological activity. The best result was obtained at the longest incubation time in combination with the highest temperature. Higher temperatures than 36 °C where not examined, but incubation times up to two days showed no increase in neurite outgrowth. Summarizing these experiments, we could define our standard coating conditions: 10 µM final concentration of **5.1**, DMSO as organic solvent and incubation for 16 h at 36 °C.

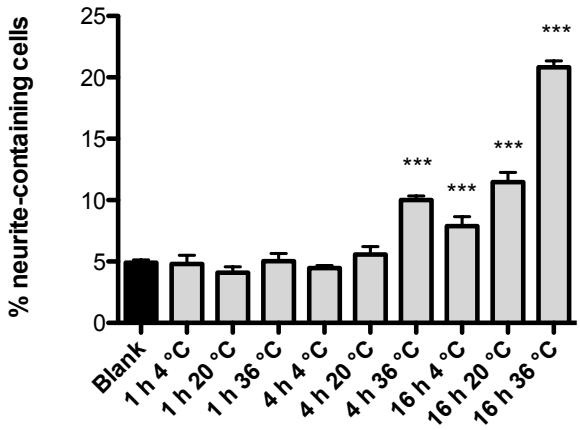

Fig. 5.5. Activity of NS using different coating conditions.

5.2.2 Scope Exploration

Concentration measurements after two days of incubation with PC12 cells showed that the actual concentration of **5.1** in the media was below our detection limit of 1 μM when standard coating conditions were applied. This indicates that we are not only dealing with slow diffusion phenomena. This hypothesis was put on an even stronger fundament by performing mixed incubation experiments (MIE). Slides coated with and without **5.1** were incubated in the same well of a 6-well plate. For this experiment the different round slides were placed at opposite ends in the same well. A small piece of the blank slide was removed to ensure differentiation (Fig. 5.6A). We repeated this experiment by fixing coated squared glass slides next to each other by melting some of the plastic well bottom (Fig. 5.6B). Again, similar results were obtained; showing diffusion of **5.1** from the surface does not play a limiting role for this method. Significant more neurite outgrowth was detected on the expected slides as shown in figure 5.7.

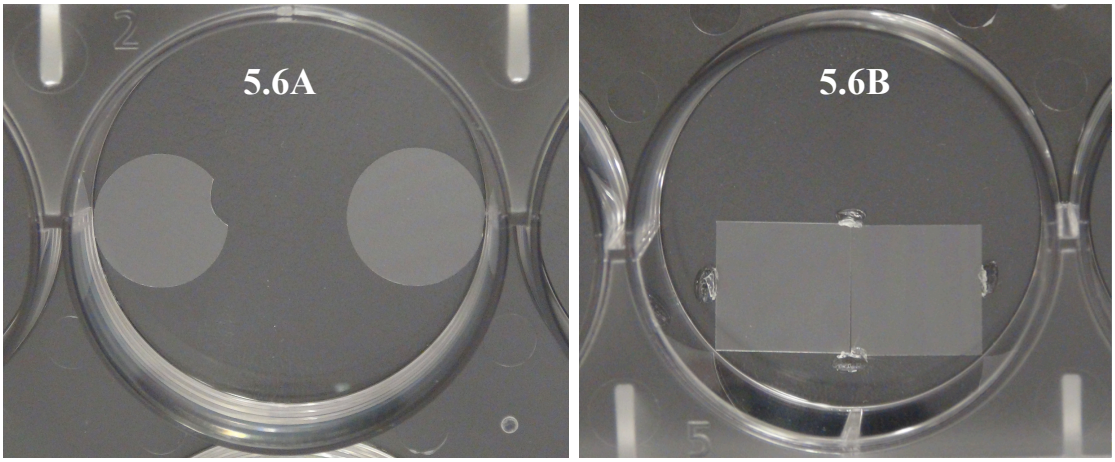

Fig. 5.6. Setting for mixed incubation experiments (MIE).

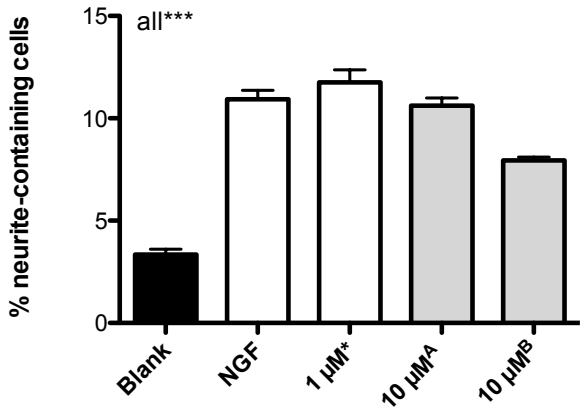

Fig. 5.7. Activity of NS for MIE experiments A: Fig. 5.6A and B: Fig. 5.6B.

All experiments performed with our method so far gave robust and reproducible results. To broaden the scope further we asked ourselves if it would be possible to recycle used glass slides. Therefore, blank and slides coated with **5.1** were placed in a 24-well plate and incubated for 2 days. Then the PC12 cells were gently removed using trypsine solution. The slides were washed twice with H_2O, transferred to a new 24-well plate, dried and sterilized by UV irradiation. Microscopic examination of the slides showed no remaining cells. The slides were then re-used for another incubation run. This experiment showed that the coated slides maintain their bioactivity for at least three cycles (Fig. 5.8).

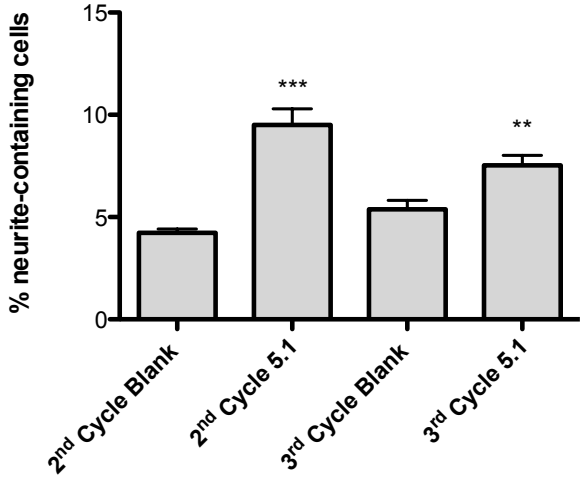

Fig. 5.8. Recycling of coated slides over three cycles.

Another widely used substance that increases the cell adherence to surfaces is poly-L-lysine.[209] Therefore MIE using 50 µg/mL of poly-L-lysine instead of collagen were performed. The obtained results clearly show that collagen could be replaced by poly-L-lysine if needed. This results also indicates, that collagen is not directly or exclusively involved in the adherence of **5.1** to the glass surface (Fig. 5.9).

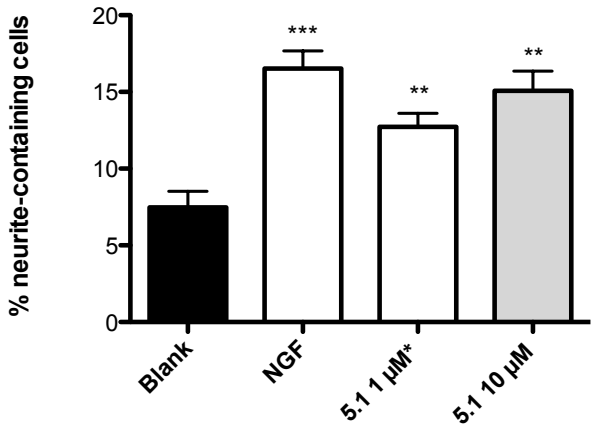

Fig. 5.9. Replacing collagen by poly-L-lysine to support cell adherence.

Since a method, which only allowed the use of a single molecule would not be of great use, we performed MIE with another two neuritogenic natural product analogs **3.5**,[210] and **3.16**[211] (Fig. 5.10). Slides coated with these structurally diverse molecules also show similar activities as compound **5.1**, albeit at higher concentrations: 100 µM (**3.5**) or 50 µM (**3.16**), respectively (Fig. 5.11). This experiment highlights the modularity of this method once more and shows that it is not limited to amphiphilic catechol type molecules.

[209] A. Khademhosseini, K. Y. Suh, J. M. Yang, G. Eng, J. Yeh, S. Levenberg, R. Langer, *Biomaterials* **2004**, *25*, 3583–3592.
[210] a) H. J. Jessen, D. Barbaras, M. Hamburger, K. Gademann, *Org. Lett.* **2009**, *11*, 3446–3449. b) B. Sellergren, L. Anderson, *J. Org. Chem.* **1990**, *55*, 3381–3383.
[211] F. Schmid, H. J. Jessen, P. Burch, K. Gademann, **2013**, *4*, 135–139.

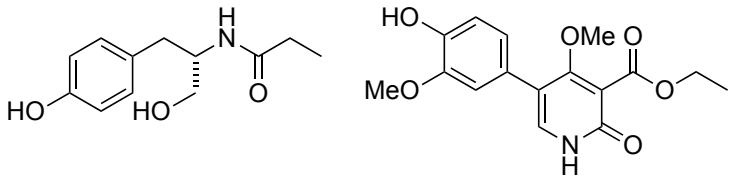

Farinosone C lead analog **3.5**

SF33 **3.16**

Fig. 5.10. Structurally diverse NP analogs **3.5** and **3.16**.

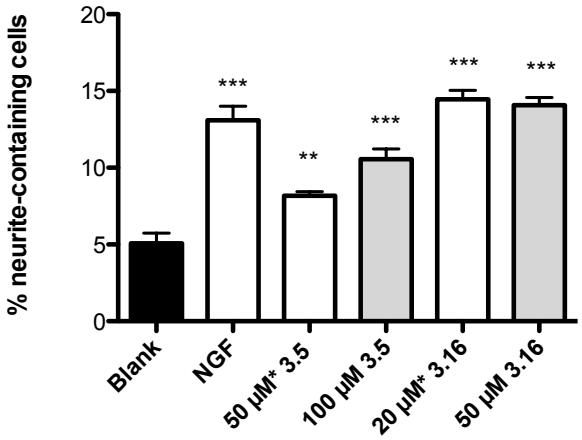

Fig. 5.11. NS assembled using different, less amphiphilic and more polar NP analogs (**3.5**, **3.16**).

5.3 Conclusions and Outlook

In conclusion, we developed a robust and modular method for the assembly of neurite outgrowth inducing glass surfaces. Figure 5.12 summarizes the coating process applying our standard conditions and visualized how straightforward the methodology is. The fact that the recycling of the slides is possible while retaining bioactivity, further demonstrates its potential utility. This work represents to the best of our knowledge the first example where NP analogs have been adapted to coat surfaces in such an uncomplicated fashion to induce neuronal differentiation. This study also follows the requirements of function-orientated synthesis (see section 1.2) in several ways. In the early stages of this project, it was essential that supply of bioactive molecules was unlimited, as a lot of material was necessary to perform the experiments. Fortunately, we were working with optimized and simplified natural

product analogs, therefore this was not a concerned issue. The project also aimed to be as function orientated as possible. In this regard, we used the intrinsic surface adherence properties of the respective molecules and herewith avoiding the attachment of linker and anchor moieties. Moreover, some limitations of previously developed neuritogenic materials such as 1) low general stability of growth factor based approaches, 2) laborious multilayer coatings or 3) the use of expensive materials could be avoided. Further work will involve the adoption of this method to different types of cells and other cell responses than neurite outgrowth such as anti-inflammatory. It is also important to use biocompatible materials instead of glass, which at the same time could also act as stabilizing bridges and ideally would be biodegradable in a slow rate. We expect that this approach will inspire the development of new and efficient methods to biologically activate surfaces in a surprisingly simple and modular way.

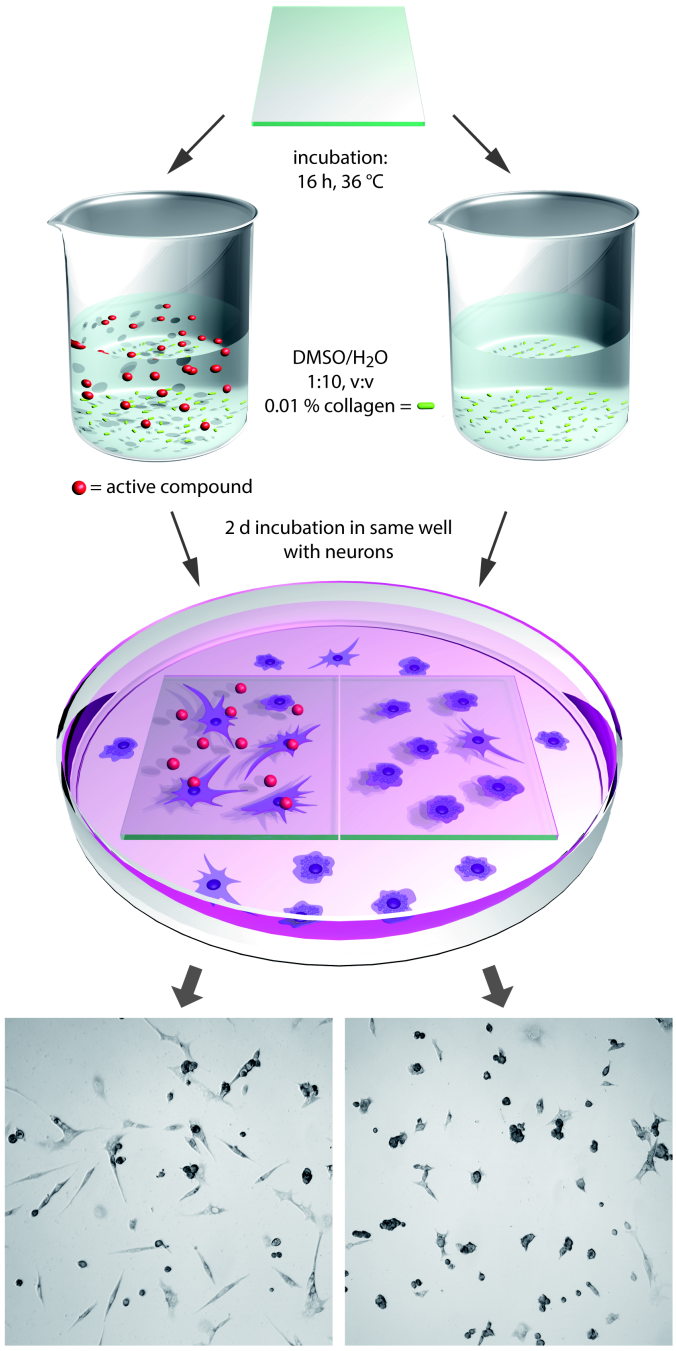

Fig. 5.11. Schematic view of the developed coating procedure using our standard conditions (graphic designed by Ruth Pfalzberger)

CHAPTER 6 -
EXPERIMENTAL PART

6

Parts of this chapter are published similarly or identically as mentioned previously.[212]

6.1 List of Abbreviations, Acronyms and Symbols

°C	Degrees centigrade
3D	Three dimensional
Ac	Acetyl
Ac_2O	Acetic anhydride
AcOH	Acetic acid
ACS	American chemical society
AD	Alzheimer's disease
AIBN	azo-bis-(isobutyronitrile)
ATDD	Amphetamine-type designer drug(s)
Aβ	β-Amyloid
BuBox	*tert*-Butylbis(oxazoline)
BuOH	Butanol
Cat.	Catalytic
$CDCl_3$	Deuterochloroform-d^1
CNS	Central nervous system
Cpd	Compound
d	Days
DAPI	4,6-diamidin-2-phenylindol
DBU	Diazabicycloundecene
DCC	*N*,*N*'-Dicyclohexylcarbodiimide
DCM	Dichloromethane
DEAD	Diethyl diazenedicarboxylate
DIBAL-H	Diisobutylaluminum hydride
DMF	Dimethylformamide
DMP	Dimethylpyridine

[212] a) P. Burch, M. Binaghi, M. Scherer, C. Wentzel, D. Bossert, L. Eberhardt, M. Neuburger, P. Scheiffele, K. Gademann, *Chem. Eur. J.* **2013**, *19*, 2589–2591. b) M. Scherer, Master Thesis, **2012**. c) D. Bossert, Master Thesis, **2012**.

DMS	Dimethyl sulfide
DMSO	Dimethyl sulfoxide
ECS	Endocannabinoid system
EDC	3-(Ethyliminomethyleneamino)-*N*,*N*-dimethyl-propan-1-amine
equiv.	Equivalent(s)
Et_2O	Diethyl ether
EtOAc	Ethyl acetate
EtOH	Ethanol
FC	Flash column chromatography
FDA	Federal drug administration
FTIR	Fourier transform infrared spectroscopy
g	Gram
Glc	Glucose
h	Hour(s)
HOBt	1-Hydroxybenzotriazol
Hz	Hertz [s^{-1}]
IEDDA	Inverse-electron demand Diels-Alder
IR	Infrared
J	Coupling constant [Hz]
L	Liter
L-DOPA	L-3,4-Dihydroxyphenylalanine
Lit.	Literature
M	Molarity [mol/Liter]
M.P.	Melting point
MDMA	3,4-Methylenedioxymethamphetamine, "ecstasy"
MeOH	Methanol
MIE	Mixed incubation experiments
MS	Mass spectroscopy
M_W	Molecular weight
NAD+	Nicotinamide adenine dinucleotide
NGF	Nerve growth factor
NMR	Nuclear magnetic resonance
NPG	Nature publishing group

NS	Neuritogenic surfaces
o.n.	Over night
PCC	Pyridinium chlorochromate
PEP	Pseudoephedrinepropionamide
PFP	Pentafluorophenol
PhMe	Toluene
ppm	Part per million
PTSA	*p*-Toluenesulfonic acid
Py	Pyridine
PyBOP	Benzotriazol-1-yl-oxytripyrrolidinophosphonium hexafluorophosphate
r.t.	Room temperature
R&D	Research and developement
Ref.	Reference
R_f	Retention factor
sat.	Saturated
SEM	Single electron microscopy
TBTA	Tris[(1-benzyl-1H-1,2,3-triazol-4-yl)methyl]amine
tert	Tertiary
TFA	Trifluoroacetic acid
THF	Tetrahydrofuran
TIPSCl	Triisopropylsilyl chloride

6.2 General Materials and Methods

6.2.1 Synthesis

Nuclear magnetic resonance (NMR) spectra were performed using a Bruker Avance 400 MHz spectrometer. Coupling constants *J* are quoted in Hertz (Hz). Splitting patterns are abbreviated as follows: singlet (s), doublet (d), doublet of doublet (dd), doublet of doublet of doublet (ddd), doublet of triplet (dt), triplet (t), quartet (q), quartet of triplet (qt), multiplet (m). Chemical shifts are reported in parts per million (ppm). NMR-solvents were obtained from Cambridge Isotope Laboratories, Inc. (Andover, MA, USA). Dry solvents were used from the Solvent System PS-MD5 (Innovative Technology, Inc., USA) or obtained from Sigma-Aldrich. Technical

solvents used for extractions and purifications (pentane, Et_2O, EtOAc, MeOH and CH_2Cl_2) were distilled prior to use. Chemicals obtained from commercial suppliers were used without further purification, except Et_3N that was distilled prior to use. Thin layer chromatography (TLC) was performed on Merck silica gel 60 F254 glass precoated plates. TLCs were analyzed by UV and $KMnO_4$-dip stain (1.50 g $KMnO_4$, 10 g K_2CO_3, 1.25 ml 10% NaOH in 200 ml dist. H_2O). Flash column chromatography (FC) was performed with the declared solvents using Silicycle SiliaFlash® P60 (230–400 mesh) silica. Reactions were performed in flame-dried glassware under an argon atmosphere. Product purification was performed on an ultimate 3000 semi-preperative HPLC from Thermo Scientific applying a Gemini-NX5 10u C18 column. High-resolution mass spectra (HRMS) were recorded on a Bruker maXis 4G mass spectrometer using electrospray ionisation. Infrared spectroscopy and melting point measurements were performed on a Varian 800 FT-IR machine or on a Büchi melting point B-545 apparatus, respectably. The melting points are uncorrected. The optical rotation was measured on a JASCO P-2000 digital polarimeter (sodium D lamp) adding 1.0 mL of solution in a 3.5 x 100 mm glass cuvette. The concentration is referred as g/100 ml.

6.2.2 PC12 Assay

Collagen coated 6- or 24-well plates (Becton Dickinson Labware, UK), Giemsa stain (modified solution), NGF-7S from murine submaxillary gland, penicillin-streptomycin solution, phosphate-buffered saline (PBS) (10X, 7.4 pH), culture flasks (Corning® cell culture flasks, 75 cm^2) were ordered from Sigma-Aldrich. Horse serum, MEM GlutaMAX™, fetal bovine serum (heat inactivated) and F-12K media were purchased from Invitrogen. Adherent PC12 cells were obtained from LTC Standards, Paris. The cells were cultured in growth media (GM) (F-12K media, 15% horse serum, 2.5% fetal bovine serum, 100 U/mL Penicillin, 100 mg/mL streptomycin). Cells were then scratched off the surface using a cell scraper (BD Falcon) and disaggregated by passage several times through a 21-gauge needle. The cell suspensions (35K cells/mL) was then subjected to the 24-well plates and incubated (36 °C, 5% CO_2) for 4 h. The GM was replaced by differentiation media (DM) (MEM GlutaMAX™, 1% horse serum, 0.5% fetal bovine serum) containing

NGF 7S (20 ng mL^{-1}) and incubated for 16 h. After the media was replaced by DM without NGF the cells were incubated for 2 d with the compounds of interest. Thereafter, cells were fixed with 4% buffered formaldehyde solution for 2 h at 4 °C, then stained with Giemsa stain (modified solution), washed twice with PBS and pictured under a phase contrast microscope (Leica DMI 4000B). The ratio of differentiated cells (at least one neurite with a length equal to at least one cell diameter) to the total cell number per picture was evaluated by manual counting. At least six photographs were taken form three different wells with the same compound. On average 200-300 cells per picture were examined. Samples with DMSO (0.1%) and NGF 7S (10 ng mL^{-1}) were used as controls. All experiments were performed in triplicate and carried out under sterile conditions. Plots were drawn using the Prism software (National Security Agency, Inc., USA).

6.3 Experimental Procedure

6.3.1 Total Synthesis of Gelsemiol

Bis(cyclopentadienyl)zirconium(IV) chloride hydride (Schwartz's Reagent)[213]

Bis(cyclopentadienyl)zirconium(IV) dichloride (10.2 g, 34.5 mmmol, 1.00 equiv.) was dissolved in dry THF (120 mL) under argon and excluded from light. To this solution was added dropwise $LiAlH_4$ (1 M solution in THF, 8.64 mL, 8.64 mmol, 0.25 equiv.). The mixture was stirred for 4 h at r.t. and was then filtered under argon. The filter cake was washed with dry THF (3x30 mL), CH_2Cl_2 (30 mL) and Et_2O (20 mL). The obtained white solid was dried over night under vacuum, yielding the desired product as colorless solid (7.63 g, 33.8 mmol, 85%). **^{1}H-NMR** (400 MHz, MeOD) δ = 6.34 (s, 10H). **^{13}C-NMR** (101 MHz, MeOD) δ = 115.2. (NMR spectra not added)

[213] S. L. Buchwald, S. J. LaMaire, R. B. Nielsen, B. T. Watson, S. M. King, *Org. Synth.* **1998**, *9*, 162.

(*E*)-(3-(benzyloxy)prop-1-en-1-yl)(phenyl)selane (2.41)

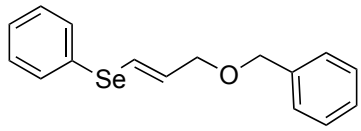

In a 250 mL three necked round bottom flask excluded from light the benzyl protected propagyl alcohol (3.77 g, 25.8 mmol, 1.00 equiv.) was added to a solution of $Cp_2Zr(H)Cl$ (6.65 g, 25.8 mmol, 1.00 equiv.) in dry THF (160 mL) under argon. The resulting mixture was stirred for 30 min at r.t. before a solution of phenylselenyl bromide (6.01 g, 25.8 mmol, 1.00 equiv.) in dry THF (50 mL) was added. The suspension was stirred for 4 h at r.t. and was then treated with pentane (500 mL). The obtained white precipitate was filtered off through a short plug of silica gel and the filter cake was washed with a mixture of pentane/Et_2O (2:1, 2x100 mL). The solvents were removed under reduced pressure and the residue dissolved in pentane (100 mL) and filtered again. The crude product was purified by FC (pentane/CH_2Cl_2/Et_2O 100:5:1) to yield selane **2.41** as slightly yellow oil (5.62 g, 18.5 mmol, 72%).

$\mathbf{R}_f$= 0.35 (pentane/Et_2O 30:1). **^{1}H-NMR** (400 MHz, $CDCl_3$) δ = 7.57 - 7.47 (m, 2H), 7.38 - 7.27 (m, 8H), 6.74 (dt, *J* = 15.4, 1.2 Hz, 1H), 6.07 (dt, *J* = 15.3, 5.9 Hz, 1H), 4.53 (s, 2H), 4.06 (dd, *J* = 5.9, 1.4 Hz, 2H). **^{13}C-NMR** (101 MHz, $CDCl_3$) δ = 138.1, 132.8, 132.0, 129.6, 129.3, 128.5, 127.8, 127.7, 127.5, 122.1, 72.2, 71.0. **FTIR** $\tilde{\nu}$ = 3060*m*, 3029*m*, 2909*w*, 2850*s*, 1610*w*, 1578*m*, 1495*w*, 1477*s*, 1453*m*, 1356*m*, 1250*w*, 1203*w*, 1101*s*, 1070*s*, 1023*s*, 1001*w*, 945*m*, 736*s*, 694*s*, 631*s* cm^{-1}.

Selane 2.44

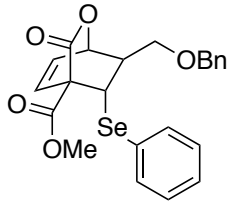

Tert-BuBox (678 mg, 2.30 mmol, 0.12 equiv.) was added to a stirred solution of copper(II) triflate (694 mg, 1.92 mmol, 0.10 equiv.) in dry CH_2Cl_2 (140 mL). The resulting green solution was stirred for 2 h at r.t. and was then cooled to –18 °C before 3-carbomethoxy-2-pyrone **2.42** (2.96 g, 19.2 mmol, 1.00 equiv.) in dry CH_2Cl_2 (15 mL) and phenylvinylselenide derivate **2.41** (5.82 g, 19.2 mmol, 1.00 equiv.) in CH_2Cl_2 (15 mL) were added. The resulting red mixture was stirred for 5 min at –18 °C and was then allowed to warm up to r.t.. The solvent was removed under reduced pressure at r.t. and the obtained red viscous residue was stirred under high vacuum for 20 h. The

crude mixture was directly purified by FC (pentane/EtOAc 5:1) to yield selane **2.44** as colorless solid (7.95 g, 17.4 mmol, 91%, 83% ee).

R_f = 0.58 (pentane/EtOAc 4:1). **M.P.** = 63 - 64 °C, **^{1}H-NMR** (400 MHz, $CDCl_3$) δ = 7.57-7.48 (m, 2H), 7.44-7.18 (m, 8H), 6.90 (d, 7.4 Hz, 1H), 6.57 (m, 1H), 5.31 (m, 1H), 4.62-4.43 (m, 2H), 3.65 (dd, *J* = 5.57, 9.23 Hz, 1H), 3.55 (s, 3H), 3.54 (t, *J* = 9.5 Hz, 1H), 3.29 (m, 1H), 2.45 (m, 1H), **^{13}C-NMR** (101 MHz, $CDCl_3$) δ = 168.7, 166.9, 137.6, 135.6, 132.0, 131.6, 129.1, 128.7, 128.5, 128.5, 127.9, 127.8, 74.7, 73.5, 68.2, 60.1, 52.5, 49.1, 39.1. **FTIR** $\tilde{\nu}$ = 3062*w*, 3032*w*, 2952*w*, 2861*w*, 1747*s*, 1616*w*, 1578*w*, 1477*m*, 1453*m*, 1364*m*, 1310*m*, 1282*s*, 1197*m*, 1170*w*, 1102*s*, 1066*s*, 1024*m*, 1000*w*, 984*w*, 739*s*, 694*s*, 612*s* cm^{-1}. **Optical rotation:** $[\alpha]_D^{25}$= –47.3 (c = 0.50, MeOH). For X-Ray see Annexes

The *tert*-BuBox ligand was either purchased by Sigma-Aldrich (*S*,*S*) or prepared following the Evans' protocol (*S*,*S and R*,*R*).[314]

(3*S* or 3*R*, 3a*S*,4*R*,6a*S*)-methyl 4-((benzyloxy)methyl)-2-oxo-3,3a,4,6a-tetrahydro-2*H*-cyclopenta[*b*]furan-3-carboxylate (2.39a/b)

2.39a = (*R*)
2.39b = (*S*)

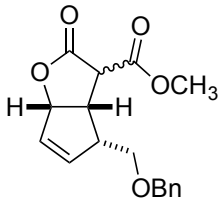

A solution of selenide **2.44** (7.42 g, 16.2 mmol, 1.00 equiv.), triphenyltinhydride (7.57 g, 21.6 mmol, 1.33 equiv.) and AIBN (879 mg, 5.35 mmol, 0.33 equiv.) in dry benzene (1250 mL) was degassed four times under argon. The solution was maintained under argon and stirred under reflux for 4.5 h. The mixture was allowed to reach r.t. and dry silica gel (220 g) was added. The suspension was vigorously stirred at r.t. for 60 h. The solvent was evaporated and the silica gel washed with Et_2O (900 mL). The solvent was removed and the obtained yellow oil was purified by FC (pentane/EtOAc 3:1) to yield a mixture of lactones **2.39a** and **2.39b** (d.r. 3:2) as colorless liquid (4.05 g, 13.4 mmol, 83%).

[314] D. A. Evans, G. S. Peterson, J. S. Johnson, D. M. Barnes, K. R. Campos, K. A. Woerpel, *J. Org. Chem.* **1998**, *63*, 4541–4544.

R_f = 0.58 (pentane/EtOAc 1:1). **HRMS-ESI** calcd. for $C_{10}H_{16}O_4^+$: [100%, M]$^+$ 303.1227, found 303.1217. **FTIR** $\tilde{\nu}$ = 3064*w*, 3032*w*, 2953*w*, 2927*w*, 2862*w*, 2801*w*, 1774*s*, 1737*s*, 1619*w*, 1496*w*, 1454*w* 1437*w*, 1367*m*, 1279*m*, 1160*m*, 1141*m*, 1085*m*, 1015*m*, 935*w*, 832*w*, 741*m*, 700*m*, 642*w* cm^{-1}.

2.39a: **^{1}H-NMR** (400 MHz, $CDCl_3$): δ = 7.42 - 7.22 (m, 5H), 5.99 - 5.90 (m, 2H), 5.57 - 5.53 (m, 1H), 4.51 - 4.39 (m, 2H), 3.75 - 3.71 (m, 1H), 3.69 (s, 3H), 3.68 - 3.67 (m, 1H), 3.63 (dd, *J* = 9.8, 4.6 Hz, 1H), 3.41 (dd, *J* = 9.8, 8.3 Hz, 1H), 3.27 - 3.19 (m, 1H). **^{13}C-NMR** (101 MHz, $CDCl_3$): δ = 172.26, 168.57, 137.55, 137.49, 132.19, 128.57, 127.94, 127.7, 87.77, 73.2, 69.04, 53.08, 48.07, 46.56, 43.40.
2.39b: **^{1}H-NMR** (400 MHz, $CDCl_3$) δ = 7.42 - 7.22 (m, 5H), 6.77 (ddd, *J* = 7.7, 1.9, 0.8 Hz, 1H), 6.57 (dd, *J* = 7.8, 5.1 Hz, 1H), 5.35 (dt, *J* = 5.1, 1.6 Hz, 1H), 4.59 - 4.50 (m, 2H), 3.87 (s, 3H), 3.60 - 3.54 (m, 1H), 3.53 - 3.46 (m, 1H), 2.28 - 2.20 (m, 1H), 1.89 (dd, *J* = 13.3, 10.7 Hz, 1H), 1.80 - 1.73 (m, 1H). **^{13}C-NMR** (101 MHz, $CDCl_3$) δ = 170.35, 168.57, 137.83, 132.23, 132.1, 128.49, 127.86, 127.75, 75.49, 73.54, 69.92, 54.6, 53.18, 38.37, 26.51.

(3*R*,3a*S*,4*S*,5*R*,6*R*,6a*R*)-4-((benzyloxy)methyl)-6-iodo-5-methyl-2-oxohexahydro-2*H*-cyclopenta[*b*]furan-3-carboxylic acid (2.49)

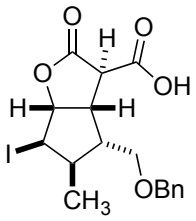

To a solution of CuBr-DMS complex (4.49 g, 21.8 mmol, 4.00 equiv.) in THF (200 mL) was added dropwise methyllithium (1.6 M solution in Et_2O, 27.3 mL, 43.7 mmol, 8.00 equiv.) at –18 °C. The mixture was stirred for 15 min at the same temperature, before it was cooled to –48 °C and lactones **2.39a/b** and (1.65 g, 5.46 mmol, 1.00 equiv.) in THF (40 mL) and TMSCl (1.74 mL, 13.6 mmol, 2.50 equiv.) were added. The mixture was stirred for 3.5 h at –48 °C and was then quenched with aqueous H_2SO_4 solution (160 ml, 1 M) at the same temperature. The suspension was allowed to reach r.t., the aqueous and the organic phases were separated after brine (40 mL) has been added. The aqueous phase was extracted with Et_2O (3x200 mL). The combined organic layers were washed with sat. NH_4Cl solution (600 mL) dried (Na_2SO_4) and concentrated. The mixture was dissolved in aqueous NaOH (80 mL, 1.0 M) and the resulting suspension stirred for 24 h at r.t.. Solid CO_2 was added in small portions to

set pH of the solution to 8 - 9. The mixture was cooled to 0 °C and a solution of I_2 (1.82 g, 7.26 mmol, 1.33 equiv.) in THF (45 mL) was added. The resulting brown solution was stirred for 50 min, quenched with aqueous sat. $Na_2S_2O_3$ solution (8 mL) and treated with aqueous H_2SO_4-solution (180 mL, 1 M). The aqueous phase was extracted with Et_2O (3x50 mL), the combined organic layers were dried (Na_2SO_4) and evaporated under reduced pressure. The crude residue was purified by FC (pentane/EtOAc 4:1 + 0.01 TFA) to yield **4.49** as a slightly yellow solid (1.05 g, 2.44 mmol, 45%).

R_f = 0.68 (pentane/EtOAc 1:1 + 0.1 AcOH). **M.P.** = 95 - 97 °C. **^{1}H-NMR** (400 MHz, $CDCl_3$) δ = 7.51 - 7.03 (m, 5H), 5.39 (d, *J* = 6.2 Hz, 1H), 4.57 (d, *J* = 4.6 Hz, 1H), 4.55 - 4.43 (m, 2H), 3.92 (d, *J* = 2.7 Hz, 1H), 3.64 - 3.58 (m, 1H), 3.54 (ddd, *J* = 9.4, 6.2, 2.7 Hz, 1H), 3.46 (dd, *J* = 10.3, 6.7 Hz, 1H), 2.31 (tdd, *J* = 12.1, 6.8, 2.8 Hz, 1H), 1.38 (tt, *J* = 11.7, 6.0 Hz, 1H), 0.98 (d, *J* = 6.2 Hz, 3H). **^{13}C-NMR** (101 MHz, $CDCl_3$) δ = 171.8, 171.7, 137.2, 128.6, 128.1, 127.9, 90.9, 73.6, 66.3, 48.9, 45.5, 43.7, 41.6, 36.9, 18.9. **HRMS-ESI** calcd. for $C_{17}H_{18}IO_5^-$: [100%, M]$^-$ 429.0204, found 429.0208; **FTIR** $\tilde{\nu}$ = 3056*w*, 2962*w*, 2899*w*, 2872*w*, 1755*m*, 1721*s*, 1453*w*, 1380*w*, 1362*w*, 1308*w*, 1292*w*, 1260*m*, 1209*m*, 1182*s*, 1152*s*, 1105*m*, 1082*m*, 1058*m*, 985*m*, 963*s*, 878*m*, 853*m*, 807*m*, 736*s*, 716*s*, 653*m* cm^{-1}. **Optical rotation:** $[\alpha]_D^{25}$= +1.5 (c = 1.00, MeOH). For X-Ray data see Annexes.

Gelsemiol (2.1)

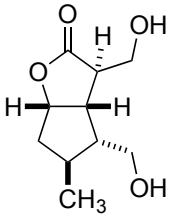

Acid **2.49** (100 mg, 0.24 mmol, 1.00 equiv.) was dissolved in THF (8 mL). The solution was cooled to 0 °C and BH_3-DMS complex (2.0 M solution in THF, 3.02 mL, 6.04 mmol, 26.0 equiv.) was added dropwise to the solution and the mixture stirred for 3 h at 0 °C. The reaction was carefully quenched with MeOH (10 mL) and the solvents were removed under reduced pressure. The crude mixture was dissolved in EtOH (30 mL) and added to a decanted solution of Raney-Nickel (20 mL, 50% w/w solution in water). The resulting suspension was stirred for additional 60 h at r.t. under an atmosphere of H_2 and was then filtered over a short plug of silica gel and washed with EtOAc (3x30 mL). The solvents were removed and the crude product purified by FC

(EtOAc) to give gelsemiol (**2.1**) as a white solid and the diasteromeric lactols **2.50a/b** as side products, which were again stirred for 24 h in a solution of Raney-Nickel (10 mL, 50% w/w solution in water) in EtOH (15 mL) under an argon atmosphere. The suspension was again filtered over a short plug of silica gel and washed with EtOAc (3x30 mL). The solvents were removed and the crude product purified by FC (EtOAc) to gain additional **2.1** (30 mg, 0.15 mmol, 65% combined yield over two steps).

R_f = 0.25 (EtOAc), **M.P.** = 89 - 91 °C **^{1}H-NMR** (600 MHz, D_2O) δ = 5.09 (ddt, *J* = 7.0, 6.3, 0.6, 0.6 Hz, 1H), 3.93 (dd, *J* = 11.3, 4.3 Hz, 1H), 3.83 (dd, *J* = 11.6, 4.5 Hz, 1H), 3.81 (dd, *J* = 11.3, 4.0 Hz, 1H), 3.59 (dd, *J* = 11.5, 9.5 Hz, 1H), 3.10 (td, *J* = 7.7, 5.2 Hz, 1H), 2.95 (dt, *J* = 5.1, 4.2 Hz, 1H), 2.12 (dd, *J* = 14.6, 6.2 Hz, 1H), 1.85 (dddd, *J* = 11.6, 9.5, 8.1, 4.5 Hz, 1H), 1.74 (dtq, *J* = 6.0, 12.1, 6.2 Hz, 1H), 1.54 (ddd, *J* = 14.6, 12.1, 6.3 Hz, 1H), 0.99 (d, *J* = 6.3 Hz, 3H). **^{13}C-NMR** (151 MHz, D_2O) δ = 183.2, 86.5, 62.6, 61.3, 51.1, 44.7, 44.7, 41.9, 33.5, 17.4. **HRMS-ESI** calcd. for $C_{10}H_{16}O_4^+$: [100%, M]$^+$ 201.1121, found 201.1119. **FTIR** $\tilde{\nu}$ = 3247*s*, 2964*w*, 2928*m*, 2885*m*, 2864*w*, 1756*s*, 1481*w*, 1462*m*, 1379*m*, 1330*w*, 1314*w*, 1218*s*, 1204*s*, 1080*s*, 1012*s*, 989*s*, 956*w*, 939*w*, 920*w*, 879*w*, 845*w*, 705*m*, 679*m*, 645*m* cm^{-1}. **Optical rotation:** $[\alpha]_D^{25}$= +12.8 (c = 0.50, MeOH). The reported data is in accordance with the literature.[215]

2.50a: **R_f** = 0.18 (EtOAc). **^{1}H-NMR** (500 MHz, $CDCl_3$) δ = 5.45 (d, *J* = 4.7 Hz, 1H), 4.71 (t, *J* = 6.7 Hz, 1H), 3.84 - 3.72 (m, 2H), 3.71 - 3.63 (m, 2H), 2.57 (dt, *J* = 8.9, 7.3 Hz, 1H), 2.27 (tt, *J* = 9.3, 5.1 Hz, 1H), 1.84 (dd, *J* = 14.3, 5.5 Hz, 1H), 1.71 - 1.59 (m, 2H), 1.38 - 1.29 (m, 1H), 0.95 (d, *J* = 5.9 Hz, 3H). **^{13}C-NMR** (126 MHz, D_2O) δ = 98.2, 82.8, 60.9, 60.0, 50.6, 47.0, 44.7, 40.7, 32.0, 16.4.
2.50b: **R_f** = 0.18 (EtOAc). **^{1}H-NMR** (500 MHz, $CDCl_3$) δ = 5.10 (d, *J* = 4.9 Hz, 1H), 4.49 (t, *J* = 6.5 Hz, 1H), 3.83 - 3.73 (m, 2H), 3.70 - 3.63 (m, 2H), 2.62 (dd, *J* = 8.5, 6.6 Hz, 1H), 0.98 - 0.95 (m, 1H), 2.08 (p, *J* = 6.0 Hz, 1H), 1.92 (d, *J* = 13.7 Hz, 1H), 1.69 - 1.60 (m, 1H), 1.34 (dd, *J* = 11.7, 6.3 Hz, 1H), 0.96 (d, *J* = 6.2 Hz, 3H); **^{13}C-NMR** (126 MHz, D_2O) δ = 100.7, 82.1, 62.1, 60.6, 50.4, 48.8, 46.2, 41.6, 32.5, 16.7.

[215] S. R. Jensen, O. Kirk, B. J. Nielsen, R. Norrestam, *Phytochem.* **1987**, *6*, 1725–1731.

(3*R*,3*S*,4*S*,5*R*,6*R*,6*R*)-4-((benzyloxy)methyl)-3-(hydroxymethyl)-6-iodo-5-methylhexa-hydro-2*H*-cyclopenta[*b*]furan-2-one (2.51)

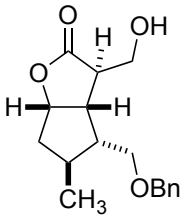

Oxalyl chloride (148 µL, 1.75 mmol, 6.00 equiv) was added to a solution of dry DMF (45 µL, 0.58 mmol, 2.00 equiv) in dry CH_2Cl_2 (6 mL) at 0 °C under an atmosphere of Ar. After 5 min the ice-bath was removed and the solution was stirred for 1 h at r.t.. The solvent was evaporated by first bubbling Ar into the solution and then by applying a vacuum. The residual white powder was dissolved in dry CH_3CN (8 mL) and dry THF (8 mL) before a solution of **2.49** (125 mg, 0.29 mmol, 1.00 equiv) in dry THF (8 mL) was added at –48 °C under argon. The reaction mixture was stirred for 3.5 h at the same temperature. At this point, to the reaction mixture was added a solution of $NaBH_4$ (66 mg, 1.75 mmol, 6.00 equiv) in dry DMF (5 mL) and dry THF (5 mL) at –48 °C, stirred for additional 3 h at the same temperature and quenched with aqueous H_2SO_4-solution (1.0 M, 25 mL). The aqueous phase was extracted with Et_2O (3x40 mL) and the combined organic layers were washed with brine (100 mL), dried over Na_2SO_4 and evaporated under reduced pressure. The crude residue was purified by FC (pentane/Et_2O, 1:2) to give the benzyl protected alcohol as viscous oil (80 mg, 0.195 mmol, 67%).

$\mathbf{R}_f$ = 0.78 (EtOAc). **^{1}H-NMR** (500 MHz, $CDCl_3$) δ = 7.55 - 7.25 (m, 5 H), 5.35 (d, *J* = 6.8 Hz, 1H), 4.60 - 4.44 (m, 3H), 3.91 (dd, *J* = 10.5, 5.2 Hz, 1H), 3.80 (dd, *J* = 10.5, 4.9 Hz, 1H), 3.63 (dd, *J* = 10.0, 3.9 Hz, 1H), 3.51 (dd, *J* = 10.0, 8.8 Hz, 1H), 3.14 (ddd, *J* = 9.0, 6.9, 3.4 Hz, 1H), 2.93 - 2.87 (m, 1H), 2.42 (dtd, *J* = 12.6, 8.9, 3.9 Hz, 1H), 1.22 - 1.13 (m, 1H), 1.02 (d, *J* = 6.2 Hz, 3H). **^{13}C-NMR** (126 MHz, $CDCl_3$) δ = 178.1, 137.3, 128.6, 128.1, 128.0, 90.7, 73.6, 67.6, 63.5, 45.8, 44.1, 42.7, 42.7, 37.4, 19.1. **HRMS-ESI** calcd. for $C_{10}H_{16}O_4^+$: [100%, M]$^+$ 417.0557, found 417.0560. **FTIR** $\tilde{\nu}$ = 3453*m*, 2858*m*, 1764*s*, 1454*m*, 1366*m*, 1309*m*, 1261*m*, 1176*s*, 1092*s*, 999*s*, 794*m*, 741*m*, 700*m*, 647*m* cm^{-1}. **Optical rotation:** $[\alpha]_D^{25}$= +12.1 (c = 0.38, $CHCl_3$).

Raney Nickel (about 3 mL activated catalyst, 50% slurry in water) was decanted and the solid added to a solution of benzyl protected alcohol **2.51** in EtOH (5 mL). The reacting mixture was stirred over night under an atmosphere of H_2. The catalyst was

then removed by filtration and the solution was concentrated under reduced pressure. The crude residue was purified by FC on silica gel (pure EtOAc) to give gelsemiol (**2.1**) as white solid (4.0 mg, 0.02 mmol, 52%). The analytical data matched the reported above.

Diacylated gelsemiol 2.51

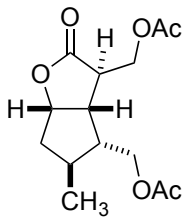

To a solution of gelsemiol (**2.1**, 1.9 mg**,** 1.0 mmol) in dry pyridine (0.5 mL) at 0 °C were added three drops of acetic anhydride. The mixture was stirred overnight and extracted with EtOAc and sat. NH_4Cl solution. The crude product was then purified by FC (pentane/Et_2O, 1:2) to give the diacetylated gelsemiol (**2.1**) (1.8 mg, 0.76 mmol, 93%).

$\mathbf{R}_f$ = 0.68 (MeOH/CH_2Cl_2, 1:20). **^{1}H-NMR** (600 MHz, $CDCl_3$) δ 4.96 (t, *J* = 6.7 Hz, 1H), 4.38 - 4.29 (m, 3H), 3.99 (dd, *J* = 11.8, 9.2 Hz, 1H), 3.03 - 2.93 (m, 1H), 2.82 (q, *J* = 4.2 Hz, 1H), 2.22 (dd, *J* = 14.5, 6.2 Hz, 1H), 2.08 (s, 3H), 2.07 (s, 2H), 2.00 - 1.90 (m, 1H), 1.84 (tp, *J* = 12.4, 6.2 Hz, 1H), 1.49 (ddd, *J* = 14.5, 12.1, 6.3 Hz, 1H), 1.05 (d, *J* = 6.3 Hz, 3H). **^{13}C-NMR** (151 MHz, $CDCl_3$) δ 176.87, 170.88, 94.65, 83.04, 63.89, 63.06, 47.88, 44.37, 41.78, 41.08, 33.41, 20.98, 20.95, 17.31, 0.15. **HRMS-ESI** calcd. for $C_{14}H_{20}NaO_4$: [100%, M+Na]$^+$ 307.1158, found 307.1155. **FTIR** $\tilde{\nu}$ = 2961*w*, 2926*w*, 2873*w*, 2854*w*, 1769*w*, 1743*w*, 1463*w*, 1371*m*, 1242*s*, 1185*m*, 1033*w* cm^{-1}. **Optical rotation:** $[\alpha]_D^{25}$= +13.0 (c = 0.03, MeOH). The reported data is in accordance with the literature.[216]

[216] S. R. Jensen, O. Kirk, B. J. Nielsen, R. Norrestam, *Phytochem.* **1987**, *6*, 1725–1731.
[217] a) H. J. Jessen, D. Barbaras, M. Hamburger, K. Gademann, *Org. Lett.* **2009**, *11*, 3446–3449 b) B. Sellergren, L. Anderson, *J. Org. Chem.* **1990**, *55*, 3381–3383.

6.3.2 Farinosone C Analogs Collection

(*S*)-*N*-(1-hydroxy-3-(4-hydroxyphenyl)propan-2-yl)propionamide (3.5)[217]

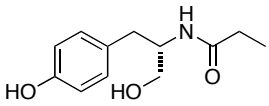

To a solution of L-tyrosinol hydrochloride (400 mg, 1.96 mmol, 1.00 equiv.) in THF (4.00 mL), K_2CO_3 (1.22 g, 8.84 mmol, 4.40 equiv.) dissolved in H_2O (3.50 mL) was added at once. The reaction mixture was stirred for 45 min at r.t. before propanoyl chloride (308 mg, 3.53 mmol, 1.80 equiv.) was added. The mixture was stirred for 15 h at r.t.. The organic solvent was then evaporated and brine was added before the aqueous layer was extracted with EtOAc (3x). The combined organic layers were dried over $MgSO_4$ and concentrated. The crude product was purified by FC on SiO_2 (CH_2Cl_2/EtOAc, 20:1) and yielded the products **3.5** (313 mg, 1.40 mmol, 71%), **3.20c** (8.0 mg, 0.028 mmol, 1%) and **3.20e** (13.4 mg, 0.048 mmol, 2%) as yellow oils.

$\mathbf{R}_f$ = 0.49 (CH_2Cl_2/MeOH, 8:2). **^{1}H-NMR** (400 MHz, MeOD) d 7.03 (d, *J* = 8.3 Hz, 2H), 6.69 (d, *J* = 8.4 Hz, 2H), 4.09 - 3.93 (m, 1H), 3.63 - 3.39 (m, 2H), 2.80 (dd, *J* = 13.8, 6.3 Hz, 1H), 2.60 (dd, *J* = 13.8, 8.2 Hz, 1H), 2.14 (q, *J* = 7.6 Hz, 2H), 1.04 (t, *J* = 7.6 Hz, 3H). **^{13}C-NMR** (101 MHz, MeOD) d 176.87, 156.86, 131.23, 130.53, 116.05, 64.19, 54.22, 37.13, 30.29, 10.51. **HRMS ESI-TOF** calcd. for $C_{12}H_{17}NO_3$ (100%, $[M+H]^+$): 224.1287; found 224.1287. **FTIR** $\tilde{\nu}$ 3276*m*, 2940*w*, 2882*w*, 1616*s*, 1545*s*, 1514*s*, 1451*m*, 1373*m*, 1236*s*, 1042*m*, 823*m*, 634*s* cm^{-1}. **Optical rotation:** $[\alpha]_D^{25}$ = –3.7 (c = 1.2, MeOH).

(*S*)-*N*-(1-hydroxy-3-phenylpropan-2-yl)propionamide (3.20a)[218]

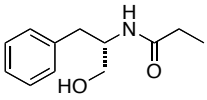

To a solution of (*S*)-(–)-2-Amino-3-phenyl-1-propanol (100 mg, 1.17 mmol, 1.00 equiv.) in H_2O/THF (1:1, 10.0 mL) was K_2CO_3 (647 mg, 4.68 mmol, 4.00 equiv.) added at r.t.. The mixture was stirred for 1 h before propionyl chlorid (204 µL, 2.34 mmol, 2.0 equiv.) was added. The reaction mixture was then stirred for 17 h under argon atmosphere. The organic solvent was evaporated and the aqueous layer was extracted with CH_2Cl_2 (3x), brine (1x), dried over Na_2SO_4

[218] H. Seki, K. Koga, S. Yamada, *Chem. Pharm. Bull.* **2013**, *15*, 1948-1954.

and concentrated. The crude product was purified by FC on SiO_2 (EtOAc/CH_2Cl_2, 1:5) to yield the product **3.20a** (200 mg, 0.97 mmol, 82%) as colorless solid.

R_f = 0.34 (MeOH/CH_2Cl_2, 1:20). **M.P.** = 77 - 78 °C. **^{1}H-NMR** (400 MHz, $CDCl_3$) δ 7.42 - 7.15 (m, 5H), 5.89 (d, *J* = 6.7 Hz, 1H), 4.31 - 4.08 (m, 1H), 3.69 (dd, *J* = 11.0, 3.3 Hz, 1H), 3.60 (dd, *J* = 11.0, 5.0 Hz, 1H), 3.04 - 2.79 (m, 2H), 2.18 (q, *J* = 7.7 Hz, 2H), 1.11 (t, *J* = 7.7 Hz, 3H). **^{13}C-NMR** (101 MHz, $CDCl_3$) δ 174.68, 137.81, 129.33, 128.73, 126.77, 64.25, 52.92, 37.10, 29.88, 9.92. **HRMS ESI-TOF** calcd. for $C_{12}H_{18}NO_2^+$ (100%, $[M+H]^+$): 208.1332; found 208.1332. **FTIR** $\tilde{\nu}$ 3325*m br*, 2962*m*, 2361*m*, 2337*m*, 1634*m*, 1615*m*, 1515*s*, 1453*m*, 1367*m*, 1229*m*, 1043*m*, 826*w* cm^{-1}. **Optical rotation:** $[\alpha]_D^{23} = -10.7$ (c = 1.0, MeOH).

(*S*)-*N*-(1-hydroxy-3-(4-methoxyphenyl)propan-2-yl)propionamide (3.20b)

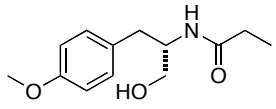

To a solution of propionamide **3.5** (120 mg, 0.538 mmol, 1.00 equiv.) in MeCN (8.0 mL) was added $CsCO_3$ (193 mg, 0.592 mmol, 1.10 equiv.) and MeI (40 µL, 0.644 mmol, 1.20 equiv.). The reaction mixture was stirred at r.t. under an argon atmosphere. After 18 h additional MeI (30 µL, 0.482 mmol, 0.9 equiv.) and $CsCO_3$ (150 mg, 0.778 mmol, 0.85 equiv) were added and the mixture was stirred for another 32 h. The solvent was evaporated and the crude products were extracted using EtOAc (3x) and brine (1x). The combined organic layers were dried over $MgSO_4$ and concentrated. The crude product was purified by FC on SiO_2 (CH_2Cl_2/MeOH 20:1) and yielded the products **3.20b** (118 mg, 0.50 mmol, 52 %) and **3.20f** (21 mg, 0.083 mmol, 9 %) as white solids.

R_f = 0.68 (MeOH/CH_2Cl_2, 1:10). **M.P.** = 80 - 82 °C. **^{1}H-NMR** (400 MHz, MeOD) δ 8.37 (dt, *J* = 8.3 Hz, 1H), 8.03 - 7.80 (m, 2H), 7.72 - 7.56 (m, 2H), 5.56 (t, *J* = 5.5 Hz, 1H), 4.74 - 4.57 (m, 2H), 4.51 (s, 3H), 4.14 - 4.00 (m, 2H), 3.56 (dd, *J* = 13.7, 5.6 Hz, 1H), 3.38 - 3.25 (m, 2H), 2.82 (q, *J* = 7.6 Hz, 2H), 1.72 (t, *J* = 7.6 Hz, 3H). **^{13}C-NMR** (101 MHz, MeOD) δ 182.10, 167.02, 140.63, 139.56, 123.00, 72.12, 64.46, 61.94, 45.21, 38.11, 19.54. **HRMS ESI-TOF** calcd. for $C_{13}H_{20}NO_3$ (100%, $[M+H]^+$): 238.1443; found 238.1451. **FTIR** $\tilde{\nu}$ 3494*w*, 3300*m*, 3080*w*, 2939*w*, 2922*w*, 1640*s*,

1540*s*, 1513*s*, 1463*m*, 1442*m*, 1247*s*, 1178*m*, 1075*m*, 1030*s*, 810*m*, 697*m* cm^{-1}. **Optical rotation:** $[\alpha]_D^{22} = -4.0$ (c = 0.68, MeOH).

(*S*)-4-(3-hydroxy-2-propionamidopropyl)phenyl propionate (3.20c)

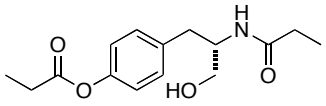

For experimental please see compound **3.5**.

$\mathbf{R}_f$ = 0.27 (EtOAc/CH_2Cl_2, 4:6). **^{1}H-NMR** (400 MHz, DMSO) δ 7.36 - 7.11 (m, 1H), 7.10 - 6.81 (m, 2H), 7.11 - 6.89 (m, 2H), 4.22 - 4.02 (m, 1H), 3.61 - 3.43 (m, 2H), 2.93 (dd, *J* = 13.7, 5.3 Hz 1H), 2.72 (dd, *J* = 13.7, 5.4 Hz, 1H), 2.65 - 2.53 (q, *J* = 7.6 Hz, 2H), 2.14 (q, *J* = 7.6 Hz, 2H), 1.22 (t, *J* = 7.5 Hz, 3H), 1.04 (t, *J* = 7.6 Hz, 3H). **^{13}C-NMR** (101 MHz, DMSO) δ 172.57, 172.52, 148.70, 136.70, 129.94, 121.25, 62.65, 52.11, 35.89, 28.56, 26.88, 9.97, 8.87. **HRMS ESI-TOF** calcd. for $C_{15}H_{21}NNaO_4^+$ (100%, $[M+Na]^+$): 302.1363; found 302.1366 **FTIR** $\tilde{\nu}$ 3454*w*, 3386*w*, 3339*w*, 3284*w*, 2976*w*, 2922*m*, 2877*w*, 2852*w*, 1753*s*, 1647*s*, 1617*s*, 1550*s*, 1510*s*, 1361*s*, 1196*s*, 1167*s*, 1074*s*, 1046*m*, 1021*m*, 900*s*, 825*m*, 667*m* cm^{-1}. **Optical rotation:** $[\alpha]_D^{22} = -17.6$ (c = 0.17, $CHCl_3$).

***(S)*-methyl 3-(4-((*tert*-butyldimethylsilyl)oxy)phenyl)-2-propionamidopropanoate (I)**

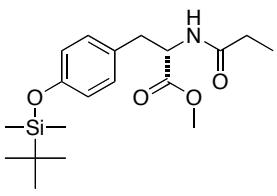

To a solution of the methyl ester **3.20h** (100 mg, 0.398 mmol, 1.00 equiv) in dry CH_2Cl_2 (5.00 mL) TBSCl (120 mg, 0.796 mmol, 2.00 equiv.), DMAP (9.72 mg, 80 µmol, 0.2 equiv.) and NEt_3 (168 mL, 1.19 mmol, 3.00 equiv.) were added. The reaction mixture was stirred for 5 h at r.t. under argon before sat. NH_4Cl-solution was added. The organic layer was separated and the aqueous layer was extracted with CH_2Cl_2 (2x). The combined organic layers were dried (Na_2SO_4) and concentrated under reduced pressure. The crude product was purified by gradiental FC on SiO_2 (first EtOAc/CH_2Cl_2, 1:4, then MeOH/CH_2Cl_2, 1:5) to yield the TBS-protected methyl ester **I** (140 mg, 0.383 mmol, 96%) as yellow oil.

$\mathbf{R}_f$ = 0.61 (CH_2Cl_2). **^{1}H-NMR** (400 MHz, $CDCl_3$) δ 7.12 - 7.04 (m, 2H), 6.80 - 6.73 (m, 2H), 4.63 (dd, *J* = 9.0, 5.8 Hz, 1H), 3.68 (s, 3H), 3.09 (dd, *J* = 13.9, 5.8 Hz, 1H),

2.89 (dd, *J* = 13.9, 9.0 Hz, 1H), 2.19 (q, *J* = 7.6 Hz, 2H), 1.05 (t, *J* = 7.6 Hz, 3H), 0.99 (s, 9H), 0.19 (s, 6H), **^{13}C-NMR** (101 MHz, MeOD) δ 176.74, 173.65, 155.79, 131.23, 131.01, 121.00, 55.19, 52.58, 37.71, 29.77, 26.17, 19.04, 10.34, –4.29. **HRMS ESI-TOF** calcd. for $C_{19}H_{31}NNaO_4Si^+$ (100%, $[M+Na]^+$): 388.1920; found 388.1912. **FTIR** $\tilde{\nu}$ 3290*w*, 2955*w*, 2933*w*, 2858*w*, 2361*w*, 2340*w*, 1745*m*, 1651*m*, 1510*s*, 1464*w*, 1439*w*, 1254*s*, 1212*m*, 1173*m*, 914*s*, 840*s*, 625*m* cm^{-1}. **Optical rotation:** $[\alpha]_D^{22}$= 20.4 (c = 2.13, MeOH).

(*S*)-*N*-(1-(4-((*tert*-butyldimethylsilyl)oxy)phenyl)-3-hydroxypropan-2-yl)propionamide (II)

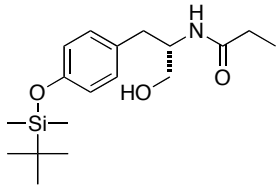

The TBDMS-protected methyl ester **I** (170 mg, 0.465 mmol, 1.00 equiv.) was dissolved in dry DMF (5.00 mL). The solution was cooled to 0 °C before $LiAlH_4$ (176 mg, 4.65 mmol, 10.0 equiv.) was added in one portion. The reaction mixture was stirred for 1 h under an argon atmosphere. The reaction mixture was quenched using H_2O (5.00 mL) followed by NaOH-solution (5.00 mL, 1 M). The mixture was then stirred for an additional hour, filtered over celite and washed with H_2O and hot EtOAc. The mixture was then extracted using statured NH_4Cl-solution, dried (Na_2SO_4) and concentrated under reduced pressure. The crude product was purified by flash chromatography on SiO_2 (MeOH/CH_2Cl_2, 1:40) to yield the product **II** (132 mg, 0.391 mmol, 84%) as colorless oil.

R_f = 0.36 (MeOH/CH_2Cl_2, 1:20). **^{1}H-NMR** (400 MHz, $CDCl_3$) 7.13 - 6.98 (m, 2H), 6.86 - 6.69 (m, 2H), 5.62 (d, *J* = 6.8 Hz, 1H), 4.19 - 4.03 (m, 1H), 3.76 - 3.65 (m, 1H), 3.63 - 3.49 (m, 1H), 2.95 - 2.70 (m, 2H), 2.17 (q, *J* = 7.4 Hz, 2H), 1.09 (t, *J* = 7.6 Hz, 3H), 0.97 (s, 9H), 0.18 (s, 6H). **^{13}C-NMR** (101 MHz, $CDCl_3$) δ 174.78, 154.60, 130.23 (2C), 120.42, 77.48, 77.16, 76.84, 64.90, 53.24, 36.30, 29.90, 25.81, 18.34, 9.93, –4.29. **HRMS ESI-TOF** calcd. for $C_{18}H_{31}NNaO_3Si^+$ (100%, $[M+H]^+$): 360.1971; found: 360.1963. **FTIR** $\tilde{\nu}$ 3326*m*, 2946*w*, 2834*w*, 1651*w*, 1511*w*, 1451*w*, 1415*w*, 1259*w*, 1115*w*, 1025*s*, 638*s* cm^{-1}. **Optical rotation:** $[\alpha]_D^{22}$= 1.9 (c = 1.0 MeOH).

(*S*)-*N*-(1-(4-hydroxyphenyl)-3-methoxypropan-2-yl)propionamide (3.20d)

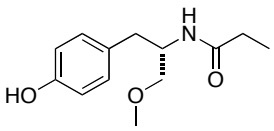

To a solution the TBS-protected alcohol **II** (500 mg, 1.48 mmol, 1.00 equiv.) in dry DMF (15.0 mL) at 0 °C was added NaH (60% in mineral oil, 89.0 mg, 2.22 mmol, 1.5 equiv.) in one portion. The mixture was allowed to reach r.t. before iodomethane (466 µL, 7.41 mmol, 5.00 equiv.) was added drop wise. The reaction mixture was stirred for 24 h under argon and then quenched using citric acid solution (5 %, 50 ml). The mixture was extracted using EtOAc (3x10 mL), brine (10mL), dried (Na_2SO_4) and concentrated under reduced pressure. The crude was filtered over a short plug of silica (EtOAc/CH_2Cl_2, 1:10) and concentrated again. The yellow residue was dissolved in dry THF (8.0 mL) and tetrabutylammonium fluoride (1 M solution in THF, 1.01 mL, 3.41 mmol, 3.00 equiv.) was added. The mixture was stirred overnight under argon before MeOH (3.0 mL) was added. The solvents were removed and the crude was extracted with CH_2Cl_2 (3x10 ml), dried (Na_2SO_4) and concentrated. The crude product was purified first by flash chromatography on SiO_2 (MeOH/CH_2Cl_2, 1:40) followed by preparative HPLC separation to yield the ether **3.20d** (80 mg, 0.337 mmol, 23%) as white solid.

R_f = 0.54 (MeOH/CH_2Cl_2, 1:10). **^{1}H-NMR** (400 MHz, $CDCl_3$) δ 7.16 - 6.94 (m, 2H), 6.84 - 6.70 (m, 2H), 5.79 (d, *J* = 8.6 Hz, 1H), 4.10 - 4.19 (m, 1H), 3.47 - 3.24 (m, 4H), 2.77 (d, *J* = 7.4 Hz, 2H), 2.27 - 2.11 (m, 2H), 1.10 (t, *J* = 7.6 Hz, 3H). **^{13}C-NMR** (101 MHz, $CDCl_3$) δ 173.91, 155.01, 130.47, 129.61, 115.54, 77.48, 77.16, 76.84, 72.65, 59.19, 50.50, 36.84, 30.01, 9.98. **HRMS ESI-TOF** calcd. for $C_{13}H_{20}NO_3^+$ (100%, $[M+H]^+$): 238.1438; found: 238.1438. **FTIR** $\tilde{\nu}$ 3286*br*, 2938*w*, 2830*w*, 2362*m*, 2339*w*, 1644*m*, 1546*m*, 1515*s*, 1457*m*, 1239*m*, 1124*w*, 1025*w*, 770*m*, 634*s* cm^{-1}. **Optical rotation**: $[\alpha]_D^{21} = -10.4$ (c = 0.35 MeOH).

(*S*)-3-(4-hydroxyphenyl)-2-propionamidopropyl propionate (3.20e)

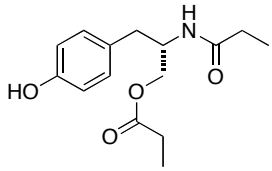

For experimental procedure please see compound **3.5**

R$_f$ = 0.43 (EtOAc/CH_2Cl_2, 4:6). **^{1}H-NMR** (400 MHz, DMSO) δ 9.17 (s, 1H), 7.72 (d, *J* = 8.3 Hz, 1H), 6.98 (d, *J* = 8.4 Hz, 2H), 6.66 (d, *J* = 8.5 Hz, 2H), 4.13 - 4.02 (m, 1H), 3.99 (dd, *J* = 10.9, 4.8 Hz, 1H), 3.86 (dd, *J* = 10.9, 6.6 Hz, 1H), 2.61 (m, 2H), 2.02 (q, *J* = 7.5 Hz, 3H), 2.02 (q, *J* = 7.4 Hz, 2H), 1.03 (t, *J* = 7.5 Hz, 3H), 0.93 (t, *J* = 7.6 Hz, 3H). **^{13}C-NMR** (101 MHz, DMSO) δ 173.49, 172.63, 155.64, 129.88, 128.21, 114.95, 64.77, 49.13, 35.82, 28.54, 26.76, 9.95, 8.96. **HRMS ESI-TOF** calcd. for $C_{14}H_{20}NO_4^-$ (100%, $[M]^-$): 279.1471; found 279.1392. **FTIR** $\tilde{\nu}$ 3365*m*, 3312*m*, 2986*w*, 2929*w*, 2853*w*, 1706*s*, 1650*s*, 1536*s*, 1515*s*, 1444*m*, 1363*m*, 1268*m*, 1209*s*, 1030*m*, 980*m*, 823*m*, 657*m* cm^{-1}. **Optical rotation:** $[\alpha]_D^{22}$= –12.1 (c = 0.14, $CHCl_3$).

(*S*)-*N*-(1-methoxy-3-(4-methoxyphenyl)propan-2-yl)propionamide (3.20f)

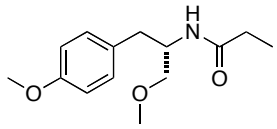

For experimental procedure please see compound **3.20b**

R$_f$ = 0.40 (EtOAc/CH_2Cl_2, 4:6). **^{1}H-NMR** (400 MHz, $CDCl_3$) δ 7.17 - 7.01 (m, 2H), 6.83 (d, *J* = 8.4 Hz, 2H), 5.71 (d, *J* = 6.0 Hz, 1H), 4.19 - 4.24 (m, 1H), 3.82 (s, 3H) 3.34 (s, 3H), 3.29 (d, *J* = 3.8 Hz, 2H), 2.79-2.85 (m, 2H), 2.18 (q, *J* = 7.6 Hz, 2H), 1.12 (t, *J* = 7.7 Hz, 3H). **^{13}C-NMR** (101 MHz, $CDCl_3$) δ 173.27, 158.21, 130.37, 130.07, 113.88, 72.16, 59.00, 55.26, 50.13, 36.46, 29.86, 9.85. **HRMS ESI-TOF** calcd. for $C_{14}H_{22}NO_3^+$ (100%, $[M+H]^+$): 252.1600; found 252.1564. **FTIR** $\tilde{\nu}$ 3290*w*, 3072*w*, 2923*w*, 1743*w*, 1644*s*, 1512*s*, 1462*m*, 1444*m*, 1245*s*, 1179*m*, 1123*m*, 1083*m*, 1035*m*, 966*w*, 912*w*, 816*w*, 659*m* cm^{-1}. **Optical rotation:** $[\alpha]_D^{22}$= –7.2 (c = 0.06, MeOH).

(*S*)-3-(4-hydroxyphenyl)-2-propionamidopropanoic acid (3.20g)[219]

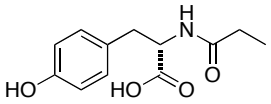

To a solution of L-tyrosine hydrochloride (3.00 g, 16.6 mmol, 1.00 equiv.) in H_2O/THF (1:1, 40.0 mL) was K_2CO_3 (9.15 g, 66.2 mmol, 4.00 equiv.) added at r.t. The mixture was stirred for 1 h before propionyl chlorid (1.59 mL, 18.2 mmol, 1.1 equiv.) was added. The reaction mixture was then stirred for 16 h under an argon atmosphere. The organic solvent was evaporated and HCl-soluiton (10 %, 50.0 mL) was added. The aqueous layer was extracted with EtOAc (3x), dried over Na_2SO_4 and concentrated. The crude product was purified by flash chromatography on SiO_2 (CH_2Cl_2/MeOH, 15:1 + 2‰ TFA) to yield the acid **3.20g** (3.42 g, 14.3 mmol, 87%) as viscous colorless oil.

R_f = 0.15 (MeOH/CH_2Cl_2, 1:15). **^{1}H-NMR** (400 MHz, D_2O) δ 7.18 - 7.11 (m, 2H), 6.88 - 6.81 (m, 2H), 4.57 (dd, *J* = 8.9, 5.4 Hz, 1H), 3.15 (dd, *J* = 14.0, 5.4 Hz, 1H), 2.92 (dd, *J* = 14.0, 9.0 Hz, 1H), 2.19 (q, *J* = 7.7 Hz, 2H), 0.99 (t, *J* = 7.7 Hz, 3H). **^{13}C-NMR** (101 MHz, D_2O) δ 177.72, 175.10, 173.85, 154.34, 130.50, 130.46, 128.38, 128.22, 115.34, 54.17, 54.00, 52.79, 35.77, 28.73, 9.27 (rotamer present) **HRMS ESI-TOF** calcd. for $C_{12}H_{16}NO_4^+$ (100%, $[M+H]^+$): 238.2625; found 238.1074. (100%, $[M]^+$). **FTIR** $\tilde{\nu}$ 3320*w br*, 2979*w*, 2941*w*, 1721*m*, 1638*m*, 1613*m*, 1514*s*, 1444*m*, 1377*w*, 1221*s*, 1125*m*, 1016*w*, 911*w*, 828*m*, 660*m* cm^{-1}. **Optical rotation:** $[\alpha]_D^{22}$= 34.9 (c = 0.35, H_2O). The reported data is in accordance with the literature.[219]

(*S*)-methyl 3-(4-hydroxyphenyl)-2-propionamidopropanoate (3.20h)

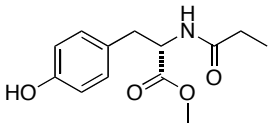

To a solution of L-tyrosinol methyl ester (1.01 g, 5.07 mmol, 1.00 equiv.) in H_2O/THF (1:1, 9.00 mL) was K_2CO_3 (2.10 g, 15.2 mmol, 3.00 equiv.) added at r.t.. The mixture was stirred for 1 h before propionyl chloride (0.531 µL, 6.08 mmol, 1.20 equiv.) was added. The reaction mixture was then stirred for 2 d under an argon atmosphere. The organic solvent was evaporated and the aqueous layer was extracted with CH_2Cl_2 (3x). The combined organic layers were washed with brine, dried over Na_2SO_4 and

[219] K. Ueda, M. Yoshihara, M. Nakao, T. Tanaka, *J. Agric. Food Chem.* **2010**, *58*, 6053–6063.

concentrated. The crude product was purified by flash chromatography on SiO_2 (CH_2Cl_2/MeOH 30:1) to yield the methyl ester **3.20h** (1.24 g, 4.93 mmol, 97%) as white solid.

R_f = 0.43 (MeOH/CH_2Cl_2, 1:20). **M.P.** = 103 - 104 °C. **^{1}H-NMR** (400 MHz, $CDCl_3$) δ 6.93 (m, 2H), 6.84 - 6.64 (m, 2H), 6.08 (m, 1H), 4.87 (dt, *J* = 8.0, 6.0 Hz, 1H), 3.74 (s, 3H), 3.09 (dd, *J* = 14.0, 5.7 Hz, 1H), 2.97 (dd, *J* = 14.0, 6.2 Hz, 1H), 2.21 (q, *J* = 7.8 Hz, 2H), 1.11 (t, *J* = 7.6 Hz, 3H). **^{13}C-NMR** (101 MHz, $CDCl_3$) δ 174.25, 172.57, 155.76, 130.35, 126.97, 115.71, 77.48, 77.16, 76.84, 53.32, 52.57, 37.32, 29.68, 9.80. **HRMS ESI-TOF** calcd. for $C_{13}H_{18}NO_4^+$ (100%, $[M+H]^+$): 252.1230; found: 252.1230. **FTIR** $\tilde{\nu}$ 3300*m*, 3024*w*, 2981*w*, 2953*w*, 2361*m*, 2340*m*, 1736*m*, 1650*m*, 1516*s*, 1444*m*, 1373*m*, 1225*m* cm^{-1}. **Optical rotation:** $[\alpha]_D^{22}$= 19.1 (c = 1.6, MeOH).

(*R*)-*N*-(1-hydroxy-3-(4-hydroxyphenyl)propan-2-yl)propionamide (3.20i)

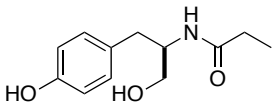

Amide **3.20i** was prepared similar than **3.5** but D-tyrosinol hydrochloride was used as starting material instead. The analytical data is in accordance with the one of its enantiomer **3.5**. Yield: 92%, **Optical rotation:** $[\alpha]_D^{21}$= 1.8 (c = 0.25, MeOH).

***N*-(4-hydroxyphenethyl)propionamide (3.20j)**

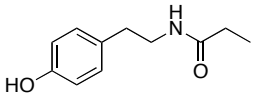

Tryamine (300 mg, 2.19 mmol, 1.00 equiv.) was dissolved in H_2O/THF (1:1, 10.0 mL). To this solution K_2CO_3 (907 mg, 6.56 mmol, 3.00 equiv.) was added at r.t.. The mixture was stirred for 1 h before propionyl chloride (263 µL, 2.19 mmol, 1.3 equiv.) was added. The reaction mixture was then stirred for 2 h under an argon atmosphere. The organic solvent was evaporated and the aqueous layer was extracted with EtOAc (3x), brine (1x), dried over Na_2SO_4 and concentrated. The crude product was purified by flash chromatography on SiO_2 (MeOH/CH_2Cl_2, 1:30) to yield the product **3.20j** (432 mg, quant.) as colorless solid.

R_f = 0.31 (MeOH/CH_2Cl_2, 1:20). **M.P.** = 109 - 110 °C. **^{1}H-NMR** (400 MHz, $CDCl_3$) δ 7.05 - 6.98 (m, 2H), 6.74 - 6.67 (m, 2H), 3.33 (t, *J* = 7.3 Hz, 2H), 2.68 (t, *J* = 7.3 Hz,

2H), 2.15 (q, *J* = 7.6 Hz, 2H), 1.09 (t, *J* = 7.6 Hz, 3H). **^{13}C-NMR** (101 MHz, MeOD) δ 176.98, 156.88, 131.25, 130.71, 116.19, 42.26, 35.69, 30.22, 10.56. **HRMS ESI-TOF** calcd for $C_{11}H_{16}NO_2^+$ (100%, $[M+H]^+$): 194.1176; found 194.1176. (100%, $[M+H]^+$). **EA**: calc. (%) for $C_{11}H_{15}NO_2$: C 68.37, H 7.82, N 7.25; found C 68.16, H 7.65, N 7.25. **FTIR** $\tilde{\nu}$ 3393*m br*, 2978*m*, 2938*m*, 2360*m*, 2343*m*, 1638*s*, 1615*s*, 1546*m*, 1515*s*, 1454*m*, 1364*m*, 2337*m*, 829*w*, 632*s* cm^{-1}.

N-(3,4-dihydroxyphenethyl)propionamide (3.20k)

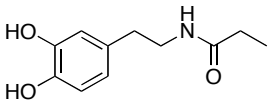

To a solution of dopamine hydrochloride (1.00 g, 5.27 mmol, 1.00 equiv.) in a mixture of H_2O/THF (1:1, 4.00 mL) was K_2CO_3 (2.19 g, 15.8 mmol, 3.00 equiv.) added. The mixture was stirred for 1 h under argon before propionyl chloride (24.7 µL, 0.223 mmol, 1.05 equiv.) was added. The mixture was then stirred overnight at r.t.. The solvent was removed and the dark residue was purified directly by flash chromatography on SiO_2 (CH_2Cl_2/MeOH 20:1) to yield the amide **3.20k** as brown oil (420 mg, 2.01 mmol, 38%).

R_f = 0.55 (MeOH/CH_2Cl_2, 1:20). **M.P.** = 112 - 113 °C. **^{1}H-NMR** (400 MHz, D_2O) δ 6.85 - 6.58 (m, 2H), 6.60 - 6.30 (m, 2H), 3.34 - 3.27 (m, 2H), 2.61 (t, *J* = 7.4 Hz, 2H), 2.14 (q, *J* = 7.6 Hz, 2H), 1.08 (t, *J* = 7.6 Hz, 3H). **^{13}C-NMR** (101 MHz, D_2O) δ 176.98, 146.16, 144.67, 132.02, 121.01, 116.84, 116.32, 42.22, 35.87, 30.20, 10.55. **HRMS ESI-TOF** calcd. for (100%, $[M+H]^+$): 210.1130; found: 210.1130. **FTIR** $\tilde{\nu}$ 3373*m*, 3100*m br*, 2974*w*, 2941*w*, 1631*m*, 1608*s*, 1545*s*, 1529*m*, 1440*s*, 1376*m*, 1276*m*, 1252*s*, 1192*s*, 1114*m*, 949*m*, 873*m*, 821*m*, 660*m* cm^{-1}.

(*S*)-4-(3-hydroxy-2-(propylamino)propyl)phenol (3.20l)

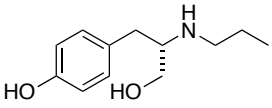

To a solution of L-tyrosinol hydrochloride (60 mg, 0.295 mmol, 2.00 equiv.) in a mixture of H_2O/THF (1:1, 2.00 mL) was K_2CO_3 (100 mg, 0.442 mmol, 3.00 equiv.) added. The mixture was stirred for 10 min at r.t. before prior to use distilled 1-bromopropane (9 µL, 0.73 mmol, 1.00 equiv.) was added. The mixture was then stirred overnight at 70 °C under an argon atmosphere. The organic solvent was removed and the residue was first directly

purified by flash chromatography on SiO_2 (CH_2Cl_2/MeOH, 20:1) followed by reverse phase preparative HPLC separation to yield the amine **3.20l** (12 mg, 57.3 µmol, 39%) as colorless fluffy solid.

$\mathbf{R}_f$ = 0.17 (MeOH/CH_2Cl_2, 1:5). **^{1}H-NMR** (400 MHz, D_2O) δ 7.24 - 7.17 (m, 2H), 6.93 - 6.86 (m, 2H), 3.81 (dd, *J* = 12.7, 3.5 Hz, 1H), 3.63 (dd, *J* = 12.7, 5.2 Hz, 1H), 3.56 - 3.45 (m, 1H), 3.11 - 2.88 (m, 4H), 1.68 (hept, *J* = 7.5 Hz, 2H), 0.95 (t, *J* = 7.5 Hz, 3H). **^{13}C-NMR** (101 MHz, D_2O) δ 154.79, 130.65, 127.23, 115.79, 60.01, 57.96, 46.44, 32.51, 19.23, 10.15. **HRMS ESI-TOF** calcd. for $C_{12}H_{20}NO_2^+$ (100%, $[M+H]^+$): 210.1489; found 210.1489. **FTIR** $\tilde{\nu}$ 3365*w*, 3241*m*, 3098*w*, 2975*w*, 2822*w*, 1614*w*, 1573*m*, 1514*s*, 1458*s*, 1260*s*, 1224*s*, 1172*w*, 1094*m*, 1073*m*, 1031*m*, 968*s*, 844*m*, 828*m* cm^{-1}. **Optical rotation:** $[\alpha]_D^{22} = -10.4$ (c = 0.14, H_2O).

(*S*)-*N*-(1-hydroxy-3-(4-hydroxyphenyl)propan-2-yl)benzamide (3.20m)[220]

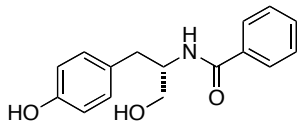

To a solution of L-tyrosinol hydrochloride (100 mg, 0.49 mmol, 1.00 equiv.) and benzyl chloride (60 mL, 0.51 mmol, 1.05 equiv.) in MeCN (4.00 mL) was added K_2CO_3 (311 mg, 2.25 mmol, 4.50 equiv.) dissolved in H_2O (3.00 mL) drop wise during 0.3 h at r.t.. The reaction mixture was then stirred for 3.5 h at r.t.. The organic solvent was evaporated and the aqueous layer was extracted with EtOAc (4x). The combined organic layers were washed with brine, dried over Na_2SO_4 and concentrated. The crude product was purified by flash chromatography on SiO_2 (CH_2Cl_2/MeOH, 20:1) to yield the products **3.20m** (98 mg, 0.361 mmol, 73%) as colorless solid.

$\mathbf{R}_f$ = 0.43 (EtOAc/ CH_2Cl_2, 4:6). **M.P.** = 37 - 41°C. **^{1}H-NMR** (400 MHz, MeOD) δ 8.09 (d, *J* = 8.4 Hz, 1H), 7.82 - 7.64 (m, 2H), 7.56 - 7.35 (m, 2H), 7.19 - 6.95 (m, 2H), 6.80 - 6.59 (m, 2H), 4.37 - 4.17 (m, 1H), 3.63 (d, *J* = 5.4 Hz, 2H), 2.91 (dd, *J* = 13.8, 6.4 Hz, 1H), 2.77 (dd, *J* = 13.8, 8.2 Hz, 1H). **^{13}C-NMR** (101 MHz, DMSO) δ 165.98, 155.43, 134.84, 130.93, 129.93, 129.41, 128.11, 127.22, 114.90, 62.78, 53.54, 35.67. **FTIR** $\tilde{\nu}$ 3448*w*, 3308*m*, 2956*w*, 2928*w*, 1630*s*, 1602*m*, 1519*s*, 1488*m*, 1332*m*, 1239*s*, 1030*s*, 820*m*, 805*m*, 689*s*, 658*s* cm^{-1}. **HRMS ESI-TOF** calcd. for $C_{16}H_{18}NO_3$ (100%,

[220] H. Gershon, R. Rodin, *J. Med. Chem.* **1965**, *8*, 864–866.

[M+H]$^+$): 272.1287; found 272.1482. **Optical rotation:** $[\alpha]_D^{24}$= –67.7 (c = 0.26, MeOH).

(*S*)-*N*-(1-hydroxy-3-(4-hydroxyphenyl)propan-2-yl)isobutyramide (3.20n)

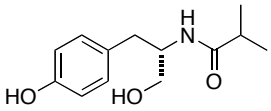

To a solution of L-tyrosinol (3.00 g, 16.6 mmol, 1.00 equiv.) in H_2O/THF (1:1, 4.0 mL) was K_2CO_3 (61 mg, 0.442 mmol, 3.00 equiv.) added at r.t.. The mixture was stirred for 1 h before isobutyryl chloride (19 µL, 0.177 mmol, 1.20 equiv.) was added. The reaction mixture was then stirred for 15 h under argon atmosphere. The organic solvent was evaporated and sat. NH_4Cl-solution (5.0 mL) was added. The aqueous layer was extracted with CH_2Cl_2 (3x). The combined organic layers were washed with brine, dried over Na_2SO_4 and concentrated. The crude product was purified by flash chromatography on SiO_2 (CH_2Cl_2/MeOH, 30:1) to yield the product **3.20n** (33 mg, 0.139 mmol, 94%) as colorless oil.

R$_f$ = 0.21 (MeOH/CH_2Cl_2, 1:20). **^{1}H-NMR** (400 MHz, MeOD) δ 7.08 - 7.01 (m, 2 H), 6.79 - 6.56 (m, 2H), 4.13 - 3.94 (m, 1H), 3.51 (d, 5.4 Hz, 2H), 2.82 (dd, *J* = 13.9, 6.0 Hz, 1H), 2.60 (dd, *J* = 13.9, 8.5 Hz, 1H), 2.38 (hept, *J* = 6.9 Hz, 1H), 1.01 (dd, *J* = 27.9, 6.9 Hz, 6H). **^{13}C-NMR** (101 MHz, MeOD) δ 179.94, 156.82, 131.26, 130.56, 116.03, 64.33, 53.96, 37.12, 36.32, 20.04, 19.68. **HRMS ESI-TOF** calcd. for $C_{13}H_{20}NO_3^+$ (100%, [M+H]$^+$): 238.1438; found 238.1438. (100%, [M]$^+$). **FTIR** $\tilde{\nu}$ 3299*m br*, 2970*m*, 2932*m*, 2876*w*, 2357*w*, 2339*w*, 1639*s*, 1615*s*, 1542*s*, 1515*s*, 1456*m*, 1373*m*, 1241*s*, 1097*w*, 1041*m*, 771*m*, 630*s* cm^{-1}. **Optical rotation:** $[\alpha]_D^{23}$= –10.7 (c = 0.1, MeOH).

(*S*)-*N*-(1-hydroxy-3-(4-hydroxyphenyl)propan-2-yl)pivalamide (3.20o)

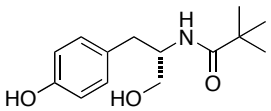

To a solution of L-tyrosinol (100 mg, 0.491 mmol, 1.00 equiv.) in H_2O/THF (1:1, 5.0 mL) was K_2CO_3 (204 mg, 1.470 mmol, 3.00 equiv.) added at r.t.. The mixture was stirred for 0.5 h before trimethylacetyl chloride (73 µL, 0.589 mmol, 1.20 equiv.) was added. The reaction mixture was then stirred overnight under argon atmosphere. The organic solvent was evaporated and

sat. NH_4Cl-solution (10.0 mL) was added. The aqueous layer was extracted with CH_2Cl_2 (3x). The combined organic layers were washed with brine, dried over Na_2SO_4 and concentrated. The crude product was purified by flash chromatography on SiO_2 (CH_2Cl_2/MeOH, 30:1) to yield the product **3.20o** (114 mg, 0.454 mmol, 92%) as colorless oil.

R_f = 0.26 (MeOH/CH_2Cl_2, 1:20). **M.P.** = 116 - 117 °C. **^{1}H-NMR** (400 MHz, MeOD) δ 7.11 - 7.00 (m, 2H), 6.75 - 6.57 (m, 2H), 4.13 - 4.02 (m, 1H), 3.61 - 3.45 (m, 2H), 2.83 (dd, *J* = 13.8, 6.1 Hz, 1H), 2.65 (dd, *J* = 13.8, 8.6 Hz, 1H), 1.09 (s, 9H). **^{13}C-NMR** (101 MHz, MeOD) δ 180.99, 156.80, 131.27, 130.54, 116.03, 64.18, 54.14, 39.63, 36.94, 27.76. **HRMS ESI-TOF** calcd. for $C_{14}H_{22}NO_3^+$ (100%, $[M+H]^+$): 252.1594; found 252.1594. **FTIR** $\tilde{\nu}$ 3478*w*, 3441*w*, 3360*w*, 3335*w*, 3183*w broad*, 2962*w*, 2935*w*, 2868*w*, 2360*w*, 1706*w*, 1615*w*, 1530*s*, 1366*w*, 1227*s*, 1038*m*, 822*m* cm^{-1}. **Optical rotation:** $[\alpha]_D^{22} = -8.8$ (c = 1.0, MeOH).

(*S*)-*N*-(1-hydroxy-3-(4-hydroxyphenyl)propan-2-yl)hex-5-ynamide (III)

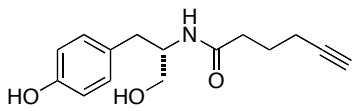

To a solution of L-tyrosinol hydrochloride (1.00 g, 4.91 mmol, 1.00 equiv.) in THF/H_2O (1:1, 16.0 mL) K_2CO_3 (1.69 g, 12.27 mmol, 4.40 equiv.) was added. The reaction mixture was stirred for 1 h at r.t. before hex-5-ynoyl chloride (770 mg, 5.89 mmol, 1.20 equiv.) was added. After stirring for 4 h additional hex-5-ynoyl chloride (150 mg, 1.15 mmol, 0.23 equiv.) was added. The mixture was then stirred for another 1.2 h. The organic solvent was evaporated and the aqueous layer was extracted with EtOAc (4x). The combined organic layers were washed with brine, dried over $MgSO_4$ and concentrated. The crude product was purified by gradiental flash chromatography on SiO_2 (MeOH in CH_2Cl_2, 1-10%) to yield alkin **III** (1.03 g, 3.93 mmol, 85%) as white solid.

R_f = 0.51 (MeOH/CH_2Cl_2, 1:10). **M.P.** = 91 - 93 °C **^{1}H-NMR** (400 MHz, MeOD) δ 7.61 (d, *J* = 8.5 Hz, 1H), 7.13 - 6.89 (m, 2H), 6.78 - 6.57 (m, 2H), 4.14 - 3.91 (m, 1H), 3.57 -3.38 (m, 2H), 2.80 (dd, *J* = 13.9, 6.0 Hz, 1H), 2.58 (dd, *J* = 13.8, 8.5 Hz, 1H), 2.31 - 2.15 (m, 3H), 2.13 - 1.97 (m, 2H), 1.76 - 1.56 (m, 2H). **^{13}C-NMR** (101 MHz, MeOD) δ 175.22, 156.86, 131.22, 130.51, 116.07, 84.25, 70.08, 64.38, 54.37, 54.27,

37.04, 36.01, 25.99, 18.54. **HRMS ESI-TOF** calcd. for $C_{15}H_{20}NO_3$ (100%, $[M+H]^+$): 262.1443; found 262.1443. **FTIR** $\tilde{\nu}$ 3483*w*, 3314*m*, 3300*m*, 3208*m*, 2690*w*, 2927*w*, 2881*w*, 1633*s*, 1615*m*, 1530*s*, 1517*s*, 1453*m*, 1247*m*, 1214*m*, 1031*s*, 821*m*, 744*m*, 681*m*, 650*s*, 627*s* cm^{-1}. **Optical rotation:** $[\alpha]_D^{22} = -19.5$ (c = 0.82, MeOH).

(*S*)-4-(1-(adamantan-1-yl)-1H-1,2,3-triazol-4-yl)-N-(1-hydroxy-3-(4-hydroxyphenyl)propan-2-yl)butanamide (3.20p)

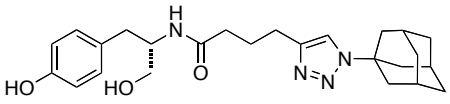

(*S*)-*N*-(1-hydroxy-3-(4-hydroxyphenyl) propan-2-yl)hex-5-ynamide **III** (50 mg, 0.191 mmol, 1.00 equiv.), 1-azidoadamantane (37.3 mg, 0.210 mmol, 1.10 equiv.), L-ascorbic acid sodium salt (37.9 mg, 0.191 mmol, 1.00 equiv.), copper(II) sulfate pentahydrate (1.9 mg, 0.008 mmol, 0.04 equiv.) and tris-(benzyltriazolylmethyl)amine (4.2 mg, 0.008 mmol, 0.04 equiv.) were dissolved in DMSO (2.00 mL). The reaction mixture was stirred for 2 d at r.t. under an argon atmosphere. The organic solvent was removed and the crude was extracted with EtOAc (3x). The combined organic layers were washed with brine, dried over Na_2SO_4 and concentrated. Purification of the crude product by gradiental FC on SiO_2 (MeOH in EtOAc 2-5%) yielded the product **3.20p** (64 mg, 0.146 mmol, 76%) as white solid.

$\mathbf{R}_f$ = 0.15 (EtOAc/CH_2Cl_2, 4:6), **M.P.** = 76 - 77 °C, **^{1}H-NMR** (500 MHz, DMSO) δ 7.74 (s, 1H), 7.13 - 6.97 (m, 2H), 6.74 - 6.61 (m, 2H), 4.10 (dd, *J* = 8.8, 5.6 Hz, 1H), 3.51 (h, *J* = 5.7 Hz, 2H), 2.83 (dd, *J* = 13.9, 5.8 Hz, 1H), 2.67 - 2.44 (m, 3H), 2.25 (s, 10H), 2.18 (t, *J* = 7.3 Hz, 2H), 1.85 (d, *J* = 7.0 Hz, 8H). **^{13}C-NMR** (101 MHz, $CDCl_3$) δ 175.51, 156.87, 131.25, 130.55, 119.94 (2C), 116.10, 64.48, 60.90, 54.16, 37.16, 36.94, 36.46, 31.00, 26.78, 25.58. **HRMS ESI-TOF** calcd. for $C_{25}H_{36}N_4O_3^+$ (100%, $[M+H]^+$): 439.2709; found 439.2709. (100%, $[M+H]^+$). **FTIR** $\tilde{\nu}$ 3263*m*, 2915*s*, 2854*m*, 1732*m*, 1640*s*, 1548*m*, 1515*s*, 1452*s*, 1233*s*, 1144*m*, 1103*m*, 1064*s*, 818*m*, 685*m*, 662*m*, 649*m* cm^{-1}. **Optical rotation:** $[\alpha]_D^{22} = -7.8$ (c = 0.12, MeOH).

_N_-((_R_)-1-hydroxy-3-(4-hydroxyphenyl)propan-2-yl)-_N_-((_S_)-1-hydroxy-3-(4-hydroxyphenyl)propan-2-yl)succinamide (3.20q)

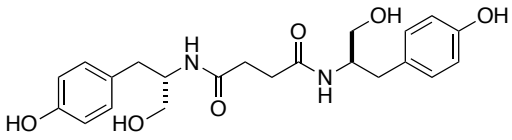

To a solution of L-tyrosinol hydrochloride (100 mg, 0.491 mmol, 2.00 equiv.) in a mixture of H_2O/THF (1:1, 4.00 mL) was K_2CO_3 (154 mg, 1.120 mmol, 5.00 equiv.) added. The mixture was stirred for 1 h under argon before succinyl chloride (24.7 µL, 0.223 mmol, 1 equiv.), which was distilled prior to use, was added. The mixture was stirred for 2 d under an argon atmosphere at r.t.. The organic solvent was removed and the pale yellow residue was purified directly by FC on SiO_2 (CH_2Cl_2/MeOH, 40:1) to yield the dimer **3.20q** as colorless solid (51 mg, 0.122 mmol, 55%).

R_f = 0.37 (MeOH/CH_2Cl_2, 1:20). **M.P.** = 167 - 169 °C. **^{1}H-NMR** (400 MHz, MeOD) 7.18 - 6.80 (m, 5H), 6.86 - 6.45 (m, 4H), 4.39 (td, *J* = 10.3, 9.8, 5.5 Hz, 2H), 4.06 (dd, *J* = 11.4, 9.4 Hz, 2H), 3.72 (dd, *J* = 11.4, 5.0 Hz, 2H), 3.00 (dd, *J* = 13.8, 10.3 Hz, 2H), 2.89 (dd, *J* = 13.8, 6.1 Hz, 2H), 2.63 - 2.41 (m, 4H). **^{13}C-NMR** (101 MHz, MeOD) δ 180.25, 157.14, 130.92, 129.64, 116.21, 61.85, 57.50, 33.81, 28.76. **FTIR** $\tilde{\nu}$ 3204*w*, 2995*w*, 2963*w*, 2946*w*, 2506*w*, 2383*m*, 1758*w*, 1676*s*, 1613*m*, 1517*m*, 1401*m*, 1372*m*, 1257*m*, 1172*s*, 1021*m*, 889*w*, 810*s*, 668*s,* 620*m* cm^{-1}.

(_S_)-_N_-(1-hydroxy-3-(4-hydroxyphenyl)propan-2-yl)nonanamide (3.20r)

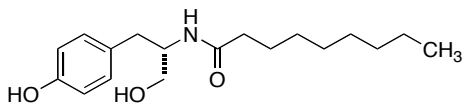

To a solution of L-tyrosinol (200 mg, 0.982 mmol, 1.00 equiv.) in H_2O/THF (1:1, 8.0 mL) was K_2CO_3 (543 mg, 3.93 mmol, 4.00 equiv.) added at r.t. under an argon atmosphere. The mixture was stirred for 0.33 h before nonanoyl chloride (248 µL, 1.37 mmol, 1.40 equiv.) was added. The reaction mixture was then stirred overnight. The organic solvent was evaporated and sat. NH_4Cl-solution (10.0 mL) was added. The aqueous layer was extracted with CH_2Cl_2 (3x). The combined organic layers were dried over Na_2SO_4 and concentrated. The crude product was purified by FC on SiO_2 (CH_2Cl_2/MeOH 30:1) to yield the product **3.20r** (213 mg, 0.693 mmol, 71%) as slight yellow solid.

R_f = 0.25 (MeOH/CH_2Cl_2, 1:20). **M.P.** = 101 - 102 °C. **^{1}H-NMR** (400 MHz, MeOD) δ 7.14 - 6.98 (m, 2H), 6.77 - 6.62 (m, 2H), 4.17 - 3.98 (m, 1H), 3.52 (d, *J* = 5.4 Hz, 2H), 2.84 (dd, *J* = 13.9, 6.0 Hz, 1H), 2.61 (dd, *J* = 13.9, 8.6 Hz, 1H), 2.14 (t, *J* = 7.5 Hz, 2H), 1.52 (p, *J* = 7.5 Hz, 2H), 1.44 - 1.15 (m, 10H), 0.92 (t, *J* = 6.9 Hz, 3H). **^{13}C-NMR** (101 MHz, MeOD) δ 176.13, 156.88, 131.20, 130.51, 116.05, 64.38, 54.19, 37.27, 37.14, 33.02, 30.44, 30.27, 30.20, 27.06, 23.70, 14.44. **HRMS ESI-TOF** calcd. for $C_{18}H_{29}NNaO_3^+$ (100%, $[M+Na]^+$): 330.4232; found; 330.2042. **FTIR** $\tilde{\nu}$ 3300*m broad*, 2933*m*, 2859*w*, 2361*w*, 2338*w*, 1629*w*, 1550*w*, 1516*m*, 1452*w,* 1373*w*, 1243*s*, 1044*w*, 631*s* cm^{-1}. **Optical rotation:** $[\alpha]_D^{22} = -13.7$ (c = 1.00, MeOH).

8-oxo-8-(perfluorophenoxy)octanoic acid (IV)[221]

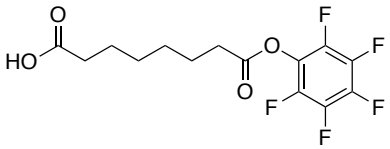

Pentaflourobenzoic acid (1.32 g, 7.176 mmol, 1.00 equiv.), octanedioic acid (2.50 g, 14.352 mmol, 2.00 equiv.) and EDC (1.65 g, 8.61 mmol, 1.20 equiv.) were dissolved in DMF/THF (1:3, 135 mL). This reaction mixture was then stirred overnight under nitrogen. The solvents were removed, first under slightly reduced pressure then under high vacuum while heating. The residue was extracted with EtOAc (4x) and aqueous HCl-solution (10 %, v:v). The combined organic layers were dried ($MgSO_4$) and concentrated. The crude product was first purified by FC on SiO_2 (CH_2Cl_2/EtOAc/TFA, 200:20:1) followed by recrystallization from pentane to yield the activated acid **IV** (680 mg, 0.361 mmol, 35%) as white crystals.

R_f = 0.59 (EtOAc). **M.P.** = 50 - 52 °C. **^{13}C-NMR** (101 MHz, MeOD) δ 34.78, 33.80, 29.73, 29.56, 25.83, 25.66, 14.46. **HRMS ESI-TOF** calcd. for $C_{14}H_{12}O_4F_5^-$ (100%, $[M]^-$): 339.0661; found 339.0656. The analytical data was in accordance with the literature.[221]

[221] P. Imming, M.-H. Jung, *Arch. Pharm.* **1995**, *1*, 87–91.

(*S*)-8-((1-hydroxy-3-(4-hydroxyphenyl)propan-2-yl)amino)-8-oxooctanoic acid (3.20s)

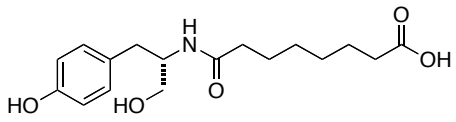

To a solution of the mono-activated acid **IV** (350 mg, 1.03 mmol, 1.20 equiv.) in DMF/THF (1:3, 6.0 mL) was L-tyrosinol hydrochloride (175 mg, 0.857 mmol, 1.00 equiv.) and NEt_3 (631 µL, 2.57 mmol, 3.00 equiv.) added. The mixture was stirred for 16 h under an argon atmosphere at r.t.. Solvent removal was accomplished under high vacuum while heating. The brown residue was extracted with EtOAc (4x) and aqueous HCl-solution (10 %, v:v). The crude product was first purified by FC on SiO_2 (CH_2Cl_2/MeOH/TFA, 100:10:1) followed by preparative HPLC separation to yield the acid **3.20s** (70 mg, 0.216 mmol, 25%) as colourless solid.

(*S*)-8-hydroxy-*N*-(1-hydroxy-3-(4-hydroxyphenyl)propan-2-yl)octanamide (3.20t)

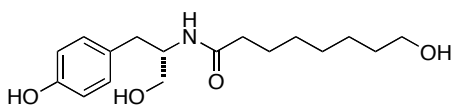

To a solution of L-tyrosinol (150 mg, 0.736 mmol, 1.00 equiv.) in MeCN (14.0 mL) was 8-hydroxyoctanoic acid (118 mg, 0.736 mmol, 1.00 equiv.), NEt_3 (311 µL, 2.21 mmol, 3.00 equiv.), EDC (282 mg, 1.47 mmol, 2.00 equiv.) and 1-hydroxybenzotriazole hydrate (149 mg, 1.1 mmol, 1.5 equiv.) added. The mixture was stirred at r.t. under argon for 12 h. The organic solvent was evaporated and sat. NH_4Cl-solution was added. The aqueous layer was extracted with CH_2Cl_2 (4x). The combined organic layers were washed with brine, dried over Na_2SO_4 and concentrated. The crude product was purified by FC on SiO_2 (CH_2Cl_2/EtOAc 5:1) to yield the triol **3.20t** (42 mg, 0.136 mmol, 19%) as slight yellow solid.

$\mathbf{R}_f$ = 0.17 (MeOH/CH_2Cl_2 1:20). **M.P.** = 124 - 125 °C. **^{1}H-NMR** (400 MHz, MeOD) δ 7.12 - 6.96 (m, 2H), 6.76 - 6.62 (m, 2H), 4.11 - 4.00 (m, 1H), 3.60 - 3.44 (m, 4H), 2.82 (dd, *J* = 13.9, 5.9 Hz, 1H), 2.59 (dd, *J* = 13.9, 8.7 Hz, 1H), 2.12 (t, *J* = 7.4 Hz, 2H), 1.60 - 1.41 (m, 4H), 1.40 - 1.12 (m, 6H). **^{13}C-NMR** (101 MHz, MeOD) δ 176.11, 156.85, 131.20, 130.54, 116.08, 64.44, 62.98, 54.17, 37.22, 37.14, 33.60, 30.27, 30.11, 26.98, 26.75. **HRMS ESI-TOF** calcd. for $C_{17}H_{27}NNaO_4^+$ (100%, $[M+Na]^+$):

332.1832; found; 332.1832. **FTIR** $\tilde{\nu}$ 3293*m*, 2932*m*, 2858*w*, 2362*s*, 2338*s*, 1638*m*, 1560*w*, 1515*m*, 1459*w*, 1369*w*, 1243*w*, 1036*w*, 758*s*, 632*s* cm^{-1}. **Optical rotation:** $[\alpha]_D^{22} = -12.0$ (c = 0.50, MeOH).

6.3.3 Tyrosinol Fatty Acid Analogs Collection

***N*-(2-(1*H*-indol-3-yl)ethyl)hexadecanamide (4.6c)**[222]

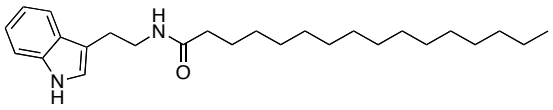

To a cooled solution (0 °C) of palamic acid (512 mg, 2.00 mmol, 2.00 equiv.) in CH_2Cl_2 (10 mL) oxalyl chloride (1.03 mL, 12.00 mmol, 12.00 equiv.) was added. The mixture was stirred for 1 h under argon in an ice-bath. The solvent was removed under reduced pressure. The curde acid chloride was dissolved in CH_2Cl_2 (5 mL) and added drop wise to a cooled (0 °C) solution of tryptamine (150 mg, 1.00 mmol, 1.00 equiv.) and TEA (281 mL, 2.00 mmol, 2.00 equiv) in CH_2Cl_2 (10 mL). The reaction mixture was stirred at r.t. under argon for 2.5 h. The solvent was evaporated and the obtained colorless residue was directly purified by FC on SiO_2 (pentane/acetone 10:1) to yield the product **4.6c** (302 mg, 0.758 mmol, 76%) as colorless solid. (NMR spectra not added)

$\mathbf{R_f}$ = 0.76 (CH_2Cl_2/MeOH 10:1). **M.P.** = 114 - 116 °C. **^{1}H-NMR** (400 MHz, $CDCl_3$) δ 8.17 (s, 1H), 7.61 (d, *J* = 7.9 Hz, 1H), 7.38 (d, *J* = 8.1 Hz, 1H), 7.21 (t, *J* = 7.5 Hz, 1H), 7.13 (t, *J* = 7.5 Hz, 1H), 7.03 (d, *J* = 2.0 Hz, 1H), 5.51 (s, 1H), 3.61 (q, *J* = 6.5 Hz, 2H), 2.98 (t, *J* = 6.7 Hz, 2H), 2.12 - 2.07 (t, *J* = 5.2 Hz, 2H), 1.66 - 1.55 (m, 2H), 1.28 (m, 24H), 0.88 (t, *J* = 6.8 Hz, 3H). **^{13}C-NMR** (101 MHz, $CDCl_3$) δ 173.29, 136.57, 127.52, 122.35, 122.13, 119.63, 118.89, 113.26, 111.39, 39.79, 37.07, 32.07, 29.84 (2C), 29.83, 29.80, 29.77 (2C), 29.63, 29.50 (2C), 29.45, 25.90, 25.53, 22.83, 14.26. **FTIR** $\tilde{\nu}$ = 3394*m*, 3250*w*, 3080*w,* 2951*w*, 2917*s*, 2847*s*, 1629*m*, 1564*m*, 1460*m*, 1287*w*, 1225*w*, 1094*w*, 1068*w*, 1011*w*, 739*s*, 725*m*. (NMR spectra not added) The reported data is in accordance with the literature.[222]

[222] F. Schmidt, P. Champy, B. Seon-Meniel, X. Franck, R. Raisman-Vozari, B. Figadère, *PLOS ONE* **2009**, *4*, e6215.

_N_-(2-(1_H_-indol-3-yl)ethyl)hexadecan-1-amine 4.6l[222]

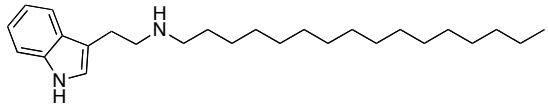

To a solution of _N_-(2-(1_H_-indol-3-yl)ethyl)hexadecanamide **4.6c** (100 mg, 0.251 mmol, 1.00 equiv.) in THF (5 mL) $LiAlH_4$ (76.2 mg, 2.01 mmol, 8.00 equiv.) was added. The mixture was then refluxed under an argon atmosphere for 4.5 h. The reaction mixture was quenched using H_2O (2 mL) followed by NaOH-solution (1 M, 1 mL). The suspension was filtered over celite and washed with EtOAc. The organic layer was separated, dried ($NaSO_4$) and concentrated. The crude was purified by FC on SiO_2 (MeOH/CH_2Cl_2 3:97 + 0.2% TEA) to yield the product **4.6l** (51 mg, 0.133 mmol, 53%) as glittery colorless solid. (NMR spectra not added) The reported data is in accordance with the literature.[222]

R_f = 0.40 (CH_2Cl_2/MeOH 10:1 + TEA). **M.P.** = 194 - 195 °C. **^{1}H NMR** (400 MHz, MeOD) δ 7.58 (d, J = 7.9 Hz, 1H), 7.37 (d, *J* = 8.1 Hz, 1H), 7.19 (s, 1H), 7.16 - 7.09 (m, 1H), 7.09 - 7.01 (m, 1H), 3.34 - 3.25 (m, 2H), 3.16 (t, *J* = 7.6 Hz, 2H), 3.07 - 2.97 (m, 2H), 1.66 (m, 2H), 1.46 - 1.16 (m, 24H), 0.90 (t, *J* = 6.9 Hz, 3H). **^{13}C-NMR** (101 MHz, MeOD) δ 138.35, 128.13, 124.21, 122.81, 120.09, 118.88, 112.58, 110.14, 49.31, 33.07, 30.38, 30.77 (2C), 30.75 (2C), 30.72, 30.62, 30.48, 30.46, 30.19, 27.57, 27.24, 23.73, 23.44, 14.43. (1 peak overlaid by MeOD) **FTIR** $\tilde{\nu}$ = 3418*s*, 3334*s broad*, 2957*w*, 2923*w*, 2850*w*, 2361*m*, 2340*m*, 1643*m*, 1460*w*, 1015*m*, 815*m*, 737*m*, 647*w*. (NMR spectra not added) The reported data is in accordance with the literature.[222]

(*S*)-4-(2-(hexadecylamino)-3-hydroxypropyl)phenol (4.22a)

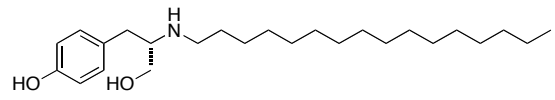

Amide **4.22e** (23.0 mg, 0.055 mmol, 1.00 equiv.), chlorotrimetyhlsilane (1.0 mg, 0.009 mmol, 0.17 equiv.) and 1,1,1,3,3,3-hexamethyldisilazane (28.3 mg, 0.175 mmol 3.20 equiv.) were dissolved in MeCN (1.5 mL) and refluxed (90 ºC) under argon for 2.5 h. The solvent was removed under reduced pressure and the residue was

[222] F. Schmidt, P. Champy, B. Seon-Meniel, X. Franck, R. Raisman-Vozari, B. Figadère, *PLOS ONE* **2009**, *4*, e6215.

dissolved in dioxane (1.50 mL). Borane dimethyl sulfide complex solution in THF (2 M) (138 mL, 0.277 mmol, 5.00 equiv.) was added and the mixture was refluxed (100 °C) under argon for 20 h. Then HCl-solution (10%, v:v, 1.0 mL) was added and the mixture was refluxed (100 °C) for another hour. The mixture was then extracted using saturated $NaHCO_3$-solution (5.00 mL) and CH_2Cl_2 (3x). The combined organic layers were concentrated and the residue was purified by FC on SiO_2 (CH_2Cl_2/MeOH 4:1 + 0.1% TFA) to yield the product **4.22a** (12.5 mg, 0.031 mmol, 56%) as white solid.

R_f = 0.28 (CH_2Cl_2/MeOH 10:1). **M.P.** = 75 - 78 °C. **^{1}H-NMR** (400 MHz, MeOH) δ 7.09 (m, 2H), 6.76 (m, 2H), 3.67 (dd, *J* = 11.8, 3.5 Hz, 1H), 3.50 (dd, *J* = 11.9, 4.9 Hz, 1H), 3.27 - 3.17 (m, 1H), 3.02 - 2.75 (m, 4H), 1.76 - 1.53 (m, 2H), 1.44 - 1.10 (m, 26H), 0.90 (t, *J* = 6.7 Hz, 3H). **^{13}C-NMR** (101 MHz, MeOH) δ 157.70, 131.35 (2C), 128.28, 116.62 (2C), 62.15, 59.67, 46.82, 34.93, 33.07, 30.78 (2C), 30.77, 30.76, 30.71, 30.65, 30.54, 30.47, 30.28, 28.04, 27.77, 23.73, 14.43. **HRMS ESI-TOF** calcd. for $C_{25}H_{46}NO_2^+$ (100%, $[M+H]^+$): 392.3523; found; 392.3525. **FTIR** $\tilde{\nu}$ 3298*w*, 2956*w*, 2917*s*, 2850*s*, 1615*w*, 1600*w*, 1564*w*, 1516*m*, 1469*m*, 1368*w*, 1249*m*, 1175*w*, 1104*w*, 1069*w*, 1041*w*, 1018*w*, 991*w*, 965*w*, 839*w*, 818*m*, 777*w*, 719*w*, 649w. **Optical rotation:** $[\alpha]_D^{25} = -8.7$ (c = 0.28, MeOH).

(*S*)-4-(3-hydroxy-2-((15-hydroxypentadecyl)amino)propyl)phenol (4.22b)

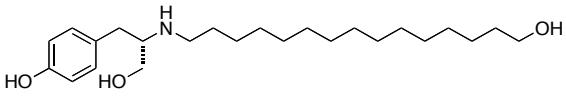

Amide **4.22f** (28.0 mg, 0.069 mmol, 1.00 equiv.), chlorotrimetyhlsilane (3.6 mg, 0.033 mmol, 0.50 equiv.) and 1,1,1,3,3,3-hexamethyldisilazane (35.5 mg, 0.220 mmol 3.20 equiv.) were dissolved in MeCN (2.00 mL) and refluxed (90 °C) under argon for 1h. The solvent was removed under reduced pressure and the residue was dissolved in dioxane (1.80 mL). Borane dimethyl sulfide complex solution in THF (2 M, 172 mL, 0.343 mmol, 5.00 equiv.) was added and the mixture was refluxed (100 °C) under argon for 13 h. Then HCl-solution (10%, v:v, 1.00 mL) was added and the mixture was refluxed (100 °C) for another hour. The mixture was extracted using sat. $NaHCO_3$-solution and CH_2Cl_2 (3x). The combined organic layers were concentrated and the residue was purified by FC on SiO_2 (CH_2Cl_2/MeOH 6:1 + 0.1% TEA) to yield the product **4.22b** (11 mg, 0.028 mmol, 41%) as white solid.

R_f = 0.14 (CH_2Cl_2/MeOH 10:1 + TEA). **M.P.** = 133 - 135 °C. **^{1}H-NMR** (500 MHz, MeOD) δ 7.13 - 7.05 (m, 2H), 6.80 - 6.73 (m, 2H), 3.69 (dd, *J* = 11.9, 3.5 Hz, 1H), 3.57 - 3.48 (m, 3H), 3.24 (td, *J* = 9.2, 4.8 Hz, 1H), 3.05 - 2.78 (m, 4H), 1.74 - 1.61 (m, 2H), 1.57 - 1.48 (m, 2H), 1.43 - 1.24 (m, 22H). **^{13}C-NMR** (125 MHz, MeOD) δ 157.73, 131.36 (2C), 128.18, 116.63 (2C), 63.00, 62.13, 59.46, 46.75, 34.79, 33.66, 30.75 (2C), 30.73 (2C), 30.64, 30.61 (2C), 30.53, 30.26, 27.91, 27.74, 26.95. **HRMS ESI-TOF** calcd. for $C_{24}H_{44}NO_3^+$ (100%, $[M+H]^+$): 394.3316; found; 394.3316. **FTIR** $\tilde{\nu}$ 3310*w*, 2919*s*, 2849*s*, 2523*w*, 2458*m*, 1612*w*, 1515*s*, 1468*s*, 1372*w*, 1258*m*, 1171*w*, 1106*w*, 1096*w*, 1064*m*, 1011*w*, 940*w*, 820*w*. **Optical rotation:** $[\alpha]_D^{25} = -11.3$ (c = 0.26, MeOH).

4-((*S*)-3-hydroxy-2-((9*Z*,12*Z*)-octadeca-9,12-dien-1-ylamino)propyl)phenol (4.22c)

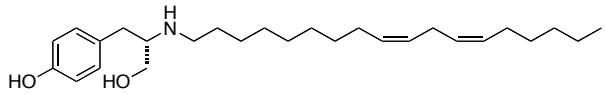

To a cooled (–78 °C) solution of ethyl linoleate (60 mg, 0.194 mmol, 1.00 equiv.) in toluene (3.00 mL) was added a precooled (–78 °C) DIBAL-H solution (1 M in *n*-hexane) (202 µL, 0.202 mmol, 1.05 equiv.) which was dissolved in toluene (1.00 mL). The mixture was stirred for 50 min at this temperature under argon before it was quenched using sat. Rochelle salt-solution (3.00 mL) and extracted with Et_2O (3x). The combined organic layers were dried over $NaSO_4$ and concentrated.

The crude linolic aldehyde was dissolved in MeOH (2.00 mL). To this solution glacial acetic acid (0.10 mL), L-tyrosinol hydrochloride (53.1 mg, 0.261 mmol, 1.35 equiv.) and sodium cyanoborohydride (18.2 mg, 0.290 mmol, 1.50 equiv.) were added. The mixture was stirred for 2.5 h at r.t. under argon before it was quenched with HCl-solution (10%, v:v, 30 mL). The mixture was extracted with Et_2O (3x10 mL). The combined organic layers were washed with brine, dried using $NaSO_4$ and concentrated. The residue was purified by FC on SiO_2 (MeOH/CH_2Cl_2 1:15 + 0.1% TEA) to yield the product **4.22c** (22 mg, 0.052 mmol, 27%) as colourless oil.

R_f = 0.50 (CH_2Cl_2/MeOH 10:1 + TEA). **^{1}H-NMR** (400 MHz, MeOH) δ 7.11 (m, 2H), 6.77 (m, 2H), 5.43 - 5.26 (m, 4H), 3.72 (dd, *J* = 12.1, 3.3 Hz, 1H), 3.53 (dd, *J* = 12.1, 4.5 Hz, 1H), 3.40 - 3.32 (m, 1H), 3.13 - 2.82 (m, 4H), 2.78 (t, *J* = 6.3 Hz, 2H), 2.15 - 2.00 (m, 4H), 1.76 - 1.59 (m, 2H), 1.60 - 1.23 (m, 18H), 0.91 (t, *J* = 6.9 Hz, 3H). **^{13}C-**

NMR (101 MHz, MeOD) δ 157.86, 131.39, 130.96, 130.84, 129.14, 129.03, 127.67, 116.68, 62.06, 58.61, 46.45, 34.25, 32.66, 30.75, 30.47, 30.42, 30.26, 30.20, 28.17, 27.67, 27.40, 26.53, 23.62, 14.43. **HRMS ESI-TOF** calcd. for $C_{27}H_{46}NO_2^+$ (100%, $[M+H]^+$): 416.3523; found; 416.3525. **FTIR** $\tilde{\nu}$ 3263*w*, 3010*w*, 2925*s*, 2854*s*, 1614*s*, 1603*w*, 1516s, 1453*m*, 1376*w*, 1260*m*, 1231*m*, 1174*w*, 1106*w*, 1044*m*, 966*w*, 840*w*, 778*w*, 660*s*, 618*s*. **Optical rotation:** $[\alpha]_D^{25} = -5.5$ (c = 0.19, MeOH).

4-((*S*)-3-hydroxy-2-((9*Z*,12*Z*,15*Z*)-octadeca-9,12,15-trien-1-ylamino)propyl)phenol (4.22d)

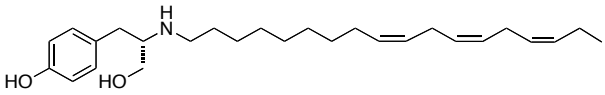

To a cooled (–78 °C) solution of ethyl linolenate (150 mg, 0.489 mmol, 1.00 equiv.) in toluene (3.00 mL) was added a precooled (–78 °C) DIBAL-H solution (1 M in *n*-hexane, 514 mL, 0.514 mmol, 1.05 equiv.) which was prior dissolved in toluene (1.00 mL). The mixture was stirred for 50 min at this temperature under argon before it was quenched using sat. Rochelle-salt-solution (5.00 mL) and extracted with Et_2O (3x). The combined organic layers were dried over $NaSO_4$ and concentrated.

The crude linolenic aldehyde was dissolved in MeOH (4.00 mL). To this solution glacial acetic acid (0.15 mL), L-tyrosinol hydrochloride (130 mg, 0.636 mmol, 1.30 equiv.) and sodium cyanoborohydride (46.1 mg, 0.734 mmol, 1.50 equiv.) were added. The mixture was stirred for 2 h at r.t. under argon before it was quenched with HCl-solution (10%, v:v, 30 mL). The mixture was extracted with Et_2O (3x10 mL). The combined organic layers were washed with brine, dried using $NaSO_4$ and concentrated. The residue was purified by FC on SiO_2 ($MeOH/CH_2Cl_2$, 1:20 + 0.1% TEA) to yield the product **4.22d** (90 mg, 0.218 mmol, 22%) as colorless oil.

$\mathbf{R_f}$ = 0.49 (CH_2Cl_2/MeOH 10:1). **^{1}H-NMR** (400 MHz, MeOD) δ 7.08 (m, 2H), 6.75 (m, 2H), 5.50 - 5.16 (m, 6H), 3.65 (dd, *J* = 11.7, 3.6 Hz, 1H), 3.49 (dd, *J* = 11.7, 5.0 Hz, 1H), 3.15 (td, *J* = 9.2, 4.9 Hz, 1H), 3.05 - 2.63 (m, 8H), 2.22 - 2.01 (m, 4H), 1.71 - 1.55 (m, 2H), 1.34 (s, 10H), 0.97 (td, *J* = 7.5, 0.7 Hz, 3H). **^{13}C-NMR** (101 MHz, MeOD) δ 157.54, 132.71, 131.31 (2C), 131.05, 129.18 (2C), 128.84, 128.66, 128.21, 116.55 (2C), 62.20, 60.29, 47.04, 35.32, 30.72, 30.45, 30.30, 30.26, 28.42, 28.17,

27.84, 26.52, 26.40, 21.48, 14.67. **HRMS ESI-TOF** calcd. for $C_{27}H_{44}NO_2^+$ (100%, $[M+H]^+$): 414.3367; found; 414.3367. **FTIR** $\tilde{\nu}$ 3283*w*, 3011*w*, 2962*w* 2926*m*, 2854*m*, 2361*w*, 2338*w*, 1614*w*, 1595*w*, 1516*m*, 1451*m*, 1393*w*, 1368*w*, 1233*m*, 1172*w*, 1106*w*, 1043*w*, 839*w*, 770*m*, 716*m*, 655*s*. **Optical rotation:** $[\alpha]_D^{25}$= –8.7 (c = 0.14, MeOH).

(*S*)-*N*-(1-hydroxy-3-(4-hydroxyphenyl)propan-2-yl)palmitamide (4.22e)

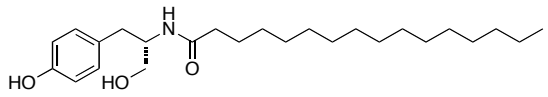

L-Tyrosinol hydrochloride (150 mg, 0.736 mmol, 1.00 equiv.), palmitic acid (189 mg, 0.736 mmol, 1.00 equiv.), EDC (283 mg, 1.472 mmol, 2.00 equiv.), 1H-benzotriazole (149 mg, 1.100 mmol, 1.50 equiv.) and TEA (311mL, 2.208 mmol, 3.00 equiv.) were suspended in MeCN (8.00 mL). The mixture was then stirred under argon at r.t. for 18 h. The solvent was evaporated and the white residue was directly purified by gradiental FC on SiO_2 (CH_2Cl_2/MeOH 10:1 to 4:1) to yield the product **4.22d** (203 mg, 0.500 mmol, 68%) as white fluffy solid.

$\mathbf{R_f}$ = 0.44 (CH_2Cl_2/MeOH 10:1). **M.P.** = 52 - 55 °C. **^{1}H-NMR** (400 MHz, MeOH) δ 7.04 (m, 2H), 6.68 (m, 2H), 4.05 (dq, *J* = 11.4, 5.6 Hz, 1H), 4.05 (dq, *J* = 11.4, 5.6 Hz, 1H), 3.50 (d, *J* = 5.3 Hz, 2H), 3.40 - 3.27 (m, 3H), 2.82 (dd, *J* = 13.9, 6.0 Hz, 1H), 2.59 (dd, *J* = 13.9, 8.5 Hz, 1H), 2.12 (t, *J* = 7.4 Hz, 2H), 1.68- 1.40 (m, 2H), 1.26 (d, *J* = 24.7 Hz, 25H), 0.90 (t, *J* = 6.8 Hz, 3H). **^{13}C-NMR** (101 MHz, MeOH) δ 176.15, 156.90, 131.21, 130.50, 116.06, 64.36, 54.19, 37.27, 37.15, 33.08, 30.81, 30.77, 30.59, 30.48, 30.20, 27.06, 23.74, 14.44. **HRMS ESI-TOF** calcd. for $C_{25}H_{44}NO_3^+$ (100%, $[M+H]^+$): 406.3316; found; 406.3320. **FTIR** $\tilde{\nu}$ 3485*w*, 3314*w,* 3202*w,* 2918*s*, 2850*s,* 2390*w,* 1636*s,* 1614*w,* 1537*s,* 1515*m,* 1462*m,* 1451*m,* 1380*w,* 1366*w,* 1246*m,* 1224*w,* 1038*s,* 830*m,* 730*w,* 720*w,* 686*m*. **Optical rotation:** $[\alpha]_D^{25}$= –12.8 (c = 0.51, MeOH).

(*S*)-15-hydroxy-*N*-(1-hydroxy-3-(4-hydroxyphenyl)propan-2-yl)pentadecanamide (4.22e)

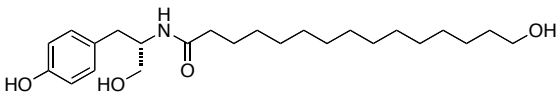

L-Tyrosinol hydrochloride (150 mg, 0.736 mmol, 1.00 equiv.), 15-hydroxypentadecanoic acid (196 mg, 0.736 mmol, 1.00 equiv.), EDC (283 mg, 1.472 mmol, 2.00 equiv.), 1H-benzotriazole (149 mg, 1.100 mmol, 1.50 equiv.) and TEA (311 µL, 2.208 mmol, 3.00 equiv.) were suspended in MeCN (8.00 mL). The mixture was then stirred under argon at to r. t. for 16 h. The solvent was evaporated and the white residue was directly purified by FC on SiO_2 (CH_2Cl_2/MeOH 2:1) followed by a recrystallization (pentane/acetone 4:1) to yield the product **33** (188 mg, 0.461 mmol, 63%) as white solid.

R_f = 0.43 (CH_2Cl_2/MeOH 10:1). **M.P.** = 40 - 43 °C. **^{1}H-NMR** (400 MHz, MeOD) δ 7.07 - 7.00 (m, 2H), 6.74 - 6.65 (m, 2H), 4.04 (dt, *J* = 11.3, 5.6 Hz, 1H), 3.58 - 3.46 (m, 4H), 2.82 (dd, *J* = 13.9, 6.0 Hz, 1H), 2.59 (dd, *J* = 13.9, 8.5 Hz, 1H), 2.12 (t, *J* = 7.5 Hz, 2H), 1.58 - 1.41 (m, 4H), 1.39 - 1.00 (m, 20H). **^{13}C-NMR** (101 MHz, MeOD) δ 176.14, 156.89, 131.20 (2C), 130.50, 116.06 (2C), 64.37, 63.02, 54.20, 37.27, 37.15, 33.68, 30.79, 30.77 (2C), 30.75 (2C), 30.62, 30.59, 30.48, 30.19, 27.07, 26.96. **HRMS ESI-TOF** calcd. for $C_{24}H_{42}NO_4^+$ (100%, $[M+H]^+$): 408.3108; found; 408.3108. **FTIR** $\tilde{\nu}$ 3451*w*, 3301*m*, 3027*w*, 2920*s*, 2848*s*, 1638*s*, 1556*s*, 1514*s*, 1459*s*, 1421*w*, 1377*m*, 1343*w*, 1313*w*, 1271*m*, 1238*s*, 1175*w*, 1083*w*, 1048*s*, 1026*w*, 952*w*, 852*w*, 816*w*, 778*w*, 726*m*. **Optical rotation:** $[\alpha]_D^{25} = -13.3$ (c = 0.26, MeOH).

(9*Z*,12*Z*)-*N*-((*S*)-1-hydroxy-3-(4-hydroxyphenyl)propan-2-yl)octadeca-9,12-dienamide (BSL34)

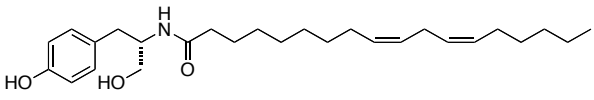

Linoleic acid (50 mg, 0.178 mmol, 1.00 equiv.), DCC (73.6 mg, 0.357 mmol, 2.00 equiv.) and pentafluorophenol (49.2 mg, 0.267 mmol, 1.50 equiv.) were suspended in DMF (4.00 mL). The mixture was stirred under argon at 60 °C for 18 h. Then L-tyrosinol hydrochloride (38.8 mg, 0.214 mmol, 1.20 equiv.) and TEA (75 mL, 0.535 mmol, 3.00 equiv.) were added and the mixture was stirred at r.t. for 30 h. The

reaction mixture was concentrated and directly purified by FC on SiO_2 (CH_2Cl_2/MeOH 20:1) without extraction to yield the product **BSL34** (22 mg, 0.461 mmol, 63%) as white solid.

R_f = 0.65 (MeOH/$CH_2Cl_2$1:20). **M.P.** = 52 - 55 °C. **^{1}H-NMR** (400 MHz, MeOD) δ 7.04 (m, 2H), 6.69 (m, 2H), 5.44 - 5.25 (m, 4H), 4.05 (tt, *J* = 11.3, 5.6 Hz, 1H), 3.50 (d, *J* = 5.4 Hz, 2H), 2.88 - 2.72 (m, 3H), 2.59 (dd, *J* = 13.9, 8.5 Hz, 1H), 2.15 - 2.02 (m, 6H), 1.56 - 1.45 (m, 2H), 1.42 - 1.15 (m, 14H), 0.90 (t, *J* = 6.8 Hz, 3H). **^{13}C-NMR** (101 MHz, MeOD) δ 176.12, 156.90, 131.21, 130.94, 130.50, 129.07, 129.06, 116.07, 64.36, 54.19, 37.26, 37.15, 32.66, 30.77, 30.48, 30.38, 30.23, 30.18, 28.18, 28.16, 27.06, 26.54, 23.63, 14.43. **HRMS ESI-TOF** calcd. for $C_{27}H_{44}NO_3^+$ (100%, $[M+H]^+$): 430.3316; found; 430.3316. **FTIR** $\tilde{\nu}$ 3491*w,* 3317*m*, 3186*w*, 3010*w*, 2923*m*, 2853*m*, 1642*s*, 1614*w*, 1534*s*, 1515*s*, 1462*m*, 1447*m*, 1384*w*, 1363*w*, 1246*m*, 1220*s*, 1113*w*, 1053*m*, 1036*s*, 954*w*, 823*w*, 724*w*, 680*m*. **Optical rotation:** $[\alpha]_D^{25}$= –12.8 (c = 0.21, MeOH).

(9*Z*,12*Z*,15*Z*)-*N*-((*S*)-1-hydroxy-3-(4-hydroxyphenyl)propan-2-yl)octadeca-9,12,15-trienamide (4.22h)

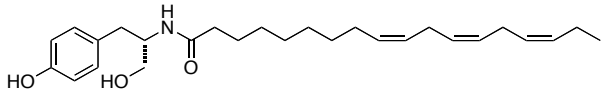

Linolenic acid (55 mg, 0.198 mmol, 1.00 equiv.), DCC (81.5 mg, 0.395 mmol, 2.00 equiv.) and pentafluorophenol (54.5 mg, 0.296 mmol, 1.50 equiv.) were suspended in DMF (4.00 mL). The mixture was stirred under argon at r.t. for 48 h. Then L-tyrosinol hydrochloride (50 mg, 0.277 mmol, 1.40 equiv.) and TEA (83 mL, 0.593 mmol, 3.00 equiv.) were added and the mixture was stirred at r.t. for 20 h. The reaction mixture was concentrated, diluted with water and extracted with Et_2O (3x). The combined organic layers were washed with brine, dried over $NaSO_4$ and concentrated. The crude product was purified by flash chromatography on SiO_2 (CH_2Cl_2/MeOH 50:1) yielded the product **4.22h** (49 mg, 0.111 mmol, 56%) as white solid.

R_f = 0.50 (CH_2Cl_2/EtOAc 8:2). **M.P.** = 70 - 72 °C. **^{1}H-NMR** (400 MHz, MeOD) δ 7.03 (m, 2H), 6.69 (m, 2H), 5.45 - 5.23 (m, 6H), 4.05 (tt, *J* = 11.3, 5.6 Hz, 1H), 3.50 (d, *J* = 5.4 Hz, 2H), 2.91 - 2.72 (m, 5H), 2.59 (dd, *J* = 13.9, 8.5 Hz, 1H), 2.17 - 1.99

(m, 6H), 1.55 - 1.45 (m, 2H), 1.41 - 1.12 (m, 8H), 0.97 (t, *J* = 7.5 Hz, 3H). **^{13}C-NMR** (101 MHz, MeOD) δ 176.09, 156.88, 132.71, 131.19, 131.12, 130.48, 129.21, 129.18, 128.79, 128.23, 116.06, 64.35, 54.18, 37.26, 37.15, 30.75, 30.37, 30.22, 30.18, 28.19, 27.06, 26.52, 26.40, 21.49, 14.66. **HRMS ESI-TOF** calcd. for $C_{27}H_{41}NNaO_3^+$ (100%, $[M+Na]^+$): 450.2979; found; 450.2979. **FTIR** $\tilde{\nu}$ 3491*w*, 3317*m*, 3182*w*, 3007*w*, 2927*m*, 2876*w*, 2852*w*, 1641*s*, 1614*w*, 1600*w*, 1533*s*, 1516*s*, 1448*m*, 1389*m*, 1363*m*, 1305*w*, 1248*m*, 1219*m*, 1114*w*, 1079*w*, 1054*m*, 1037*s*, 955*w*, 935*w*, 861*w*, 844*w*, 823*m*, 771*m*, 714*m*, 679*w*. **Optical rotation:** $[\alpha]_D^{25} = -12.9$ (c = 0.24, MeOH).

6-((5-(dimethylamino)naphthalene)-1-sulfonamido)hexanoic acid (4.28)[223]

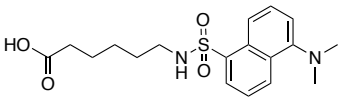

6-Aminohexanoic acid **4.27** (750 mg, 5.72 mmol, 5.00 equiv.) was dissolved in $NaHCO_3$ (1.0 M, 20 mL). To this solution 5-(dimethylamino)naphthalene-l-sulfonyl chloride **4.26** (dansyl chloride, 309 mg, 1.14 mmol, 1 equiv.) in acetone (5 mL) and Et_3N (322 mL, 2.29 mmol, 2.0 equiv.) was added. The solution was stirred for 1 h, acidified to pH 3 with HCl-solution (2 M) and extracted with ethyl acetate (3 x 15 mL). The organic layer was washed with water (1x), brine (1x) and dried (Na_2SO_4). The solvent was evaporated and the crude product was purified by FC on SiO_2 (MeOH/CH_2Cl_2 1:30) to yield **4.28** as yellow oil (180 mg, 494 mmol, 40%).

$\mathbf{R}_f$ = 0.86 (CH_2Cl_2/CH_2Cl_2, 1:10). **^{1}H-NMR** (400 MHz, $CDCl_3$) δ 8.53 (d, *J* = 8.5 Hz, 1H), 8.36 - 8.20 (m, 2H), 7.53 (ddd, *J* = 12.7, 8.5, 7.5 Hz, 2H), 7.18 (d, *J* = 7.4 Hz, 1H), 4.98 (t, *J* = 6.1 Hz, 1H), 2.88 (m, 8H), 2.17 (t, *J* = 7.4 Hz, 2H), 1.39 (m, 4H), 1.19 (m, 2H). **^{13}C-NMR** (101 MHz, $CDCl_3$) δ 179.24, 152.06, 134.86, 130.53, 129.98, 129.74 (2 peak), 128.51, 123.35, 118.88, 115.36, 45.54, 43.07, 33.71, 29.26, 25.88, 24.00. **UPLC MS** calcd for $C_{18}H_{25}N_2O_4S$ (100%, $[M+H]^+$): 362.1; found: 365.2. (NMR spectra not added) The reported data is in accordance with the literature.[223]

[223] T. H. Walls, S. C. Grindrod, D. Beraud, L. Zhang, A. R. Baheti, S. Dakshanamurthy, M. K. Patel, M. L. Brown, L. H. MacArthur, *Bioorg. Med. Chem.* **2012**, *20*, 5269–5276.

(*S*)-6-((5-(dimethylamino)naphthalene)-1-sulfonamido)-*N*-(1-hydroxy-3-(4-hydroxyphenyl)propan-2-yl)hexanamide (4.30)

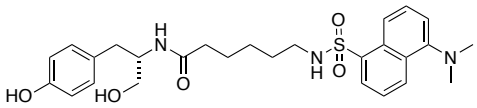

To a solution of acid **4.28** (125 mg, 0.343 mmol, 1.00 equiv.) in MeOH (10 mL), was added L-tyrosinol hydrochloride, HATU **4.29** (132 mg, 0.412 mmol, 1.20 equiv.) and Et_3N (68 mL, 0.480 mmol, 1.40 equiv.). The mixture was stirred for 4 h at r.t. under argon. The solvent was evaporated under reduced pressure and the residue was washed using CH_2Cl_2 (3x), brine (1x), dried ($NaSO_4$) and concentrated. The crude was purified by FC on SiO_2 (MeOH/CH_2Cl_2 1:15) yielding the product **4.30** as yellow oil (111 mg, 216 mmol, 63%).

$\mathbf{R}_f$ = 0.17 (CH_2Cl_2/CH_2Cl_2 1:20). **^{1}H-NMR** (400 MHz, MeOD) δ 8.53 (d, *J* = 8.5 Hz, 1H), 8.35 (d, *J* = 8.7 Hz, 1H), 8.18 (d, *J* = 7.3 Hz, 1H), 7.55 (q, *J* = 7.4 Hz, 2H), 7.23 (d, *J* = 7.5 Hz, 1H), 7.00 (m, 2H), 6.67 (m, 2H), 4.02 (m, 1H), 3.60 - 3.43 (m, 2H), 2.96 - 2.71 (m, 9H), 2.56 (dd, *J* = 13.9, 8.6 Hz, 1H), 1.94 (t, *J* = 7.4 Hz, 2H), 1.28 (dq, *J* = 13.9, 7.0 Hz, 4H), 1.04 (q, *J* = 8.1 Hz, 2H).**^{13}C-NMR** (101 MHz, MeOD) δ 175.74, 156.77, 153.11, 137.09, 131.19, 131.14, 131.06, 130.92, 130.49, 130.11, 129.04, 124.29, 120.53, 116.38, 116.06, 64.32, 54.12, 45.79, 43.66, 37.11, 36.90, 30.26, 26.91, 26.33. **HRMS ESI-TOF** calcd. for $C_{27}H_{36}N_3O_5S^+$ (100%, $[M+H]^+$): 514.2370; found: 514.2376. **FTIR** $\tilde{\nu}$ = 3280*m*, 2940*w*, 2866*w*, 2836*w*, 2792*w*, 1639*m*, 1614*m*, 1259*w*, 1573*m*, 1515*s*, 1454*m*, 1309*s*, 1232*m*, 1160*m*, 1140*s*, 1075*m*, 1024*s*, 946*w*, 824*w*, 790*s*, 653*s*, 621*s*. **Optical rotation:** $[\alpha]_D^{25}$ = –7.5 (c = 0.83, MeOH).

Compound **5.1** was synthesized following a known procedure and the obtained analytical data was in full accordance with the literature.[224] Compound **3.16**[225] was available in our laboratory originating from previous projects.

[224] Y. Luo, K. Sun, L. Li, L. Gao, G. Wang, Y. Qu, L. Xiang, L. Chen, Y. Hu, J. Qi, *ChemMedChem* **2011**, *6*, 1986–1989.
[225] F. Schmid, H. J. Jessen, P. Burch, K. Gademann, Med. Chem. Comm. **2013**, *4*, 135–139.
[226] A. Chicca, J. Marazzi, S. Nicolussi, J. Gertsch, *J. Biological Chem.* **2012**, *287*, 34660–34682.

6.4 Endocannabinoid System Screen

To obtain the biological data regarding the endocannabinoid system, established procedures were followed (**34** = **BSL34**).[226]

Figure 6.1A. CB_1 binding at 1 μM, n=2, mean ± SD

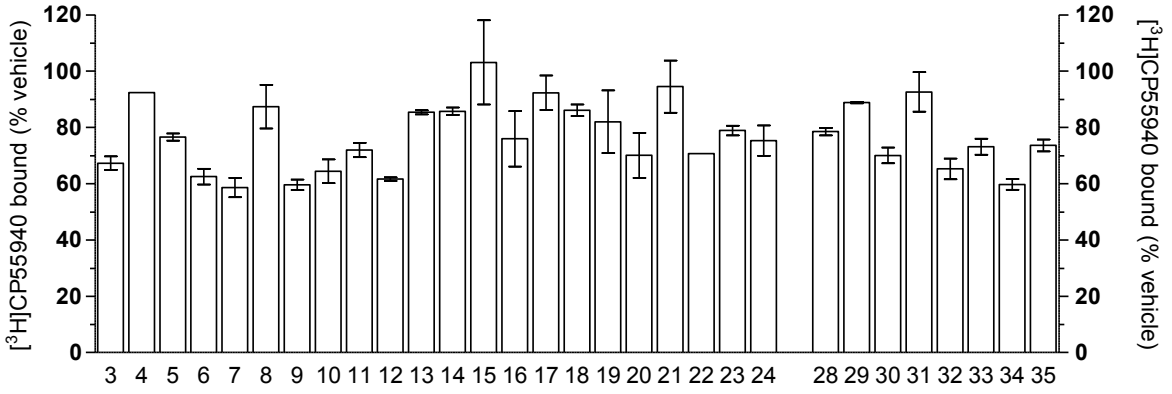

Figure 6.1B. CB_2 binding at 1 μM, n=2, mean ± SD

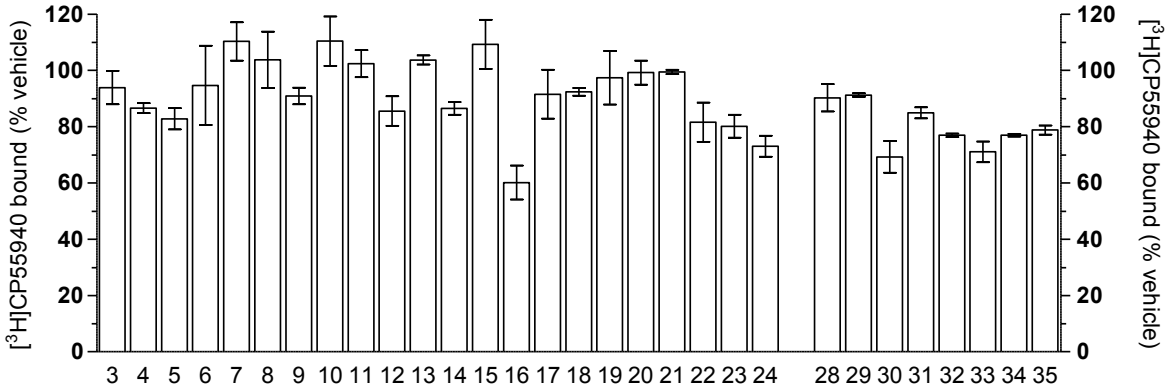

Figure 6.2. FAAH activity at 1 μM, n=2, mean ± SD

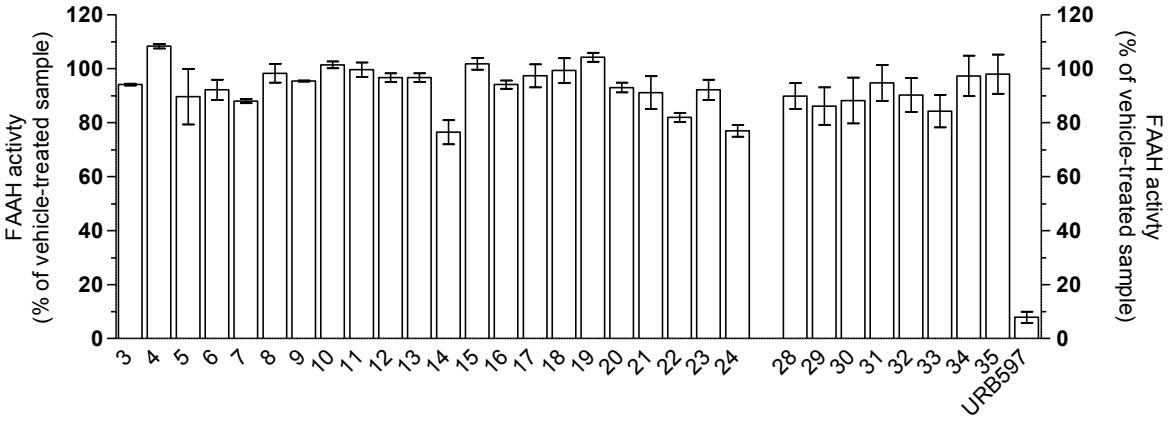

Figure 6.3A. MAGL activity at 1 μM, WWL70 10 μM, Orlistat 20 μM, JZL184 10 μM, result combined, n=2, mean ± SD

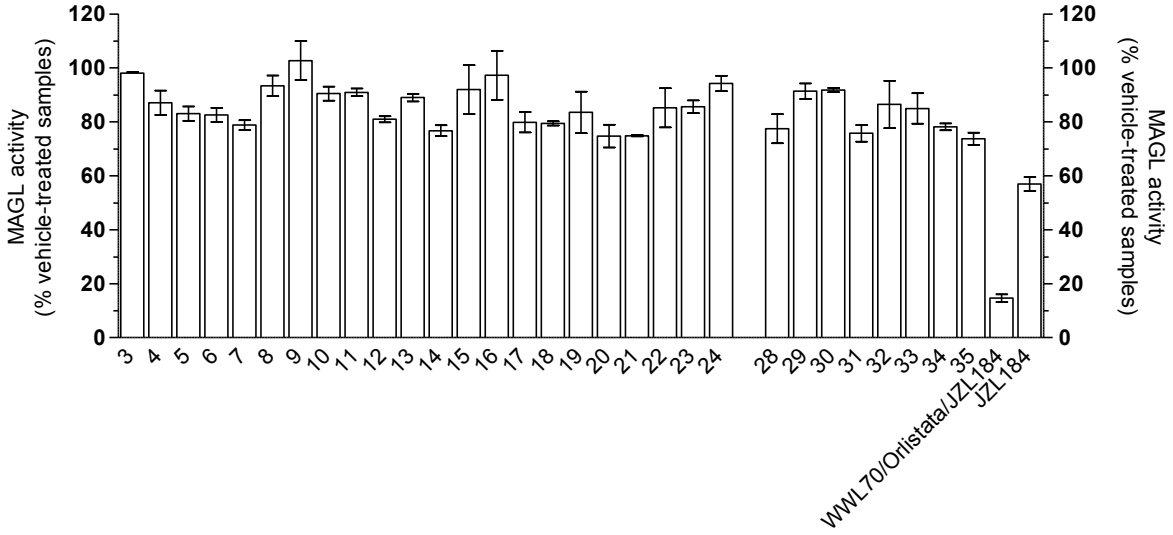

Figure 6.3B. ABHDs activity at 10 μM, WWL70 10 μM, Orlistat 20 μM, result combined, n=2, mean ± SD

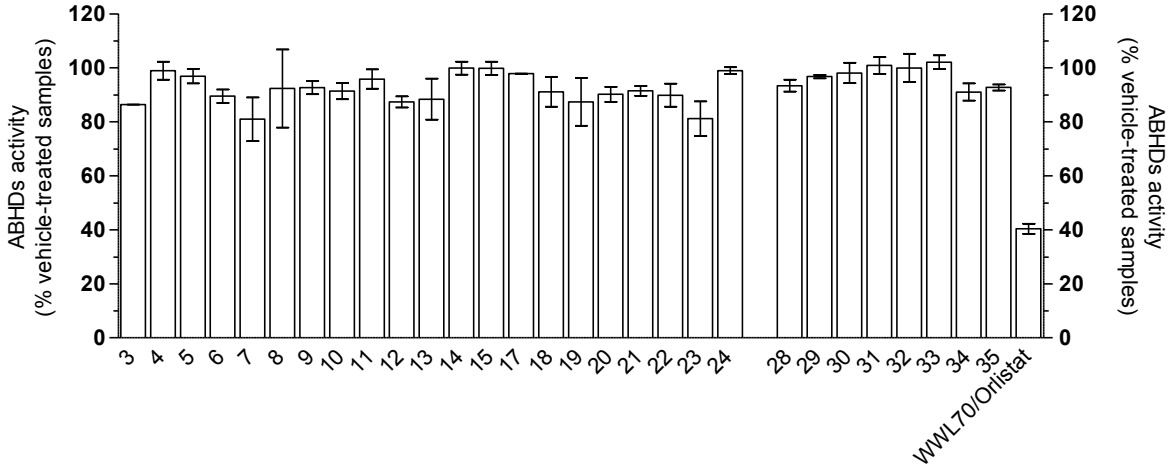

Figure 6.4. EMT activity at 10 µM, WWL70 10 µM, Orlistat 20 µM, result combined, n=2, mean ± SD

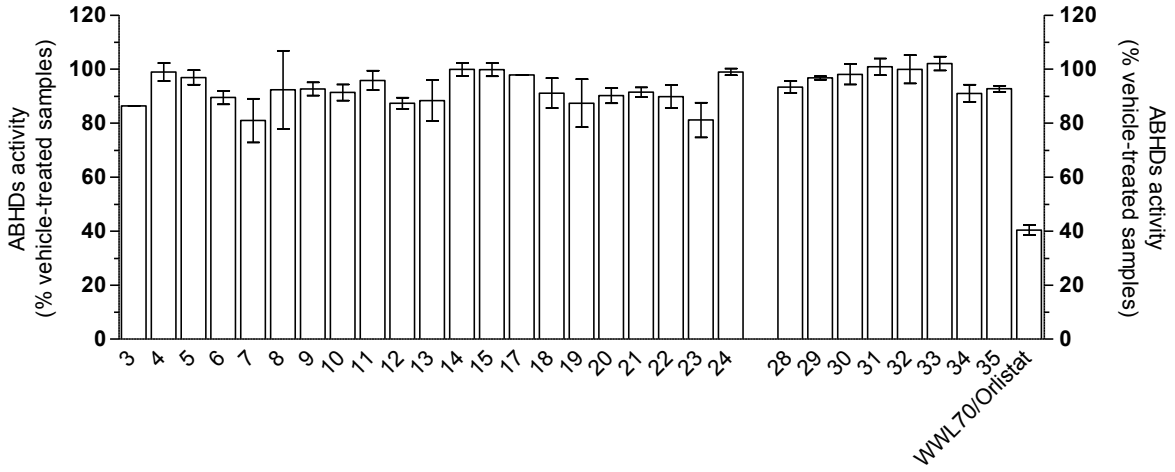

6.5 Re-Uptake Inhibition Screening[227]

For DA re-uptake inhibition assays, we used HEK 293 cells that stably overexpress human DA-, NE-, or SER-Transpoter.[228] The cells were cultured to 70% confluence in Dulbecco's Modified Eagle's Medium (4.5 g/L glucose) supplemented with 10% fetal bovine serum, 6 mM L-glutamine, 0.1 mM non-essential amino acids, 1mM sodium pyruvate, and 250 g/ml geneticin. For each re-uptake experiment, cells were detached with 0.05% trypsin/EDTA and re-suspended in re-uptake assay buffer (10 mM L-glucose, 0.5 mM $MgCl_2$, 4.6 mM KCl, 120 mM NaCl, 0.7 mM Na_2HPO_4, 1.3 mM NaH_2PO_4, and 0.015 mM sodium bicarbonate, pH 7.5) to 4 x 10^6 cells/mL. Distributed into 96-well plates, cells were incubated for 10 min at r. t. with the compounds at 20 µM (final concentration) or controls (vehicle control for 100% re-uptake and mazindol, nisoxetine, or fluoxetine at 10 µM for non-specific re-uptake). Then, 5 nM (final concentration) ^{3}H-DA, ^{3}H-NE, or ^{3}H-5-HT (specific activity = 30-50 Ci/mmol, PerkinElmer, Switzerland or ANAWA, Switzerland) were added and incubated for another 10 min at r.t.. Re-uptake was stopped separating cells from re-uptake buffer by centrifugation through a silicon oil mixture (1:2, m/m mixture of silicon oil types

[227] C. M. Hysek, L. D. Simmler, V. G. Nicola, N. Vischer, M. Donzelli, S. Krähenbühl, E. Grouzmann, J. Huwyler, M. C. Hoener, M. E. Liechti, *PLOS ONE* **2012**, *7*, e36476.
[228] M. Tatsumi, K. Groshan, R. D. Blakely, E. Richelson, *Euro. J. Pharmaco.* **1997**, *340*, 249–258.

AR20 and AR200) into a 3 M KOH layer in the tube tip. Essentially for reproducibility, the centrifuge always ran at high speed (13200 rpm) for 3 min. We then froze the tubes in liquid nitrogen and cut the tube tip containing cells underneath the silicon oil layer. The cells were disrupted with lysis buffer (0.05 M TRIS-HCl, 50 mM NaCl, 5 mM EDTA, and 1% NP- 40) and mixed with scintillation fluid (UltimaGold, PerkinElmer, Switzerland) and radioactivity was quantified on a β-counter. For data analysis, we subtracted all non-specific radioactive counts assessed with 10 µM mazindol, nisoxetine, or fluoxetine from the total counts derived from each drug. The specific vehicle control was set to define 100% re-uptake.

6.6 Surface Coating

6.6.1 Coating Procedure

Microscope cover glass slides (12 mm Ø, Marienfeld GmBH & Co, Germany) were placed in 24-well plates (Falcon) and covered with 1 mL of the respected coating solution (CS). The cover glasses were then incubated for 16 h at 36°C. The CS was removed and the slides were washed seven times with H_2O on both sides, placed in new collagen coated 6- or 24-well plates (Becton Dickinson Labware, UK), and finally subjected to UV irradiation (Lamp: Philips, TUV, 15W/G15 T8, 15 cm distance between lamp and plate) for 2 h for drying and sterilization. In case of the mixed incubation experiments where 6-well plates were used and two differently coated cover glasses were placed in the same well, a small glass piece was dismantled from the blank slide for differentiation as shown (Fig. 5.6).

6.6.2 Coating Solutions (CS)

CS Collagen: 0.01% of collagen (type 1 from rat tail, Sigma-Aldrich) in aqueous solution was mix either with:

- 100 µM DMSO solution of tetradecyl 2,3-dihydroxybenzoate (**5.1**), 1:10, v:v.
- 500 µM DMSO solution of 5-(4-hydroxy-3-methoxyphenyl)-4-methoxy-2-oxo-1,2-dihydropyridine-3-carboxylate (**3.16**), 1:10, v:v.
- 1 mM DMSO solution of (*S*)-*N*-(1-hydroxy-3-(4-hydroxyphenyl)propan-2-yl)propionamide (**3.5**), 1:10, v:v.

CS Collagen Blank: 0.01% of collagen in aqueous solution / DMSO, 1:10, v:v.

CS Poly-L-lysine: 50 µg/mL Poly-L-lysine hydrobromide 10'000-20'000 (Fluka) in aqueous solution / 100 µM DMSO solution of tetradecyl 2,3-dihydroxybenzoate (**5.1**), 10:1.

CS Poly-L-lysine Blank: 50 µg/mL Poly-L-lysine hydrobromide 10'000-20'000 (Fluka) in aqueous solution / DMSO, 1:10, v:v.

6.6.3 Biological Evaluation - General Procedure

When the PC12 cell concentration was sufficient, the growth medium (GM) in the culture flask was replaced by 12 mL of differentiation media (DM) (DMEM GlutaMAX™, 1% horse serum, 0.5% fetal bovine serum) containing NGF-7S (120 ng/mL) and incubated for 16 h. The media was removed and replaced by fresh DM without NGF-7S. The cells were scratched off the surface using a cell scraper (BD Falcon) and disaggregated by passage through a 21-gauge needle. The cell suspensions (80000 cells/mL) was then subjected to plates containing the coated cover glasses and incubated for 2 d at 36 °C. Cells were then fixed with 4% buffered formaldehyde solution for 2 h at 4 °C, then stained with Giemsa stain (modified solution), washed twice with PBS, mounted on microscope slides using Flouromount (Sigma-Aldrich), sealed with nail polisher (Express Finish, Maybelline, New York) and pictured under a phase contrast microscope (Leica DMI 4000B). The pictures were evaluated as descried in chapter 6.1.2.

6.6.4 Restricted Area Coating

A 200 µL droplet of a 1 mM solution of **5.1** in EtOH was placed on the bottom of a 6-well plate. After evaporation, the cells were incubation and fixed under identical conditions as descried before but the staining procedure was modified. The methanol content of the Giemsa stain solution was removed and replaced by an equivalent amount of water. After staining and washing with PBS twice, the cells were stained with a 300 nM DAPI solution in PBS for 5 min, washed twice with PBS and examined under the fluorescent microscope.

6.6.5 Recycling Procedure

Instead of fixing the cells after 2 d, the glass slides were incubated for 20 min with TrypLE™ Express, washed twice with H_2O, transferred in a new collagen coated 24-well plate and subjected again for 2 h to UV irradiation before being reused for another cycle using the same conditions as before.

6.6.6 Close Proximity MIE

Square microscope cover slides (12x12 mm, Marienfeld GmBH & Co, Germany) were coated under standard conditions with or without **5.1.** To fix them in close proximity in a new well, small parts of the well bottom were molten with a glowing spatula as shown (Fig. 5.6).

6.6.7 SEM Pictures

Transparent conducting oxide coated glass (TC022-7, 2.2 mm thick, Solaronix, Switzerland) was sonicated for 15 min in a cleaning solution (2% of cleaner L2 solution, Sonoswiss, Switzerland), washed with H_2O and EtOH, dried and UV irradiated (UVO Cleaner, Jetlight Company Inc., USA) for 20 min. The glass plates where then coated under standard conditions using the following CS: Collagen with **5.1**, Collagen blank, Poly-L-lysine, Poly-L-lysine blank. They where then examined with a ZEISS/LEO Supra 35 field emission scanning electron microscope. No difference on the surface could be detected.

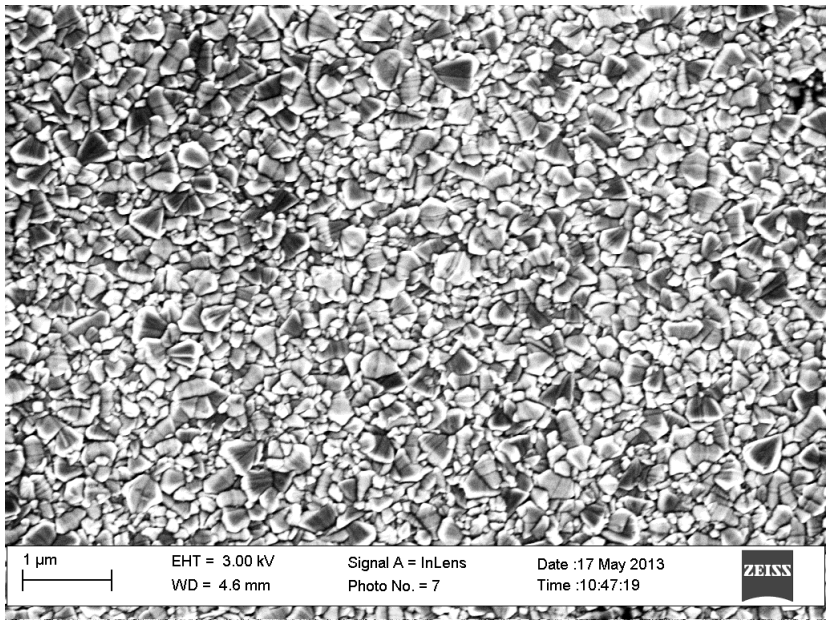

Transparent conducting oxide coated glass incubated under standard conditions with CS Collagen blank.

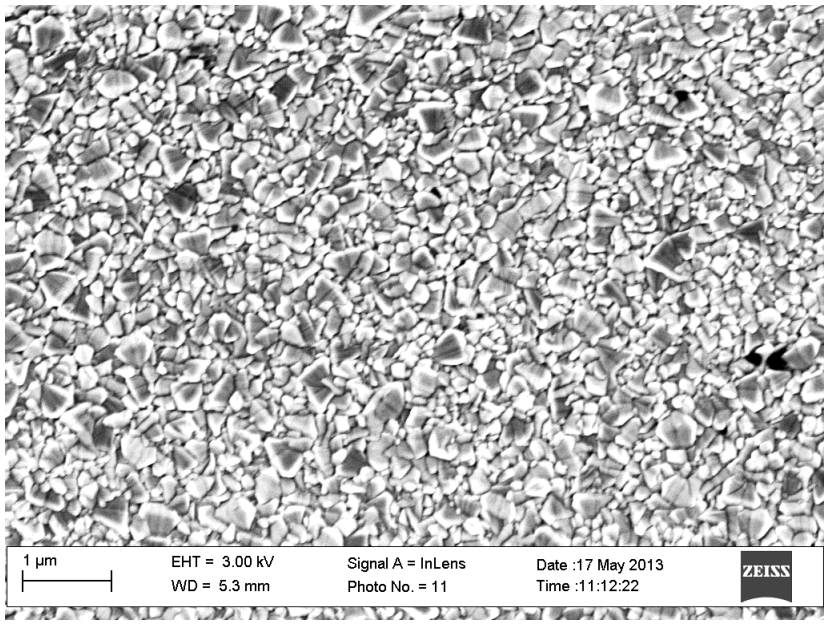

Transparent conducting oxide coated glass incubated under standard conditions with Coating: DMSO in 0.01% collagen aqueous solution, 1:10, v:v, **5.1** 10 µM.

7

CHAPTER 7 - ANNEXES

7.1 X-Ray Parameters

X-Ray parameters for **2.44**:

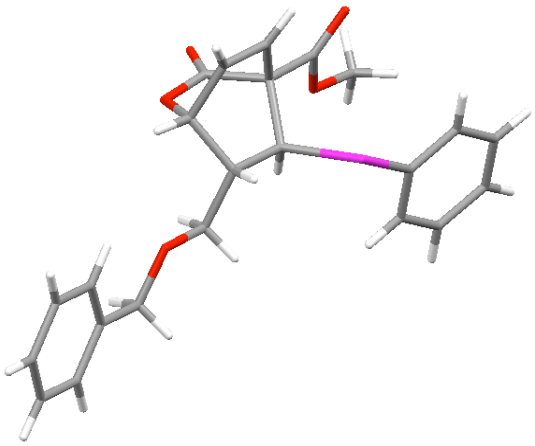

CCDC ID	**CCDC 901009**
Formula	$C_{23}H_{22}O_5Se$
Formula weight	457.37
Z, calculated density	1.461 Mg•m^{-3}
F(000)	936
Description and size of crystal	colourless block, size 0.10•0.15•0.50 mm^3
Absorption coefficient	1.838 mm^{-1}
Min/max transmission	0.4601 / 0.8376
Temperature	293(2) K
Radiation (wavelength)	Mo*K*α (λ = 0.71073 Å)
Crystal system, space group	orthorhombic, P 2_1 2_1 2_1
a	6.0133(13) Å
b	15.952(4) Å
c	21.670(5) Å
α	90°
β	90°
γ	90°
V	2078.7(8) Å^3
Max Θ	25.99°
Number of collected reflections	23949
Number of independent reflections	4070 (merging r = 0.0822)
Number of observed reflections	4070 (I>2.0σ(I))
Number of refined parameters	263
R	0.0346
wR	0.0857
Goodness of fit	1.070

X-Ray parameters for **2.49**:

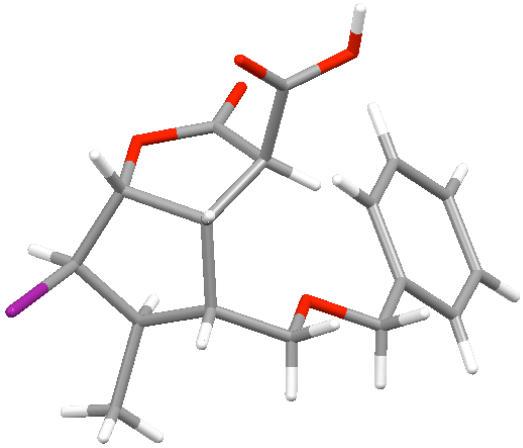

CCDC ID	**CCDC 901010**
Formula	$C_{17}H_{19}IO_5$
Formula weight	430.24
Z, calculated density	1.667 Mg•m^{-3}
F(000)	856
Description and size of crystal	colourless block, size 0.04•0.17•0.31 mm^3
Absorption coefficient	1.890 mm^{-1}
Min/max transmission	0.73 / 0.93
Temperature	123 K
Radiation (wavelength)	Mo*K*α (λ = 0.71073 Å)
Crystal system, space group	orthorhombic, P 2_1 2_1 2_1
a	7.7519(2) Å
b	9.8721(2) Å
c	22.3993(5) Å
α	90°
β	90°
γ	90°
V	1714.16(7) Å^3
Max Θ	34.503°
Number of collected reflections	53644
Number of independent reflections	7257 (merging r = 0.032)
Number of observed reflections	6374 (I>2.0σ(I))
Number of refined parameters	209
R	0.0158
wR	0.0200
Goodness of fit	1.090

X-Ray parameters for gelsemiol (**2.1**):

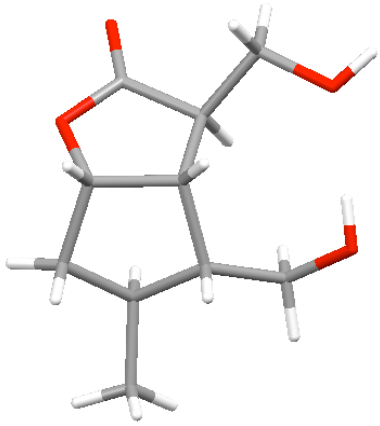

CCDC ID	**CCDC 901008**
Formula	$C_{10}H_{16}O_4$
Formula weight	200.23
Z, calculated density	1.345 Mg•m^{-3}
F(000)	432
Description and size of crystal	colorless plate, size 0.030•0.110•0.190 mm^3
Absorption coefficient	0.103 mm^{-1}
Min/max transmission	0.99 / 1.00
Temperature	123 K
Radiation (wavelength)	Mo*K*α (λ = 0.71073 Å)
Crystal system, space group	orthorhombic, P 2_1 2_1 2_1
a	5.9236(4) Å
b	7.8797(6) Å
c	21.1900(15) Å
α	90°
β	90°
γ	90°
V	989.07(12) Å^3
Max Θ	32.572°
Number of collected reflections	14382
Number of independent reflections	2078 (merging r = 0.041)
Number of observed reflections	1730 (I>2.0σ(I))
Number of refined parameters	127
R	0.0305
wR	0.0449
Goodness of fit	1.1124

X-Ray parameters for gelsemiol (**3.20h**):

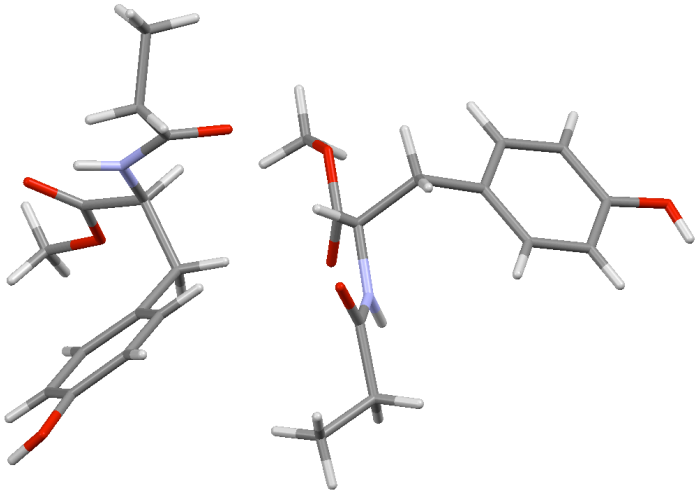

CCDC ID	**CCDC 955378**
Formula	$C_{13}H_{17}NO_4$
Formula weight	251.28
Z, calculated density	1.260 Mg•m^{-3}
F(000)	536
Description and size of crystal	colorless plate, size 0.04•0.30•0.45 mm^3
Absorption coefficient	0.094 mm^{-1}
Min/max transmission	0.95/ 1.00
Temperature	123 K
Radiation (wavelength)	Mo*K*α (λ = 0.71073 Å)
Crystal system, space group	P 2(1), Z = 4
a	9.4301(4) Å
b	14.8968(6) Å
c	10.0047(4) Å
α	90°
β	109.569(6)°
γ	90°
V	1324.26(9) Å^3
Max Θ	27.49°
Number of collected reflections	30118
Number of independent reflections	6060 (merging r = 0.0253)
Number of observed reflections	6060 (I>2.0σ(I))
Number of refined parameters	331
R	0.028
wR	0.0726
Goodness of fit	1.026

X-Ray parameters for gelsemiol (**3.20s**):

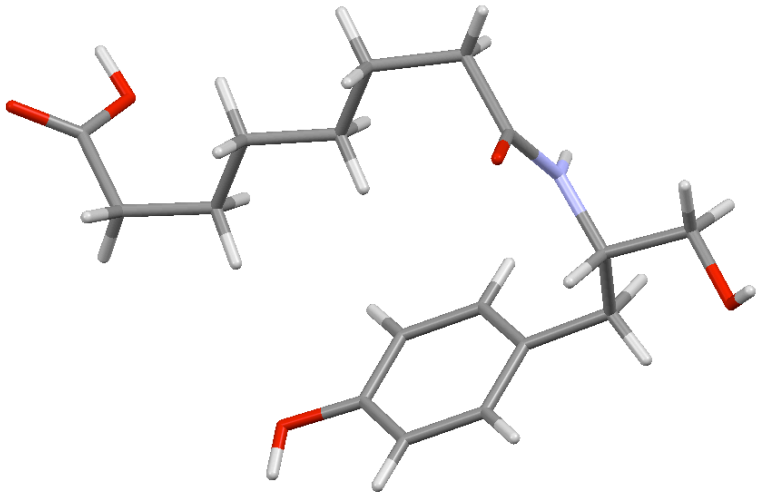

CCDC ID	**CCDC 955377**
Formula	$C_{17}H_{25}NO_5$
Formula weight	323.38
Z, calculated density	1.265 Mg•m^{-3}
F(000)	348
Description and size of crystal	colorless prismatic, size 0.10•0.24•0.30 mm^3
Absorption coefficient	0.093 mm^{-1}
Min/max transmission	0.95/ 1.00
Temperature	140 K
Radiation (wavelength)	Mo*K*α (λ = 0.71073 Å)
Crystal system, space group	P 21, Z = 2
a	5.0493(3) Å
b	16.9091(8) Å
c	10.1272 Å
α	90°
β	100.905(6)°
γ	90°
V	849.04(8) Å^3
Max Θ	26.37°
Number of collected reflections	6522
Number of independent reflections	3336 (merging r = 0.0142)
Number of observed reflections	3336 (I>2.0σ(I))
Number of refined parameters	308
R	0.026
wR	0.0616
Goodness of fit	1.038

7.2 NMR Spectra

Gelsemiol (2.1)

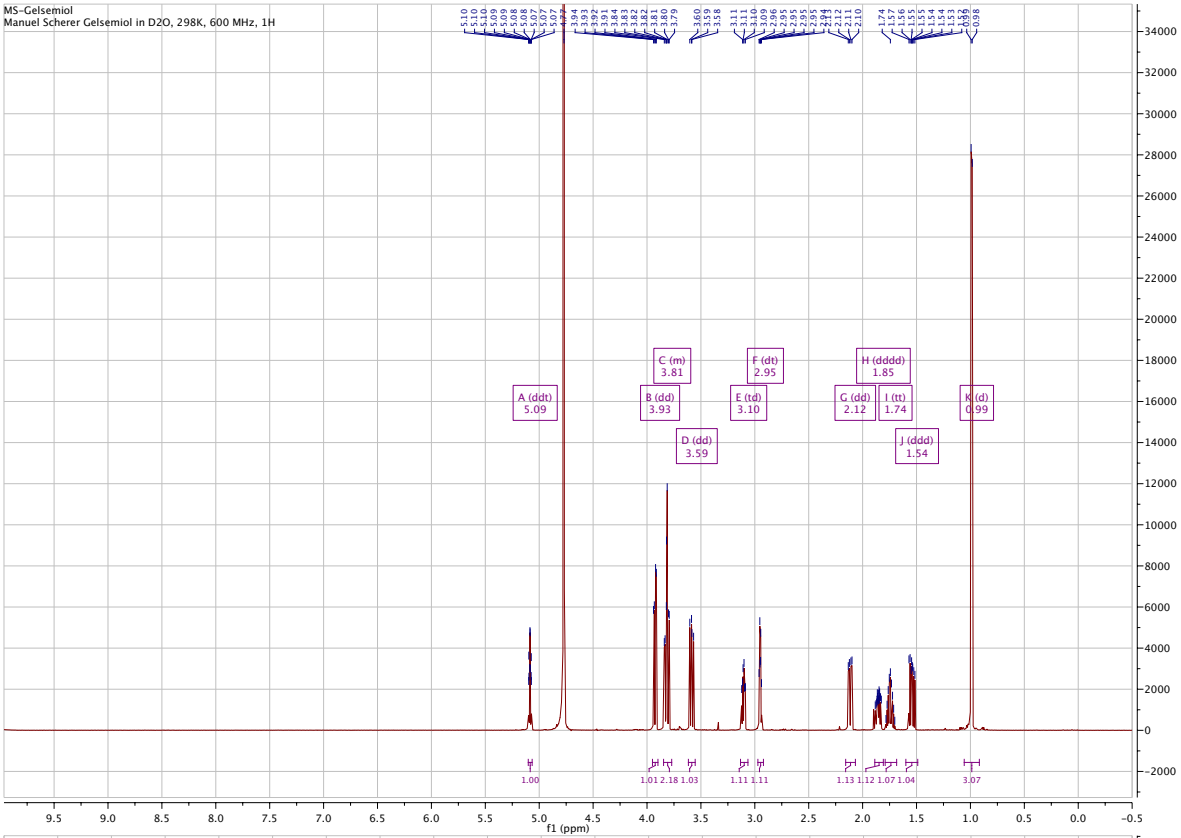

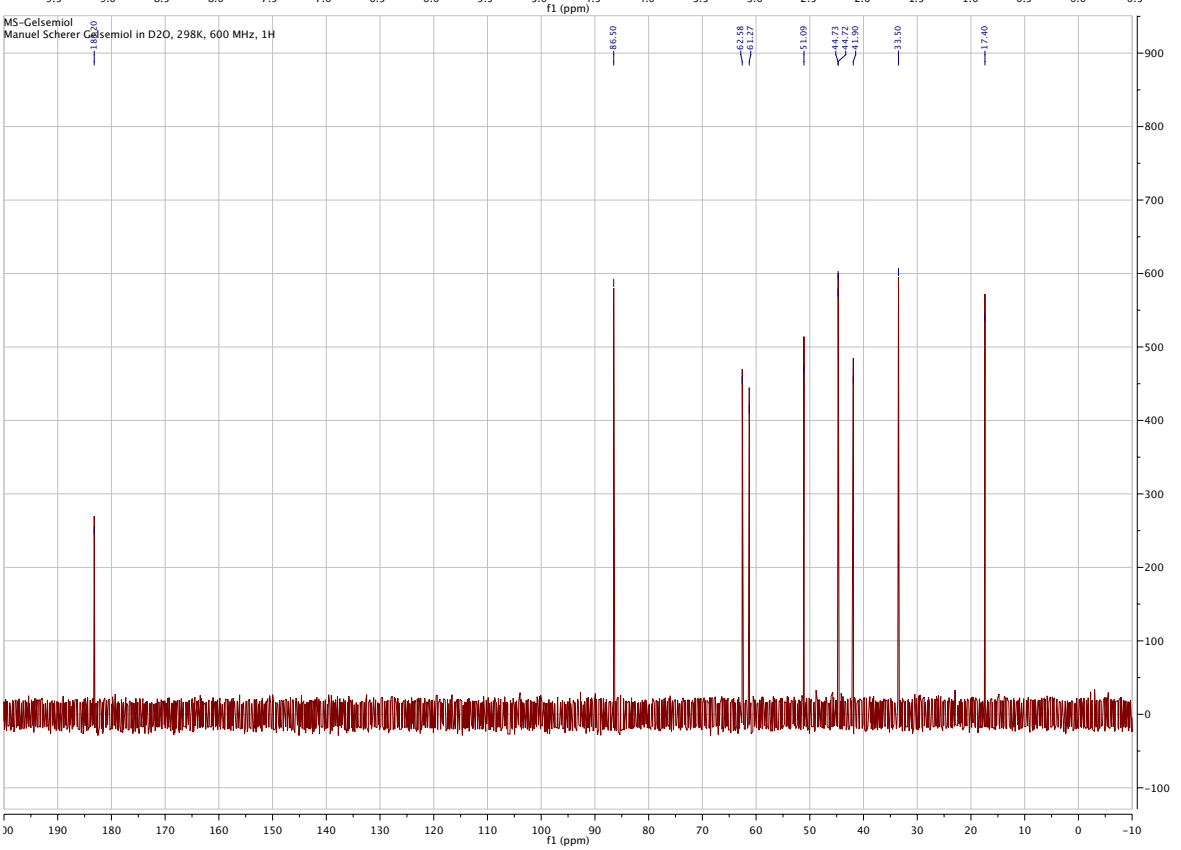

Gelsemiol (2.1) HMQC

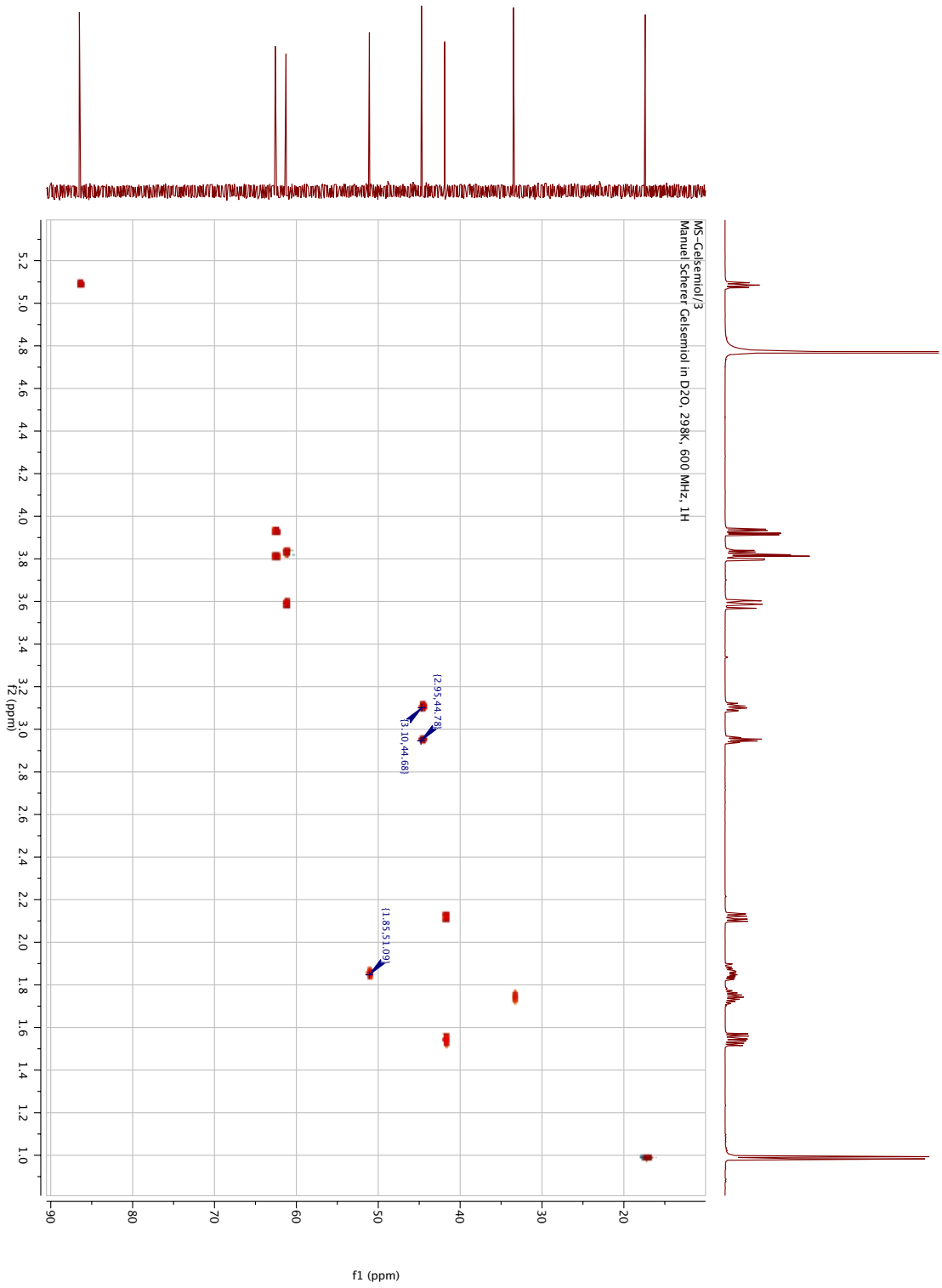

(3*S* or 3*R*, 3a*S*,4*R*,6a*S*)-methyl 4-((benzyloxy)methyl)-2-oxo-3,3a,4,6a-tetrahydro-2*H*-cyclopenta[*b*]furan-3-carboxylate (2.39a/b)

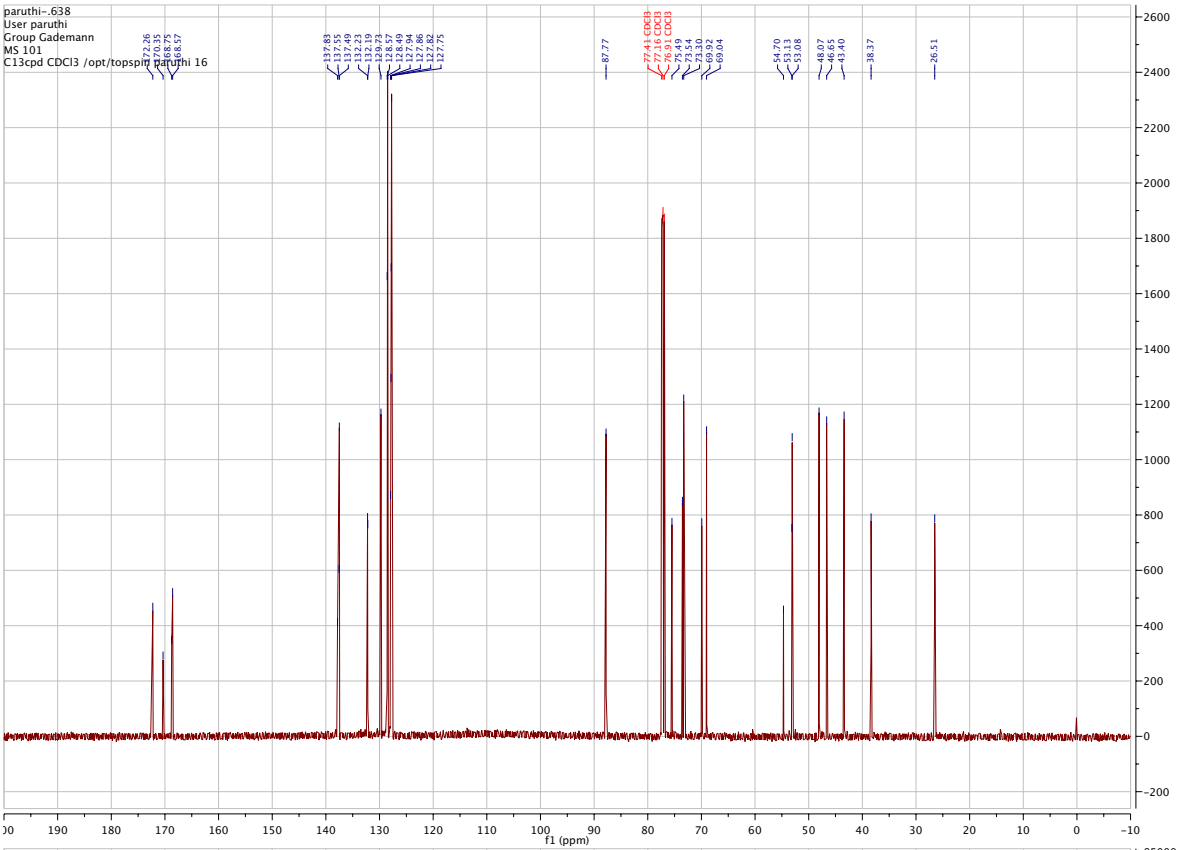

(*E*)-(3-(benzyloxy)prop-1-en-1-yl)(phenyl)selane (2.41)

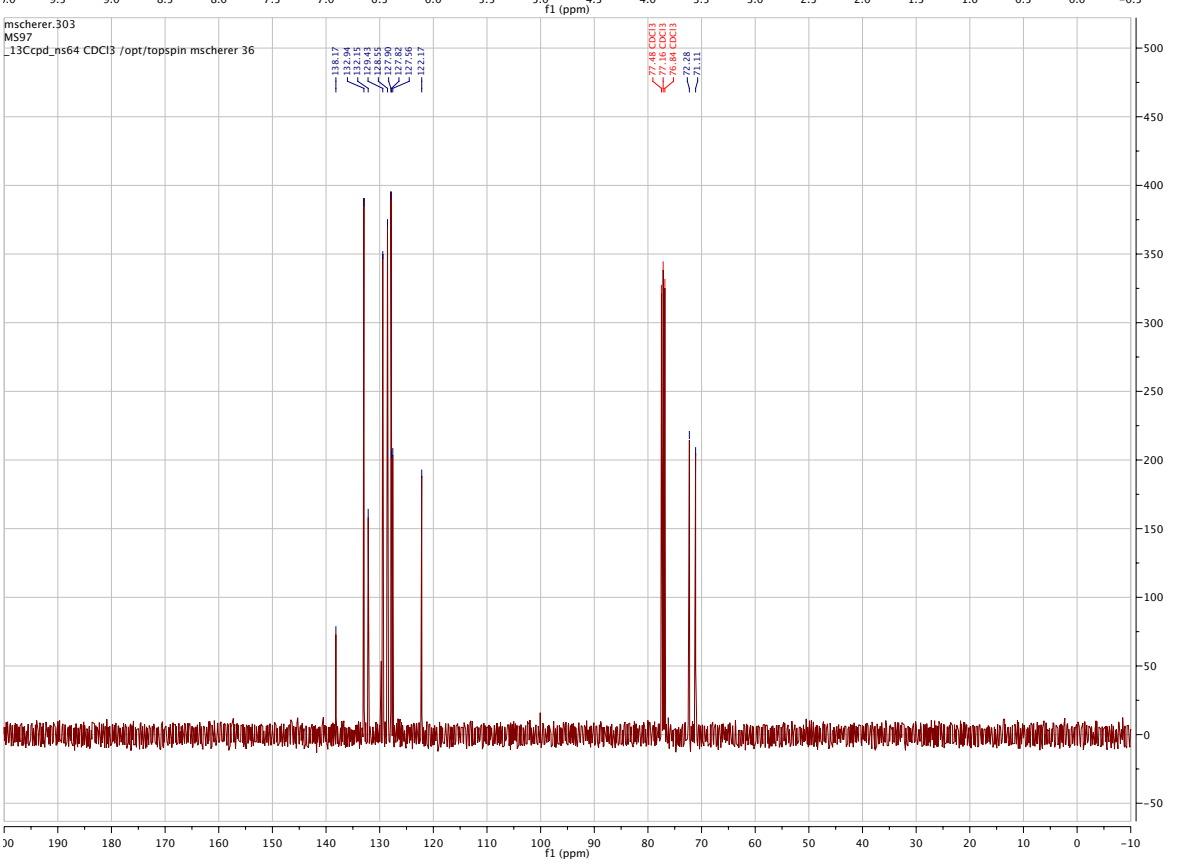

Selane 2.44

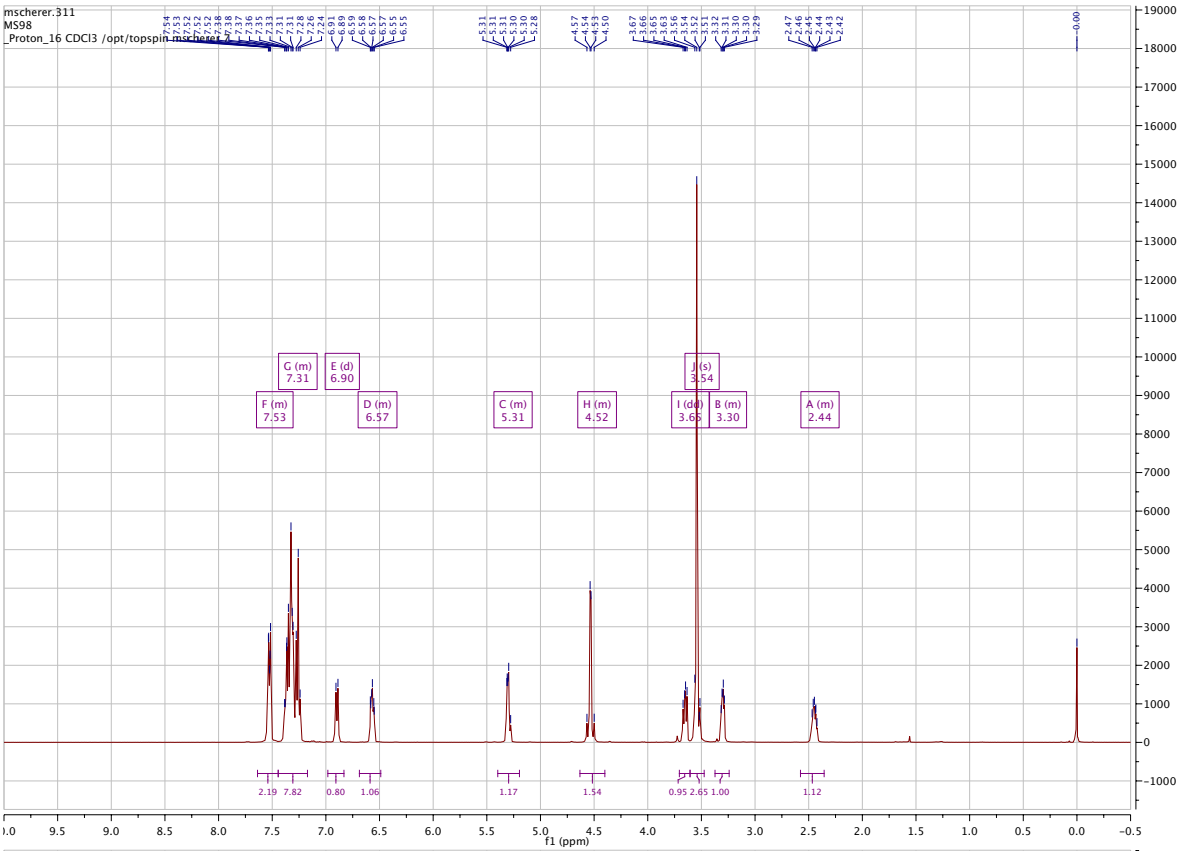
mscherer.311
MS98
_Proton_16 CDCl3 /opt/topspin mscherer 7
G (m) 7.31
E (d) 6.90
J (s) 3.54
F (m) 7.53
D (m) 6.57
C (m) 5.31
H (m) 4.52
I (dd) 3.65
B (m) 3.30
A (m) 2.44
2.19 7.82 0.80 1.06 1.17 1.54 0.95 2.65 1.00 1.12
f1 (ppm)

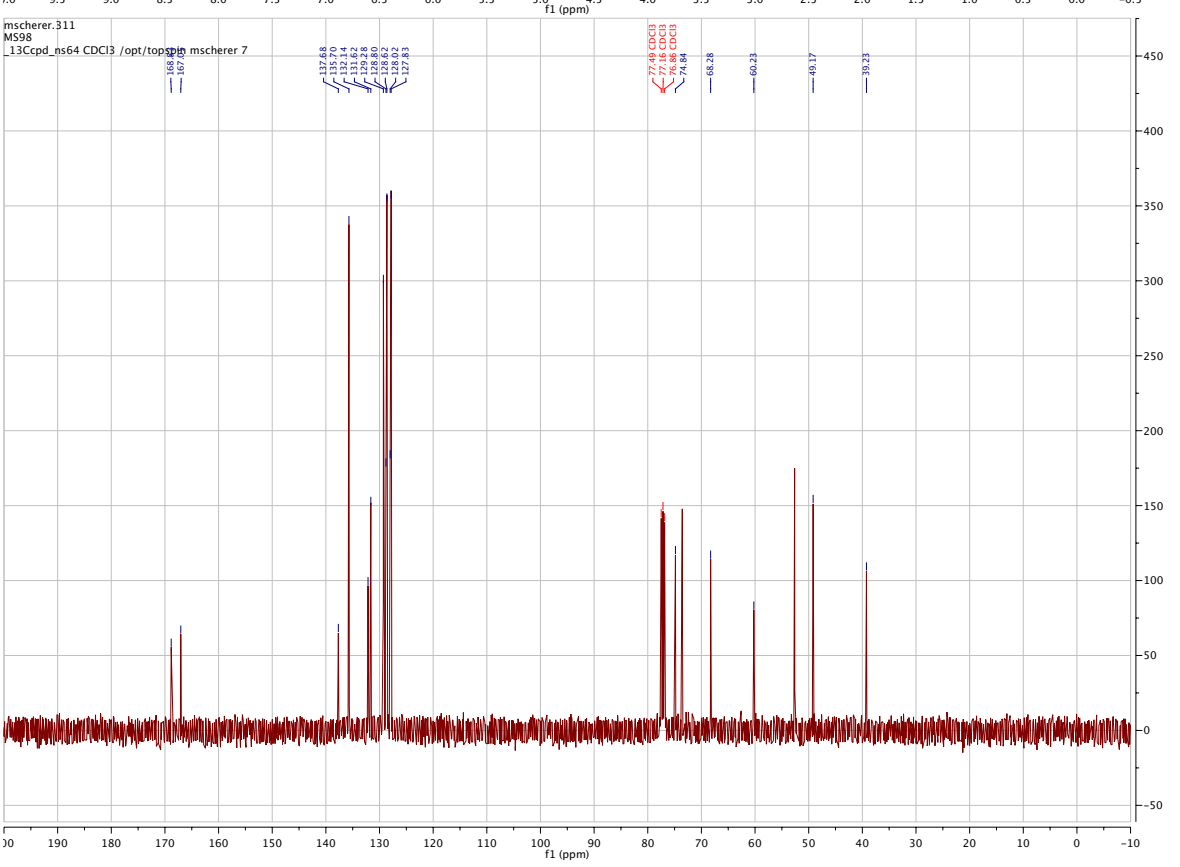
mscherer.311
MS98
_13Ccpd_ns64 CDCl3 /opt/topspin mscherer 7
168.47
167.79
137.68
135.70
132.14
131.62
129.28
129.00
128.62
128.02
127.83
77.49 CDCl3
77.16 CDCl3
76.84 CDCl3
68.28
60.23
49.17
39.23
f1 (ppm)

(3*R*,3a*S*,4*S*,5*R*,6*R*,6a*R*)-4-((benzyloxy)methyl)-6-iodo-5-methyl-2-oxohexahydro-2*H*-cyclopenta[*b*]furan-3-carboxylic acid (2.49)

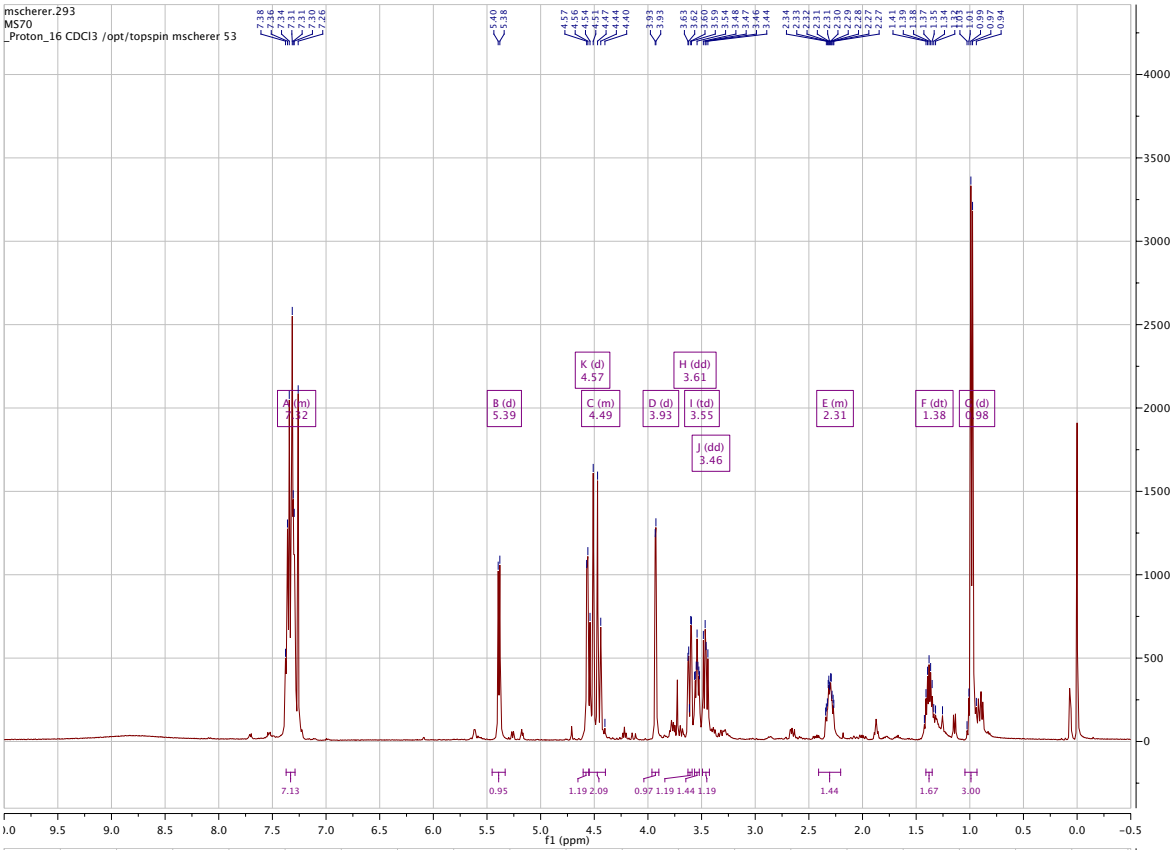

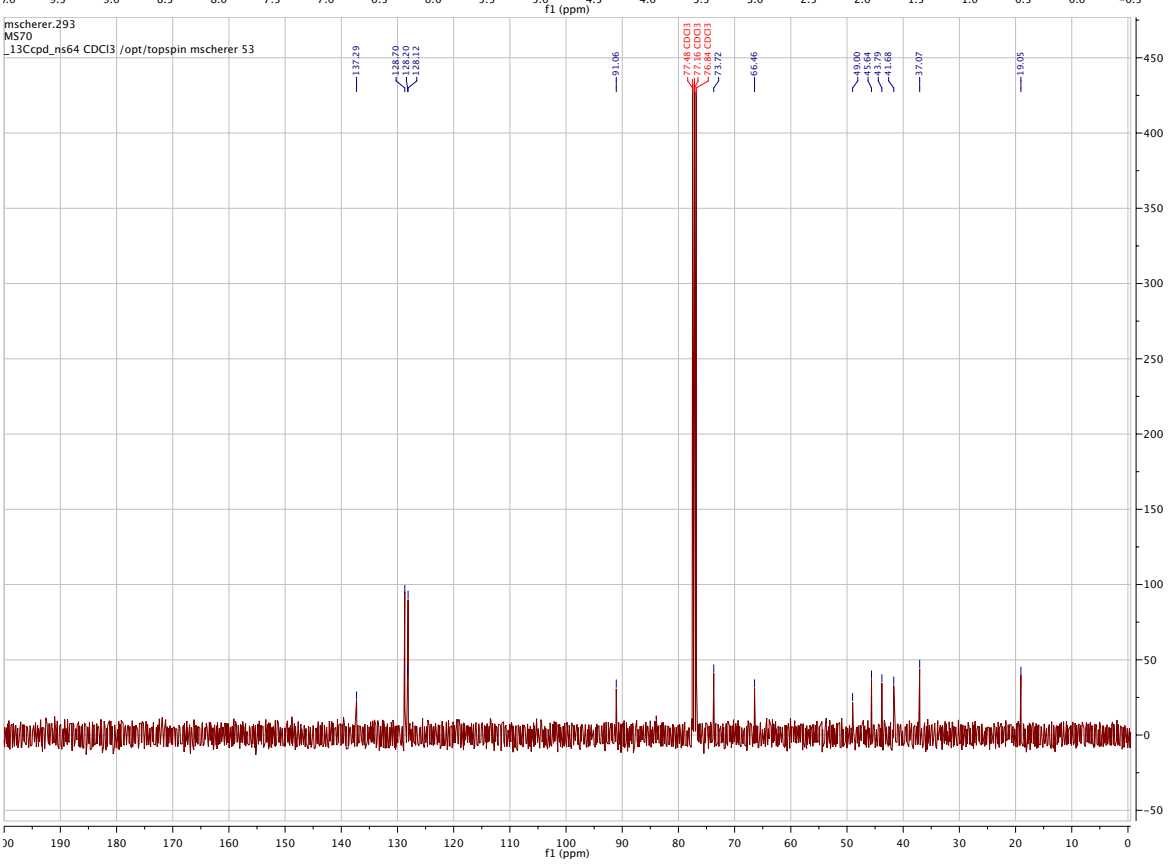

Gelsemiol lactol 2.50

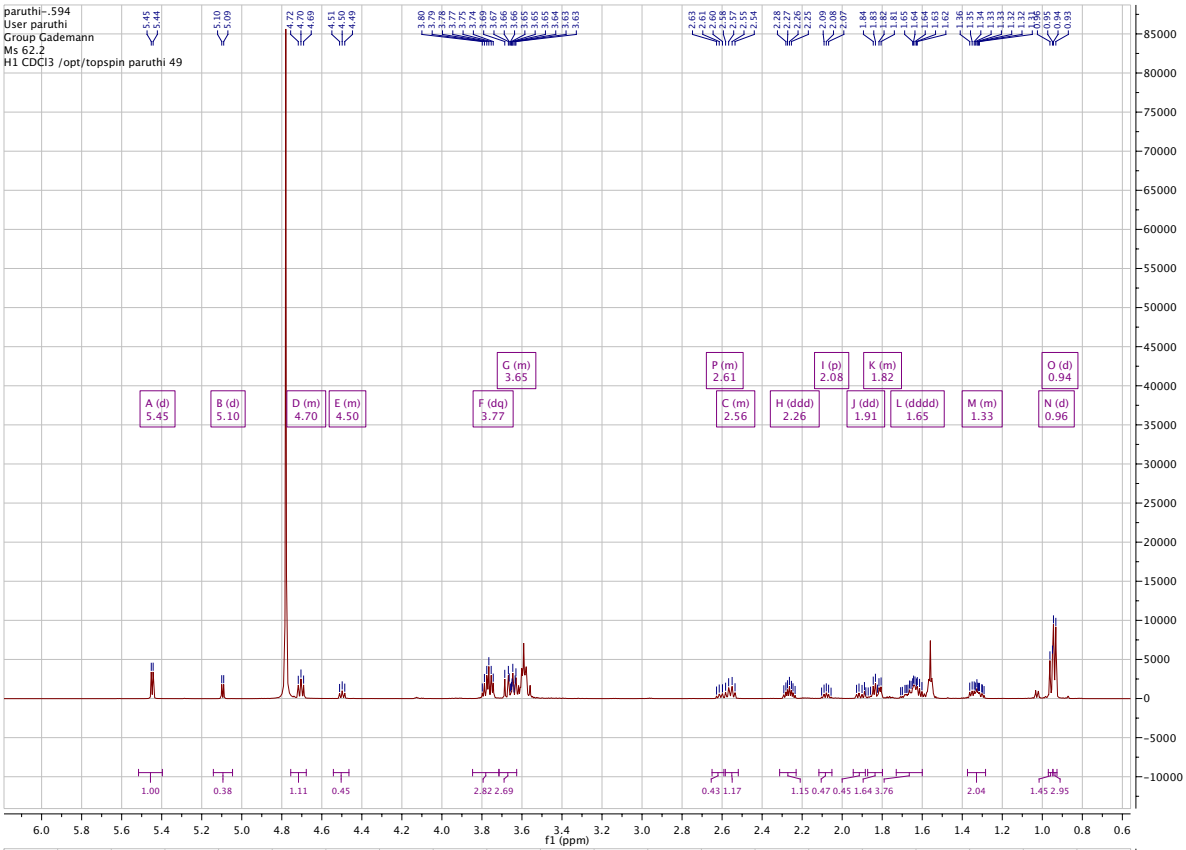

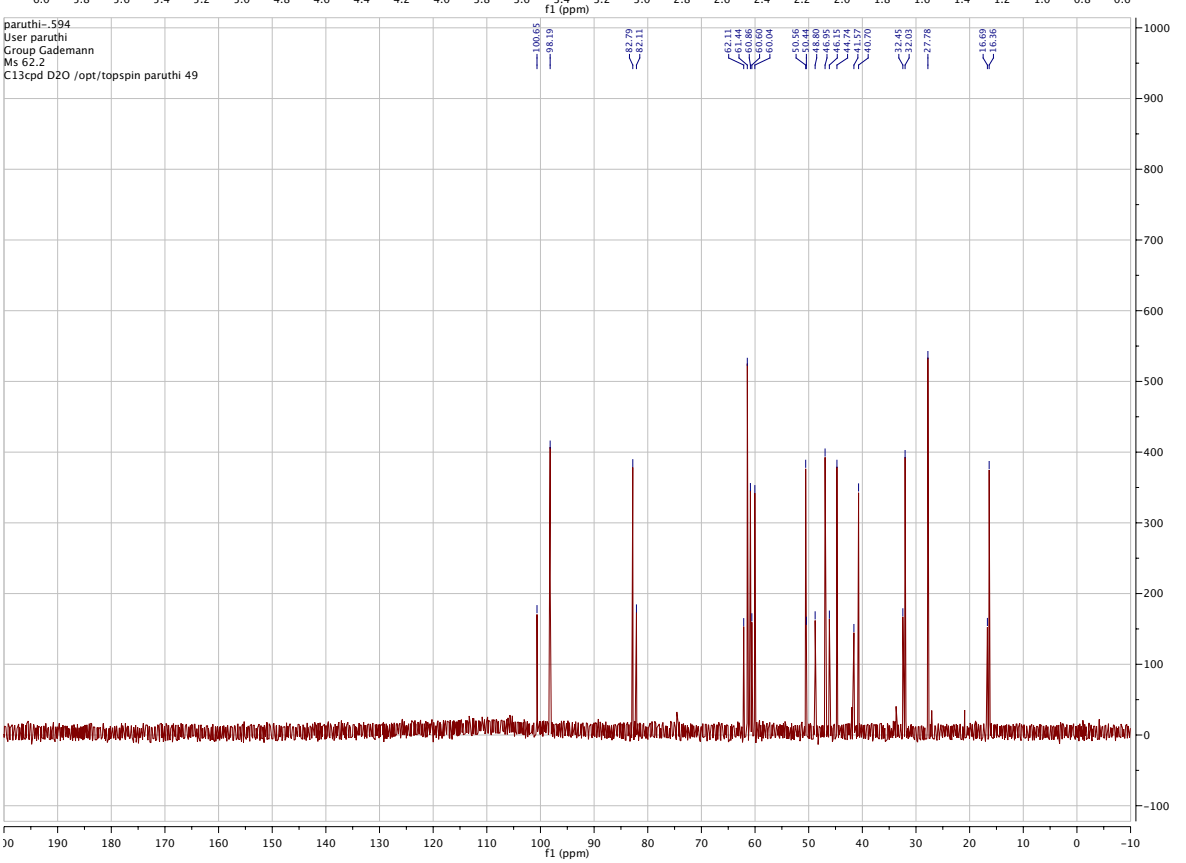

(3*R*,3*S*,4*S*,5*R*,6*R*,6*R*)-4-((benzyloxy)methyl)-3-(hydroxymethyl)-6-iodo-5-methylhexa-hydro-2*H*-cyclopenta[*b*]furan-2-one (2.51)

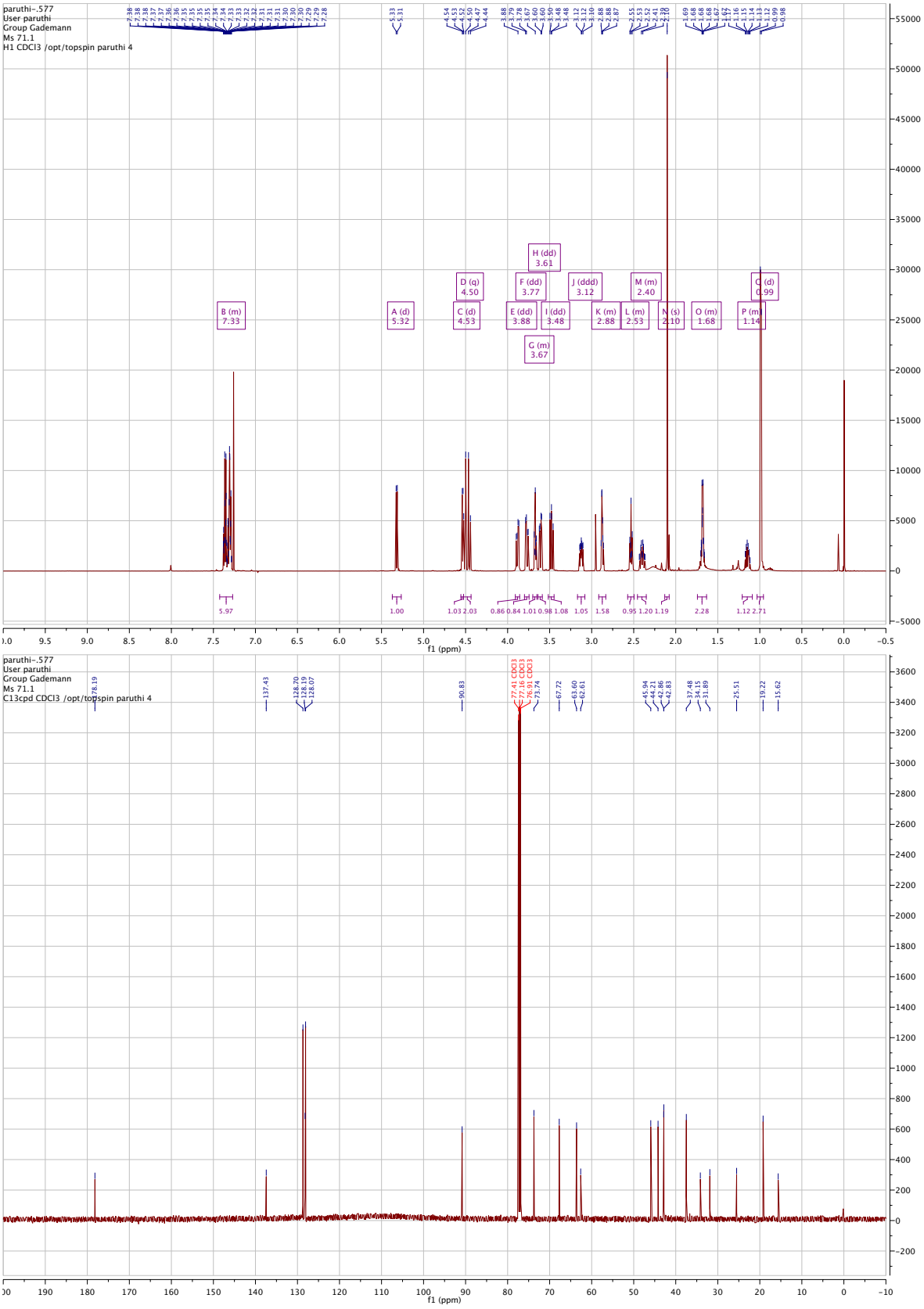

Gelsemiol acetylated (2.52)

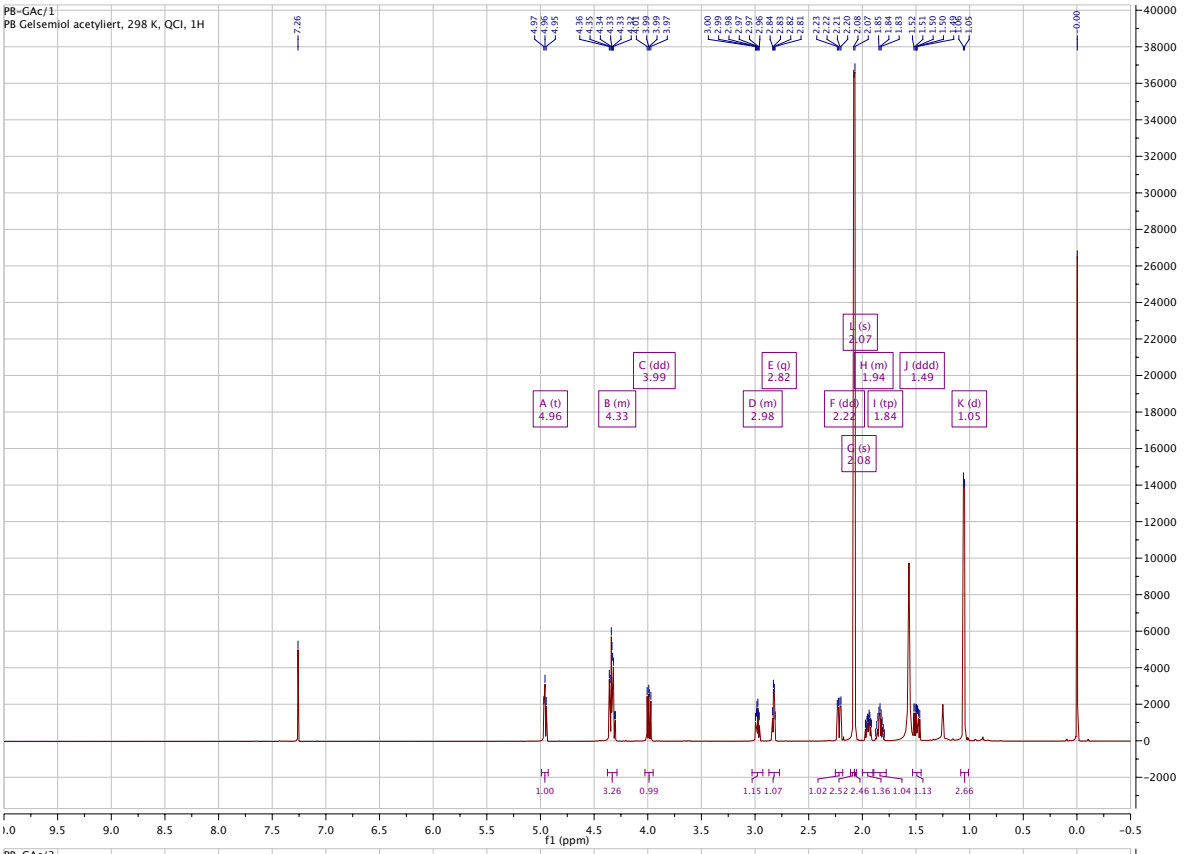

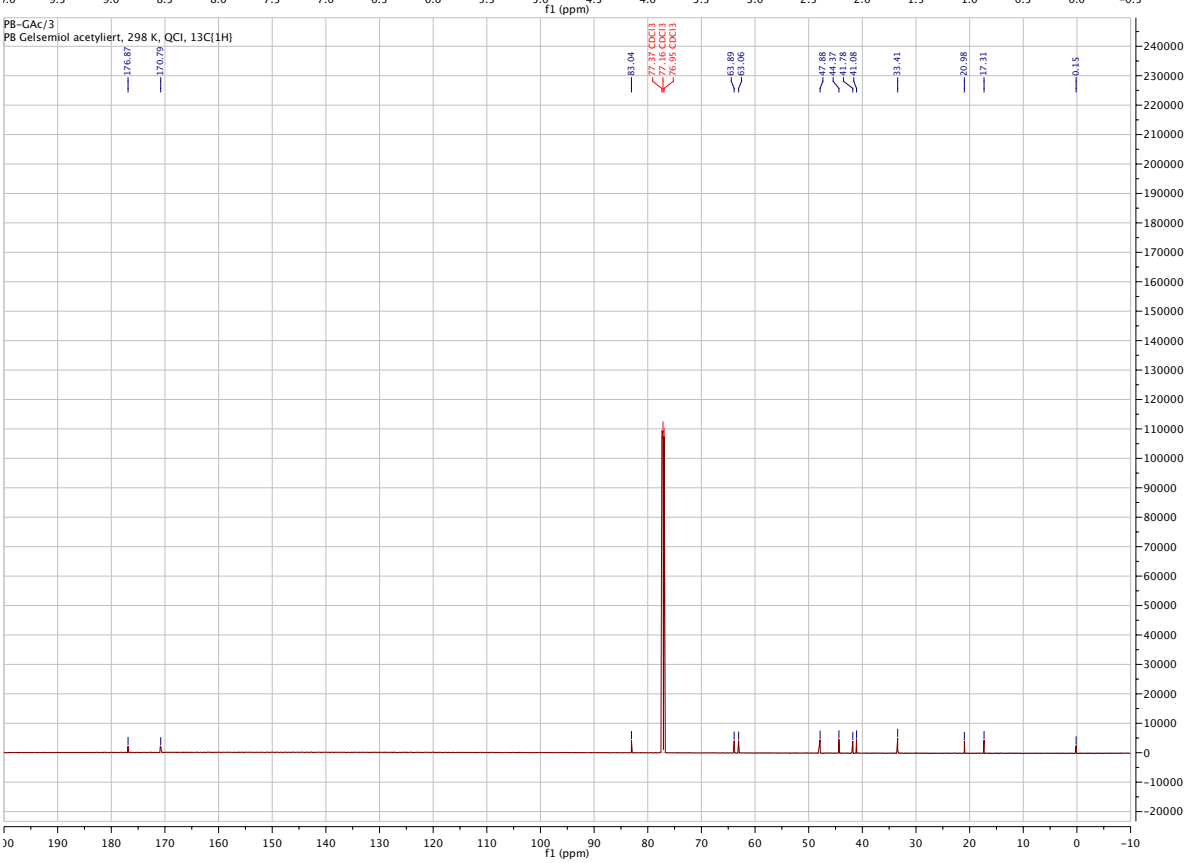

(*S*)-*N*-(1-hydroxy-3-(4-hydroxyphenyl)propan-2-yl)propionamide (3.5)

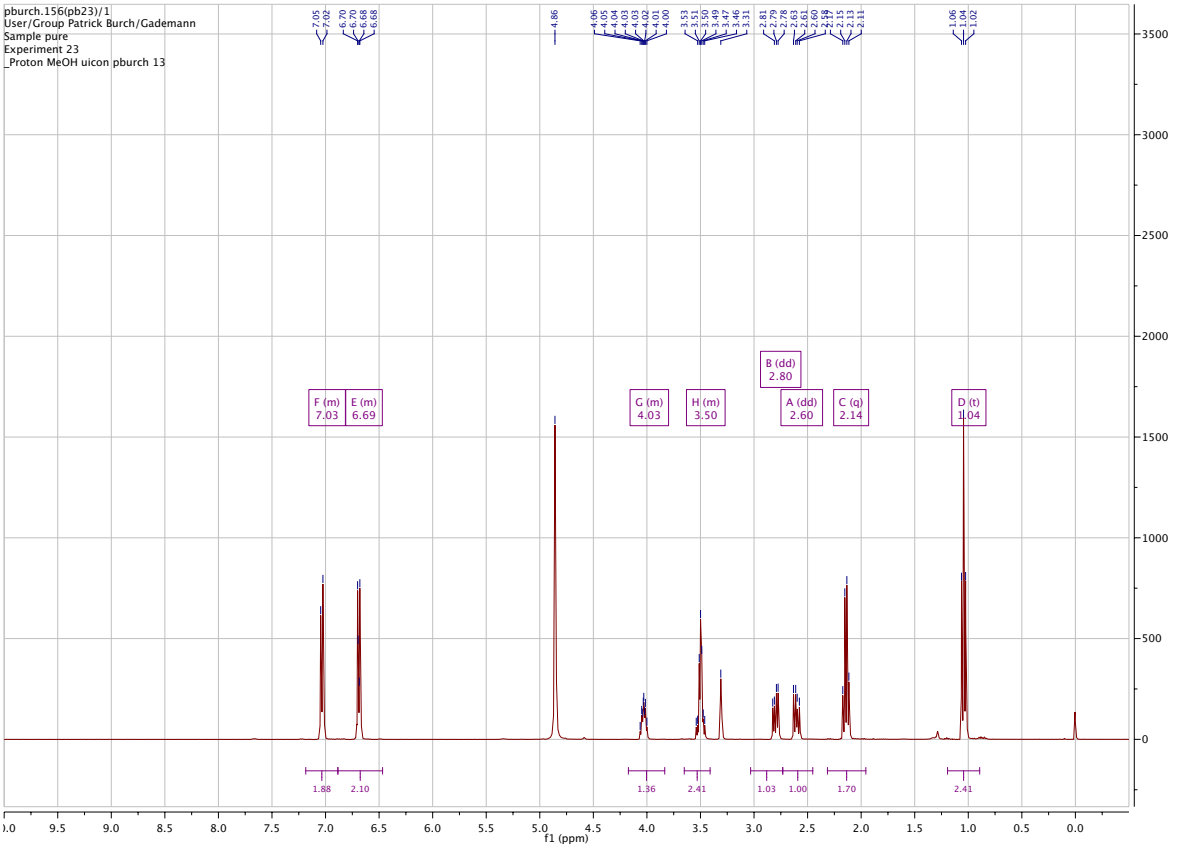

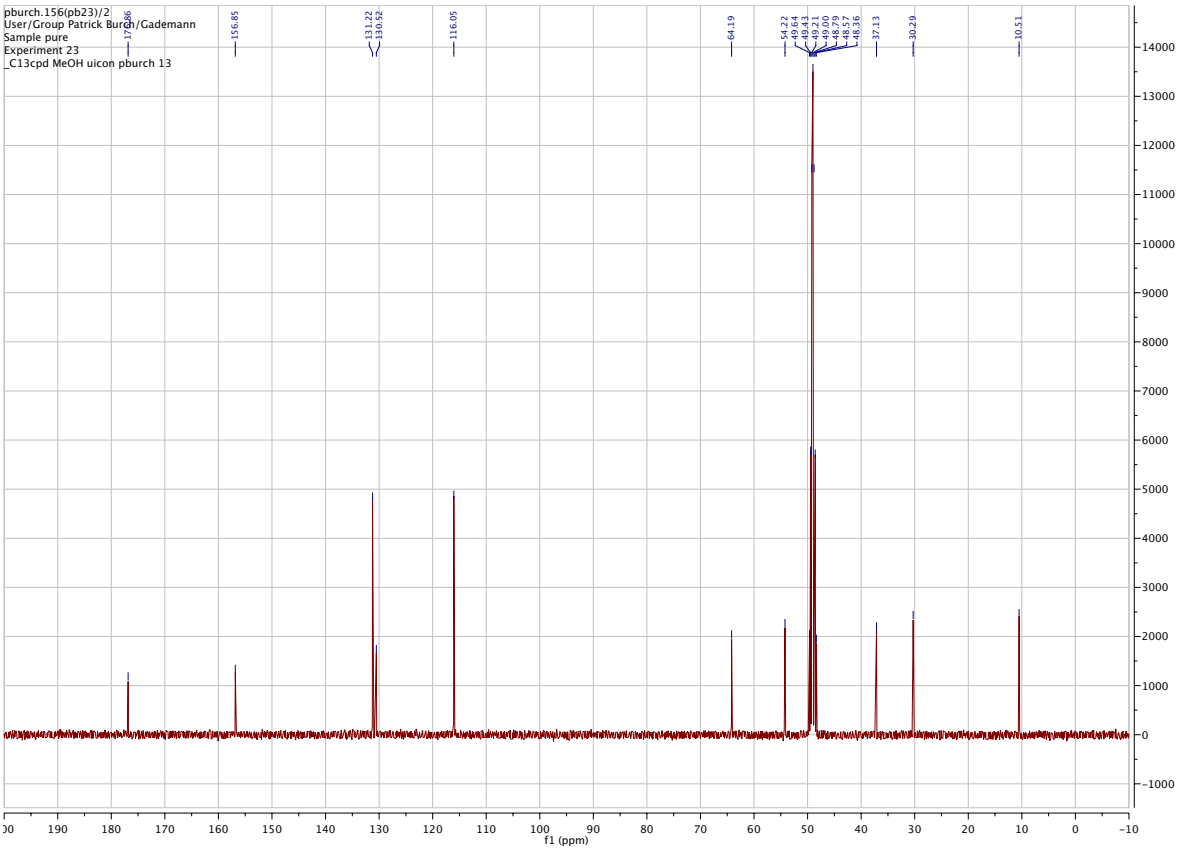

(*S*)-*N*-(1-hydroxy-3-phenylpropan-2-yl)propionamide (3.20a)

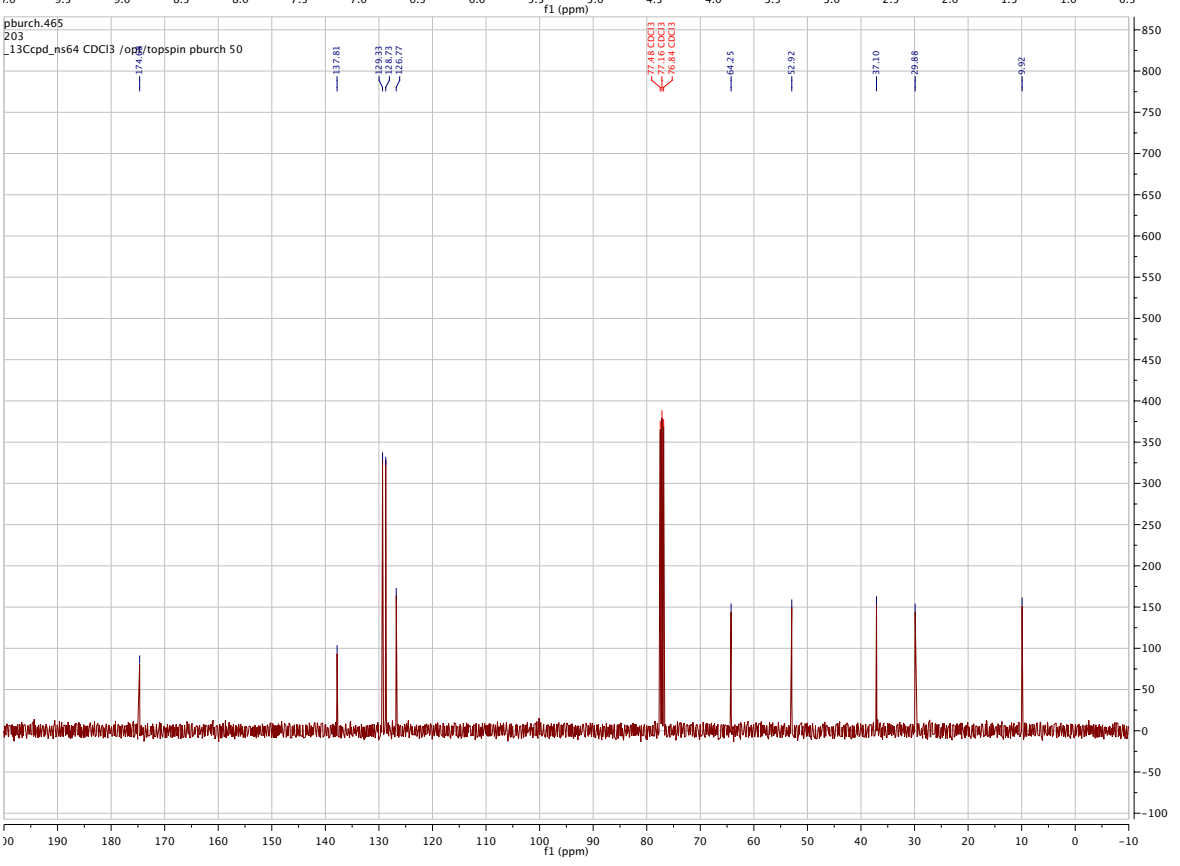

(*S*)-*N*-(1-hydroxy-3-(4-methoxyphenyl)propan-2-yl)propionamide (3.20b)

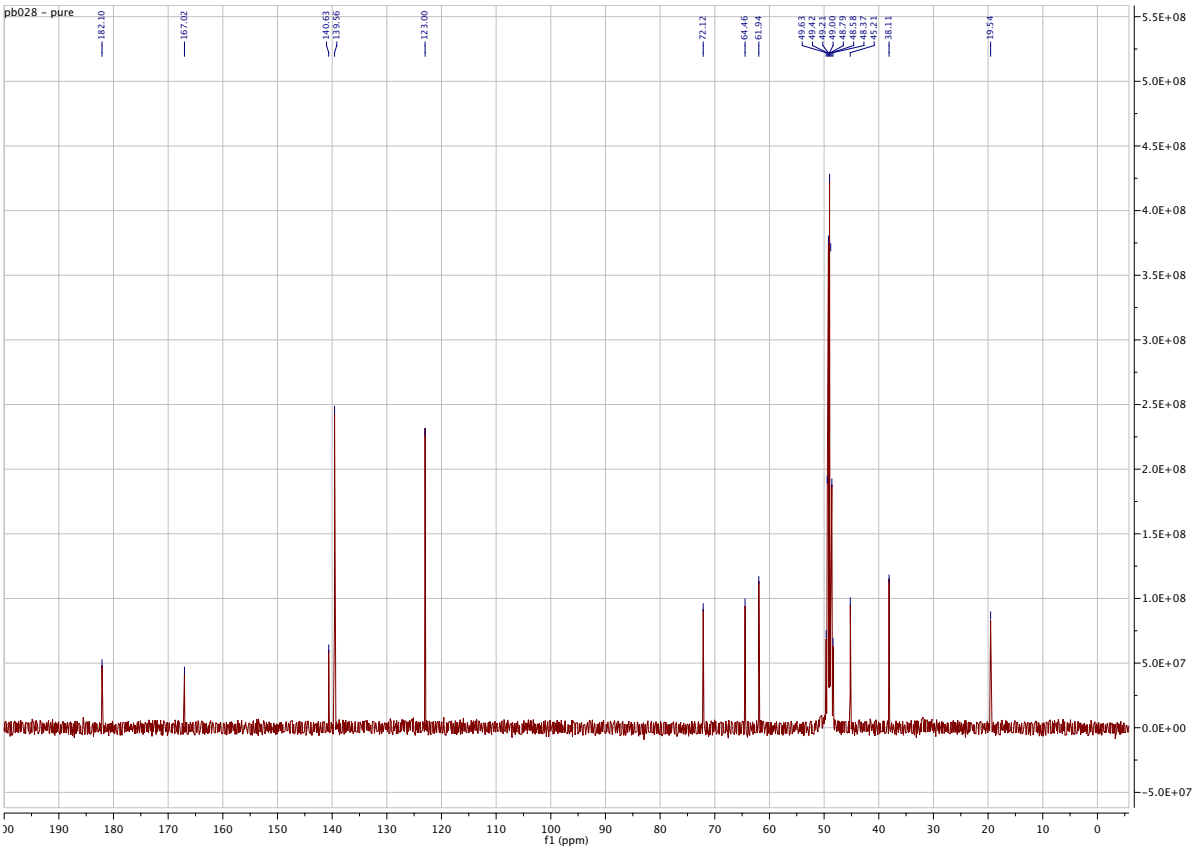

(*S*)-4-(3-hydroxy-2-propionamidopropyl)phenyl propionate (3.20c)

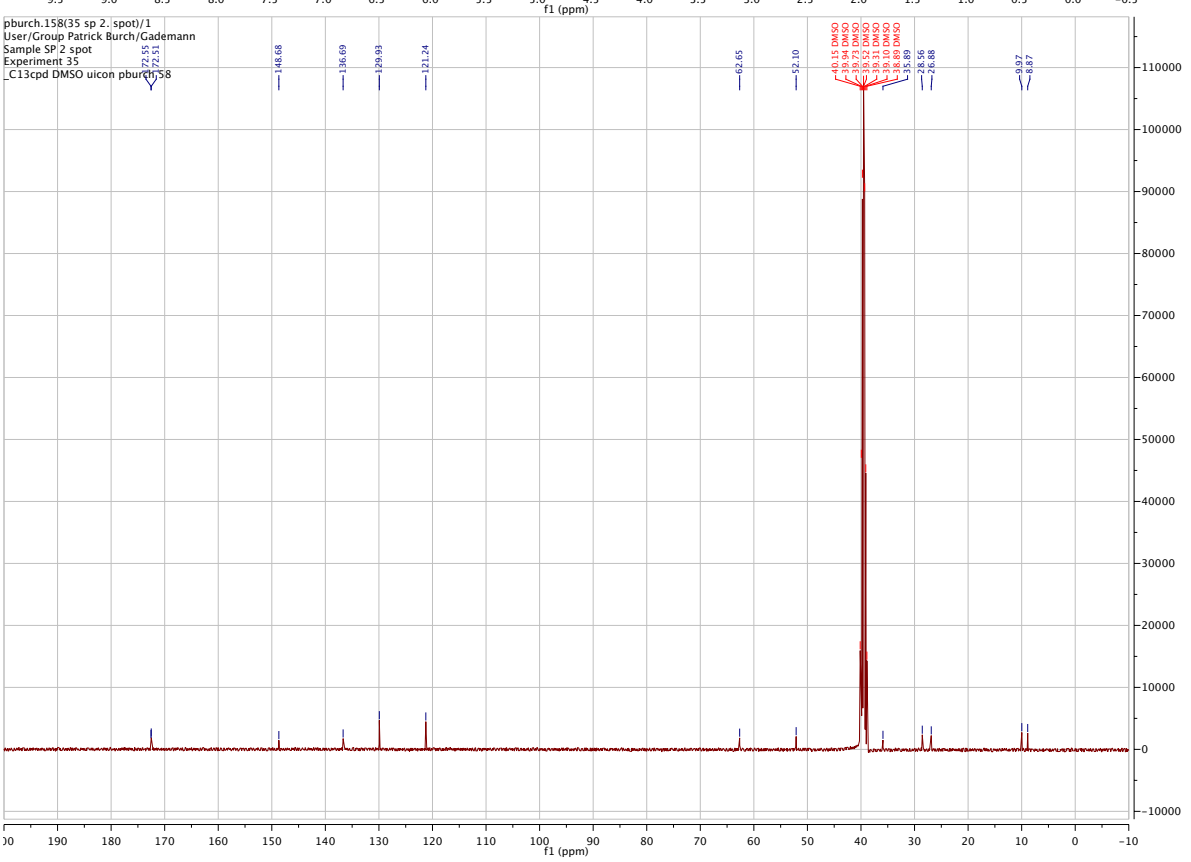

(*S*)-*N*-(1-(4-((*tert*-butyldimethylsilyl)oxy)phenyl)-3-hydroxypropan-2-yl)propionamide (I)

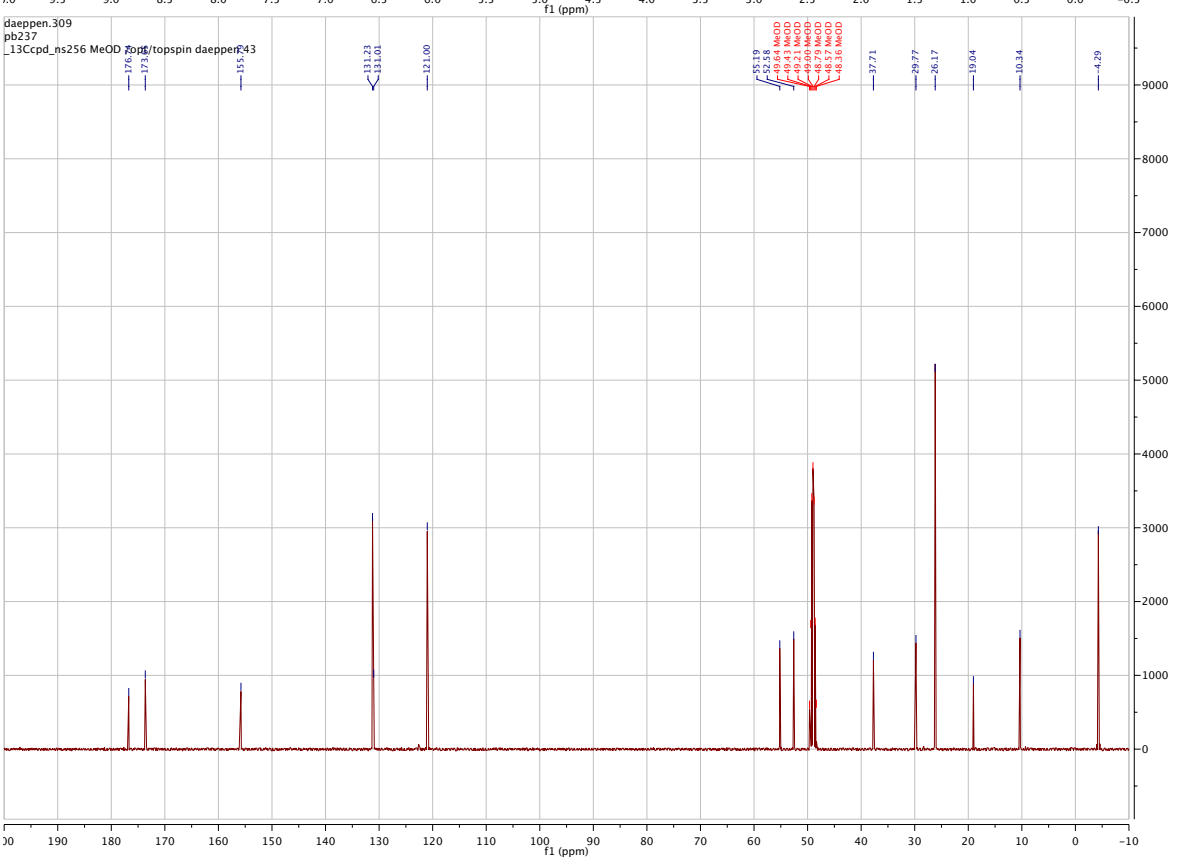

(S)-methyl 3-(4-((*tert*-butyldimethylsilyl)oxy)phenyl)-2-propionamidopropanoate (II)

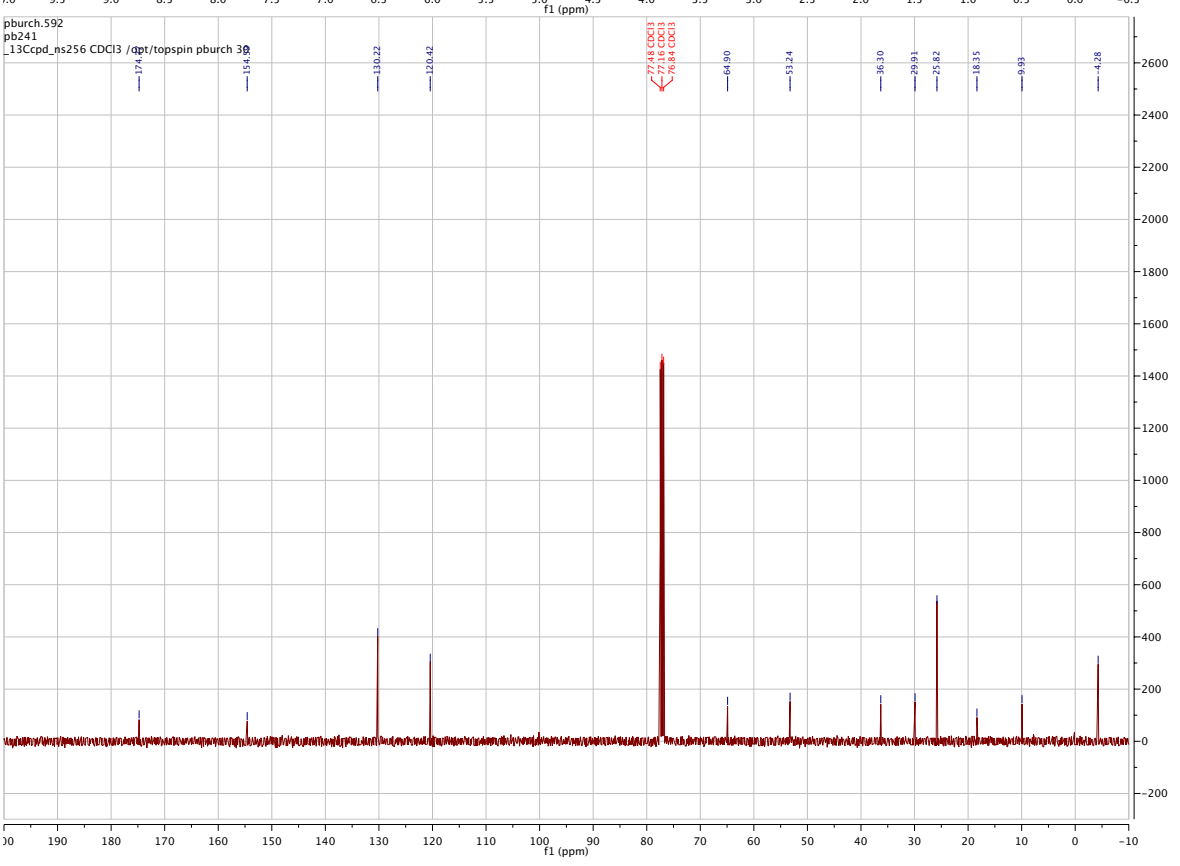

(*S*)-*N*-(1-(4-hydroxyphenyl)-3-methoxypropan-2-yl)propionamide (3.20d)

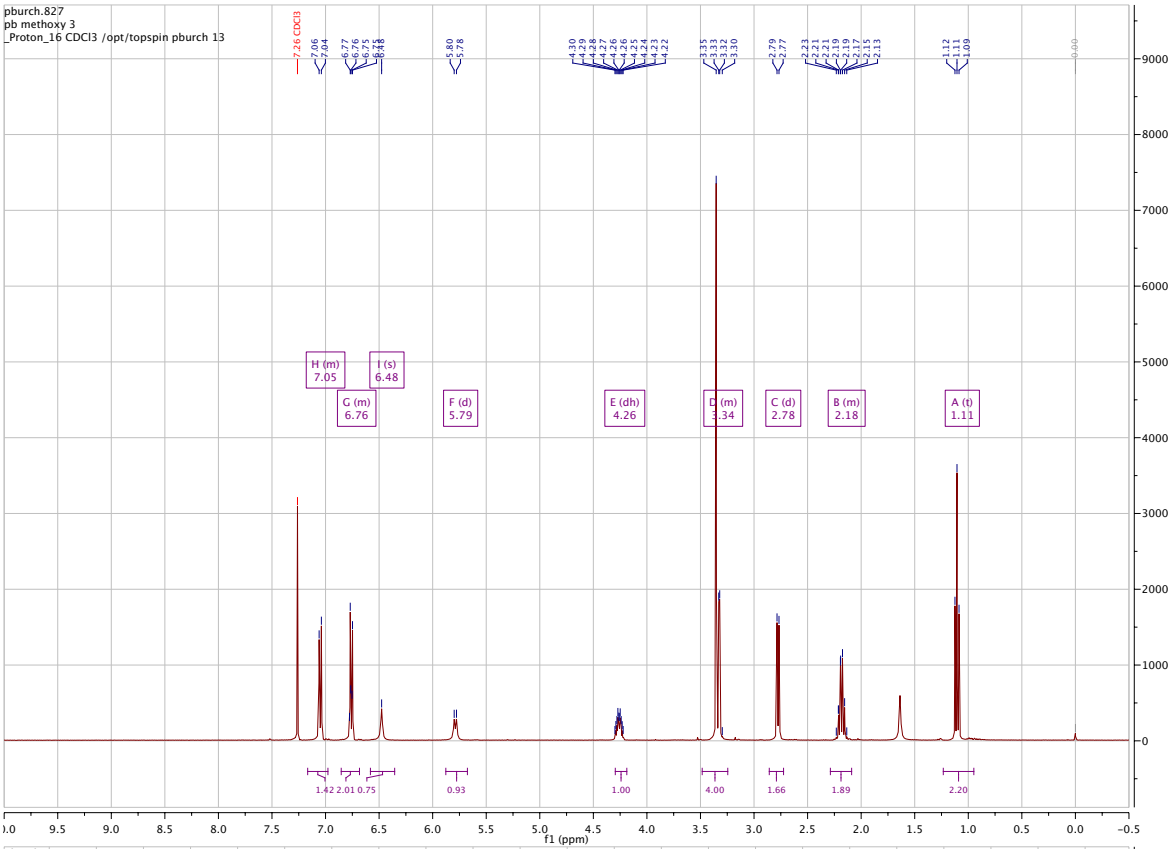

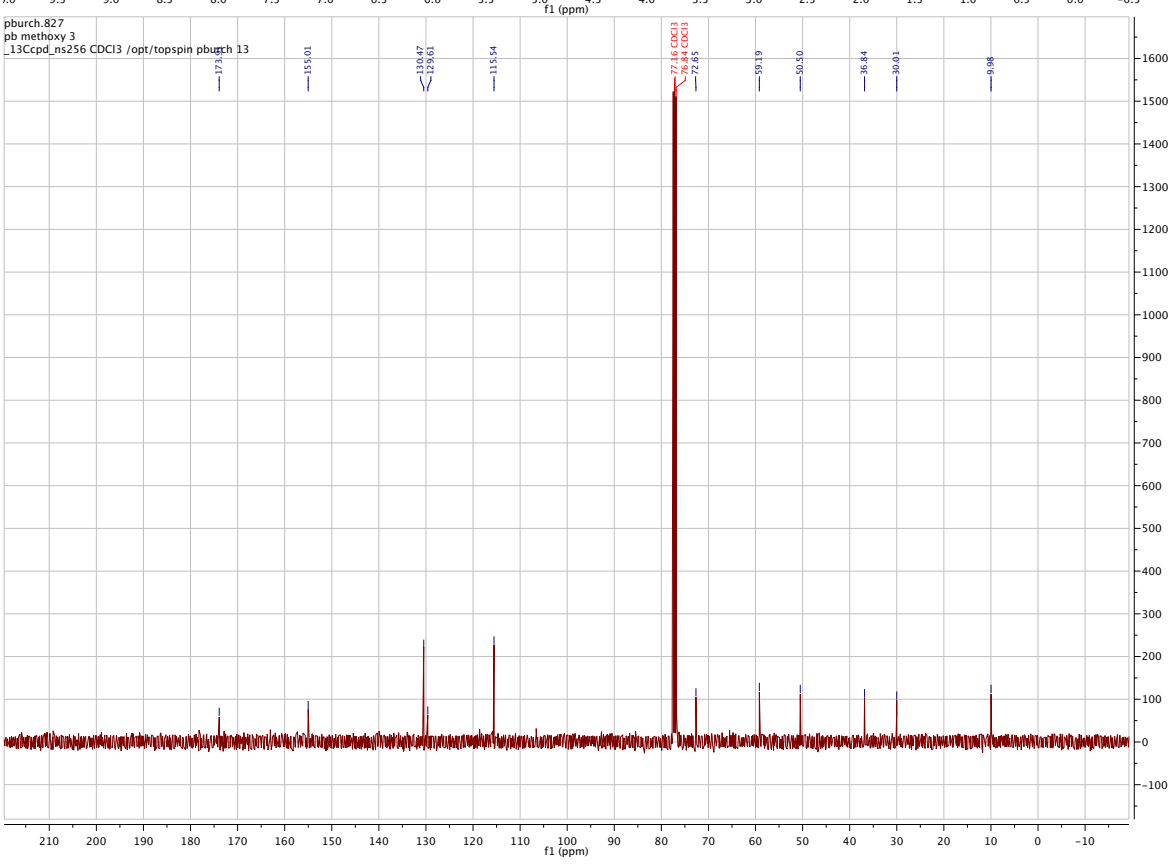

(*S*)-3-(4-hydroxyphenyl)-2-propionamidopropyl propionate (3.20e)

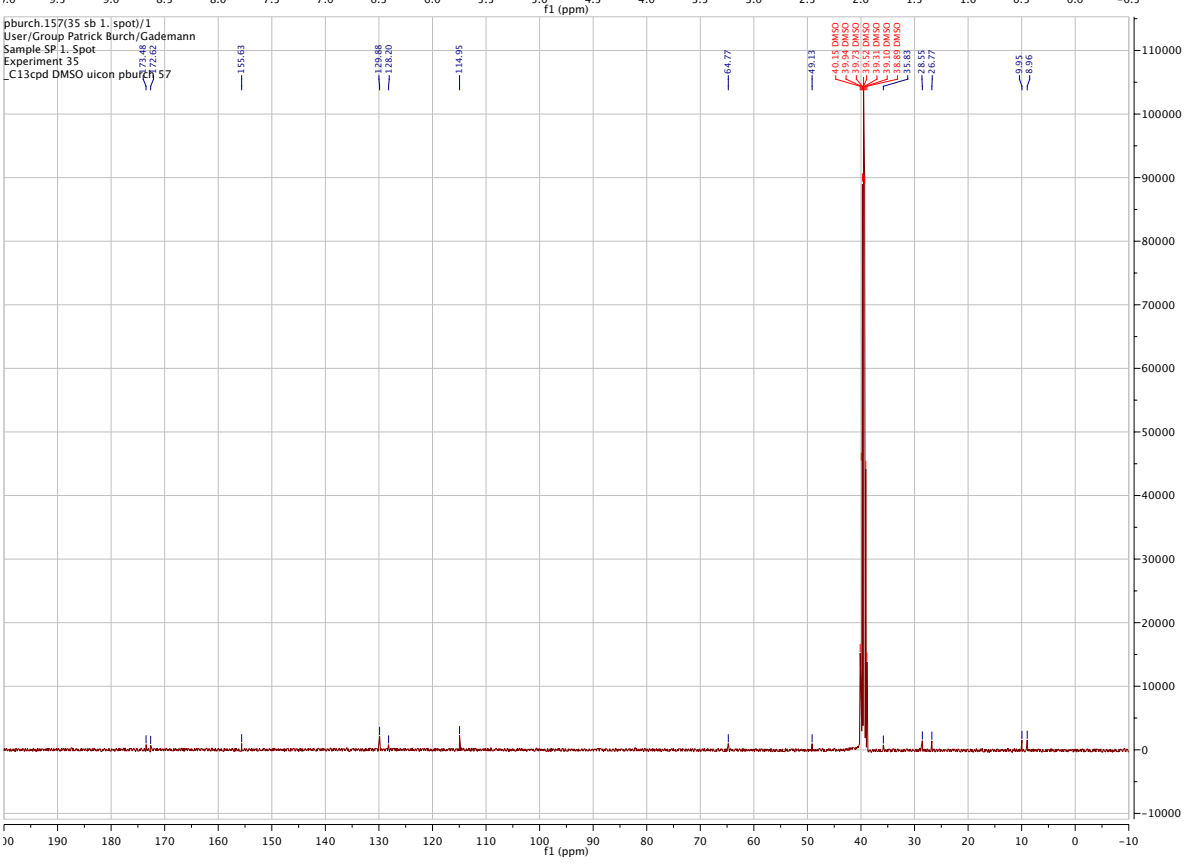

(*S*)-*N*-(1-methoxy-3-(4-methoxyphenyl)propan-2-yl)propionamide (3.20g)

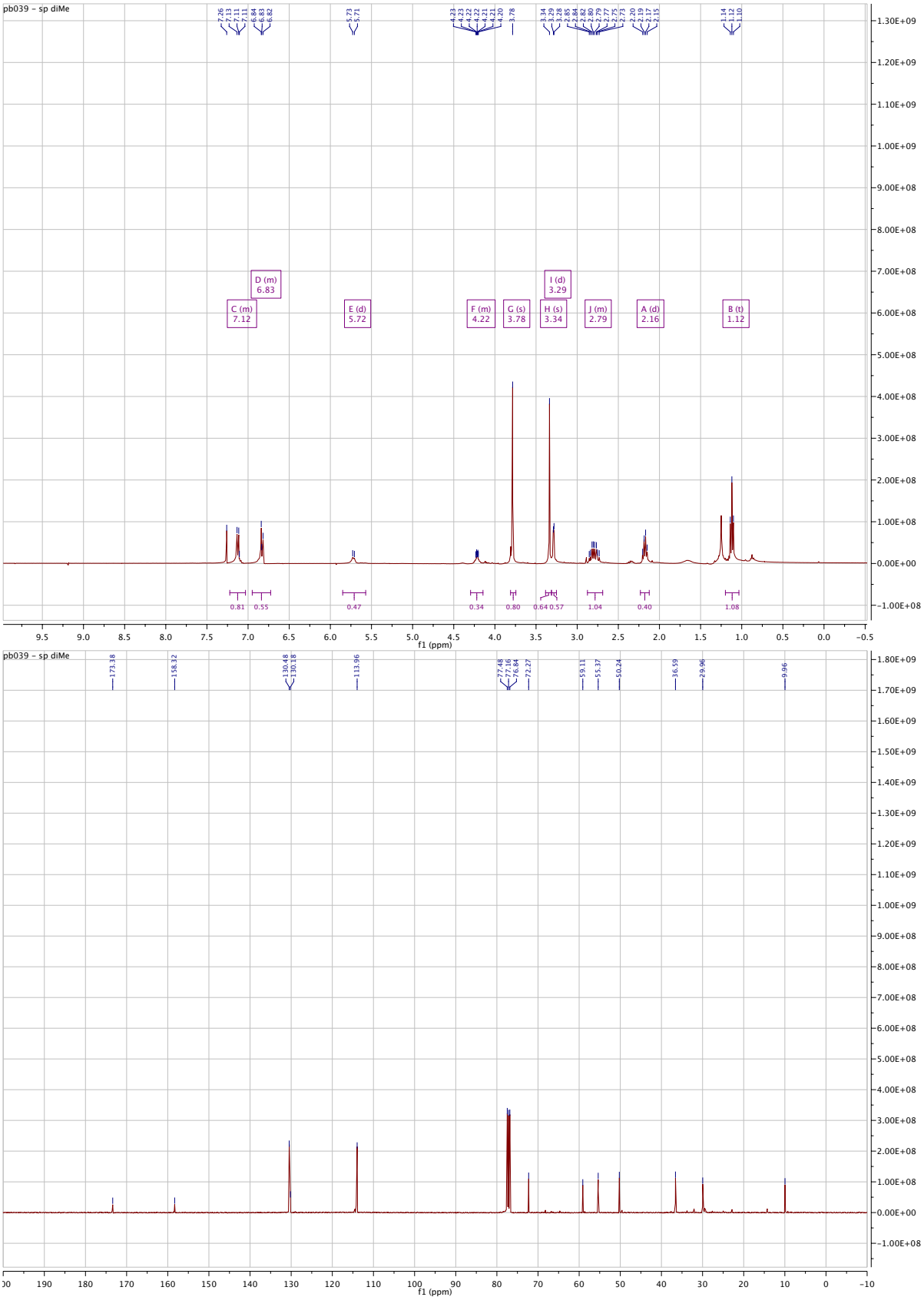

(*S*)-3-(4-hydroxyphenyl)-2-propionamidopropanoic acid (3.20h)

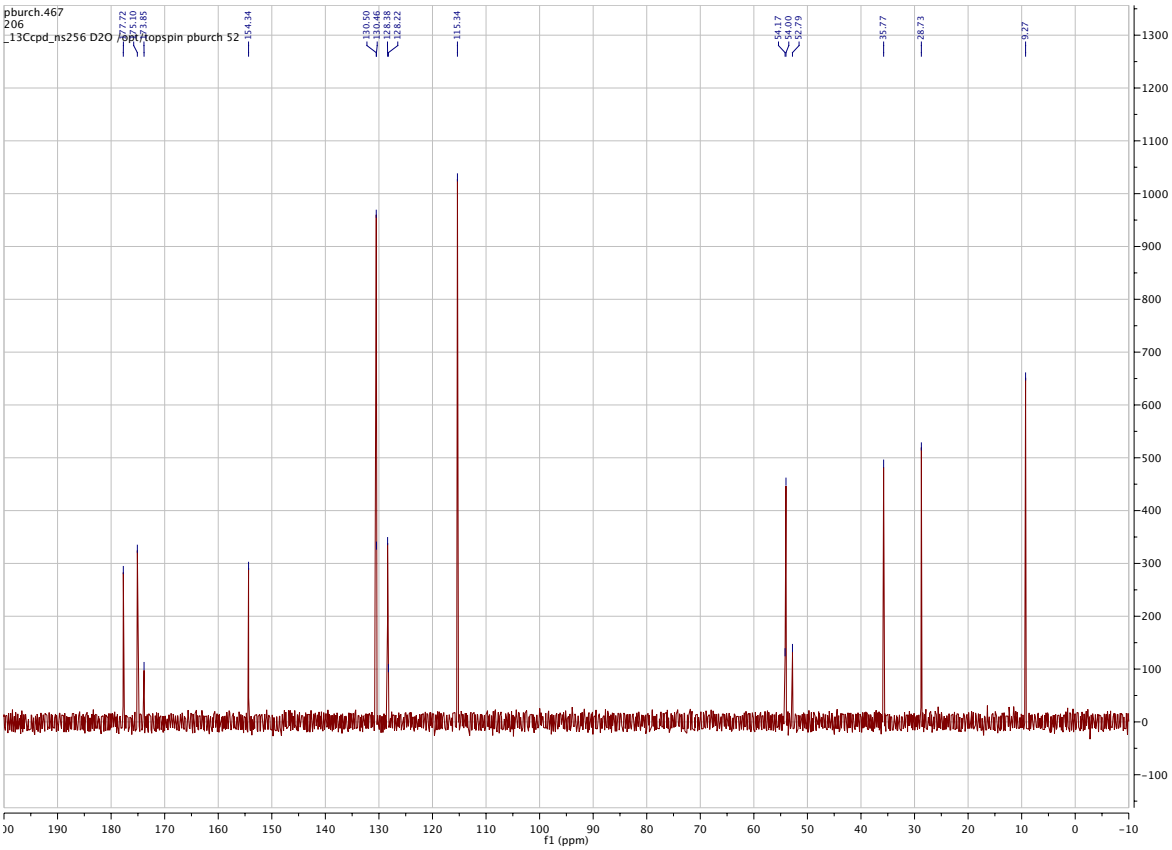

(*S*)-methyl 3-(4-hydroxyphenyl)-2-propionamidopropanoate (3.20h)

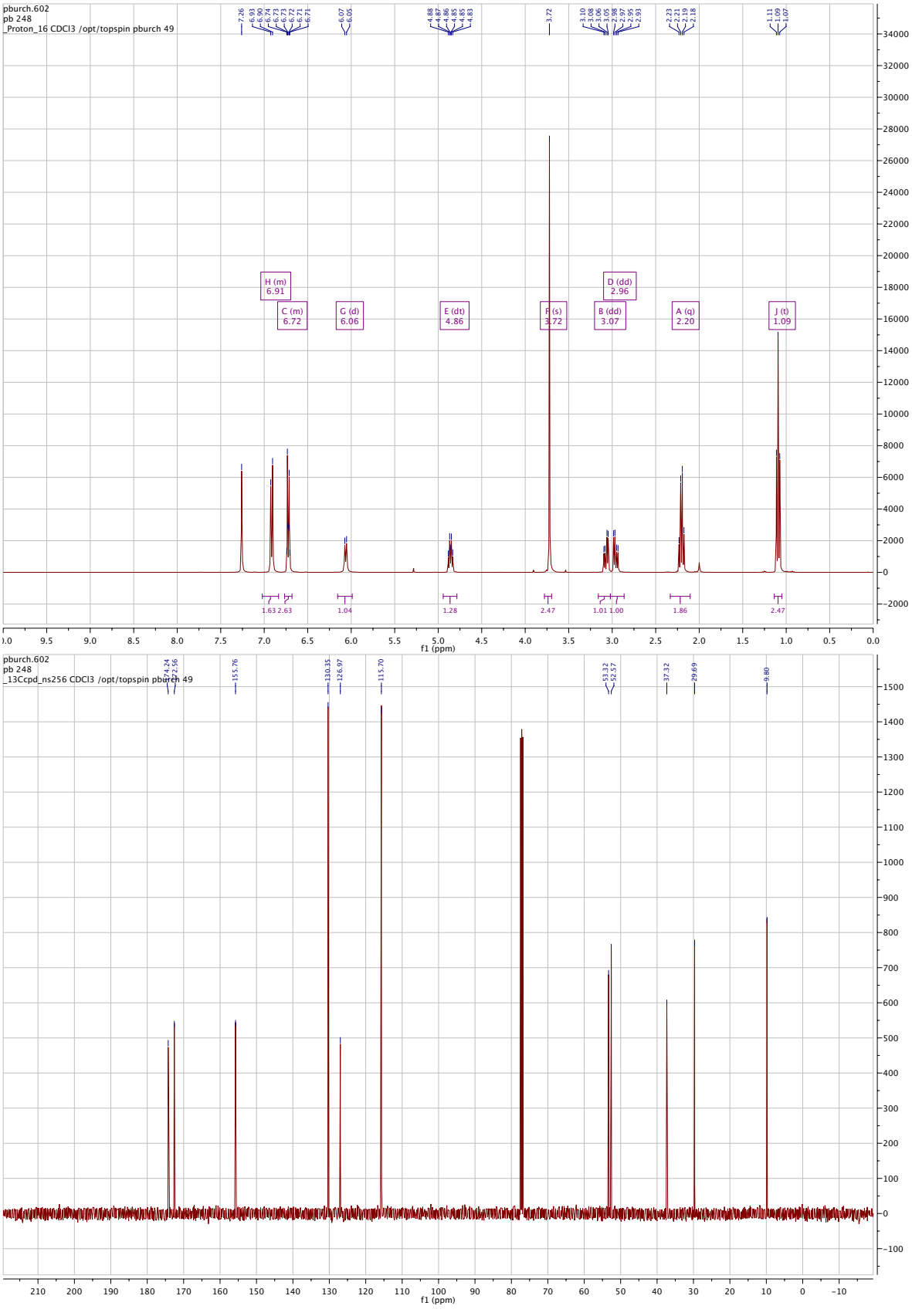

N-(4-hydroxyphenethyl)propionamide (3.20j)

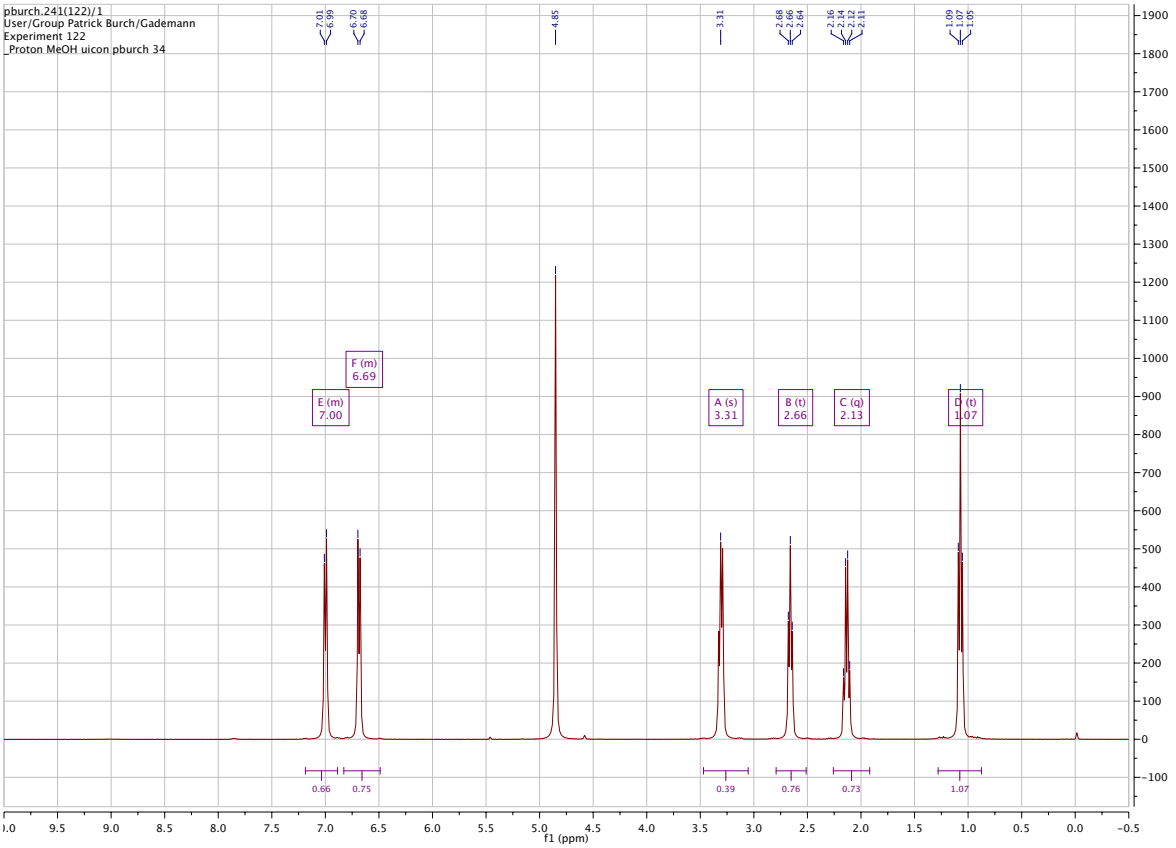

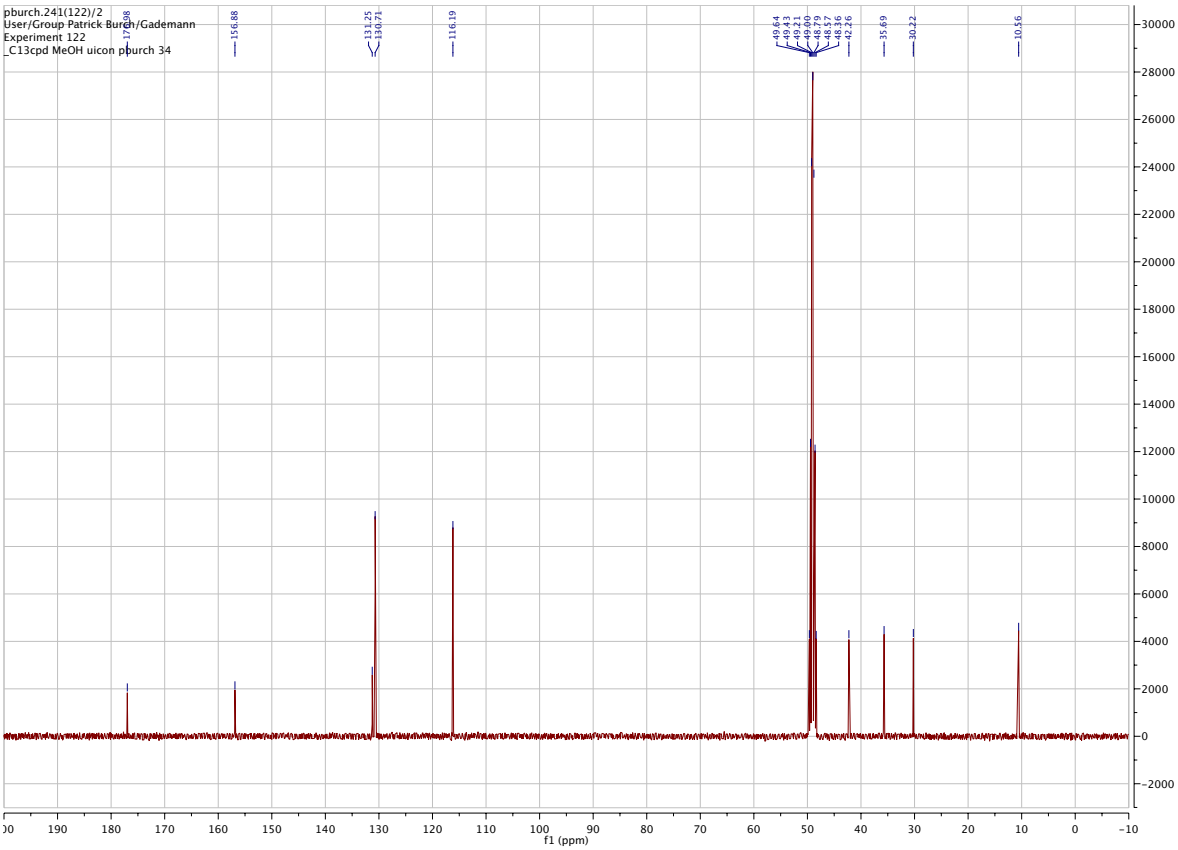

N-(3,4-dihydroxyphenethyl)propionamide (3.20k)

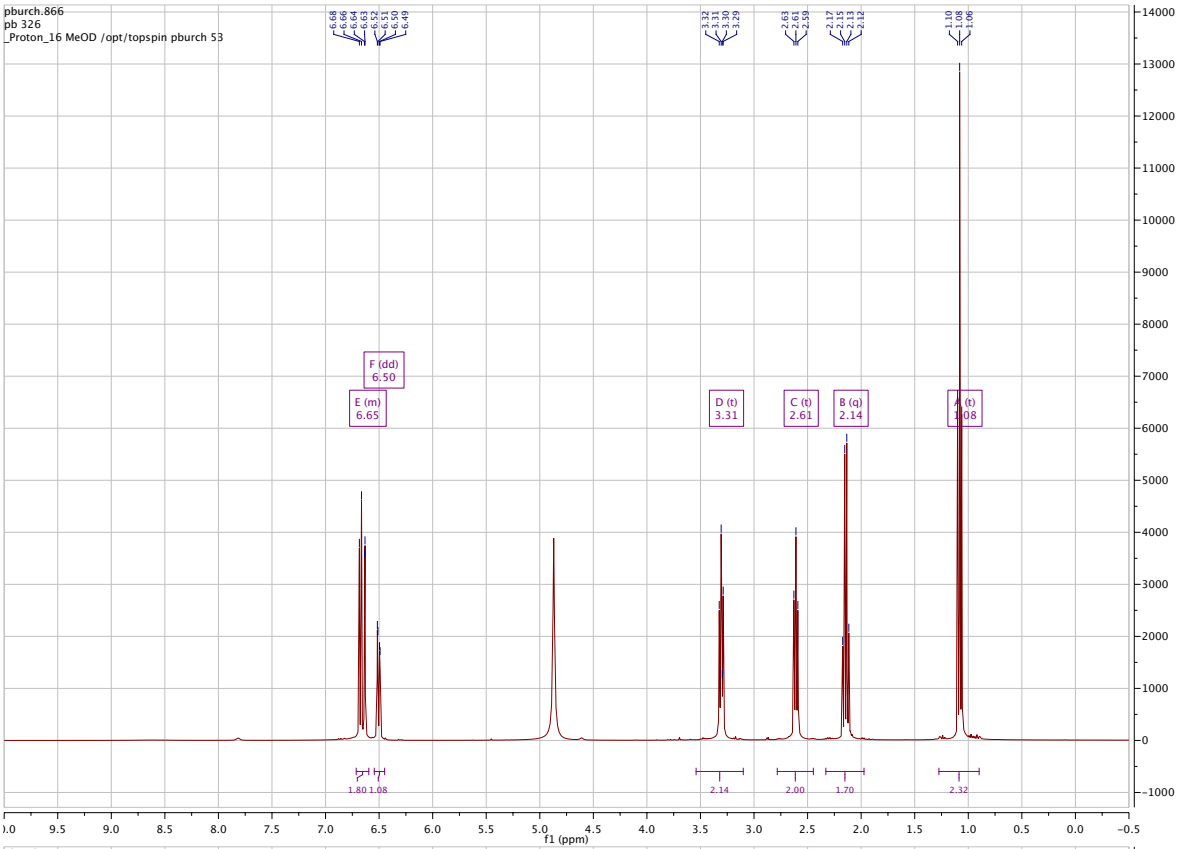

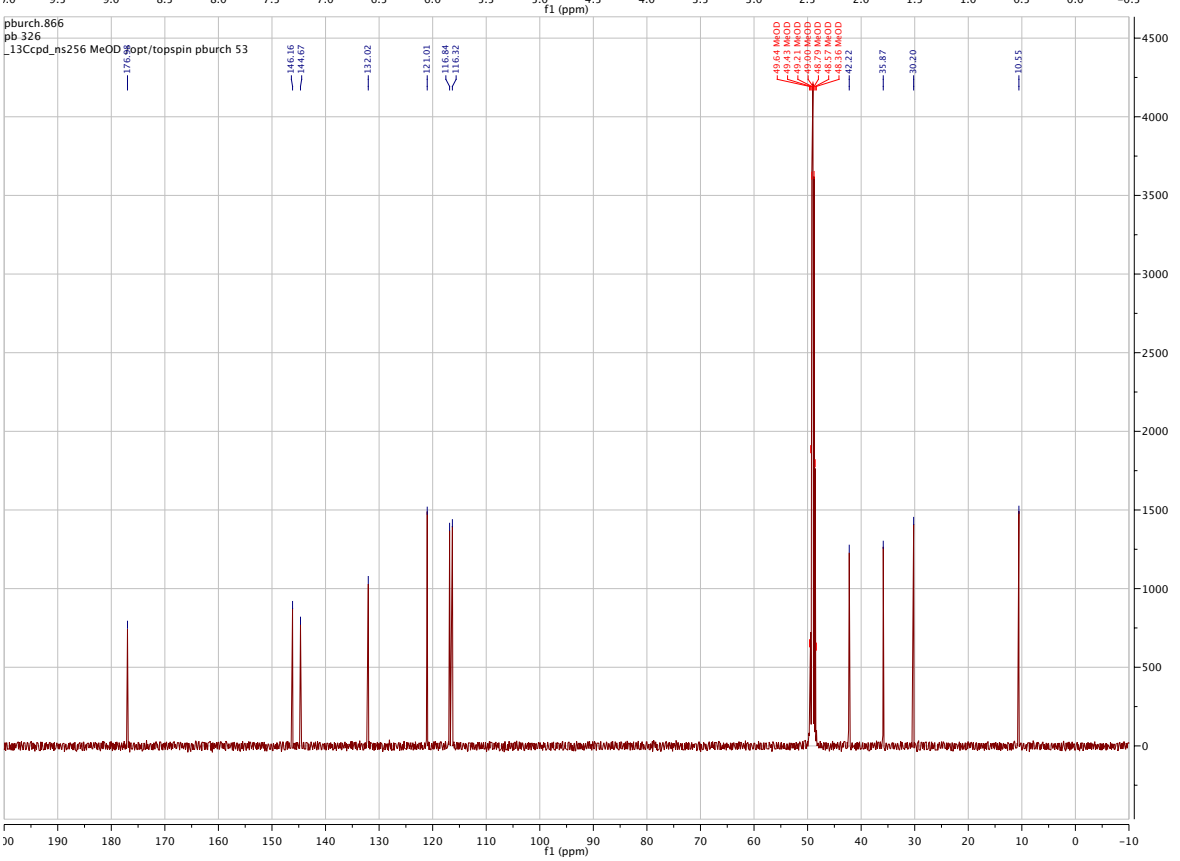

(*S*)-4-(3-hydroxy-2-(propylamino)propyl)phenol (3.20l)

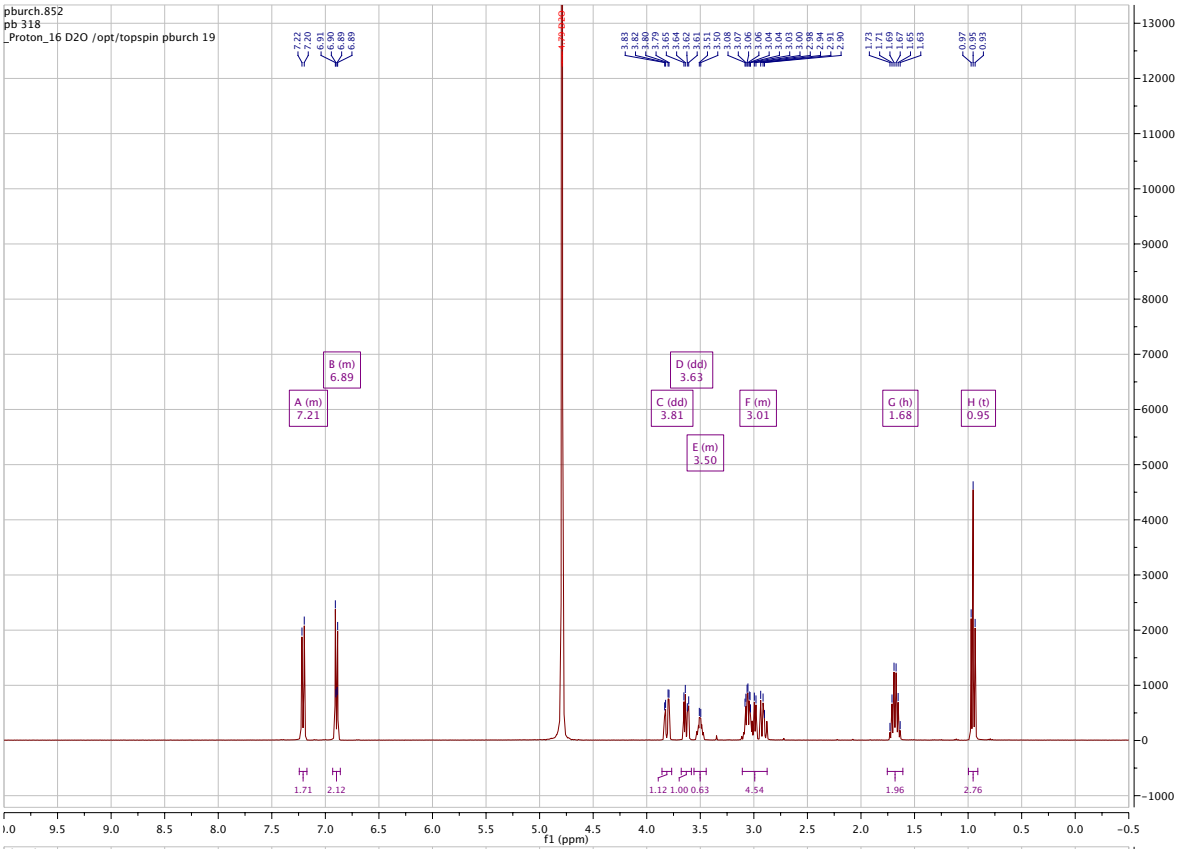

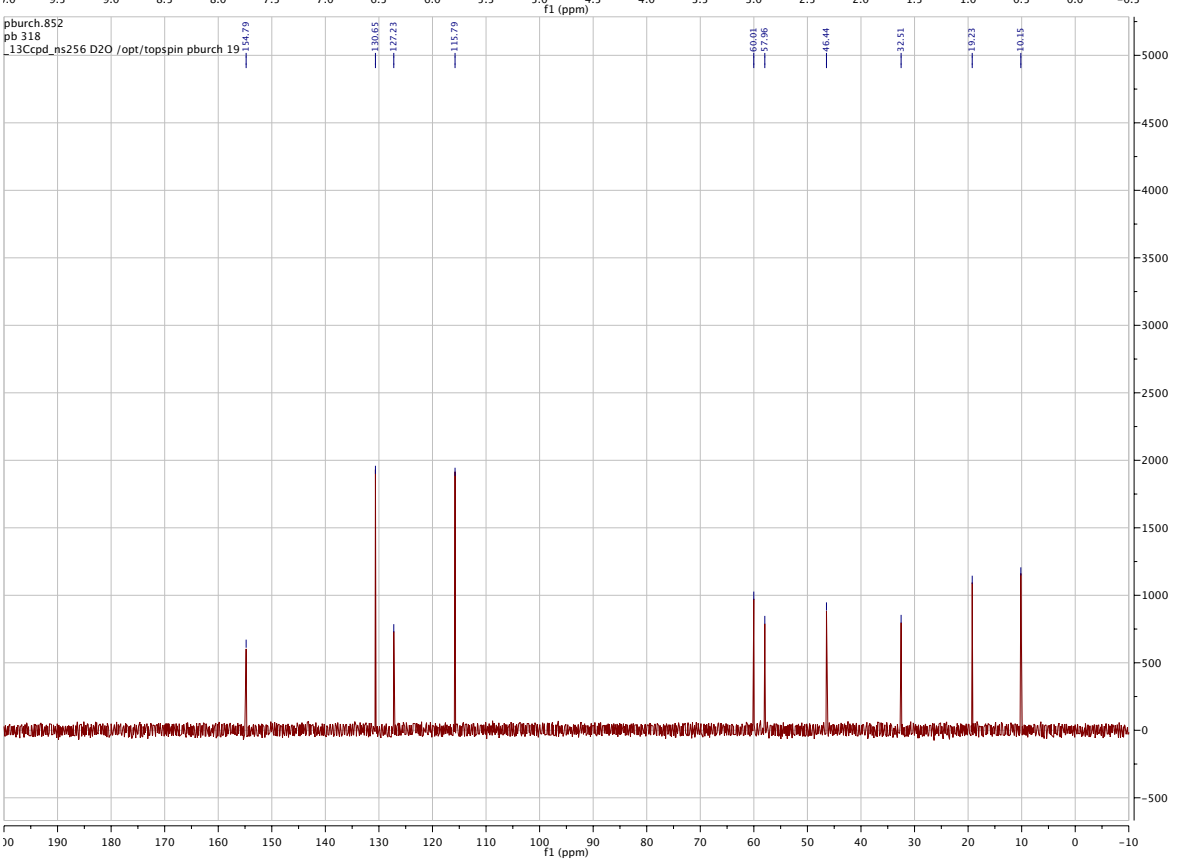

(*S*)-*N*-(1-hydroxy-3-(4-hydroxyphenyl)propan-2-yl)benzamide (3.20m)

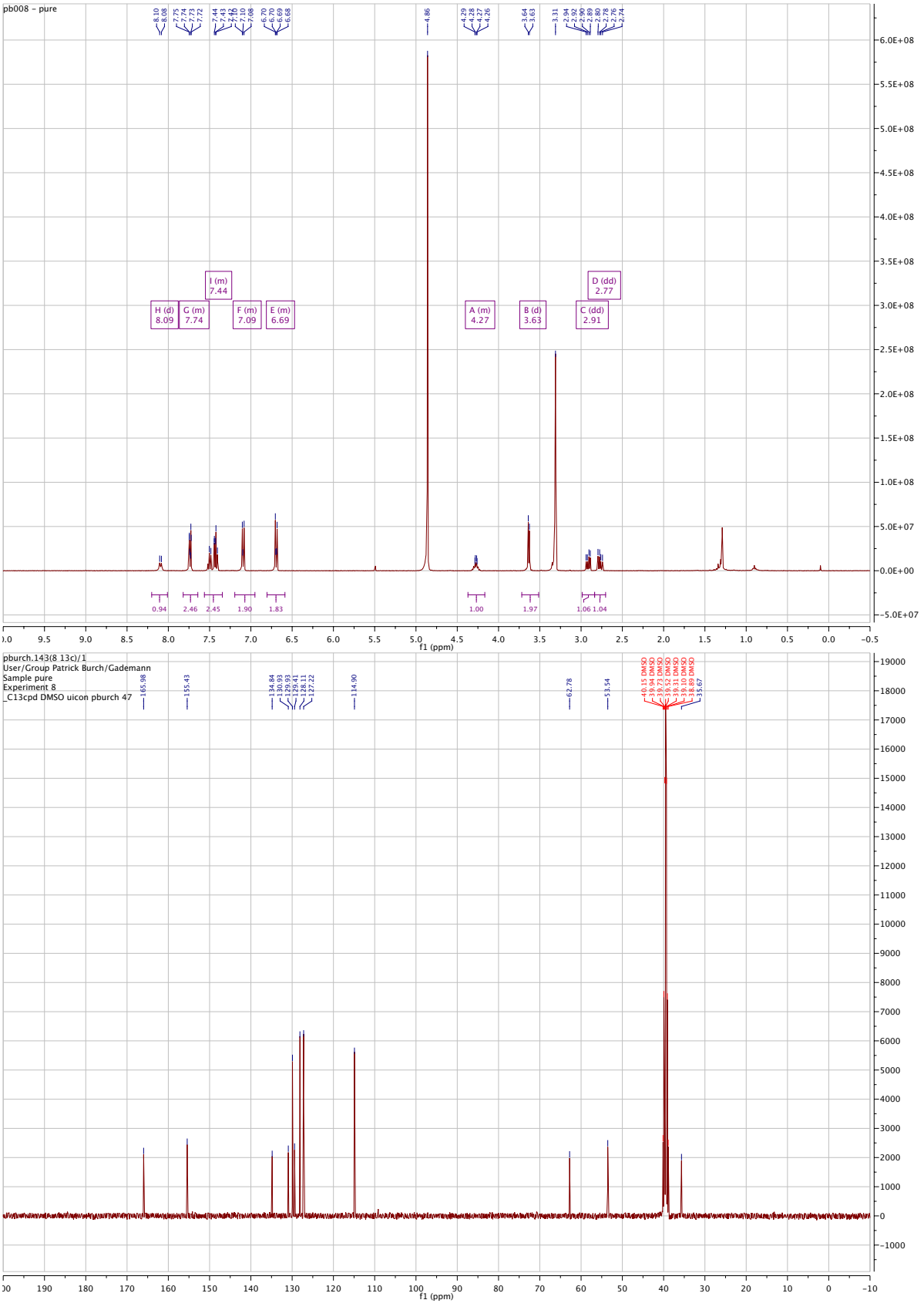

(*S*)-*N*-(1-hydroxy-3-(4-hydroxyphenyl)propan-2-yl)isobutyramide (3.20n)

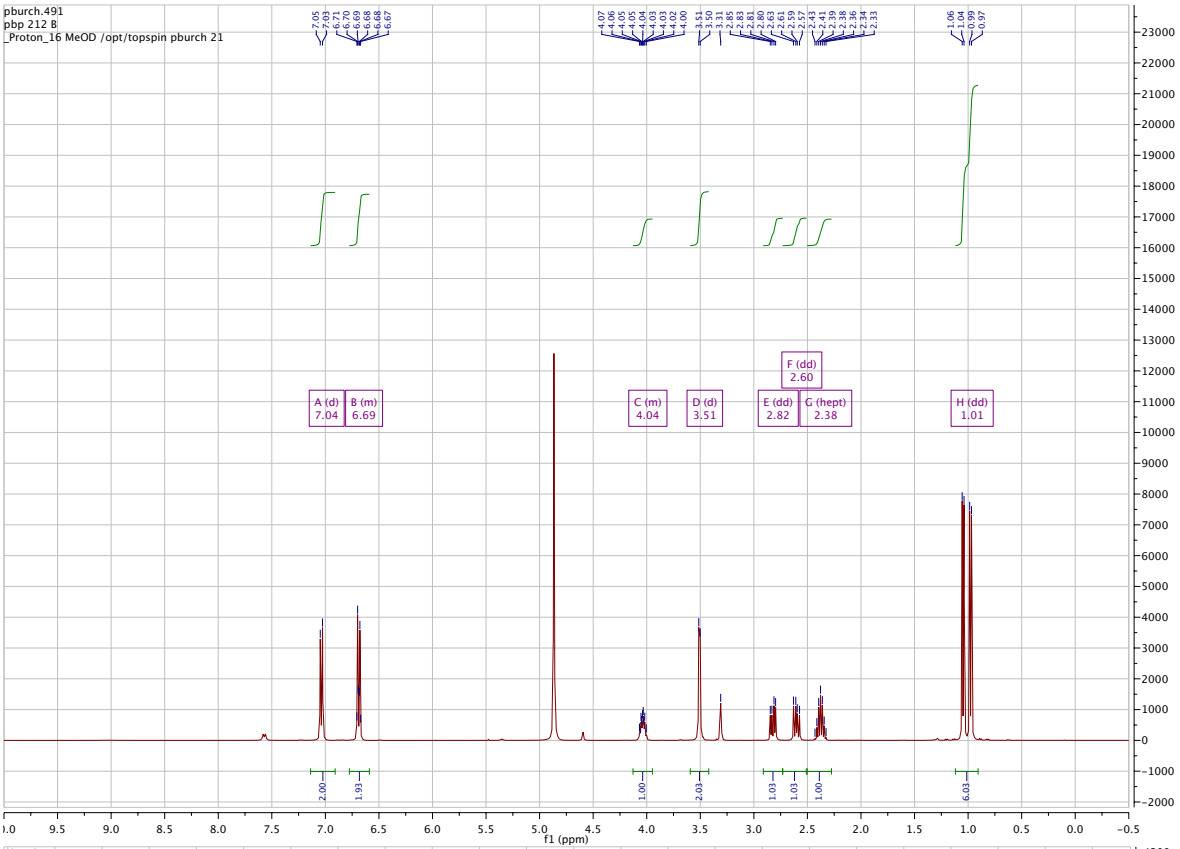

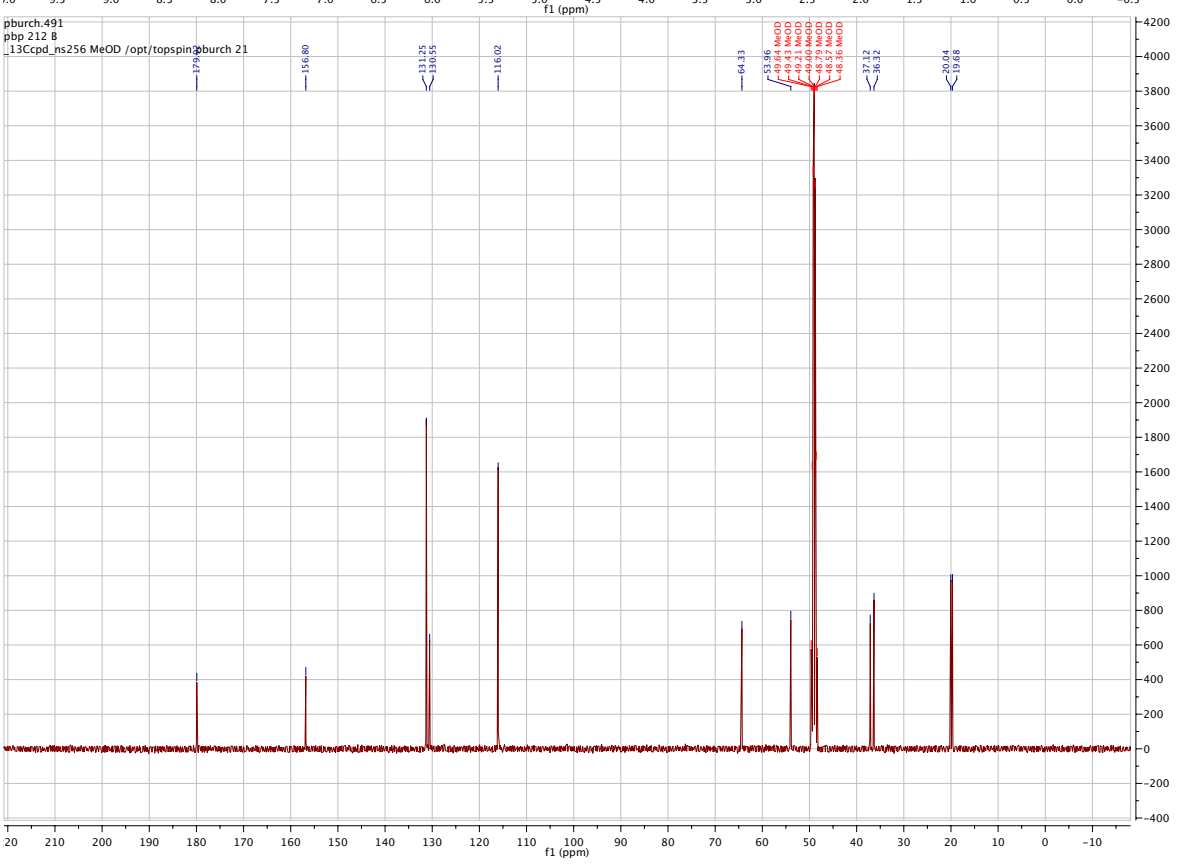

(*S*)-*N*-(1-hydroxy-3-(4-hydroxyphenyl)propan-2-yl)pivalamide (3.20o)

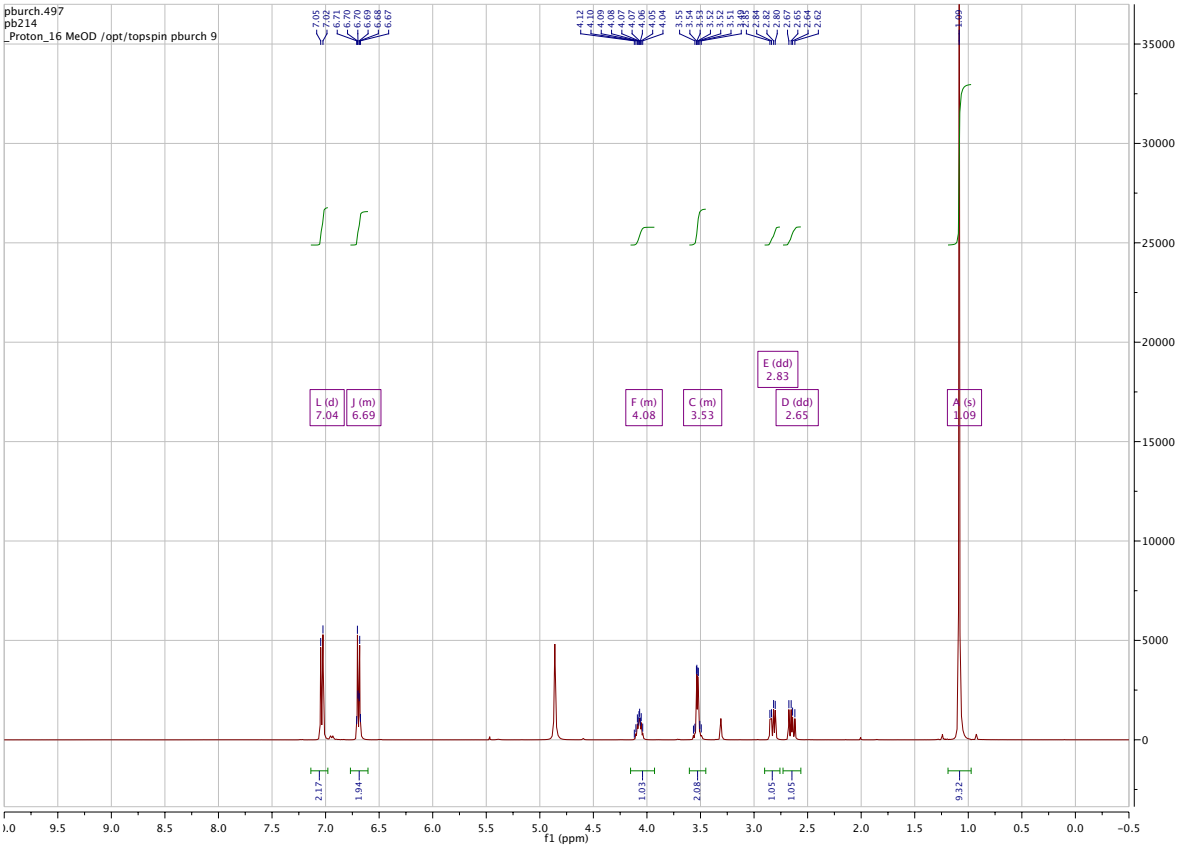

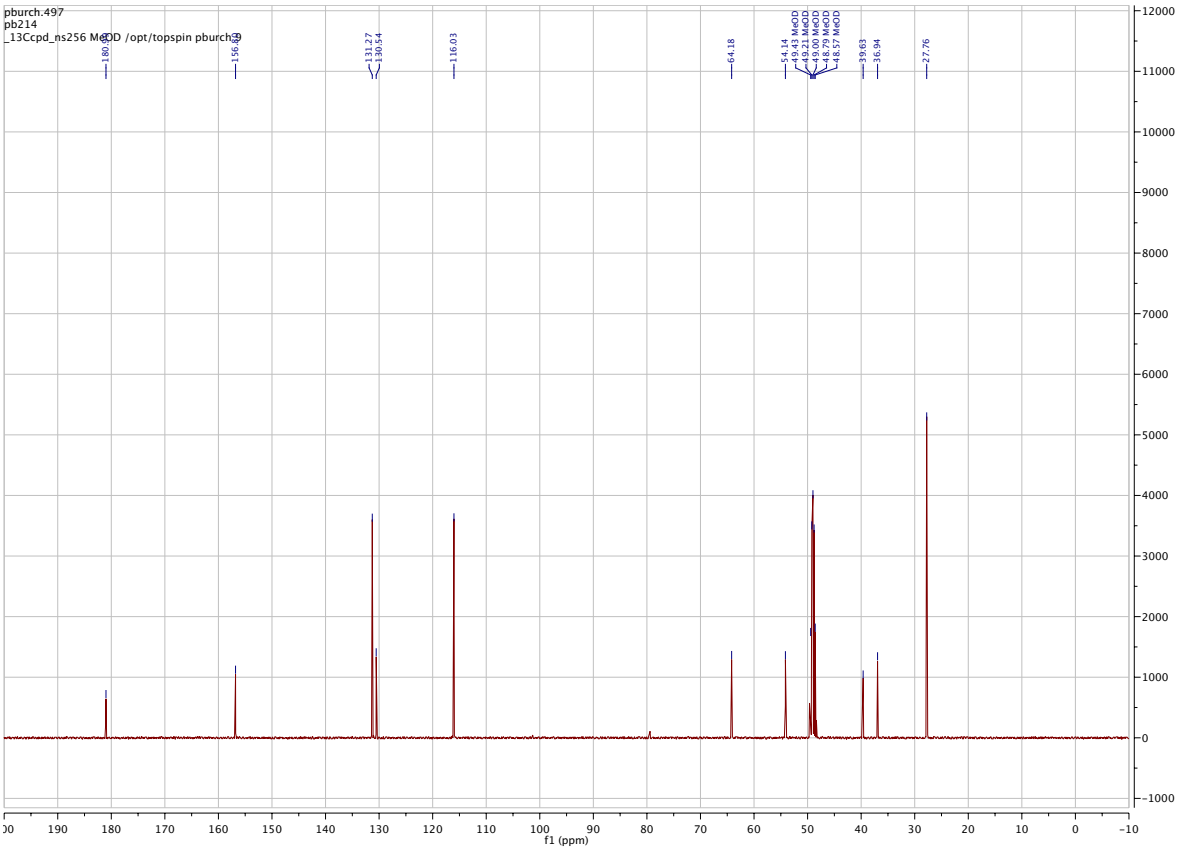

(*S*)-*N*-(1-hydroxy-3-(4-hydroxyphenyl)propan-2-yl)hex-5-ynamide (III)

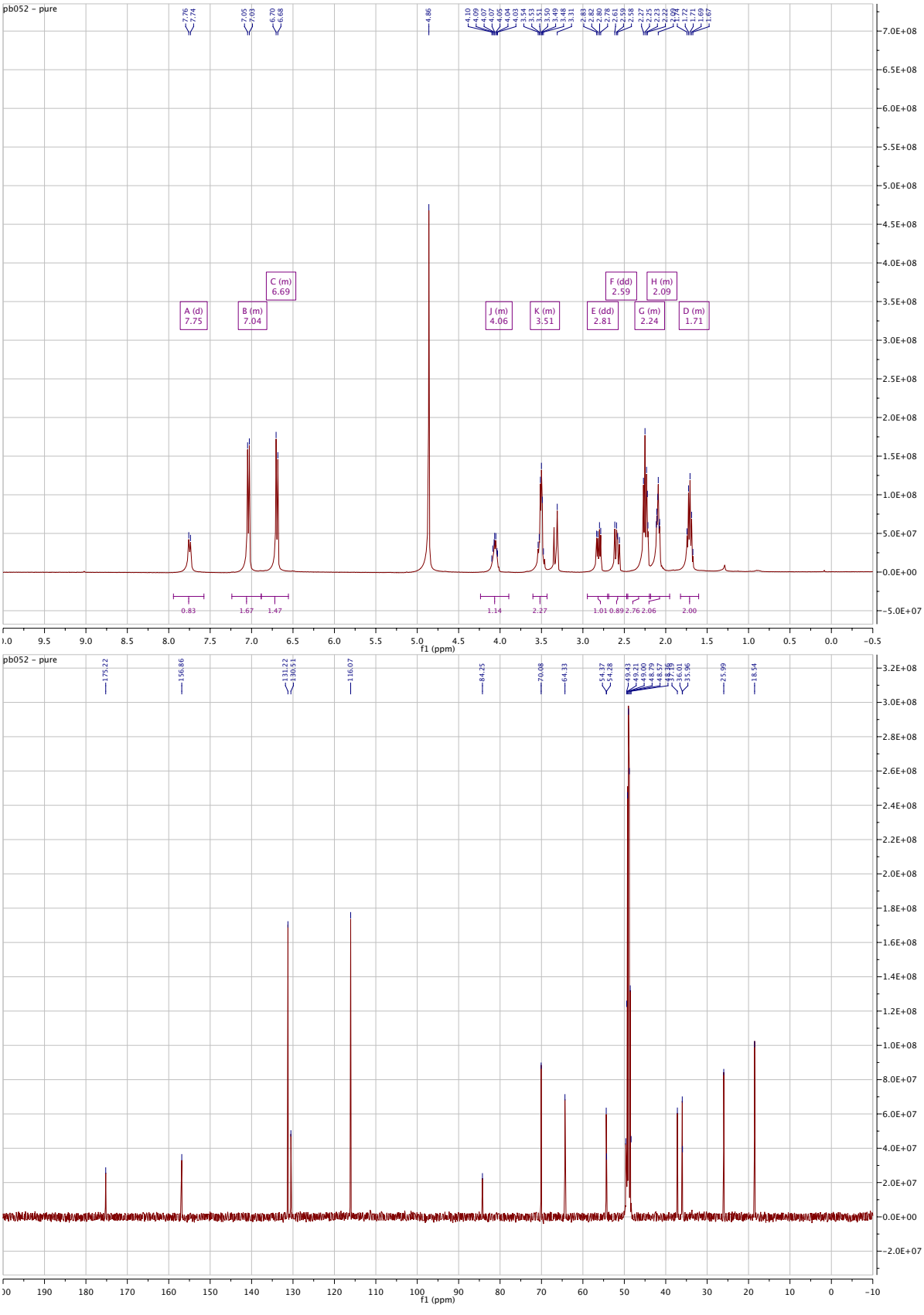

(*S*)-4-(1-(adamantan-1-yl)-1H-1,2,3-triazol-4-yl)-N-(1-hydroxy-3-(4-hydroxyphenyl)propan-2-yl)butanamide (3.20p)

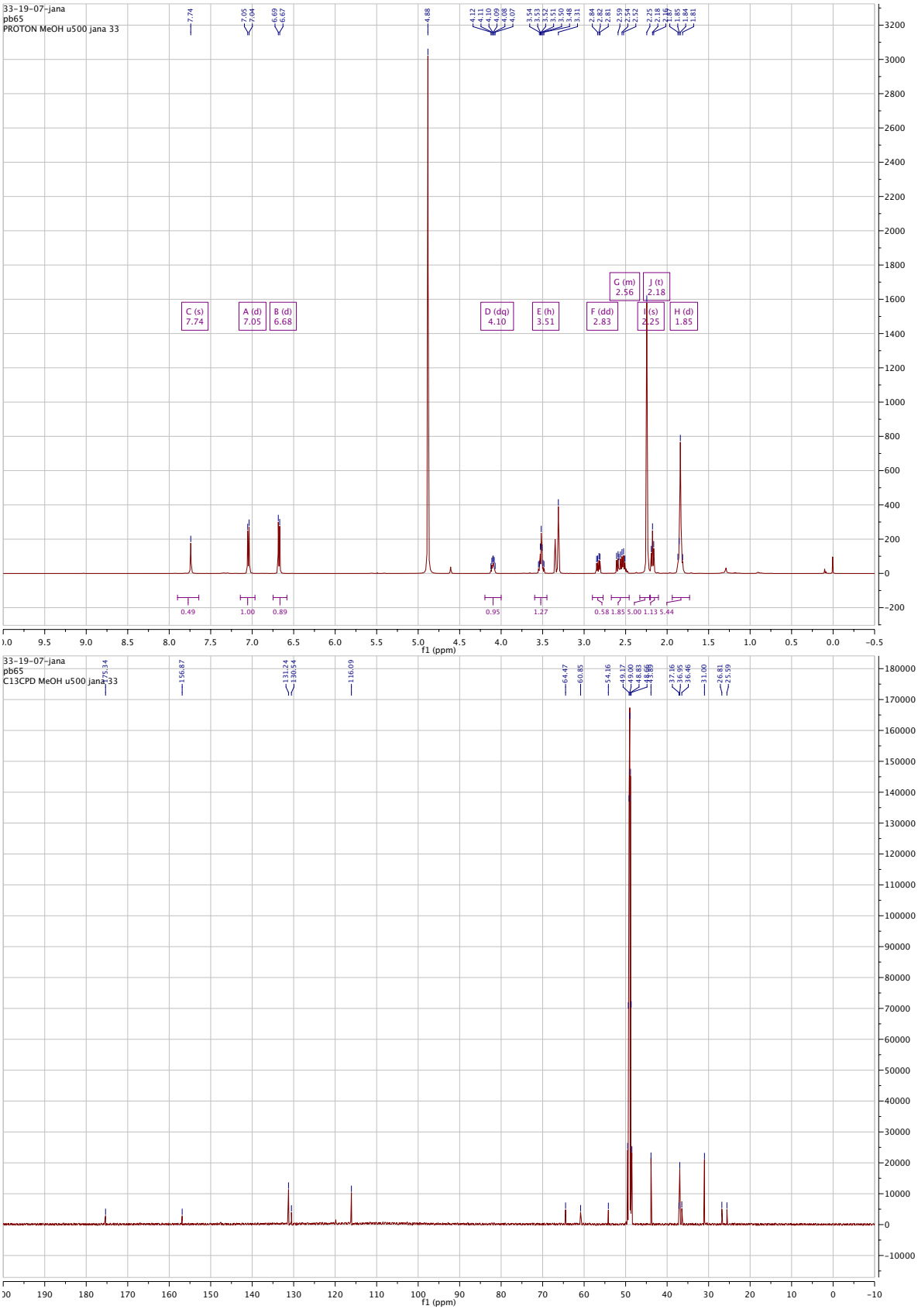

N-((*R*)-1-hydroxy-3-(4-hydroxyphenyl)propan-2-yl)-*N*-((*S*)-1-hydroxy-3-(4-hydroxyphenyl)propan-2-yl)succinamide (3.20q)

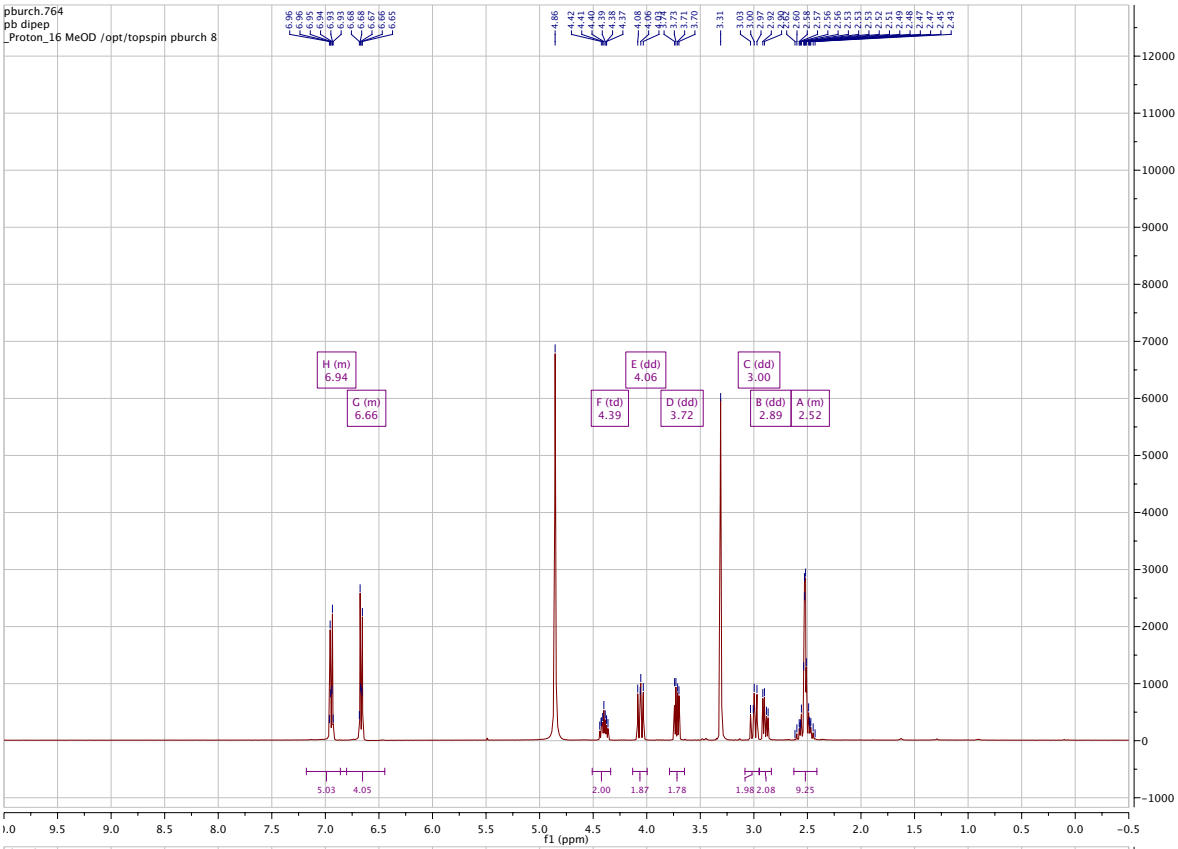

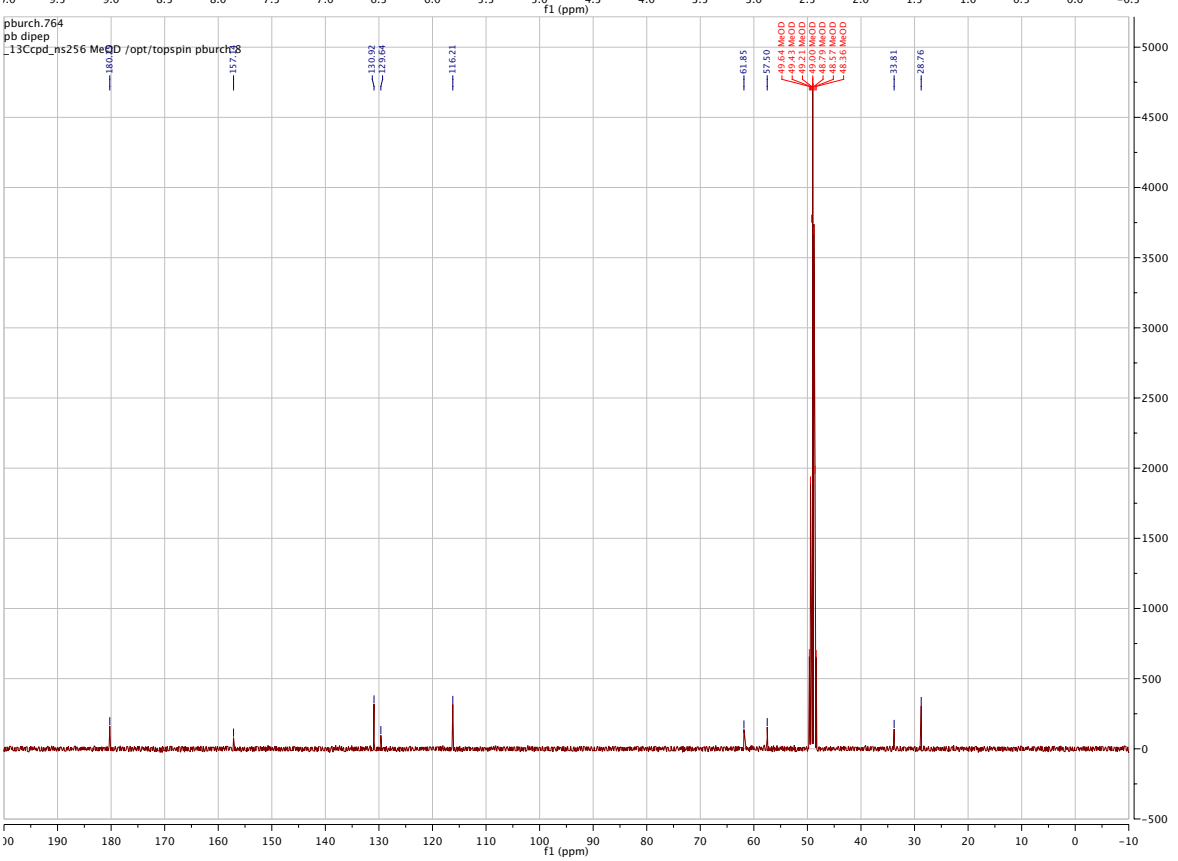

(*S*)-*N*-(1-hydroxy-3-(4-hydroxyphenyl)propan-2-yl)nonanamide (3.20r)

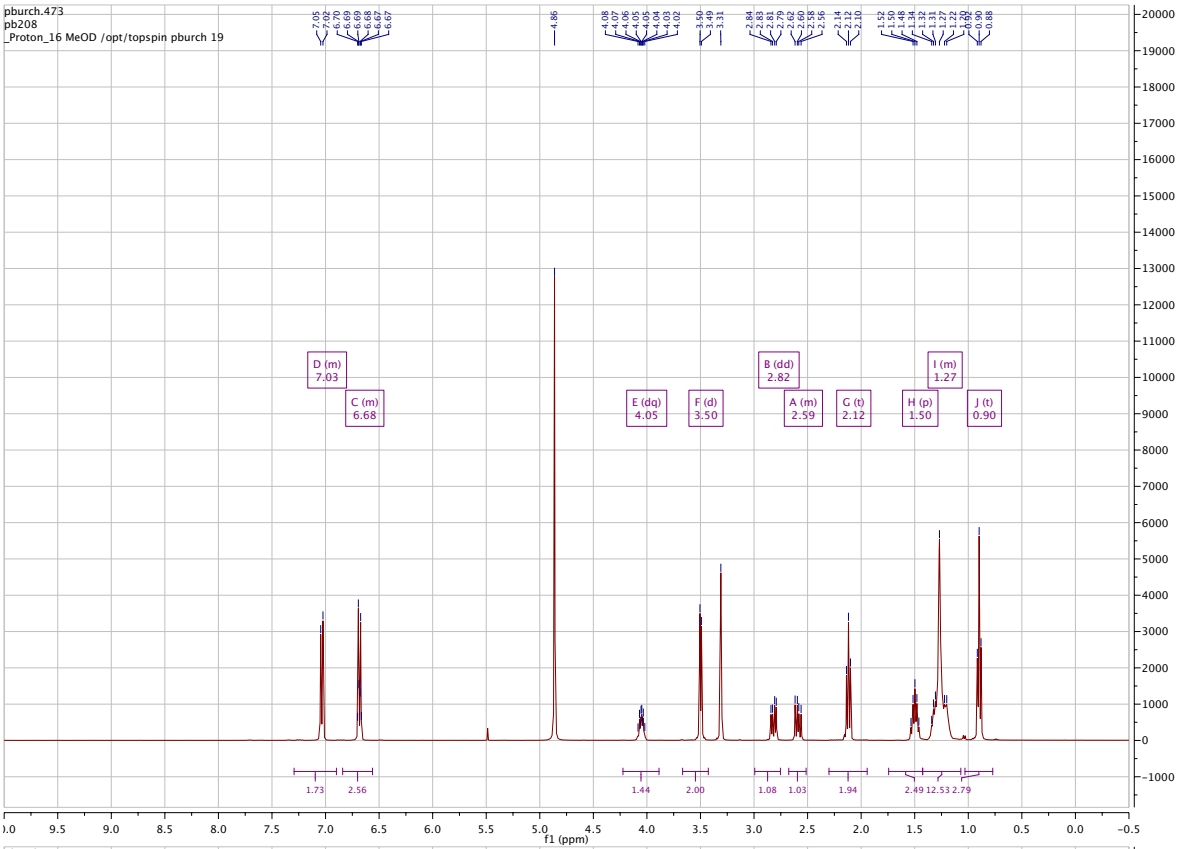

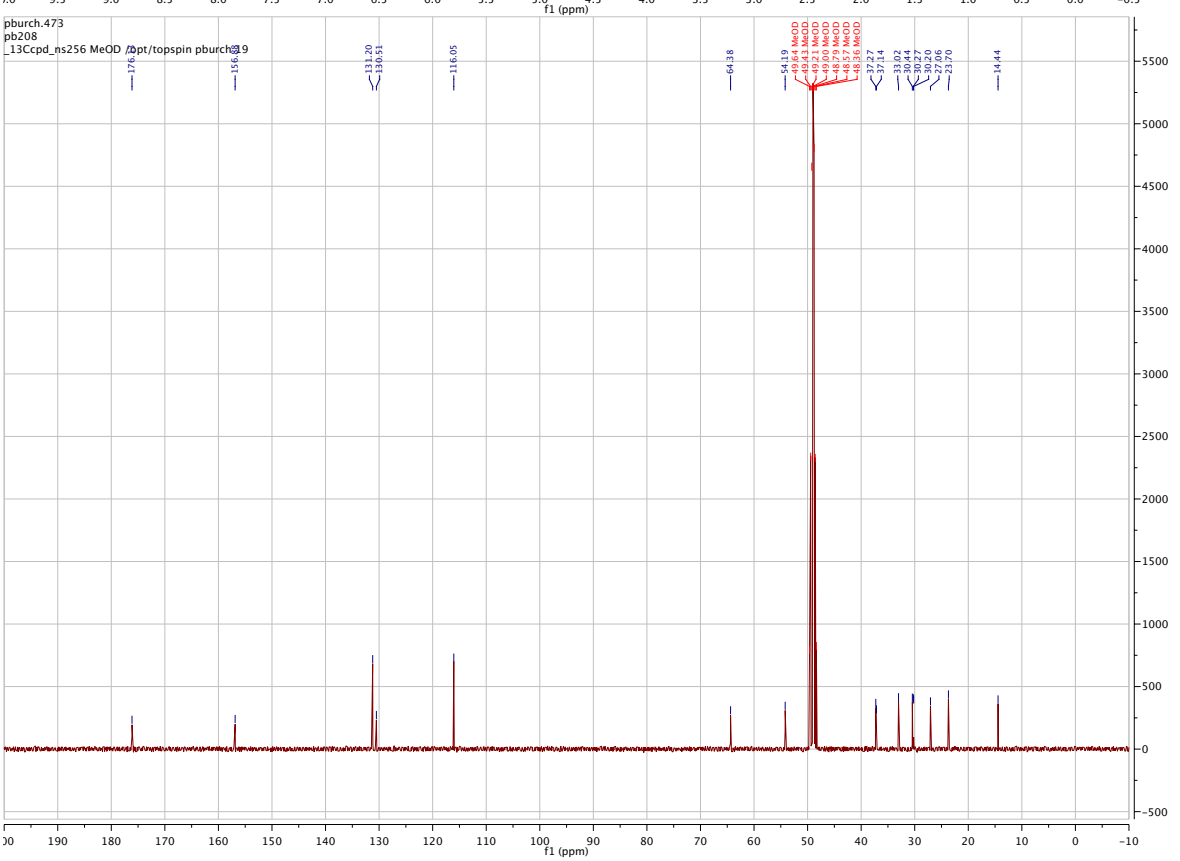

(*S*)-8-((1-hydroxy-3-(4-hydroxyphenyl)propan-2-yl)amino)-8-oxooctanoic acid (3.20s)

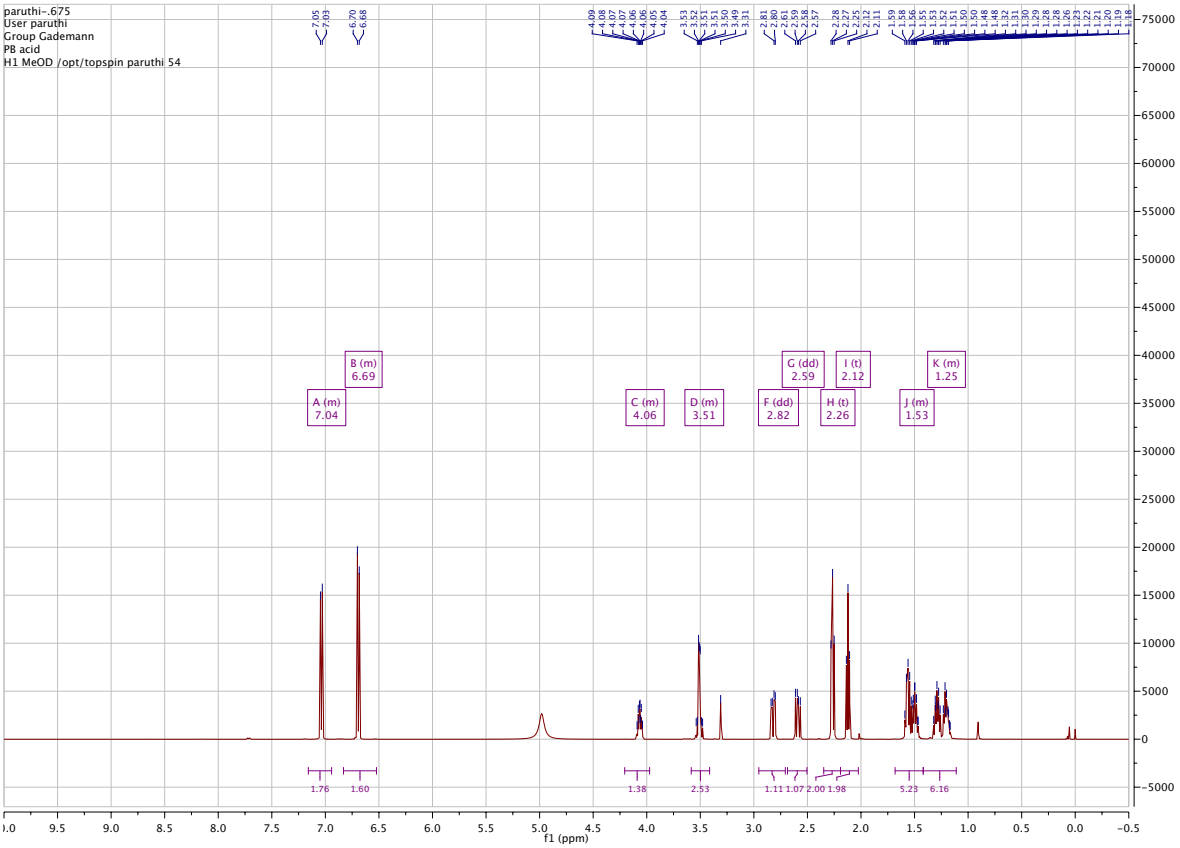

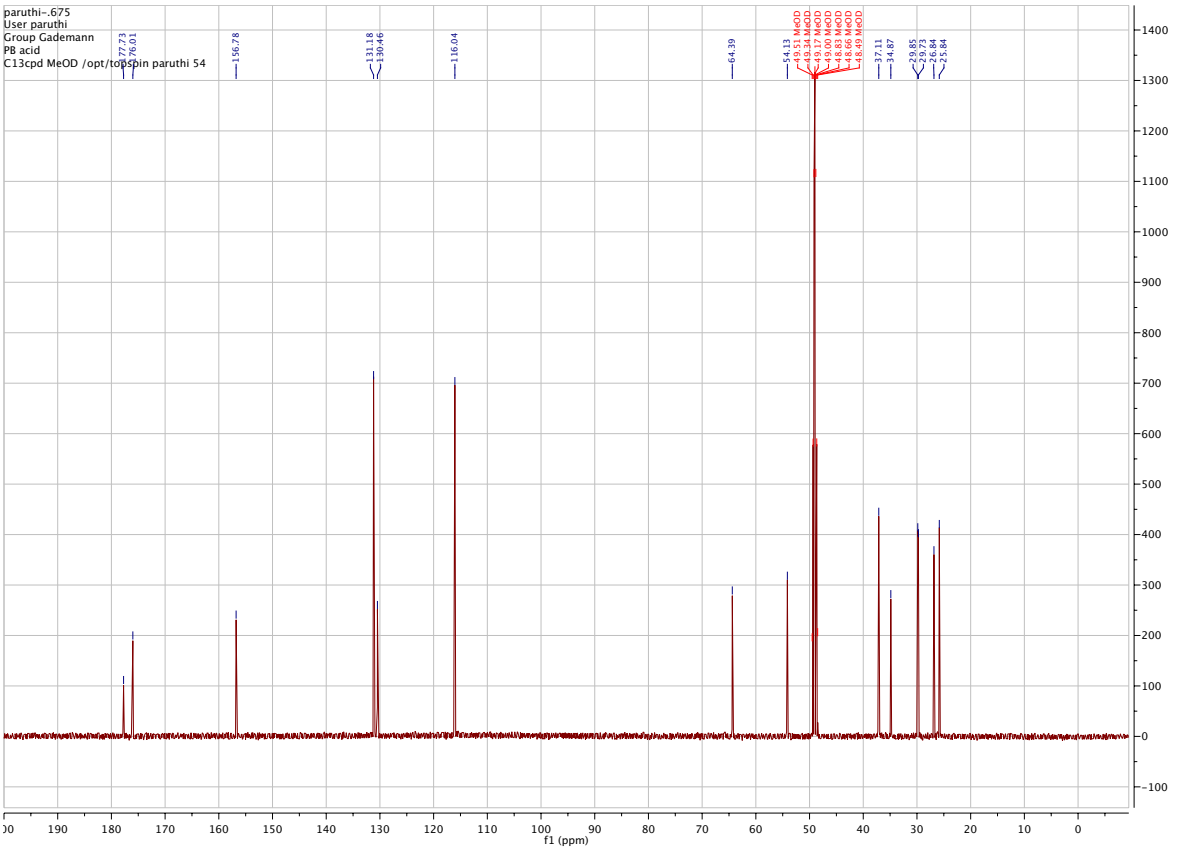

(*S*)-8-hydroxy-*N*-(1-hydroxy-3-(4-hydroxyphenyl)propan-2-yl)octanamide (3.20t)

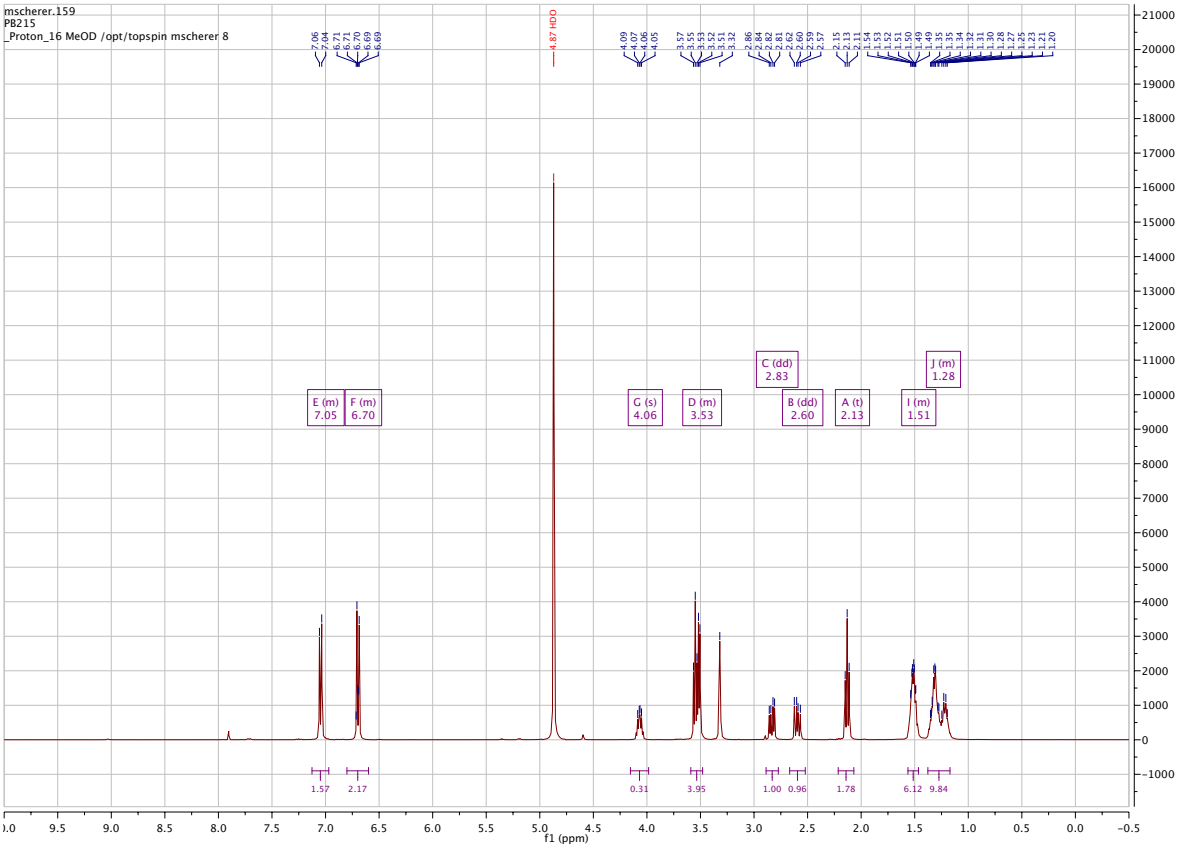

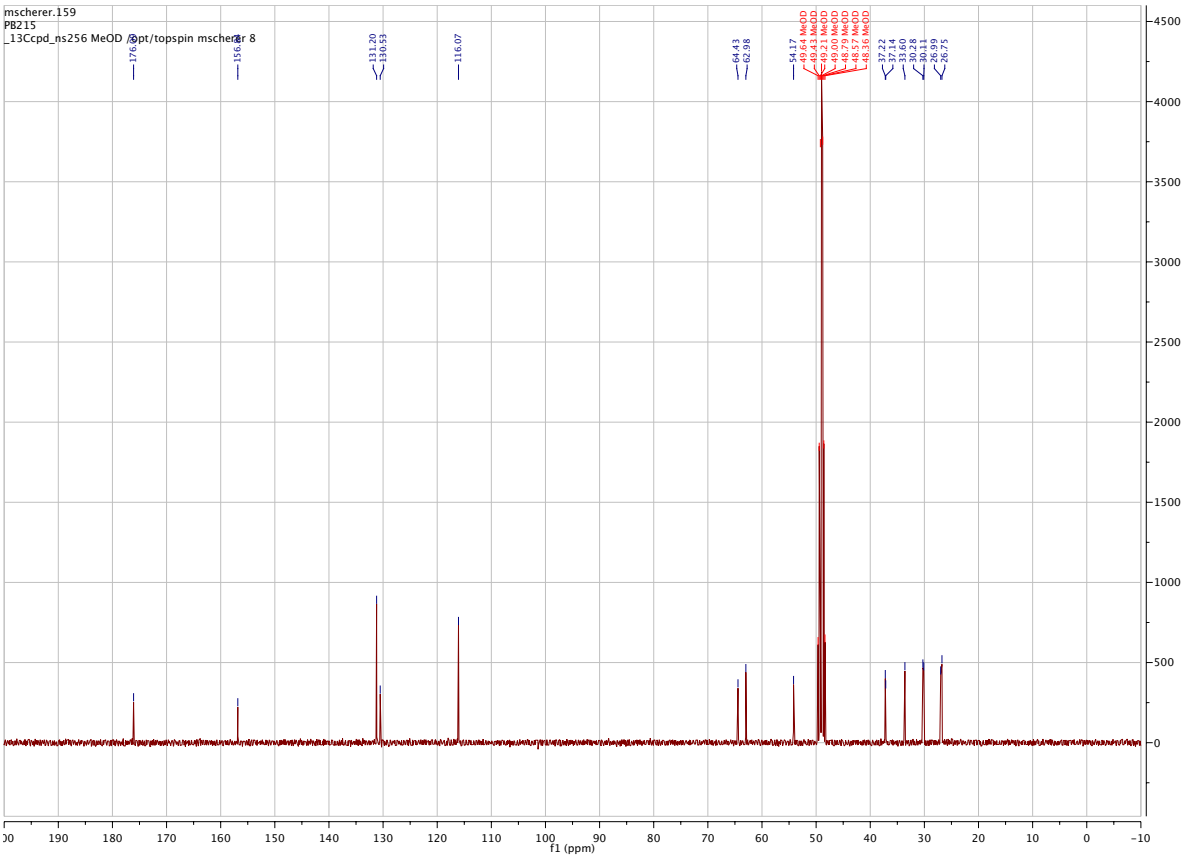

(*S*)-4-(2-(hexadecylamino)-3-hydroxypropyl)phenol (4.22a)

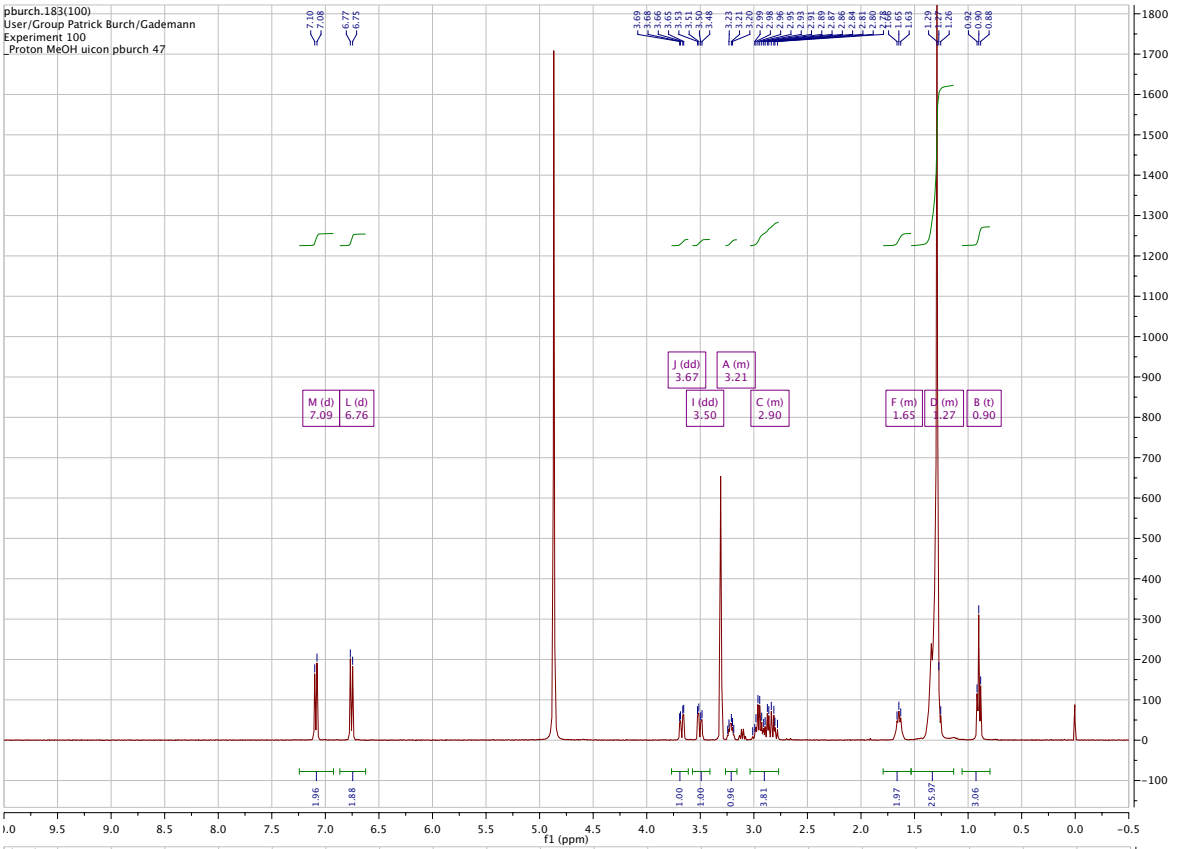

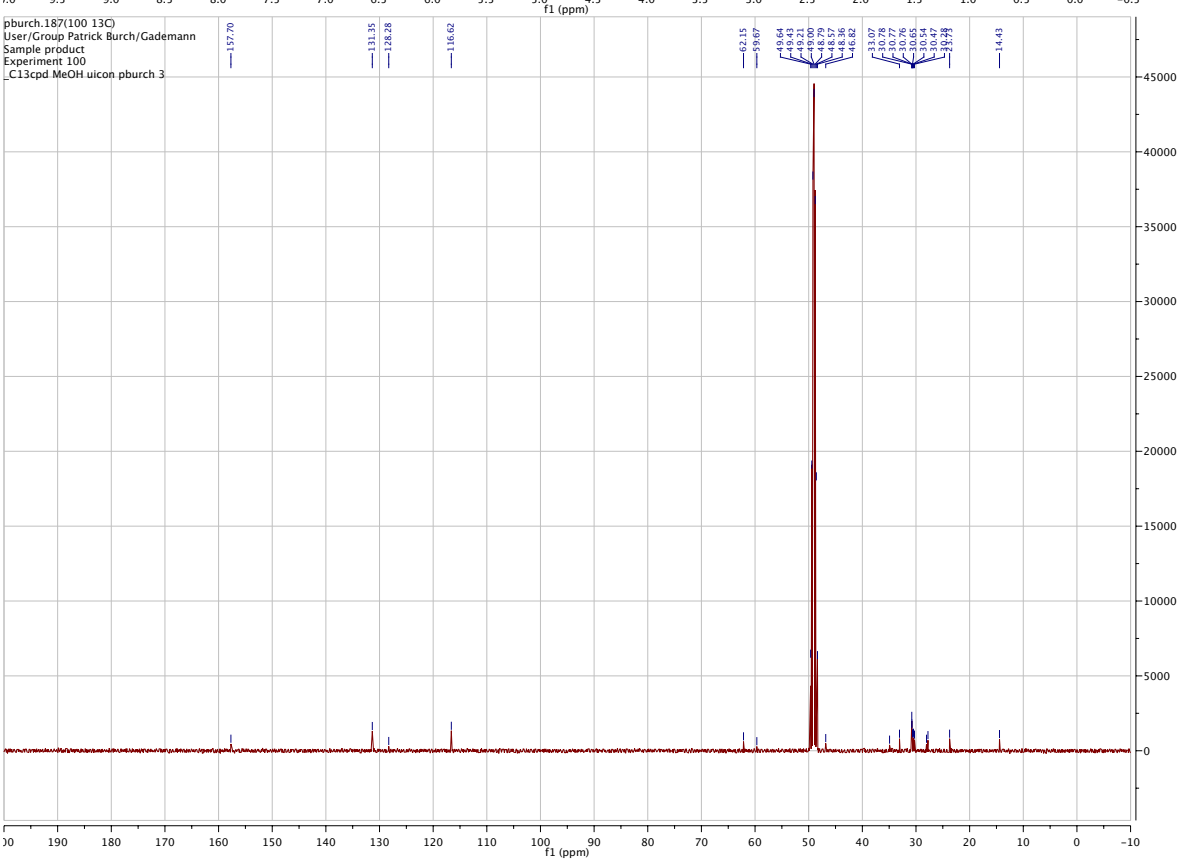

(*S*)-4-(3-hydroxy-2-((15-hydroxypentadecyl)amino)propyl)phenol (4.22b)

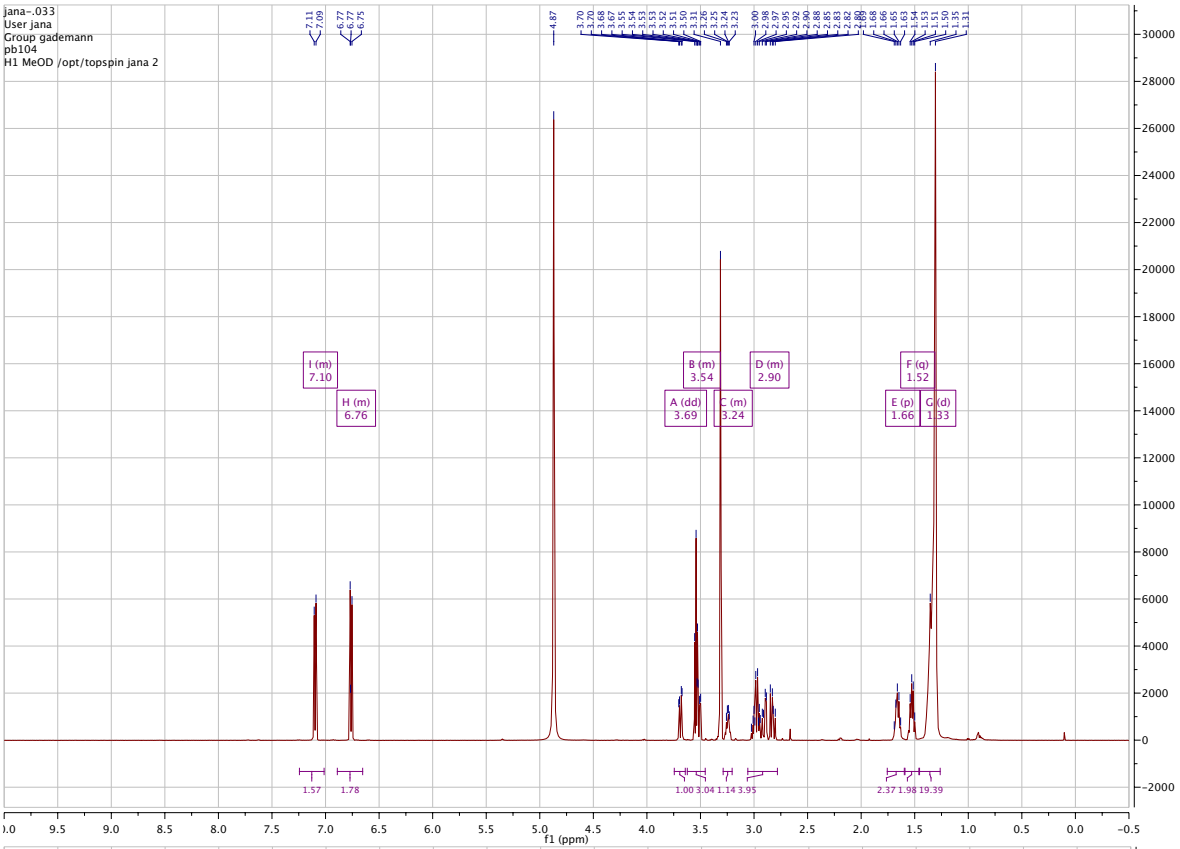

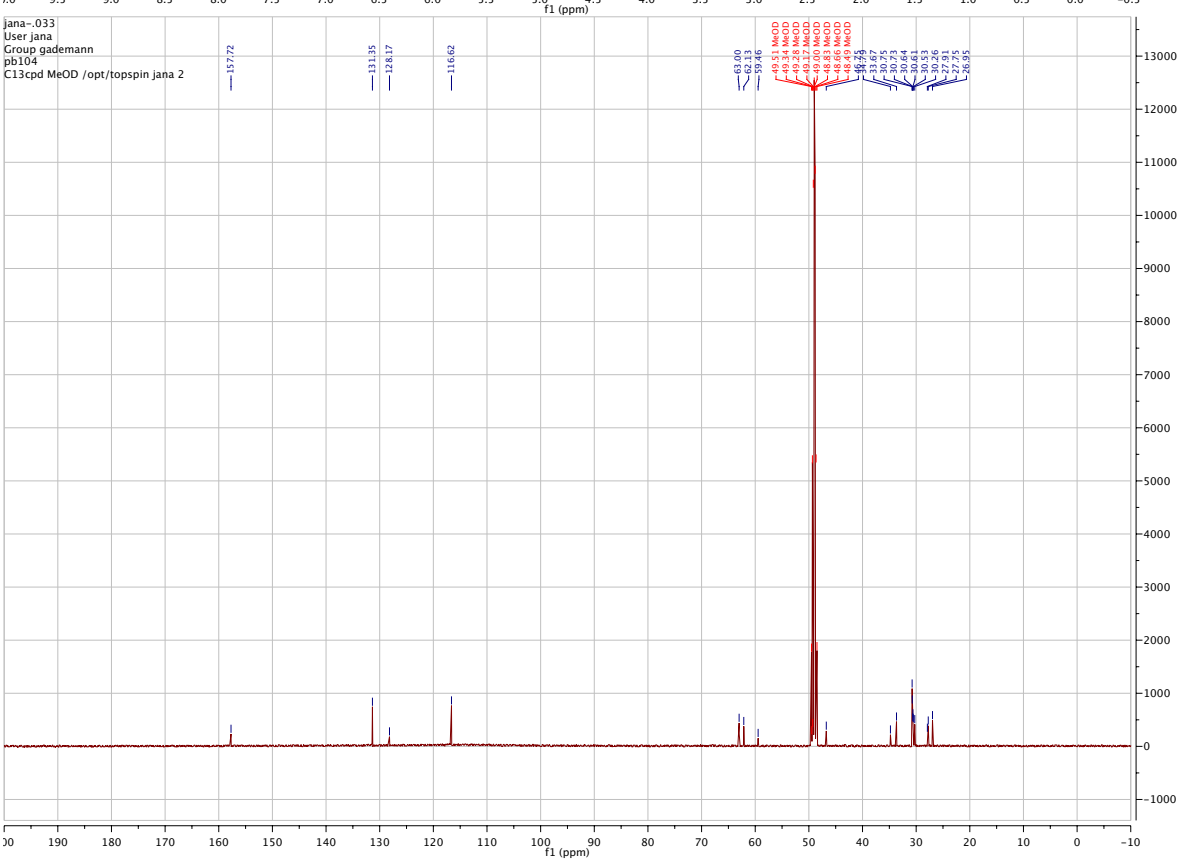

4-((*S*)-3-hydroxy-2-((9*Z*,12*Z*)-octadeca-9,12-dien-1-ylamino)propyl)phenol (4.22c)

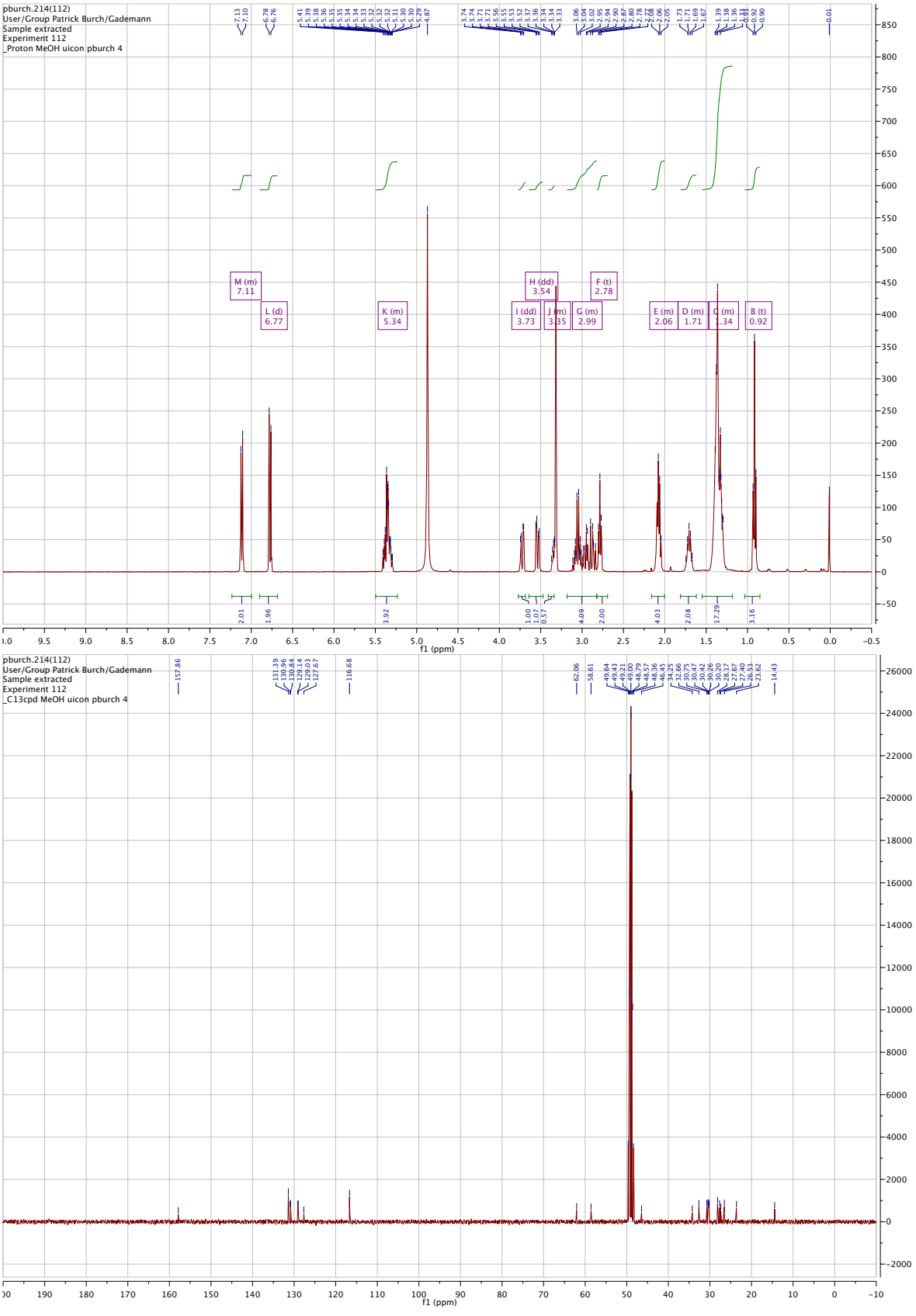

4-((*S*)-3-hydroxy-2-((9*Z*,12*Z*,15*Z*)-octadeca-9,12,15-trien-1-ylamino)propyl)phenol (4.22d)

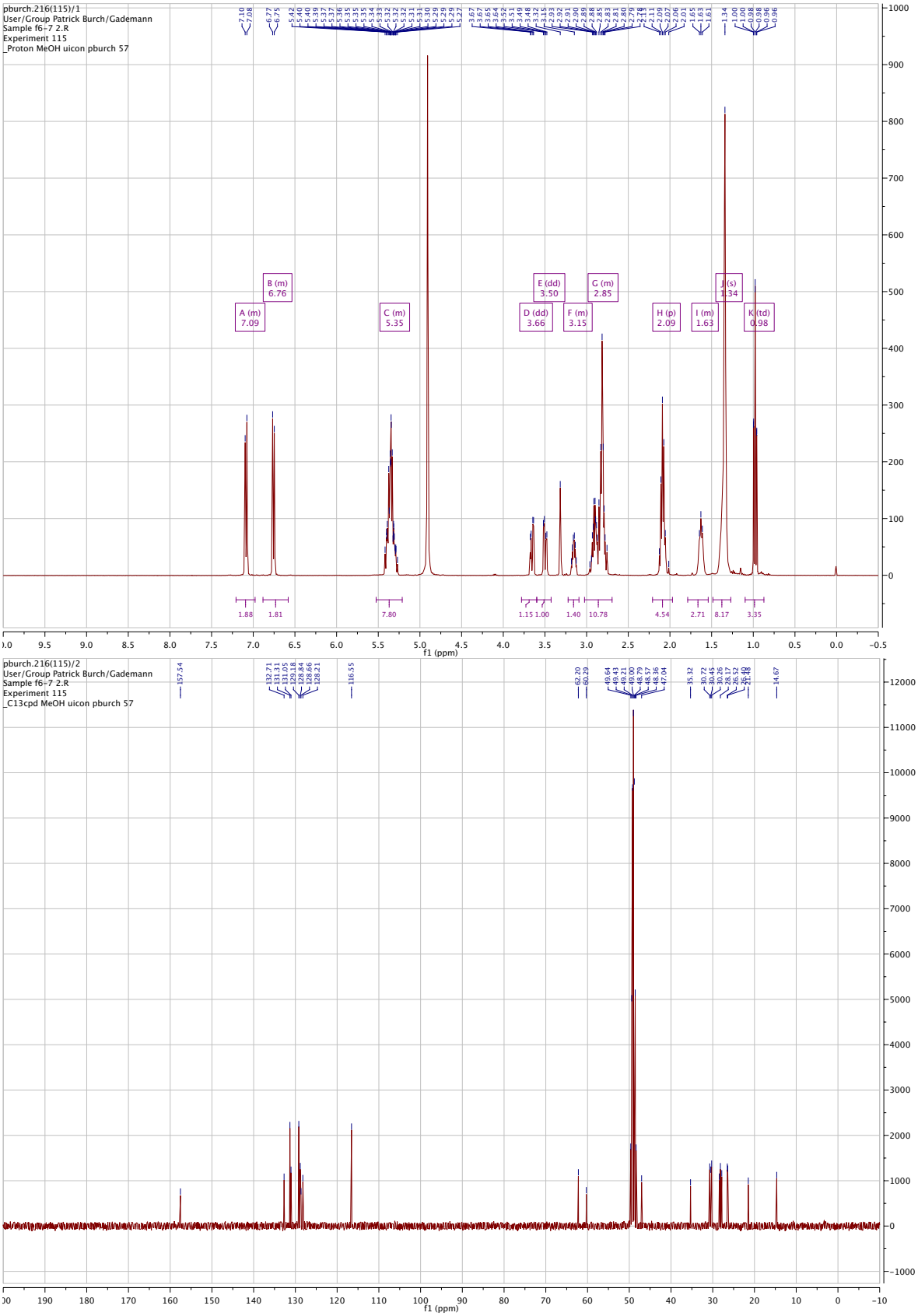

(*S*)-*N*-(1-hydroxy-3-(4-hydroxyphenyl)propan-2-yl)palmitamide (4.22e)

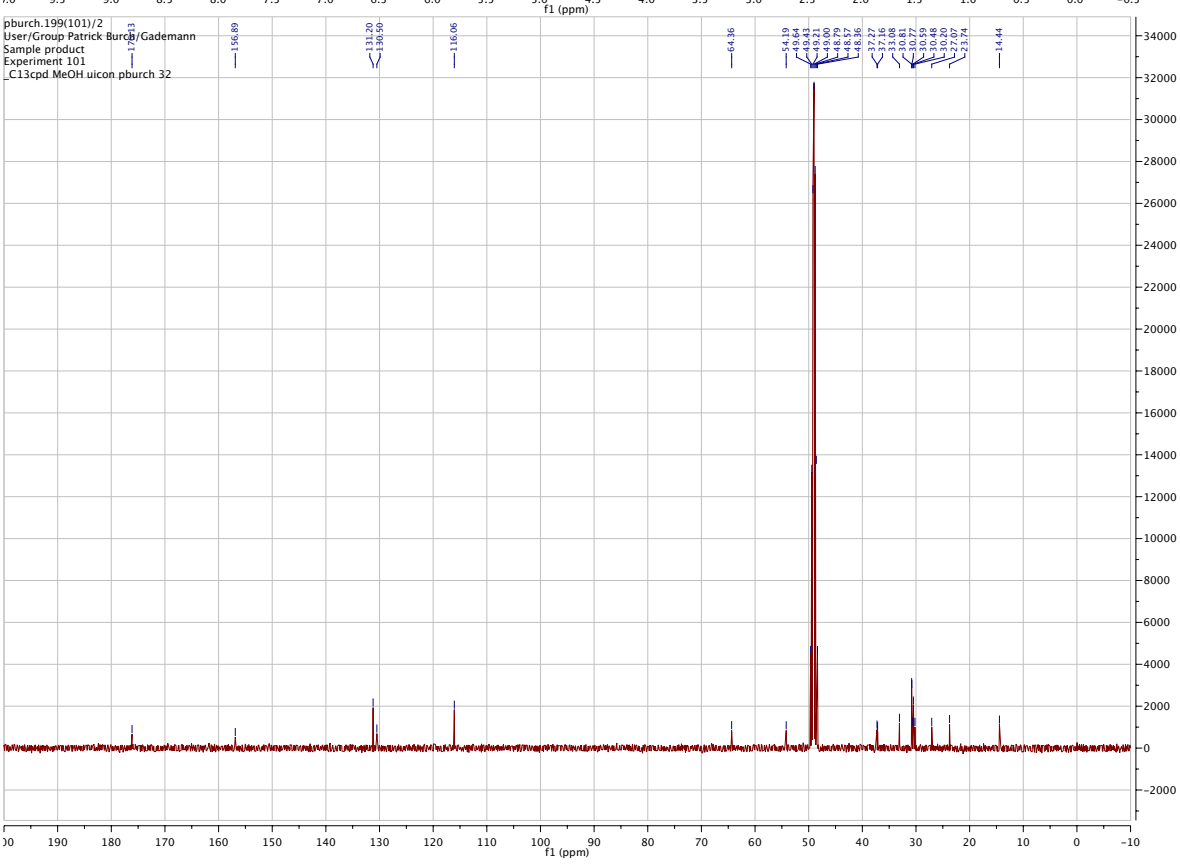

(*S*)-15-hydroxy-*N*-(1-hydroxy-3-(4-hydroxyphenyl)propan-2-yl)pentadecanamide (4.22f)

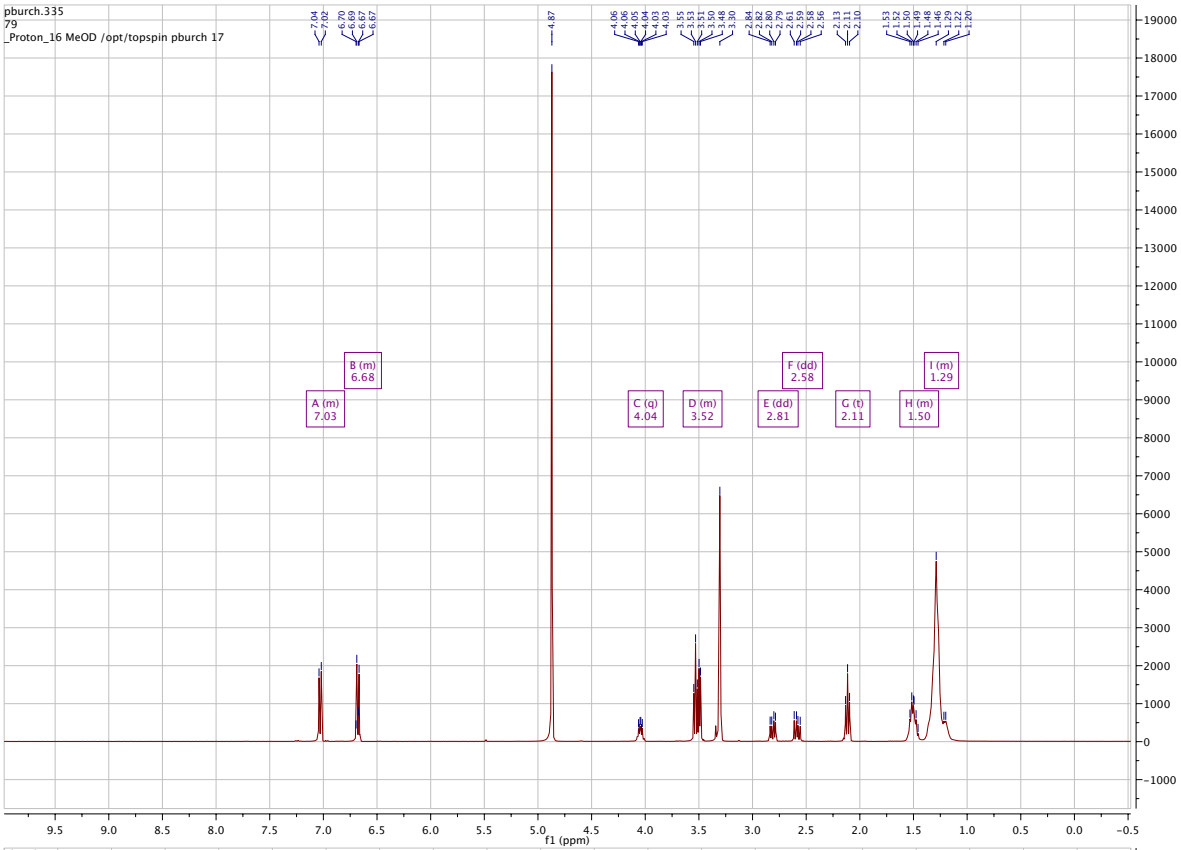

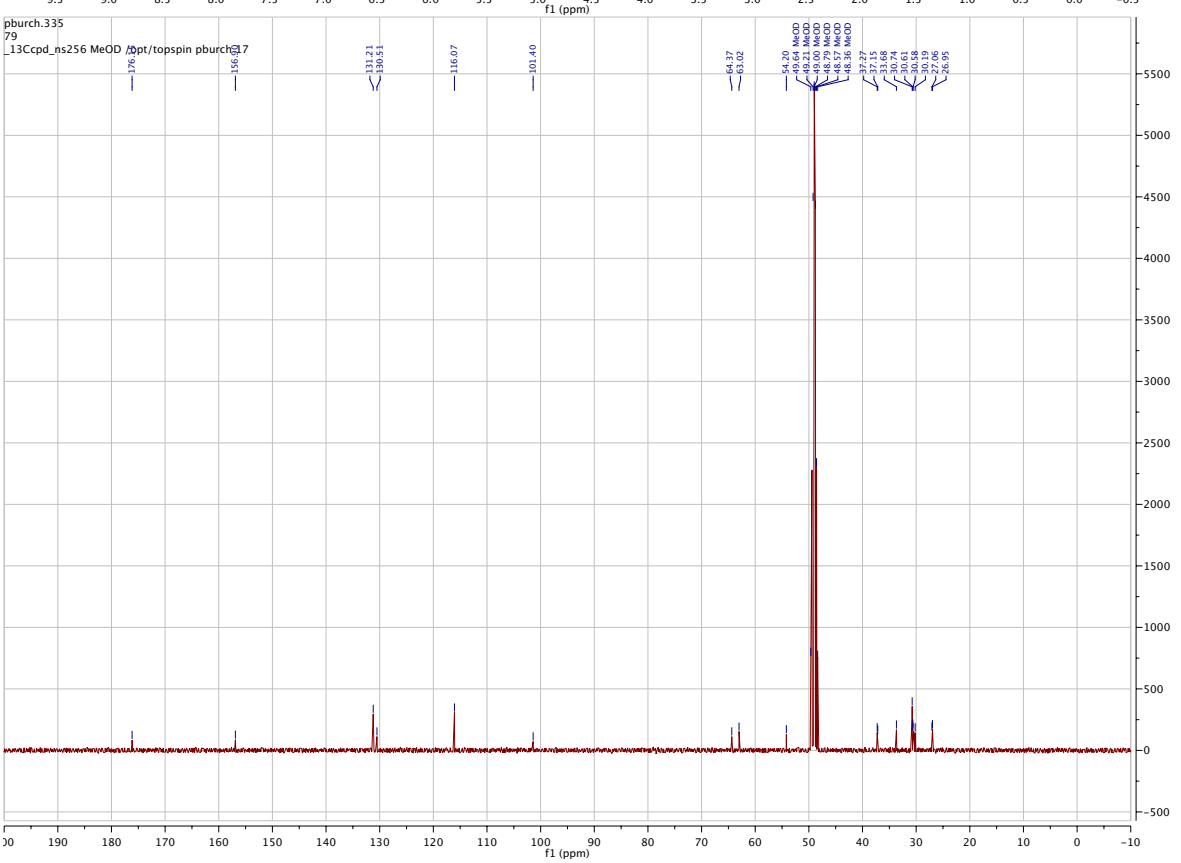

(9*Z*,12*Z*)-*N*-((*S*)-1-hydroxy-3-(4-hydroxyphenyl)propan-2-yl)octadeca-9,12-dienamide (BSL34)

(9*Z*,12*Z*,15*Z*)-*N*-((*S*)-1-hydroxy-3-(4-hydroxyphenyl)propan-2-yl)octadeca-9,12,15-trienamide (4.22h)